Preparation of Monolayer Tethers via Reduction of Aryldiazonium Salts

A thesis submitted in partial fulfilment of the requirements for

the Degree

of Doctor of Philosophy in Chemistry

in the University of Canterbury

By

Lita Lee

University of Canterbury

2015

Acknowledgements

I am thankful to Prof. Alison Downard for her encouragement, guidance and support during my years doing chemistry, without her I wouldn't have pursued PhD and let alone complete it. I would like to thank Dr. Paula Brooksby and all the (past and present) members of Downard research group. I would also like to thank Philippe Hapiot, Yann Leroux and Joanna Jalkh for their help during my stay in Rennes. Thank you also goes to Chris Fitchett for his help with organic chemistry and Matt Polson for his help with synthesis. Also, thank you to King, Siji and Rakesh for their help with organic chemistry and synthesis. Thank you to Steel and Fitchett groups for sharing their lab. I am grateful to all the staff and students in the Nanofabrication lab at the University of Canterbury for access to, and assistance with, their facilities. A thank you must also goes to all the staff of the Department of Chemistry at the University of Canterbury, especially Rob for making (and repairing) all the special glassware used in this thesis. Finally, I would like to thank the MacDiarmid Institute for the scholarships.

Table of Contents

Abstract

This thesis describes the preparation of surface-attached monolayer tethers from electroreduction of aryldiazonium ions using a protection-deprotection strategy. Monolayers of ethynylphenyl, carboxyphenyl, aminophenyl and aminomethylphenyl were prepared. Glassy carbon (GC) and pyrolysed photoresist film (PPF) surfaces were modified electrochemically and characterised by redox probe voltammetry. The monolayer tethers were coupled with electro-active ferrocenyl (Fc) and nitrophenyl (NP) groups for the indirect electrochemical estimation of the surface concentration. Film thickness measurement was carried out using an atomic force microscopy (AFM) depth profiling technique. The surface concentration and film thickness measurement results were consistent with the formation of monolayer films after removal of the protecting groups.

Preparation of mixed monolayers was studied using three different modification strategies: i) grafting from a solution containing two different protected aryldiazonium ions, ii) sequential grafting of two different protected aryldiazonium ions, and iii) grafting of protected aryldiazonium ions followed by removal of the protecting group and reaction of an amine or carboxylic acid derivative directly with the GC surface. The composition of the mixed layer prepared using the first method is difficult to control, whereas the possibility of multilayer formation cannot be discounted using the second method. Multilayer formation is unlikely using the third method. The electrocatalysis of oxygen reduction at mixed monolayer films was investigated briefly.

The origin of the two reduction peaks frequently observed for electroreduction of aryldiazonium ions at carbon surfaces was studied. Electroreduction was carried out at GC and HOPG surfaces. The reduction peak at the more positive potential is surface sensitive,

while the peak at the more negative potential is not. However, both reduction peaks lead to deposition of films and it is tentatively proposed that the more positive peak corresponds to reduction at a ‘clean’ GC electrode, and the more negative peak corresponds to reduction at the already grafted layer.

Abbreviations

Commonly used abbreviations

ACN	Acetonitrile
AFM	Atomic force microscopy
AQ	Anthraquinone
Boc	*tert*-Butyloxycarbonyl
Boc_2O	Di-*tert*-butyl dicarbonate
CE (1 M LiCl)	Calomel electrode with 1 M lithium chloride solution
$(COCl)_2$	Oxalyl chloride
DCC	Dicyclohexyl carbodiimide
DCM	Dichloromethane
DIPEA	Diisopropylethylamine
DMAP	4-(Dimethylamino) pyridine
DMF	Dimethylformamide
DMSO	Dimethylsulfoxide
EDC	1-Ethyl-3-(3-dimethylaminopropyl)carbodiimide hydrochloride
EDTA-Na_2	Disodium dihydrogen ethylenediaminetetraacetate
Et_3N	Triethylamine
Eth	Ethynyl
EtOAc	Ethyl acetate
EtOH	Ethanol
Fc	Ferrocenyl
$FcCH_2COOH$	Ferrocene acetic acid
FcCOOH	Ferrocene monocarboxylic acid
Fm	9-Fluorenemethyl

Fmoc	9-Fluorenylmethyloxycarbonyl
Fmoc-Cl	9-Fluorenylmethyl chloroformate
FmOH	9-Fluorenemethanol
GC	Glassy carbon
HBF_4	Tetrafluoroboric acid
HBTU	*O*-(Benzotriazol-1-yl)-*N*,*N*,*N*′,*N*′-tetramethyluronium hexafluorophosphate
HOBt	1-Hydroxybenzoltriazole hydrate
HOPG	Highly ordered pyrolytic graphite
NBA.HCl	4-Nitrobenzylamine hydrochloride
NBD	4-Nitrobenzenediazonium
NMR	Nuclear magnetic resonance spectroscopy
$NOBF_4$	Nitrosonium tetrafluoroborate
NP	4-Nitrophenyl
NPH	4-Nitrophenylhydrazine
PB	Phosphate buffer
PPF	Pyrolysed photoresist film
SCE	Saturated calomel electrode
t-BuONO	*tert*-Butylnitrite
$TBABF_4$	Tetrabutylammonium tetrafluoroborate
$TBAClO_4$	Tetrabutylammonium perchlorate
TBAF	Tetrabutylammonium fluoride
TBAOH	Tetrabutylammonium hydroxide
$TBAPF_6$	Tetrabutylammonium hexafluorophosphate
TFA	Trifluoroacetic acid
TFAA	Trifluoroacetic anhydride
THF	Tetrahydrofuran
TIPS	Triisopropylsilyl

XPS	X-ray photoelectron spectroscopy

Electrochemical abbreviations

CV	Cyclic voltammogram
ΔE_p	CV oxidation and reduction peak potential separation
$E_{½}$	Half wave potential
$E_{p,a}$	CV anodic peak potential
$E_{p,c}$	CV cathodic peak potential
i	Current
ν	Scan rate
Γ	Surface concentration

Publications

Lee, L., Downard, A.J., Preparation of ferrocene-terminated layers by direct reaction with glassy carbon: a comparison of methods. *Journal of Solid State Electrochemistry*, **2014**, *18*, 3369.

Lee, L., Ma, H.F., Brooksby, P.A., Brown, S.A, Leroux, Y.R., Hapiot, P., Downard, A.J., Covalently anchored carboxyphenyl monolayer via aryldiazonium ion grafting: A well-defined reactive tether layer for on-surface chemistry. *Langmuir*, **2014**, *30*, 7104.

Ma, H.F., Lee, L., Brooksby, P.A., Brown, S.A., Fraser, S.J., Gordon, K.C., Leroux, Y.R., Hapiot, P., Downard, A.J., Scanning tunneling and atomic force microscopy evidence for covalent and noncovalent interactions between aryl films and highly ordered pyrolytic graphite. *Journal of Physical Chemistry C*, **2014**, *118*, 5820.

Lee, L., Brooksby, P.A., Leroux, Y.R., Hapiot, P., Downard, A.J., Mixed monolayer organic films via sequential electrografting from aryldiazonium ion and arylhydrazine solutions. *Langmuir*, **2013**, *29*, 3133.

Chapter 1. Introduction

1.1 Carbon Electrodes

Carbon material has been widely used for electrochemistry due to its low cost compared to precious metal electrodes, relative inertness to electrochemistry, mechanical stability, and wide potential window.[1-3] The different allotropes of carbon used as electrode materials are graphite, diamond and fullerenes; graphite consists of stacked planar graphene sheets, incorporating sp^2 hybridised carbon atoms, while diamond consists of a sp^3 hybridised, tetrahedral-coordination lattice of carbon atoms. Fullerenes are also formed from sp^2 hybridised carbon, however unlike graphite, it does not consist of planar graphene sheets. The most common fullerenes used as electrode materials are carbon nanotubes.

Examples of graphitic carbon electrode materials include amorphous carbon, carbon fiber, powdered graphite, carbon black, glassy carbon (GC), pyrolytic graphite (PG), and highly ordered pyrolytic graphite (HOPG). The working electrodes used in this work are GC, HOPG and pyrolysed photoresist film (PPF), which are described in more detail in the following Section. Due to graphite-based materials being the only electrodes used in this thesis work, diamond- and fullerene-based electrodes will not be discussed.

Graphite materials are often classified by the three dimensions of the crystallites: the in-plane crystallite size (L_a), the height perpendicular to the graphene planes (L_c), and the intersheet spacing (d_{002}). The structure of graphite is shown on Figure 1.1. As seen in Figure 1.1, graphite presents two different crystallographic planes; the aromatic hexagonal plane is termed the basal-plane, while the plane perpendicular to this is known as the edge-plane, where the graphene sheets terminate in either a zig-zag or armchair conformation (Figure 1.1).

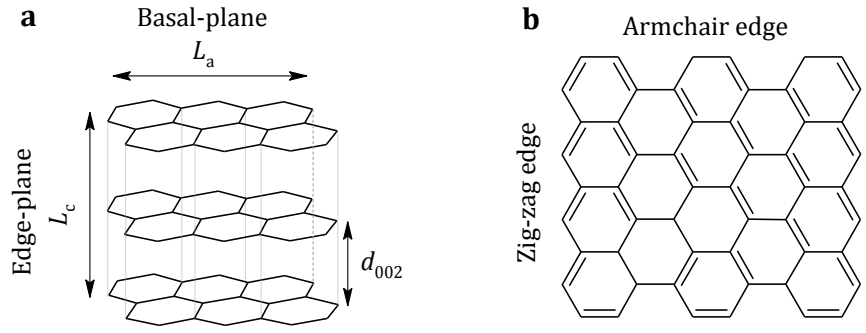

Figure 1.1 a) Structure of graphite; b) representation of zig-zag and armchair edge.

Most of the electrochemical activity of graphite is commonly considered to occur at the edge-plane rather than the basal plane.[4-10] Electron transfer is dependent on the density of states (DOS) of the materials;[11, 12] a higher DOS in the electrode promotes faster electron transfer.[1, 11] Basal-planes have low DOS at the Fermi level, whereas edge-planes have higher DOS due to dangling bonds and/or terminating impurity groups.[13] This explanation has been used to account for the proposed faster electron transfer at edge-plane than basal-plane.

Recent research by Unwin and Macpherson[14-20] suggests that it may not be correct that electron transfer at the basal-plane is very slow. Microscopic and nanoscopic study of redox couples at HOPG suggests that the pristine basal surface of HOPG has significant electron transfer activity.[16-20] The scanning micropipette contact method (SMCM) has been used to study the electron transfer of $Fe(CN)_6^{4-}$ on HOPG surface. SMCM (pipette diameter = 580 nm) allows the electrochemical reaction of solution species to be carried out on a small area of the electrode surface (e.g. pristine basal-plane only). It was found that there is no significant difference in electron transfer rate on the basal plane and edge plane of HOPG.[19] More recently, scanning electrochemical cell microscopy (SECCM) techniques were employed to study the electroactivity of basal plane HOPG.[17, 18, 20] SECCM is superior to the previous SMCM technique because SECCM provides a simultaneous map of local substrate electroactivity and topography. The SECCM results suggest that the basal plane of HOPG is

highly active towards electrochemistry.[17, 18, 20] These two different views of the electroactivity of basal plane graphite have not yet been reconciled.

1.1.1 Glassy carbon (GC)

GC is generally fabricated from polymeric resins such as polyacrylonitrile, by heat treating at 1000 – 3000 °C under pressure in an inert atmosphere.[21-25] The degree of graphitisation can be controlled by the pyrolysis conditions; increasing the annealing temperature reduces the intersheet distance and increases L_a and L_c.[23-25] Typical GCs usually have L_a and L_c in the range of 30 – 70 Å, and d_{002} ~ 3.6 Å.[1] Perfectly graphitised carbon has a d_{002} value of 3.354 Å.[26] The disordered nature of GC makes detailed microstructure characterisation at the atomic level difficult. Thus, the structure of GC is generally presented as a network of randomly intertwined ribbons of graphitic planes.[22, 23, 27] An alternative model based on detailed high resolution transmission electron microscopy (HRTEM) study revealed that GC may incorporate broken or imperfect fullerene-like structures.[21, 28]

Due to the randomly oriented crystallites in GC, GC is considered to consist mainly of edge-plane sites. The highly reactive edge-plane is prone to reaction with air and moisture, resulting in a surface terminated with a variety of oxygen-containing functional groups (Figure 1.2).[1, 2] Surface oxides on GC have been studied by a variety of methods, including, Raman spectroscopy,[29-31] X-ray photoelectron spectroscopy (XPS),[32-40] and electrochemistry.[33, 36, 40-44] Raman spectroscopy has been used to provide quantitative data identifying the surface coverage of certain oxygen-containing functionalities on the surface. For example, the surface coverage of carbonyl and hydroxyl groups on GC have been estimated using the reagents 2,4-dinitrophenylhydrazine (DNPH) and fluorescein mixed anhydride (FMA), respectively. These reagents react specifically with the particular functional groups and are also Raman active;[29, 31] DNPH gives rise to a Raman signal at 925

cm^{-1} and FMA at 765 cm^{-1}. Graphitic carbon has two characteristic Raman signals at 1360 cm^{-1} and 1600 cm^{-1}. Therefore, the 925/1360 cm^{-1} peak area ratio from the DNPH/GC adduct was used to assess the surface –C=O coverage. It was found that 1.2% of GC surface C atoms were in the form of carbonyl groups available for reaction with DNPH. Similarly the 765/1360 cm^{-1} peak area ratio from the FMA/GC adduct indicated that 0.8% of GC surface C atoms were bonded to hydroxyl groups available for reaction with FMA.[29, 31]

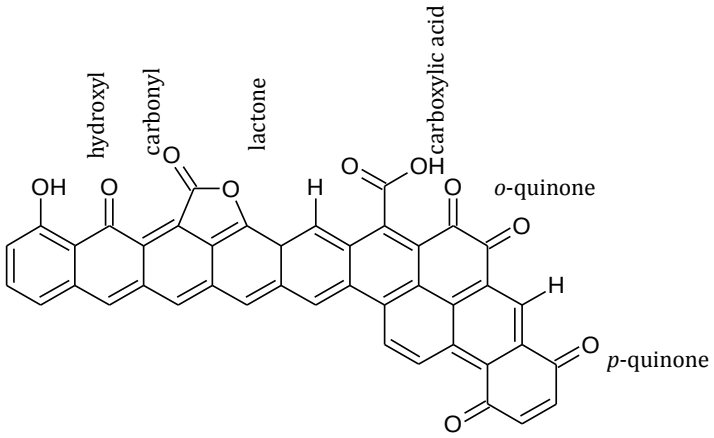

Figure 1.2 Examples of the various surface oxides that are present at the edge-plane of graphitic carbon surfaces.

XPS analysis of specific surface oxides on GC is usually carried out by deconvolution of the C 1s spectra into contributions from different carbon bonds, such as C–C, C–O, and C=O.[34-36] However, the chemical shifts in the binding energies of C atoms in different chemical environments are very small, which makes the deconvolution process difficult and introduces a large degree of uncertainty in the assignment of the relative amounts of each chemical species on the surface. To overcome this difficulty, a "tagging" molecule can be used. The tag can chemically react with a specific surface group and contains one or more atoms that are not normally present in the GC sample, such as Ti, N or F.[37, 38, 41] For instance, pentafluorophenylhydrazine (PFPH) was used to react with C=O groups and the percentage of C=O groups on the GC electrode could be calculated from the amount of F and N on the

surface.[37] The percentage of carbonyl groups estimated from the F 1s and N 1s spectra ranges from 1.4% to 2.2%.

To the best of my knowledge, there are no reports of quantitative determination of surface oxides on GC using electrochemical methods. However, electrochemistry has been used to study the effects of surface oxides on the rate of electron transfer.[33, 36, 41-44] The effect on electron transfer kinetics is dependent on the redox system used. For example, for outer sphere redox probes, such as $Ru(NH_3)_6^{2+/3+}$, electron transfer is relatively insensitive to surface chemistry, thus no difference in electron transfer rate is observed for surfaces covered with a high or low concentration of oxide, or even with a thin layer of adsorbates.[41] On the other hand, for a redox system that is dependent on surface oxides, such as $Fe^{3+/2+}$, the electron transfer rate is slower if the surface O/C ratio is decreased.[33, 36, 41-44] A third category of redox probe is surface sensitive but not oxide sensitive, such as $Fe(CN)_6^{3-/4-}$. Changes in the surface O/C ratio has little effect on the electron transfer kinetics, however a thin layer of adsorbates will slow down the electron transfer rate.[33, 41, 42]

Different pre-treatment processes lead to different surface O/C ratios on GC. Methods include electrochemical pre-treatment,[32-35, 42, 45-47] vacuum heat treatment (VHT),[31, 41, 48-51] radio frequency (RF) plasma treatment,[52, 53] laser activation,[54-58] and polishing.[36, 59-61] Electrochemical pre-treatment and RF oxygen plasma treatment usually result in an increase of surface oxides, with O/C ratios typically in the range of 0.13 – 0.42[32-35, 45] and 0.22 – 0.33,[52, 53] respectively. In contrast, VHT and laser activation usually yield a decrease in surface oxides, with O/C ratio ~ 0.04.[31, 48, 49, 55] Polishing with alumina or diamond paste, the most common pre-treatment procedure, gives a reported O/C ratio of 0.08 – 0.33.[31, 34-38, 41, 45] Polishing with alumina/H_2O slurry was employed in this thesis to prepare GC surfaces prior

to modification. Further detailed discussion of surface oxides on polished GC is included in Chapter 3.

1.1.2 Highly ordered pyrolytic graphite (HOPG)

HOPG is produced by high-temperature deposition of gaseous hydrocarbons, often acetylene, followed by compression at high pressure and temperature. The graphite crystallites of HOPG are much larger than those in GC, usually having L_a and L_c values exceeding 1 μm.[1] A key difference between GC and HOPG is that HOPG has a much lower density of edge plane than GC. The amount of step edges and defect sites depends on the history and preparation of the HOPG. The HOPG surface is atomically flat, which makes it a suitable carbon substrate for scanning tunnelling microscopy (STM) investigation.[62] In this thesis, HOPG was only used to investigate the cyclic voltammograms (CVs) of electroreduction of aryldiazonium salts (Chapter 7).

1.1.3 Pyrolysed photoresist film (PPF)

The process of pyrolysing photoresist for photolithography was first reported in 1985 by Lyons and co-workers,[63, 64] and in 1997, it was used to fabricate microelectromechanical systems (MEMs).[65] It was not until 1998 that carbon films prepared from pyrolysed photoresist were characterised electrochemically and routinely used as electrode materials.[66] For investigations of the pyrolysis procedure, Novolak photoresist (phenol formaldehyde resin) was spin-coated onto a silicon wafer and pyrolysed at temperatures ranging from 600 to 1000 °C under a N_2 atmosphere.[66] The thickness of the film decreased from 8 μm to 2 μm after pyrolysis at 1000 °C.[66, 67] As the pyrolysis temperature increased the sheet resistance decreased; film pyrolysed at 600 °C had a sheet resistance of 10^5 Ω □$^{-1}$ and film pyrolysed at 1000 °C had sheet resistance of 10 Ω □$^{-1}$.[67] After pyrolysis at > 700 °C, atomic force microscopy (AFM) showed an atomically smooth surface with root mean square (rms)

roughness of 0.2 nm over an area of 0.5 μm × 0.5 μm.[67] Raman spectra showed that the films have graphitic character but are highly disordered and XPS measurement showed that the O/C ratio decreases gradually with increasing pyrolysis temperature, reaching a limiting value of ~ 0.05 at temperatures > 700 °C.[67] Electrochemical activity for the $Fe(CN)_6^{4-/3-}$ redox reaction was shown to improve as the pyrolysis temperature increased. For CVs obtained at 60 mV s^{-1}, ΔE_p decreased as temperature increased; at 700 °C ΔE_p was 170 mV while at 1000 °C, ΔE_p was 80 mV.[66]

McCreery and co-workers[68] reported a PPF preparation procedure that has formed the basis of electrode preparation by other groups and for this thesis work. In McCreery's method, positive photoresist was spin-coated onto a silicon wafer and pyrolysed at 1100 °C in a reducing atmosphere (5% H_2 and 95% N_2). McCreery and co-workers characterised their PPF by Raman spectroscopy, XPS, AFM, scanning electron microscopy (SEM), transmission electron microscopy (TEM) and electrochemistry.[68, 69] The film prepared in this way reduced in thickness from 5 – 6 μm to 1 – 2 μm during pyrolysis. The 1 μm thick PPF samples had a resistivity of 5.1 × 10^{-3} Ω cm, which is similar to the resistivity of GC prepared at 1000 °C (4.5 – 5.0) × 10^{-3} Ω cm.[68] SEM images of the PPF samples showed a featureless surface and HRTEM indicated the presence of graphite-like structures.[68] Raman bands at ~ 1380 cm^{-1} (D band) and ~1600 cm^{-1} (E_{2g}) band were examined to assess the disordered nature of the carbon film; the larger the D/E_{2g} ratio the greater the disorder. PPF was shown to be less disordered than GC (i.e. PPF had higher basal plane to edge plane ratio compared to GC). XPS studies indicated an O/C ratio of 0.023 ± 0.005 for freshly prepared PPF. The O/C ratio increased upon exposure to air to ~0.05 – 0.06. AFM images of 1 μm × 1 μm regions were featureless with rms roughness of ~0.5 nm.[68, 69] In contrast, the rms roughness of HOPG surface determined by scanning tunnelling microscopy (STM) is 0.24 nm,[70] while for GC the rms

roughness has been reported to be 4.1 ± 0.1 nm (from STM).[70] CVs obtained at 200 mV s^{-1} at PPF and GC electrodes in $Fe(CN)_6^{3-/4-}$ solution gave ΔE_p of 80 mV and 65 mV, respectively.[68] Although, PPF shows small differences to GC, its GC-like nature makes it a good substitute for GC when a flat surface is required, for example, for film thickness measurement using AFM, as carried out in this work.

1.2 Surface Modification via Reduction of Aryldiazonium Salts

Since the first demonstration by Pinson and co-wokers,[71] aryldiazonium salts have been widely used to covalently modify surfaces with organic films.[72] Grafting via aryldiazonium salts involves the reduction of the aryldiazonium ion, followed by homolytic cleavage of the C–N bond to generate an aryl radical which may subsequently react with the substrate to form a covalent bond (Scheme 1.1). The formation of the covalent bond makes it a robust method for surface modification. The reduction of aryldiazonium salt can be carried out under a variety of conditions: electrochemically,[71, 73, 74] by reduction by the substrate,[75, 76] by addition of a reducing agent (hypophosphorous acid,[77-79] iron powder,[80] or ascorbic acid[81, 82]), or by photosensitised reduction.[83, 84] Grafting through aryldiazonium ion chemistry is of particular interest not only because of the stability of the surface attachment but also due to the wide range of derivatives that can be synthesised.[85, 86] Furthermore, grafting can be performed on various substrates (such as carbons, metals, semiconductors, and polymers).[87, 88] In addition to grafting using an isolated aryldiazonium salt, the aryldiazonium ion can be grafted *in situ* (in the reaction solution) after mixing the aromatic amine with sodium nitrite (in acidic aqueous condition) or with *tert*-butyl nitrite or isoamyl nitrite (in acetonitrile solution).[86, 89, 90] The advantage of this route is that some aryldiazonium salts that are difficult (or impossible) to isolate can be grafted onto a substrate.

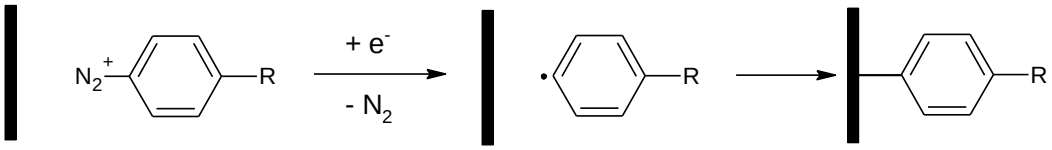

Scheme 1.1 Reaction scheme for the reduction of aryldiazonium ion that leads to formation of aryl radical that subsequently reacts with a substrate to form a covalent bond.

Surface grafting through the reduction of aryldiazonium ions usually results in a disorganised multilayer film.[72, 73] A mechanism for the formation of multilayers has been proposed by Pinson and co-workers[91] (Scheme 1.2). This mechanism also accounts for the observed formation of azo bonds within the layers. The reaction pathway involves the reduction of aryldiazonium ion to give an aryl radical, which attacks the already grafted aryl group to generate a grafted cyclohexadienyl radical (step iii). To restore the aromaticity, the cyclohexadienyl radical must lose a hydrogen radical, this is possible either through an electron transfer to the electrode and loss of a proton or by reoxidation of the cyclohexadienyl radical by an aryldiazonium ion (step iv). Repetition of this reaction cycle (step i – iv) would lead to formation of thick polyphenyl layers (step v). Grafted cyclohexadienyl radicals can also react with an aryldiazonium ion giving rise to a radical cation that is readily reduced to give an azo link (steps vi and vii). The recovery of the aromaticity is achieved by reoxidation of the cyclohexadiene (step viii). This second pathway leads to incorporation of azo bonds in the film. The azo linkage can also form directly with the substrate.[92, 93] The presence of azo linkages from aryldiazonium derived films is supported by XPS and time-of-flight secondary ion mass spectroscopy (ToF-SIMS).[91-95]

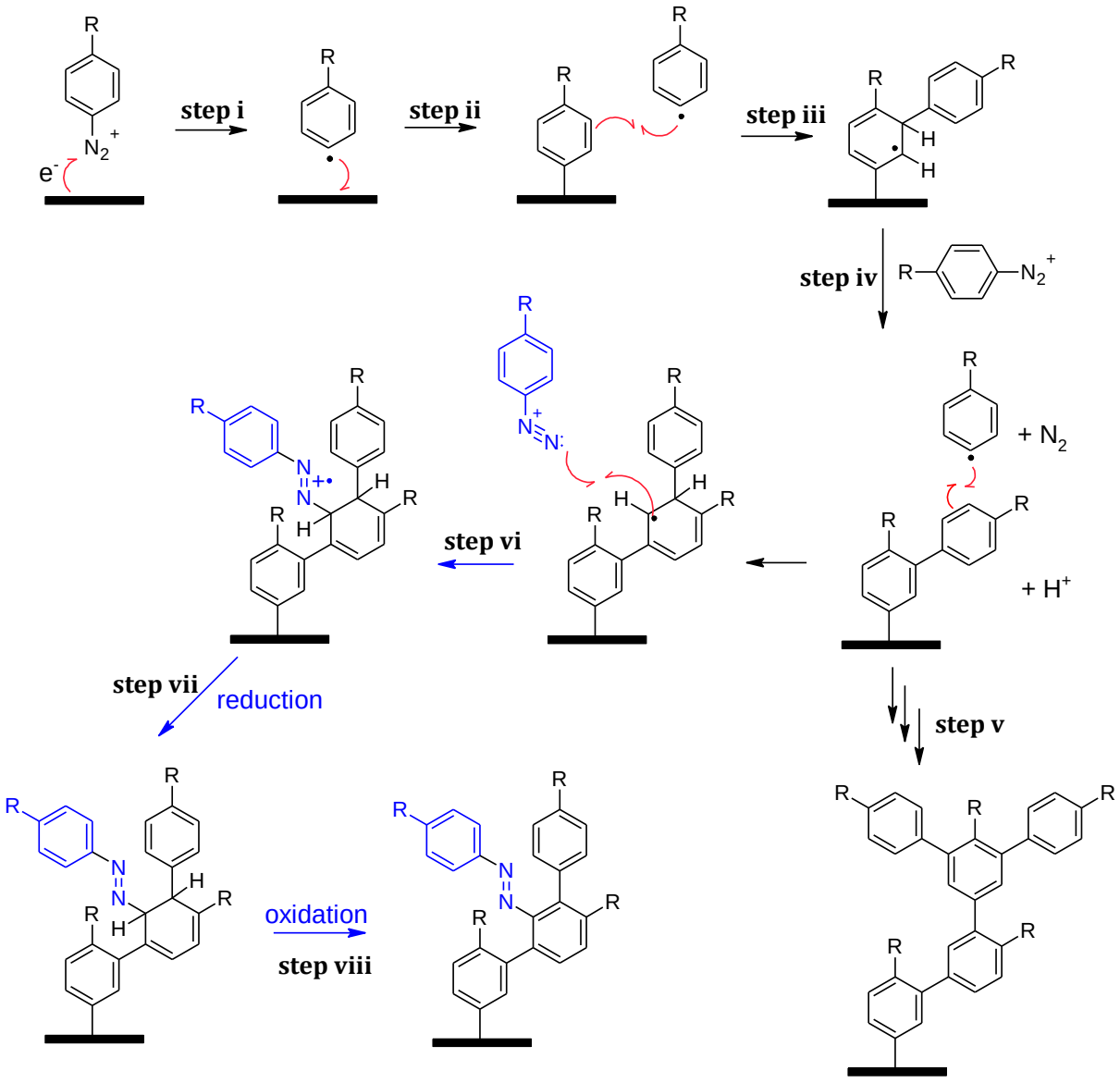

Scheme 1.2 Proposed mechanism, based on that of Pinson and co-workers,[91] for the grafting of multilayer films by reduction of aryldiazonium salts. Adapted from reference 76.

Surface modification via aryldiazonium ion is also proposed to proceed via aryl cation intermediates (Scheme 1.3).[77, 93, 96, 97] Formation of an aryl cation is through heterolytic cleavage of the C–N bond. Unlike the homolytic pathway, the heterolytic process does not involve electron transfer from an external source (electrode or reducing agent), rather it is similar to an S_N1 reaction.[98] Whether the homolytic or heterolytic pathway occurs depends on the experimental conditions. In the presence of an electron source (electrode or reducing agent), the homolytic pathway is preferred, while high temperature favours the heterolytic

pathway.[98] In addition, increasing the nucleophilicity of the solvent or increasing the electrophilicity of the *β*-nitrogen atom of the diazonium salt (by placing suitable substituents on the aromatic ring), favours the homolytic pathway. This effect can be accounted for by a mechanism in which the solvent acts as an electron donor to the diazonium cation, leading to the production of aryl radicals (Scheme 1.4).[98]

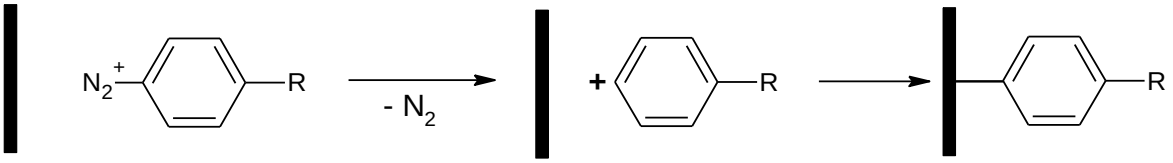

Scheme 1.3 Reaction scheme for the modification of a substrate via aryl cation intermediates.

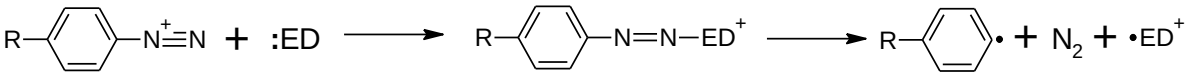

Scheme 1.4 Reaction scheme for the stabilisation of aryldiazonium ion by electron donating solvent leading to dediazoniation via homolytic pathway.

Both the homolytic and heterolytic pathways can result in covalent bonds between the substrate and the modifier.[71, 85, 94, 99-107] Evidence for covalent bonding includes the stability of the film formed towards ultrasonication,[71-73, 85, 99, 101, 102] and direct spectroscopic evidence.[72, 73, 100, 103-105, 107] For example, ultrasonication of modified GC electrodes for 15 min in acetonitrile (ACN), dimethylformamide (DMF), dimethylsulfoxide (DMSO), benzene, benzonitrile, acetone, ethanol, methanol, dichloromethane (DCM) and chloroform does not change the voltammetric signal of the nitrophenyl (NP) group.[85] A ToF-SIMS analysis of GC modified with polyphenylene films revealed the presence of fragments assigned to the modifier bonded to the GC surface, through direct C–C bonds and through C–O bonds.[94] The presence of C–O bonds suggests that the reaction of aryl radicals with oxygen containing functionalities on the GC surface is possible.

The existence of a covalent metal–C bond between a metallic substrate and the aryl groups has been demonstrated using XPS. For a modified Cu substrate, XPS signals were consistent with both Cu–O–C and Cu–C linkages.[104] Evidence of a bond between an Fe substrate and aryl modifier has also been observed on iron plates electrografted with 4-carboxybenzene diazonium salt.[100] Recently, evidence of covalent bonding between a Au substrate and aryl moieties was provided by McDermott and co-workers.[107] A combination of surface-enhanced Raman scattering (SERS) and density functional theory (DFT) modelling of gold-nanoparticles (Au-NPs) modified with 4-nitrobenzenediazonium salt (NBD) revealed a Raman band at 412 cm^{-1}, which was assigned to a Au–C stretch.[107] A high-resolution electron energy loss spectroscopy (HREELS) study was then performed on a planar Au (111) surface modified with NBD by electrochemical and spontaneous grafting. The observation of a peak at 420 cm^{-1}, on the spontaneously and electrochemically modified Au (111) surfaces, gave direct evidence of the formation of Au–C bond.[107] Furthermore, ToF-SIMS analysis of Al plates grafted from $^{+}N_2$-C_6H_4-CH_2-S-C(=S)-N(C_2H_5)$_2$ revealed fragments corresponding to Al–C and Al–O–C linkages.[108] The data indicated that the aryl radicals were mainly bonded to the surface through Al–O–C linkages.[108] XPS analysis of MnO_2 nanorods modified with NBD and 4-aminobenzenediazonium salts also provided evidence of Mn–O–C bonds.[109]

On the other hand, surface modification by aryldiazonium salts has also been reported to result in mainly physisorbed layers.[110-113] STM investigation of HOPG surfaces modified by electrografting in NBD solution showed that films were mainly physisorbed on the basal-plane. Physisorbed films were stable to brief sonication but were removed by the STM tip while imaging.[113] Spontaneous modification of Au surfaces with diazonium derivatives in aqueous acidic solution has been reported to result in mostly physisorbed material, which was removed by sonication in ACN.[110, 112]

1.2.1 Preparation of films with controlled thickness

The thickness of layers grafted from aryldiazonium salts can be controlled to some extent by controlling the charge consumed during the grafting process. In practice, this involves controlling the grafting potential, electrolysis time and the concentration of aryldiazonium salt.[73, 114] For example, preparation of a NP layer was performed by chronoamperometry at a potential located 150 mV negative to the diazonium ion reduction peak potential. As the modification time increased, the average film thickness (measured by AFM) and the surface concentration (determined from the voltammetric peak area) of the NP groups increased.[114] From the film thickness and surface concentration data, a NP surface concentration of $(2.5 \pm 0.5) \times 10^{-10}$ mol cm^{-2} was found for a 'slice' of NP film equivalent to monolayer thickness.[114] It was also reported that under the same conditions, thinner films are formed in aqueous acid medium than in ACN.[114]

Electrografting of diazonium salts has been investigated in ionic liquids.[115, 116] Under conditions where electrografting of NBD in ACN gave a film thickness and surface concentration of NP groups of 4 nm and 2×10^{-9} mol cm^{-2}, respectively, the corresponding values for a film grafted in the ionic liquid *N*-tributyl-*N*-methylammonium bis(trifluoromethylsulfonyl)imide ([Bu_3MeN][NTf_2]), were 1 nm and 2×10^{-10} mol cm^{-2}, respectively.[115] Hence, it appears that thinner films are grafted in ionic liquid than in ACN. This finding was attributed to the higher viscosity and therefore lower diffusion coefficient for the diazonium ion in the ionic liquid than in ACN.[115] Thus a lower amount of NP radicals would be generated close to the electrode surface in ionic liquid than in ACN.

1.2.2 Preparation of monolayer films

The major theme of this thesis work is preparation of monolayer films using aryldiazonium salts. Compared with the disorganised multilayer films that usually result from diazonium ion

grafting, a monolayer has the advantages of being more organised and allows faster electron transfer between the electrode and immobilised groups, due to its lower thickness. This is an important factor for potential applications involving electrochemical or electrical measurements, such as electrochemical sensors. Typically a sensor consists of a transducer or detector device that produces a signal, and a recognition element that enables a selective response to a particular analyte (Figure 1.3).[117] The distance between the recognition element and the transducer must be small to ensure the electrical signal (electron transfer) can be detected. Furthermore, better control of the composition and orientation of the recognition layer is possible with a monolayer compared to a multilayer. To ensure long-term performance of the sensor, the recognition element must be stably immobilised onto the electrode surface. This can be achieved using aryldiazonium ion grafting giving a covalently attached modifier. Thus, monolayer preparation via aryldiazonium ion grafting is an important research goal.

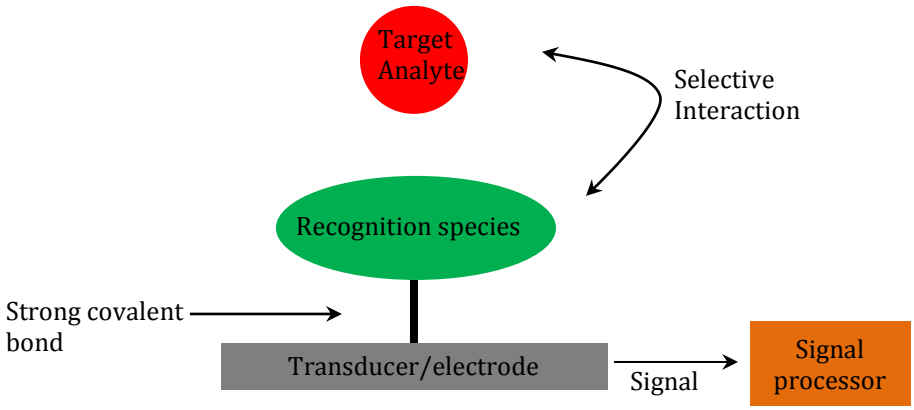

Figure 1.3 Schematic of a sensor with electrochemical transducer.

As mentioned earlier, choice of the grafting conditions can limit the amount of film grafted from aryldiazonium salts. Thin films can also be formed with the use of a radical scavenger.[118] Electrografting of NBD in the presence of 2,2-diphenyl-1-picyrlhydrazyl (DPPH) in excess, resulted in a surface concentration of NP groups of 6.7×10^{-10} mol cm^{-2}

compared to 17.5×10^{-10} mol cm^{-2} when no DPPH was added to the grafting solution.[118] The low surface concentration of NP groups suggests a thinner layer, however no film thickness measurement was carried out by the authors. It was also noted that the grafting process occurs even at high concentration of DPPH, and the authors tentatively suggest that the reaction of aryl radicals with the surface occurs more readily than coupling of aryl radicals with DPPH, which in turn occurs more readily than the coupling of aryl radicals with the already grafted aryl groups.[118]

A sub-monolayer of anthraquinonyl groups immobilised on edge-plane pyrolytic graphite was reported by Compton and co-workers.[119] Firstly, anthraquinone-2-diazonium salt (AQ-N_2^+) was adsorbed to pyrolytic graphite at 0 °C, followed by thermal decomposition of the diazonium ion, in diazonium ion free solution, at room temperature. The authors propose that this results in covalently attached anthraquinone (AQ) groups via ester linkages (Scheme 1.5).[119] The amount of AQ adsorbed on the surface could be tuned by varying the adsorption time. It was proposed that the amount of AQ bonded to the surface is limited by the amount of AQ pre-adsorbed on the surface and thus only a monolayer was possible. The maximum surface concentration of bonded AQ groups was 7.4×10^{-10} mol cm^{-2} after 300 s of pre-adsorption.[119] However, films were only characterised by electrochemistry.[119] The stability of the AQ layer upon repetitive scanning was taken as evidence for covalent attachment, as was a linear plot between peak current and scan rate and ideal CV peak shapes.[119] However, similar CVs are also expected if AQ groups were bonded directly to the surface after formation of the corresponding radical or cation, and the formation of physisorbed layers also cannot be discounted.[120] It is well known that AQs readily physisorb on graphitic surfaces,[121] and hence, the nature of the interaction between AQ groups and the surface is not clear.

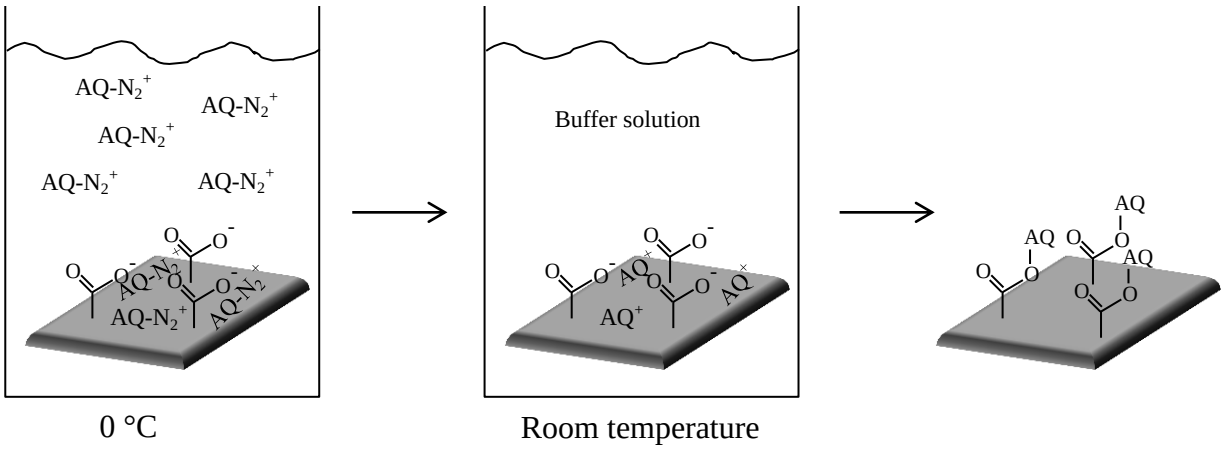

Scheme 1.5 Illustration of the proposed pathway for derivatising graphitic electrodes via the adsorption-transfer method. Adapted from reference 119.

Using a different strategy, grafting of sterically hindered 3,5-bis-*tert*-butylbenzene diazonium was shown to give a monolayer film on a gold electrode (thickness = 1 nm).[122] It was proposed that substitution at the 3 and 5 positions prevents attack of radicals at already grafted aryl groups. While this finding supports the generally assumed multilayer film growth mechanism (Scheme 1.2), it does not give a layer that can be used for further coupling reactions. On the other hand, a sterically hindered diazonium ion which includes reactive functionalities has been shown to limit film growth to a monolayer. Calix[4]tetra-diazonium ions (Scheme 1.6) have been electrografted to carbon and gold surfaces giving monolayer films. On PPF, AFM measurements gave a film thickness of (1.3 ± 0.1) nm, and on Au, ellipsometry gave a thickness of (1.09 ± 0.20) nm.[123] These thicknesses are consistent with the theoretical calculated height of the calix[4]arene (~ 1 nm).[123] The constrained cone conformation of the macrocycle and the methylene links at the *ortho* positions of the phenoxy substituents were proposed to prevent the formation of multilayers.[123]

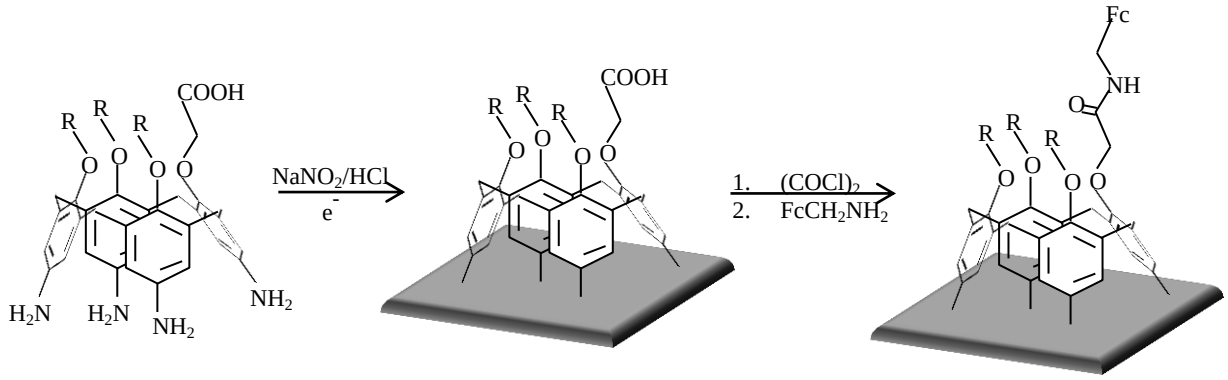

Scheme 1.6 Schematic representation of electrograting of calix[4]arene via the *in situ* diazotation of the calix[4]tetraanilines in the presence of $NaNO_2$ in acidic aqueous solution followed by functionalisation with ferrocenyl (Fc) moiety. R = C_3H_7, CH_2COOH. Adapted from reference 123[123].

1.2.3 Preparation of monolayers via reduction of aryldiazonium ions bearing a cleavable group

Another strategy for forming a monolayer via aryldiazonium ions is by the use of cleavable groups. This is the method used in this thesis. The first reported example of 'near' monolayer formation by grafting of a cleavable molecule was based on an aryldiazonium ion containing a disulfide (S-S) bond.[124] As shown in Scheme 1.7, electrochemical grafting of diaryl disulfide at a GC electrode resulted in a covalently bonded multilayer and subsequent reductive cleavage of the disulfide bond resulted in a 'near' monolayer of thiophenolate groups.[124] AFM measurement of film thickness gave values of 3 ± 1 and 1.5 ± 0.5 nm before and after cleavage respectively.[124] The calculated height of a thiophenolate molecule is 0.6 nm, suggesting that some multilayer film remained even after cleavage of the disulfide bond.[124] This is presumably due to the outer phenyl groups having insufficient bulk to protect the inner aryl moieties from aryl radical attack, thus yielding some areas of multilayer film after cleavage (Scheme 1.7). The same method was applied to single-walled (SW) and multi-walled carbon nanotubes (MWCNTs) and the decrease in film thickness after cleavage of the disulfide bond was evidenced by TEM.[125]

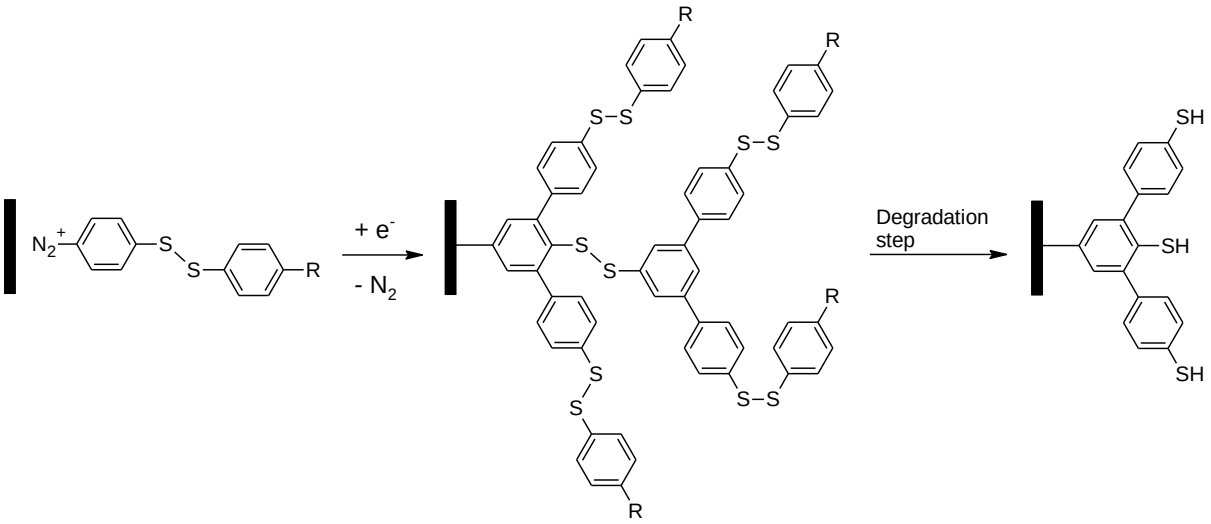

Scheme 1.7 Grafting of aryldiazonium salts containing cleavable disulfide bonds to form a near monolayer film. R = N_2^+ or Cl. Adapted from reference 124.

A similar formation-degradation approach using a hydrazone substituted benzene diazonium ion has also been reported.[126] The positively charged hydrazone group is expected to decrease access of further diazonium ions to the surface, and the hydrazone groups are readily cleaved by hydrolysis in acidic medium to give benzaldehyde groups (Scheme 1.8). The surface concentration was found to be 4×10^{-10} mol cm^{-2}, determined from the CVs of the irreversible reduction of the benzaldehyde group.[126] AFM measurement of the film thickness before and after hydrolysis gave values of 1.9 ± 0.6 and 1.2 ± 0.4 nm, respectively,[126] again suggesting that more than a monolayer film remained after hydrolysis.

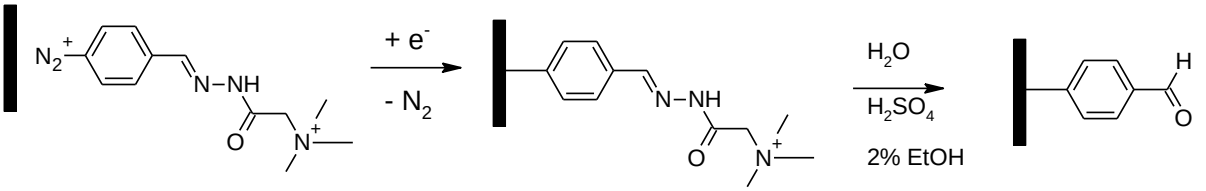

Scheme 1.8 Grafting of benzaldehyde Girard's reagent T hydrazone diazonium salt followed by acid hydrolysis to form a near monolayer of benzaldehyde groups. Adapted from reference 126.

Bartlett and co-workers[127-131] have reported on the use of Boc-protected amine derivatives of aryldiazonium salts to avoid the formation of multilayers during the grafting process. Electrochemical reduction of (*N*-Boc-aminomethyl)benzene diazonium salt on a GC

electrode resulted in a surface bearing a Boc-amine group, that was deprotected under acidic conditions. AQ, anthracene, and dihydroxybenzene derivatives have been immobilised on the surface via amide coupling reaction with the amine tether.[127-129, 131] No film thickness measurements were undertaken in the study, however the surface concentration of coupled AQ was ~6×10^{-10} mol cm^{-2}, while the surface concentrations of coupled dihydroxybenzene derivatives ranged from $0.74 - 7.6 \times 10^{-10}$ mol cm^{-2} depending on the substituent on the dihydroxybenzene molecule. As mentioned earlier, a monolayer equivalent of NP groups has a surface concentration of $(2.5 \pm 0.5) \times 10^{-10}$ mol cm^{-2}.[114] Hence, the surface concentration of AQ and dihydroxybenzene derivatives coupled to the deprotected aminomethylphenyl surface suggests that more than a monolayer of aminomethylphenyl groups were immobilised on the surface after deprotection. Boc-protected amine derivatives of aryldiazonium salts are further investigated in this thesis (Chapter 6).

More recent work by Leroux and co-workers[132] has combined the use of a sterically bulky protecting group and the formation-degradation approach to prepare monolayer films. This method is termed the 'protection-deprotection' strategy. In this strategy, the bulky protecting group should prevent radical attack at the already grafted aryl rings. The protecting group can be subsequently removed (deprotected) to reveal a functionality that can be used for further coupling reactions (Scheme 1.9). In Leroux and co-workers' work, ethynylphenyl groups were protected by silyl moieties (trimethylsilyl (TMS), triethylsilyl (TES) and triisopropylsilyl (TIPS)) and after deprotection, post-functionalisation was carried out using the well-known 'click' coupling (Cu(I)-catalysed Huisgen 1,3-dipolar cycloaddition) reaction (Scheme 1.10).[133] It was shown that even the smallest TMS group is bulky enough to protect the already attached aryl groups from the attack of aryl radicals.[133] Film thickness measurements by AFM gave values ranging from 0.8 to 2 nm for the three protected films and after deprotection all of the films had thickness close to 0.6 nm, consistent with a

monolayer.[133] Moreover, after post-functionalisation with a Fc moiety, surface concentrations of 3.3, 2.5 and 2.0 × 10^{-10} mol cm^{-2} were found for films initially protected with TMS, TES and TIPS groups, respectively.[133] This is consistent with the increased size of the protecting groups and therefore expected decreased density of the grafted molecules.

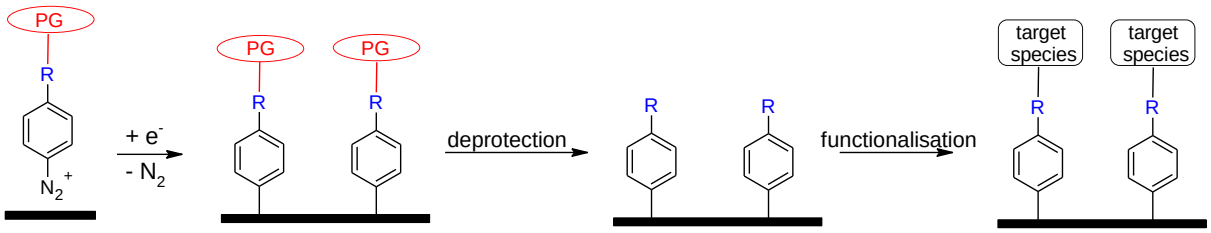

R = functionality that can be further used for coupling reactions

PG = protecting group

Scheme 1.9 Schematic representation of preparation of monolayer films via the protection-deprotection strategy.

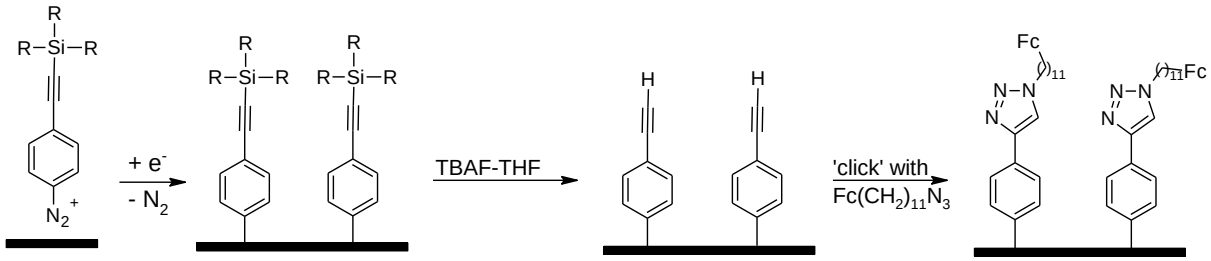

R = Me, Et and *i*Pr

Scheme 1.10 Strategy for preparation of monolayers based on silyl protecting groups. Adapted from reference 133.

TIPS protected ethynylbenzene diazonium salt has also been grafted at carbon paper electrodes.[134] The functionality of the ethynyl group was compared using the 'click' reaction, Sonogashira coupling, and Glasier coupling with the appropriate Fc derivatives. Surface concentrations of the Fc groups were not determined by the authors, but inspection of the CVs of surface immobilised Fc shows the yield of reactions is in the order of: 'click' reaction

> Sonogashira coupling > Glasier coupling.[134] The use of the TIPS protecting group is also investigated in this thesis (Chapter 4).

1.2.4 Preparation of mixed layers via reduction of aryldiazonium ions

The ability to form mixed layers (films incorporating more than one modifier) is useful especially for biosensing applications. The incorporation of a diluent component helps in increasing the sensor sensitivity by giving a better accessibility of the active species and at the same time reducing nonspecific adsorption.[87, 135] For example, Gooding and co-workers have modified GC surfaces with two modifiers: oligo(phenylethynylene) derivatives as molecular wires and poly (ethylene glycol) (PEG) derivatives as the diluent molecules (Figure 1.4).[136, 137] The molecular wire serves as a conduit for electron transfer and the PEG diluent layer blocks the access of other species in solution to the electrode surface.[136, 137] Ferrocene was attached to the end of the molecular wires to demonstrate the ability of the interface to facilitate efficient electron transfer. It was shown electrochemically that the electrode interface is able to resist nonspecific interactions of proteins, and only protein (antibody, Figure 1.4) specifically interacting with the attached receptor (biotin) influenced the electrochemistry of ferrocene.[136, 137] Note, Figure 1.4 shows a monolayer film however, this was not specifically characterised in their work.

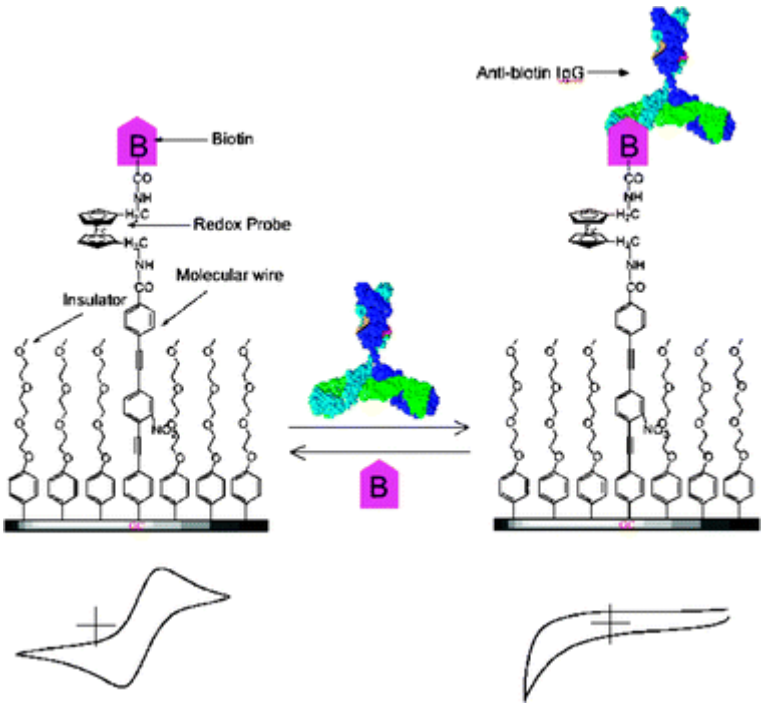

Figure 1.4 Schematic representation of GC interface consisting of molecular wire coupled with biotin and PEG diluent layer for immunobiosensing application. Bottom figures depicting the expected electrochemistry of ferrocene in the absence and presence of the complementary antibody. Figure is reproduced from reference 136.

Surfaces containing multiple functionalities can be prepared by electrografting from mixtures of aryldiazonium salts in solution.[136-144] However, the control of the surface composition using this method is difficult. Bélanger and co-workers[142] and Gooding and co-workers[139] have investigated the deposition behaviour of mixed aryldiazonium salts solutions. Bélanger and co-workers[142] studied two sets of binary mixtures of *para*-substituted aryldiazonium ions on GC electrode: Br-Ar-N_2^+/NO_2-Ar-N_2^+ and Br-Ar-N_2^+/$N(Et)_2$-Ar-N_2^+, while Gooding and co-workers[139] examined eight sets of binary mixtures of *para*-substituted aryldiazonium ions on GC and Au electrodes: Br-Ar-N_2^+/HS-Ar-N_2^+, COOH-Ar-N_2^+/HS-Ar-N_2^+, COOH-Ar-N_2^+/Br-Ar-N_2^+, SH-Ar-N_2^+/NH_2-Ar-N_2^+, Br-Ar-N_2^+/NH_2-Ar-N_2^+, Br-Ar-N_2^+/NO_2-Ar-N_2^+, NH_2-Ar-N_2^+/COOH-Ar-N_2^+, and NO_2-Ar-N_2^+/COOH-Ar-N_2^+. Both groups investigated the influence of the ratios of the two aryldiazonium ions in solution on the composition of the grafted mixed layers. It was concluded by those authors that the composition of the modified

binary mixed layers is dominated by the aryldiazonium ion that is easier to reduce, i.e. the more easily reduced aryl diazonium ion has a higher concentration on the surface than in the corresponding solution mixture.

On the other hand, when electrografting was carried out in a binary mixture of *para*-substituted aryldiazonium ions bearing two oppositely charged moieties, SO_3^--Ar-N_2^+/$N^+(Me)_3$-Ar-N_2^+, equal concentrations of the two species were found on the modified surface regardless of the ratio of the two aryldiazonium ions in the solution.[138] The authors suggest that this is due to the electrostatic interaction of the two diazonium ion species in solution prior to electroreduction. The CVs of the mixed aryldiazonium ions solution (SO_3^--Ar-N_2^+/$N^+(Me)_3$-Ar-N_2^+) show only one reduction peak and this peak is more positive than either of the individual diazonium ion reduction peaks.[138] This indicates that it is easier to reduce SO_3^--Ar-N_2^+ and $N^+(Me)_3$-Ar-N_2^+ in the mixed system. It was proposed that this may be due to charge neutralisation in the mixed system, which decreases the energy barrier for reducing the aryldiazonium ions.[138] Moreover, the XPS spectra of the single component layers showed the presence of adsorbed counterions required to neutralize the surface charge (Na signal from Na^+ for SO_3^--Ar film, and F signal from BF_4^- for $N^+(Me)_3$-Ar film), but these Na and F signals were not present for the mixed component layers.[138] DFT calculations of the two diazonium molecules demonstrated favourable interactions between the molecular orbitals of the two diazonium species in the gas phase, induced by electrostatic interaction.[138] The experimental and theoretical results suggest that electrostatic interaction between the two diazonium ions in solutions is expected.

In contrast, XPS analysis of grafting from a binary mixture of *para*-substituted aryldiazonium ions, SO_3^--Ar-N_2^+/NH_3^+-Ar-N_2^+, by Vilà and Bélanger[144] showed that films always had a

higher concentration of SO_3^--Ar groups than NH_3^+-Ar groups in comparison to the corresponding concentrations in solution. This was surprising because NH_3^+-Ar-N_2^+ is more easily reduced than SO_3^--Ar-N_2^+. The authors suggest the reason for the apparent lower grafting efficiency of NH_3^+-Ar groups may be the lower reactivity of the NH_3^+-Ar$^\bullet$ radical towards the electrode surface.[144] In these experiments, the NH_3^+-Ar-N_2^+ ion was produced *in situ* and so it is also possible that the second amine was also diazotised and decomposed with loss of N_2. Another tentative explanation is that already grafted aminophenyl groups were diazotised and lose N_2. All of these processes would lead to the small N signal as determined by XPS. It is clear from these findings that the composition of a binary mixed layer is not necessarily dominated by the most easily reduced diazonium ion. Hence, it is difficult to control the composition of binary mixed layers using electrografting from mixtures of two aryldiazonium ions. Moreover, formation of multilayers is expected in all of these studies.

Recently, Lagrost and co-workers[143] have reported on the preparation of binary mixed monolayers with controlled composition based on calix[4]arenes molecules. The rim of the calix[4]arenes can be prepared with up to four reactive arms (Scheme 1.6). Due to having a common scaffold, the reduction potentials of derivatives with the different reactive arms are very similar. Therefore the surface composition of the mixed layers can be controlled by tuning the molar ratio of the calix[4]arenes in the grafting solution.

An alternative method for preparation of mixed layers is via sequential grafting of two different aryldiazonium salts.[145-148] Lacroix and co-workers[148] prepared mixed layers using bulky groups as a spacer that can be subsequently removed to create free space for grafting of a second modifier (Scheme 1.11). Reduction of bithiophene benzenediazonium ion in the presence of cyclodextrin (β-CD) results in a layer consisting of grafted bithiophene phenyl

and adsorbed β-CD (step i). Removal of the bulky β-CD creates pinholes in the film (step ii). These pinholes can be used to graft a second modifier (step iii). The surface concentration of NP groups on the mixed layer was calculated to be between 1×10^{-10} and 2×10^{-10} mol cm^{-2} and similar thickness (~5 nm), was found by AFM for the bithiophene phenyl single component films and the mixed films, suggesting that the NP groups are predominately grafted to the free carbon surface. However, the film thickness measurement clearly indicates that the first grafting procedure resulted in a multilayer film.

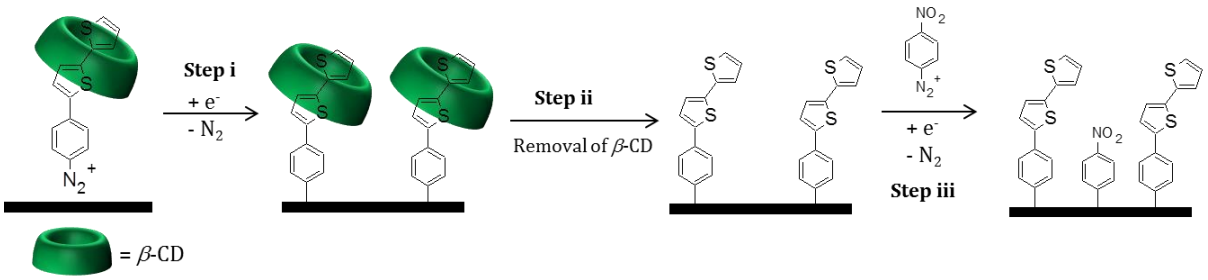

Scheme 1.11 Preparation of mixed film consisting of biothiophene phenyl and NP groups from sequential grafting of biothiophene benzenediazonium ion in the presence of β-CD followed by removal of β-CD and grafting of NBD. Adapted from reference 148.

Leroux and co-workers[147] have also prepared a mixed layer based on this strategy. Grafting a layer of TIPS-Eth-Ar followed by removal of the TIPS groups create pinholes for subsequent attachment of NP groups resulted in a mixed layer consisting of Eth-Ar and a multilayer of NP groups (Scheme 1.12). Their strategy is outlined in Chapter 4 and further studied and developed in this thesis work (Chapter 4, 5 and 6) with the aim of restricting the film to a monolayer.

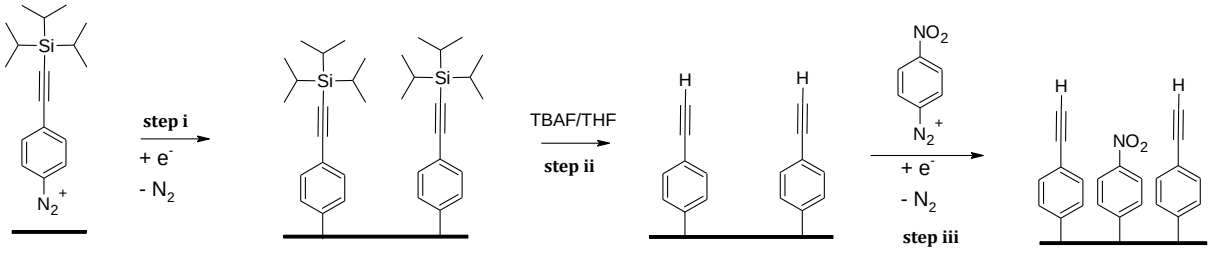

Scheme 1.12 Strategy for preparation of mixed film consist of Eth-Ar and NP groups based on the sequential grafting of two aryldiazonium ions.

1.3 Applications of Surface Modification via Reduction of Aryldiazonium Ions

A widely studied application of surface modification via reduction of aryldiazonium salts is the fabrication of biosensors and chemical sensors. As seen in Figure 1.3, a typical sensor consists of a signal transducer and recognition elements. In the case of biosensors, the recognition elements are biological species. Two different strategies have been used to covalently immobilise biological molecules on the surface via the use of aryldiazonium ions. In the first approach, the surface is modified with amine or carboxylic acid functionalities via reduction of aryldiazonium ion. The biological molecules are then covalently coupled to the surface via amide coupling, usually in the present of activating agents, such as 1-ethyl-3-(3-dimethylaminopropyl)carbodiimide hydrochloride (EDC) (Scheme 1.13).[87, 149-154] For example, enzyme cytochrome P450 2B4 (CYP450 2B4) has been immobilised onto screen printed carbon electrodes (SPCEs) for detection of phenobarbital, which is an anticonvulsant drug used to treat epilepsy.[150] Firstly, SPCEs were modified with NBD and the NP groups were subsequently reduced electrochemically to aminophenyl groups. The aminophenyl groups were then reacted with CYP450 2B4 in the presence of EDC and *N*-hydroxysuccinimide (NHS) to obtain the covalently immobilised CYP450 2B4. The sensor was then used to determine the concentration of phenobarbital in the pharmaceutical drug LUMINALETAS®. The concentration of phenobarbital was found to be (17.64 ± 2.87) mg, which was in agreement with the values given by the manufacturer (15 mg).[150] The authors also fabricated a similar biosensor based on a self-assemble monolayer of thiol molecules on gold screen printed electrodes (Au-SPEs). However, the modified Au-SPEs gave a low quality signal and were not further investigated.[150] The lower quality signal obtained from Au-SPEs than SPCEs may be due to the weaker Au–S bond than the C–C bond.

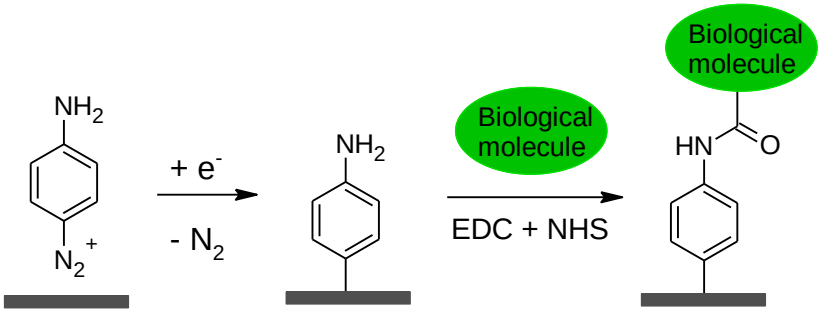

Scheme 1.13 Schematic representation of immobilisation of biological molecules via surface bound amine functionalities.

In the second approach, the biological molecules are first modified with aryldiazonium moieties prior to immobilisation on the surface (Scheme 1.14).[87, 154-160] For example, as shown in Scheme 1.15, biotinylated antibody was first functionalised with 4-carboxybenzenediazonium in the presence of EDC and NHS. The diazonium functionalised antibody was then electrogratfted onto Au and GC surfaces.[160] The deposited biotinylated antibody was reacted with streptavidin-labelled gold nanoparticles (Au-NPs) for detection by SEM (Scheme 1.15A). SEM images showed an increase in the number of Au-NPs as the number of electrografting cycles increased, reaching a maximum coverage after 10 CV cycles from 0 to -0.9 V at 100 mV s^{-1}. Comparison with the control samples, where non-biotinylated diazonium modified antibodies were used, indicated that the device is specific to the target antigen. Furthermore, to test the electrochemical performance of the biosensors, the biotinylated antibody was reacted with ExtrAvidin® horseradish peroxidase (HRP) (Scheme 1.15B). The HRP functionalised surface showed catalytic activity towards hydrogen peroxide reduction and hence electrode preparation by this approach is suitable for fabrication of electrochemical immunosensors.[160]

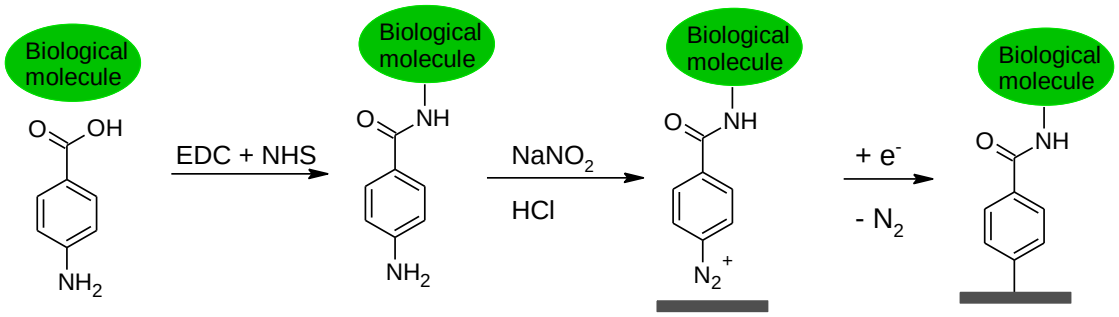

Scheme 1.14 Schematic representation of immobilisation of biological molecules via the use of biological molecules derivatised with aryldiazonium ion functionalities.

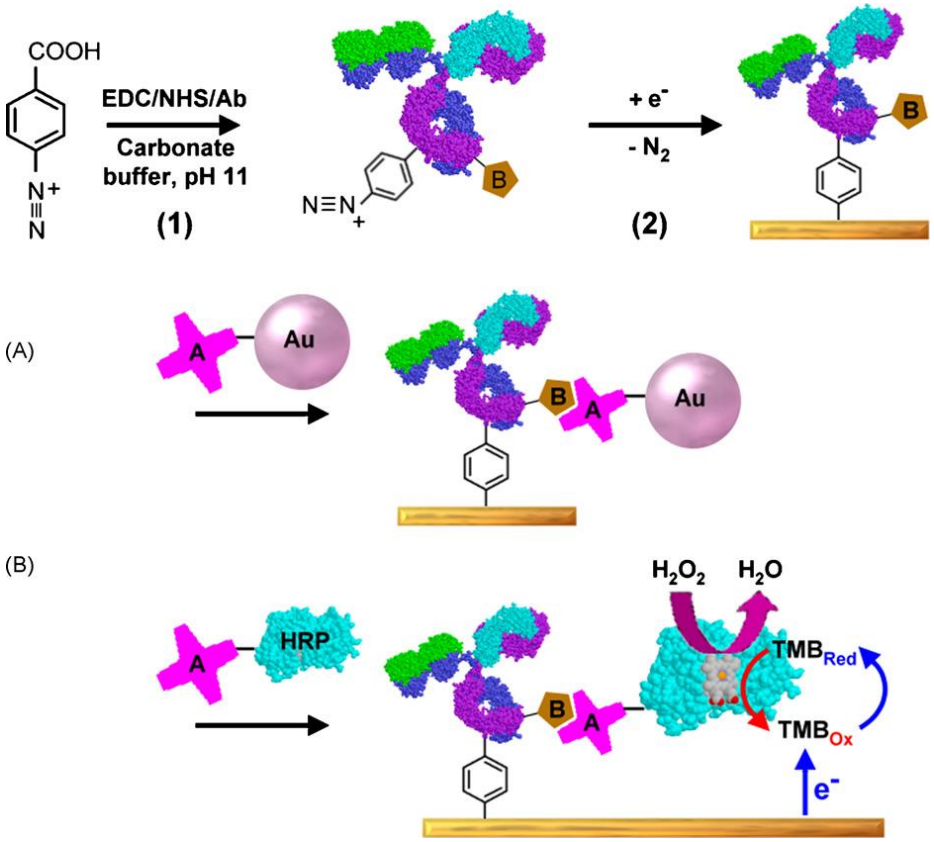

Scheme 1.15 Preparation of diazonium-modified antibody: (1) carboxyl diazonium is covalently attached to antibody by EDC/NHS coupling. (2) Diazonium-antibody is electrodeposited onto an electrode by cyclic voltammetry. (A) Attachment of streptavidin-Au NPs. (B) Attachment of ExtrAvidin-HRP and subsequent electrochemical analysis. TMB = 3,3′,5,5′-tetramethylbenzidine. Reproduced from reference 160.

Chemical sensors have been a less common target for diazonium ion modification. Electroreduction of quinone-containing diazonium ions have been used to prepare pH sensors.[161, 162] For example, a carbon fibre microelectrode grafted with a 4-benzoylamino-2,5-

dimethoxyphenyl moiety followed by electrochemical oxidation of the methoxy groups to quinone groups has been shown to be pH sensitive (Scheme 1.16).[161] As the pH increases, $E_{p,a}$ shifts to a more negative value and it was shown that the shift in potential is not affected by Na^+, Mg^{2+}, Ca^{2+} or K^+ ions. This electrode has been shown to be capable of measuring small pH changes associated with neurotransmitter release in the central nervous system of a mutant fly.[161]

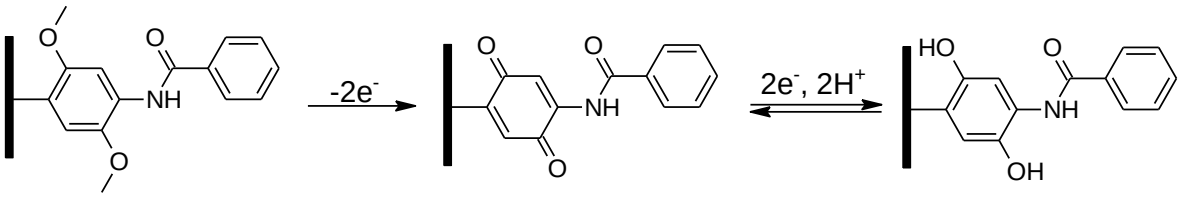

Scheme 1.16 Schematic showing the irreversible oxidation of methoxyphenyl moieties to quinone groups followed by the reversible reduction-oxidation of surface-bound quinone/hydroquinone groups.

SPCEs modified with carboxylic acid functionalities have been used to detect trace metals, including Cu^{2+},[163-165] Pb^{2+},[165, 166] and U^{6+}.[165, 167] This method is based on the accumulation of trace metals by the carboxylate layer due to the complexation ability of carboxylic groups towards metal ions in solution. The accumulated trace metals on the electrode surface are detected electrochemically. The limits of quantification for Cu^{2+}, Pb^{2+} and U^{6+} by electrodes modified with 4-carboxyphenyl groups were 10^{-8}, 5×10^{-9}, and 2×10^{-9} M, respectively.[164] It has also been shown that the detection limit can be improved by increasing the number of carboxylic acid functionalities.[165] For example, SPCEs modified with 4-carboxyphenyl have a Pb^{2+} detection limit of 10^{-9} M, while an electrode modified with 3,5-dicarboxyphenyl groups gave a detection limit of 10^{-10} M.[165]

Aryldiazonium salt grafting has also been applied industrially. For example, the fabrication of drug eluting stents (DESs) based on electrografting of aryldiazonium salts has been patented by Angiogene Inc.[168] A stent is a small mesh tube that is used to keep the coronary arteries

open for people who suffer from coronary heart disease. In a DES, the stent is coated with a drug that releases slowly upon implantation in the arteries to facilitate the healing process. Diazonium salts have been used to graft a hydrophobic layer onto the metallic stent surface to improve the adhesion of the lipophilic drug, which is passively adsorbed through hydrophobic interactions.[168] A subsequent paper described a similar modification procedure using 4(1-dodecyloxy)-phenyl diazonium tetrafluoroborate for the adhesion layer.[169] The diazonium salt was electrografted on stainless steel and CoCr stents followed by spray coating with polymer-drug solutions. The adhesion properties of the modified stents were compared with control samples, where the stent was spray coated with polymer-drug matrix directly onto the metal stents. It was found that the sample with the electrografted layer provided a better adhesion than the control sample (Figure 1.5).[169]

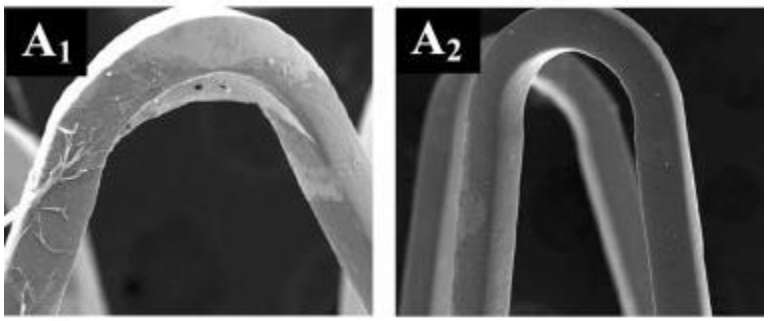

Figure 1.5 SEM images of polymer-drug coated stents following incubation under accelerated physiological conditions (0.1 M phosphate buffer, 0.3% sodium dodecyl sulphate (SDS), pH 7.4, 60 °C and 100 rpm). A_1 are controls and A_2 were electrografted prior to polymer-drug application. Adapted from reference 169.

Alchimedics has also patented the fabrication of a DES through the electrografting of aryldiazonium salts.[170] This process was based on a two-layer coating: a first polymeric layer is electrografted on the metallic stent from a mixture of aryldiazonium ion and monomer (butyl methacrylate) and a second biodegradable polymer-drug coating was then spray coated on top of the first layer.[170] This DES was trademarked as BuMA® stent and has been marketed by Sinomed Technologies Inc.[171] The process of fabricating the first polymeric

layer using a mixture of diazonium and vinylic compounds is patented by Alchimer.[172] A polymer layer prepared by electrografting is trademarked as *e*G™, and a polymer prepared from spontaneous grafting is trademarked as *c*G™.[173]

1.4 Aims

The aim of this thesis is to develop new tether monolayers using the protection-deprotection strategy and to prepare mixed monolayers using these newly developed tether monolayers. The thesis is organised as follows:

Chapter 2. *Experimental:* describes the syntheses, general experimental procedures and equipment that are relevant to this thesis.

Chapter 3. *Coupling reactions directly on glassy carbon:* describes the attachment of monolayer films directly on GC surfaces using amine and carboxylic acid derivatives. The resulting modified layers are characterised electrochemically.

Chapter 4. *Preparation of ethynyl terminated monolayers and mixed layers:* describes the use of TIPS-Eth-Ar-N_2^+ to form monolayers and mixed layers. Electrochemistry and AFM film thickness measurement are used to characterise the modified surfaces.

Chapter 5. *Preparation of carboxyphenyl monolayers and mixed layers:* describes the synthesis of 4-((9-H-fluoren-9-ylmethoxy)carbonyl)benzene-1-diazonium salt ([Fm-COO-Ar-N_2]BF_4) and the preparation of monolayers and mixed layers using this protected aryldiazonium salt. The modified surfaces are characterised using electrochemistry and AFM film thickness measurement.

Chapter 6. *Preparation of amine functionalised monolayer:* describes the synthesis of four amine protected diazonium salts: 4-(((*tert*-butoxy)carbonyl)amino)benzene-1-diazonium ([Boc-NH-Ar-N_2]BF_4), 4-(((*tert*-butoxy)carbonyl)aminomethyl)benzene-1- diazonium ([Boc-

NH-CH_2-Ar-N_2]BF_4), 4-(((9H-fluoren-9-ylmethoxy)carbonyl)amino) benzene-1-diazonium ([Fmoc-NH-Ar-N_2]BF_4), and 4-((((9H-fluoren-9-ylmethoxy)carbonyl) amino)methyl)benzene-1-dizonium ([Fmoc-NH-CH_2-Ar-N_2]BF_4). The four diazonium salts are electrografted and characterised by electrochemistry and AFM film thickness measurement. Surfaces modified with Fmoc-NH-CH_2-Ar groups are further characterised by XPS. Comparison of the reactivity of the aminophenyl and aminomethylphenyl layers towards amide coupling reactions, comparison of reactivity of ferrocene carboxylic acid and ferrocene acetic acid, and comparison of the use of Boc and Fmoc protecting groups are also described. Mixed layer preparation using Fmoc-NH-CH_2-Ar-N_2^+ is described.

Chapter 7. *Electroreduction of aryldiazonium salts at carbon electrodes: origin of two reduction peaks:* investigates the CVs obtained at carbon electrodes in ACN solutions of aryldiazonium ions in order to understand the origin of the often, but not always, observed two reduction peaks.

Chapter 8. *Conclusion:* describes the overall summary of this thesis work and suggestions for future work.

1.5 References

1 McCreery, R.L., Advanced carbon electrode materials for molecular electrochemistry. *Chem. Rev.*, **2008**, *108*, 2646.

2 Wildgoose, G.G., Abiman, P., Compton, R.G., Characterising chemical functionality on carbon surfaces. *J. Mater. Chem.*, **2009**, *19*, 4875.

3 Wildgoose, G.G., Banks, C.E., Leventis, H.C., Compton, R.G., Chemically modified carbon nanotubes for use in electroanalysis. *Microchim. Acta*, **2006**, *152*, 187.

4 Robinson, R.S., Sternitzke, K., McDermott, M.T., McCreery, R.L., Morphology and electrochemical effects of defects on highly oriented pyrolytic-graphite. *J. Electrochem. Soc.*, **1991**, *138*, 2412.

5 Banks, C.E., Davies, T.J., Wildgoose, G.G., Compton, R.G., Electrocatalysis at graphite and carbon nanotube modified electrodes: Edge-plane sites and tube ends are the reactive sites. *Chem. Commun.*, **2005**, 829.

6 Bowling, R.J., Packard, R.T., McCreery, R.L., Activation of highly ordered pyrolytic-graphite for heterogeneous electron-transfer - relationship between electrochemical performance and carbon microstructure. *J. Am. Chem. Soc.*, **1989**, *111*, 1217.

7 Davies, T.J., Hyde, M.E., Compton, R.G., Nanotrench arrays reveal insight into graphite electrochemistry. *Angew. Chem. Int. Edit.*, **2005**, *44*, 5121.

8 Kneten, K.R., McCreery, R.L., Effects of redox system structure on electron-transfer kinetics at ordered graphite and glassy-carbon electrodes. *Anal. Chem.*, **1992**, *64*, 2518.

9 McDermott, M.T., Kneten, K., McCreery, R.L., Anthraquinonedisulfonate adsorption, electron-transfer kinetics, and capacitance on ordered graphite-electrodes - the important role of surface-defects. *J. Phys. Chem.*, **1992**, *96*, 3124.

10 Cline, K.K., McDermott, M.T., McCreery, R.L., Anomalously slow-electron transfer at ordered graphite-electrodes - influence of electronic factors and reactive sites. *J. Phys. Chem.*, **1994**, *98*, 5314.

11 Royea, W.J., Hamann, T.W., Brunschwig, B.S., Lewis, N.S., A comparison between interfacial electron-transfer rate constants at metallic and graphite electrodes. *J. Phys. Chem. B*, **2006**, *110*, 19433.

12 McCreery, R.L., McDermott, M.T., Comment on electrochemical kinetics at ordered graphite electrodes. *Anal. Chem.*, **2012**, *84*, 2602.

13 Ratinac, K.R., Yang, W.R., Gooding, J.J., Thordarson, P., Braet, F., Graphene and related materials in electrochemical sensing. *Electroanal.*, **2011**, *23*, 803.

14 Dumitrescu, I., Dudin, P.V., Edgeworth, J.P., Macpherson, J.V., Unwin, P.R., Electron transfer kinetics at single-walled carbon nanotube electrodes using scanning electrochemical microscopy. *J. Phys. Chem. C*, **2010**, *114*, 2633.

15 Dumitrescu, I., Unwin, P.R., Wilson, N.R., Macpherson, J.V., Single-walled carbon nanotube network ultramicroelectrodes. *Anal. Chem.*, **2008**, *80*, 3598.

16 Edwards, M.A., Bertoncello, P., Unwin, P.R., Slow diffusion reveals the intrinsic electrochemical activity of basal plane highly oriented pyrolytic graphite electrodes. *J. Phys. Chem. C*, **2009**, *113*, 9218.

17 Lai, S.C.S., Patel, A.N., McKelvey, K., Unwin, P.R., Definitive evidence for fast electron transfer at pristine basal plane graphite from high-resolution electrochemical imaging. *Angew. Chem. Int. Edit.*, **2012**, *51*, 5405.

18 Patel, A.N., Collignon, M.G., O'Connell, M.A., Hung, W.O.Y., McKelvey, K., Macpherson, J.V., Unwin, P.R., A new view of electrochemistry at highly oriented pyrolytic graphite. *J. Am. Chem. Soc.*, **2012**, *134*, 20117.

19 Williams, C.G., Edwards, M.A., Colley, A.L., Macpherson, J.V., Unwin, P.R., Scanning micropipet contact method for high-resolution imaging of electrode surface redox activity. *Anal. Chem.*, **2009**, *81*, 2486.

20 Zhang, G.H., Kirkman, P.M., Patel, A.N., Cuharuc, A.S., McKelvey, K., Unwin, P.R., Molecular functionalization of graphite surfaces: Basal plane versus step edge electrochemical activity. *J. Am. Chem. Soc.*, **2014**, *136*, 11444.

21 Harris, P.J.F., Fullerene-related structure of commercial glassy carbons. *Philos. Mag.*, **2004**, *84*, 3159.

22 Jenkins, G.M., Kawamura, K., Structure of glassy carbon. *Nature*, **1971**, *231*, 175.

23 Jenkins, G.M., Kawamura, K., Ban, L.L., Formation and structure of polymeric carbons. *P. Roy. Soc. Lond. A. Mat.*, **1972**, *327*, 501.

24 Pesin, L.A., Structure and properties of glass-like carbon. *J. Mater. Sci.*, **2002**, *37*, 1.

25 Pesin, L.A., Baitinger, E.M., A new structural model of glass-like carbon. *Carbon*, **2002**, *40*, 295.

26 Enoki, T., Kobayashi, Y., Fukui, K.I., Electronic structures of graphene edges and nanographene. *Int. Rev. Phys. Chem.*, **2007**, *26*, 609.

27 Brown, N.M.D., You, H.X., Surface-structure of a glassy-carbon - scanning tunneling microscopy study. *J. Mater. Chem.*, **1991**, *1*, 469.

28 Harris, P.J.F., New perspectives on the structure of graphitic carbons. *Crit. Rev. Solid State*, **2005**, *30*, 235.

29 Fryling, M.A., Zhao, J., McCreery, R.L., Resonance Raman observation of surface carbonyl groups on carbon electrodes following dinitrophenylhydrazine derivatization. *Anal. Chem.*, **1995**, *67*, 967.

30 Ray, K., McCreery, R.L., Spatially resolved Raman spectroscopy of carbon electrode surfaces: Observations of structural and chemical heterogeneity. *Anal. Chem.*, **1997**, *69*, 4680.

31 Ray, K.R., McCreery, R.L., Characterization of the surface carbonyl and hydroxyl coverage on glassy carbon electrodes using Raman spectroscopy. *J. Electroanal. Chem.*, **1999**, *469*, 150.

32 Kiema, G.K., Aktay, M., McDermott, M.T., Preparation of reproducible glassy carbon electrodes by removal of polishing impurities. *J. Electroanal. Chem.*, **2003**, *540*, 7.

33 Engstrom, R.C., Strasser, V.A., Characterization of electrochemically pretreated glassy-carbon electrodes. *Anal. Chem.*, **1984**, *56*, 136.

34 Cabaniss, G.E., Diamantis, A.A., Murphy, W.R., Linton, R.W., Meyer, T.J., Electrocatalysis of proton-coupled electron-transfer reactions at glassy-carbon electrodes. *J. Am. Chem. Soc.*, **1985**, *107*, 1845.

35 Sundberg, K.M., Smyrl, W.H., Atanasoska, L., Atanasoski, R., Surface modification and oxygen reduction on glassy-carbon in chloride media. *J. Electrochem. Soc.*, **1989**, *136*, 434.

36 Kamau, G.N., Willis, W.S., Rusling, J.F., Electrochemical and electron spectroscopic studies of highly polished glassy-carbon electrodes. *Anal. Chem.*, **1985**, *57*, 545.

37 Tougas, T.P., Collier, W.G., Determination of surface carbonyl groups on glassy-carbon with X-ray photoelectron-spectroscopy preceded by derivatization with pentafluorophenylhydrazine. *Anal. Chem.*, **1987**, *59*, 2269.

38 Collier, W.G., Tougas, T.P., Determination of surface hydroxyl-groups on glassy-carbon with X-ray photoelectron-spectroscopy preceded by chemical derivatization. *Anal. Chem.*, **1987**, *59*, 396.

39 Rusling, J.F., Variations in electron-transfer rate at polished glassy-carbon electrodes exposed to air. *Anal. Chem.*, **1984**, *56*, 575.

40 Elliott, C.M., Murray, R.W., Chemically modified carbon electrodes. *Anal. Chem.*, **1976**, *48*, 1247.

41 Chen, P.H., McCreery, R.L., Control of electron transfer kinetics at glassy carbon electrodes by specific surface modification. *Anal. Chem.*, **1996**, *68*, 3958.

42 Engstrom, R.C., Electrochemical pretreatment of glassy-carbon electrodes. *Anal. Chem.*, **1982**, *54*, 2310.

43 Kepley, L.J., Bard, A.J., Ellipsometric, electrochemical, and elemental characterization of the surface phase produced on glassy-carbon electrodes by electrochemical activation. *Anal. Chem.*, **1988**, *60*, 1459.

44 McDermott, C.A., Kneten, K.R., McCreery, R.L., Electron-transfer kinetics of aquated $Fe^{+3/+2}$, $Eu^{+3/+2}$, and $V^{+3/+2}$ at carbon electrodes - inner-sphere catalysis by surface oxides. *J. Electrochem. Soc.*, **1993**, *140*, 2593.

45 Zhao, Q.L., Zhang, Z.L., Bao, L., Pang, D.W., Surface structure-related electrochemical behaviors of glassy carbon electrodes. *Electrochem. Commun.*, **2008**, *10*, 181.

46 Barbero, C., Kotz, R., Electrochemical activation of glassy-carbon - spectroscopic ellipsometry of surface phase formation. *J. Electrochem. Soc.*, **1993**, *140*, 1.

47 Blaedel, W.J., Jenkins, R.A., Study of electrochemical oxidation of reduced nicotinamide adenine-dinucleotide. *Anal. Chem.*, **1975**, *47*, 1337.

48 DuVall, S.H., McCreery, R.L., Control of catechol and hydroquinone electron-transfer kinetics on native and modified glassy carbon electrodes. *Anal. Chem.*, **1999**, *71*, 4594.

49 Fagan, D.T., Hu, I.F., Kuwana, T., Vacuum heat-treatment for activation of glassy-carbon electrodes. *Anal. Chem.*, **1985**, *57*, 2759.

50 Hance, G.W., Kuwana, T., Effect of glassy-carbon pretreatment on background double-layer capacitance and adsorption of neutral organic-molecules. *Anal. Chem.*, **1987**, *59*, 131.

51 Stutts, K.J., Kovach, P.M., Kuhr, W.G., Wightman, R.M., Enhanced electrochemical reversibility at heat-treated glassy-carbon electrodes. *Anal. Chem.*, **1983**, *55*, 1632.

52 Evans, J.F., Kuwana, T., Introduction of functional-groups onto carbon electrodes via treatment with radio-frequency plasmas. *Anal. Chem.*, **1979**, *51*, 358.

53 Miller, C.W., Karweik, D.H., Kuwana, T., Scanning electron-microscopic and X-ray photo-electron spectroscopic examination of Tokai glassy-carbon surfaces subjected to radio-frequency plasmas. *Anal. Chem.*, **1981**, *53*, 2319.

54 Pontikos, N.M., McCreery, R.L., Microstructural and morphological-changes induced in glassy-carbon electrodes by laser irradiation. *J. Electroanal. Chem.*, **1992**, *324*, 229.

55 Poon, M., McCreery, R.L., Insitu laser activation of glassy-carbon electrodes. *Anal. Chem.*, **1986**, *58*, 2745.

56 Poon, M., McCreery, R.L., Repetitive insitu renewal and activation of carbon and platinum-electrodes - applications to pulse voltammetry. *Anal. Chem.*, **1987**, *59*, 1615.

57 Poon, M., McCreery, R.L., Engstrom, R., Laser activation of carbon electrodes - relationship between laser-induced surface effects and electron-transfer activation. *Anal. Chem.*, **1988**, *60*, 1725.

58 Rice, R.J., Pontikos, N.M., McCreery, R.L., Quantitative correlations of heterogeneous electron-transfer kinetics with surface-properties of glassy-carbon electrodes. *J. Am. Chem. Soc.*, **1990**, *112*, 4617.

59 DuVall, S.H., McCreery, R.L., Self-catalysis by catechols and quinones during heterogeneous electron transfer at carbon electrodes. *J. Am. Chem. Soc.*, **2000**, *122*, 6759.

60 Kazee, B., Weisshaar, D.E., Kuwana, T., Evidence for the presence of a thin carbon-particle layer on polished glassy-carbon electrodes. *Anal. Chem.*, **1985**, *57*, 2736.

61 Weisshaar, D.E., Kuwana, T., Considerations for polishing glassy-carbon to a scratch-free finish. *Anal. Chem.*, **1985**, *57*, 378.

62 Chang, H.P., Bard, A.J., Observation and characterization by scanning tunneling microscopy of structures generated by cleaving highly oriented pyrolytic-graphite. *Langmuir*, **1991**, *7*, 1143.

63 Lyons, A.M., Photodefinable carbon-films - electrical-properties. *J. Non-Cryst. Solids*, **1985**, *70*, 99.

64 Lyons, A.M., Hale, L.P., Wilkins, C.W., Photodefinable carbon-films - control of image quality. *J. Vac. Sci. Technol. B*, **1985**, *3*, 447.

65 Schueller, O.J.A., Brittain, S.T., Marzolin, C., Whitesides, G.M., Fabrication and characterization of glassy carbon MEMS. *Chem. Mater.*, **1997**, *9*, 1399.

66 Kim, J., Song, X., Kinoshita, K., Madou, M., White, B., Electrochemical studies of carbon films from pyrolyzed photoresist. *J. Electrochem. Soc.*, **1998**, *145*, 2314.

67 Kostecki, R., Schnyder, B., Alliata, D., Song, X., Kinoshita, K., Kotz, R., Surface studies of carbon films from pyrolyzed photoresist. *Thin Solid Films*, **2001**, *396*, 36.

68 Ranganathan, S., McCreery, R., Majji, S.M., Madou, M., Photoresist-derived carbon for microelectromechanical systems and electrochemical applications. *J. Electrochem. Soc.*, **2000**, *147*, 277.

69 Ranganathan, S., McCreery, R.L., Electroanalytical performance of carbon films with near-atomic flatness. *Anal. Chem.*, **2001**, *73*, 893.

70 McDermott, M.T., McDermott, C.A., McCreery, R.L., Scanning tunneling microscopy of carbon surfaces - relationships between electrode-kinetics, capacitance, and morphology for glassy-carbon electrodes. *Anal. Chem.*, **1993**, *65*, 937.

71 Delamar, M., Hitmi, R., Pinson, J., Saveant, J.M., Covalent modification of carbon surfaces by grafting of functionalized aryl radicals produced from electrochemical reduction of diazonium salts. *J. Am. Chem. Soc.*, **1992**, *114*, 5883.

72 Pinson, J., Podvorica, F., Attachment of organic layers to conductive or semiconductive surfaces by reduction of diazonium salts. *Chem. Soc. Rev.*, **2005**, *34*, 429.

73 Belanger, D., Pinson, J., Electrografting: A powerful method for surface modification. *Chem. Soc. Rev.*, **2011**, *40*, 3995.

74 Downard, A.J., Electrochemically assisted covalent modification of carbon electrodes. *Electroanal.*, **2000**, *12*, 1085.

75 Adenier, A., Cabet-Deliry, E., Chausse, A., Griveau, S., Mercier, F., Pinson, J., Vautrin-Ul, C., Grafting of nitrophenyl groups on carbon and metallic surfaces without electrochemical induction. *Chem. Mater.*, **2005**, *17*, 491.

76 Barriere, F., Downard, A.J., Covalent modification of graphitic carbon substrates by non-electrochemical methods. *J. Solid State Electr.*, **2008**, *12*, 1231.

77 Abiman, P., Wildgoose, G.G., Compton, R.G., A mechanistic investigation into the covalent chemical derivatisation of graphite and glassy carbon surfaces using aryldiazonium salts. *J. Phys. Org. Chem.*, **2008**, *21*, 433.

78 Masheter, A.T., Wildgoose, G.G., Crossley, A., Jones, J.H., Compton, R.G., A facile method of modifying graphite powder with aminophenyl groups in bulk quantities. *J. Mater. Chem.*, **2007**, *17*, 3008.

79 Simons, B.M., Lehr, J., Garrett, D.J., Downard, A.J., Formation of thick aminophenyl films from aminobenzenediazonium ion in the absence of a reduction source. *Langmuir*, **2014**, *30*, 4989.

80 Mevellec, V., Roussel, S., Tessier, L., Chancolon, J., Mayne-L'Hermite, M., Deniau, G., Viel, P., Palacin, S., Grafting polymers on surfaces: A new powerful and versatile diazonium salt-based one-step process in aqueous media. *Chem. Mater.*, **2007**, *19*, 6323.

81 Mesnage, A., Esnouf, S., Jegou, P., Deniau, G., Palacin, S., Understanding the redox-induced polymer grafting process: A dual surface-solution analysis. *Chem. Mater.*, **2010**, *22*, 6229.

82 Derouich, S.G., Rinfray, C., Izzet, G., Pinson, J., Gallet, J.J., Kanoufi, F., Proust, A., Combellas, C., Control of the grafting of hybrid polyoxometalates on metal and carbon surfaces: Toward submonolayers. *Langmuir*, **2014**, *30*, 2287.

83 Bouriga, M., Chehimi, M.M., Combellas, C., Decorse, P., Kanoufi, F., Deronzier, A., Pinson, J., Sensitized photografting of diazonium salts by visible light. *Chem. Mater.*, **2013**, *25*, 90.

84 Busson, M., Berisha, A., Combellas, C., Kanoufi, F., Pinson, J., Photochemical grafting of diazonium salts on metals. *Chem. Commun.*, **2011**, *47*, 12631.

85 Allongue, P., Delamar, M., Desbat, B., Fagebaume, O., Hitmi, R., Pinson, J., Saveant, J.M., Covalent modification of carbon surfaces by aryl radicals generated from the electrochemical reduction of diazonium salts. *J. Am. Chem. Soc.*, **1997**, *119*, 201.

86 Mahouche-Chergui, S., Gam-Derouich, S., Mangeney, C., Chehimi, M.M., Aryl diazonium salts: A new class of coupling agents for bonding polymers, biomacromolecules and nanoparticles to surfaces. *Chem. Soc. Rev.*, **2011**, *40*, 4143.

87 Gooding, J.J., Advances in interfacial design sensors: Aryl diazonium salts for electrochemical biosensors and for modifying carbon and metal electrodes. *Electroanal.*, **2008**, *20*, 573.

88 Gooding, J.J., Ciampi, S., The molecular level modification of surfaces: From self-assembled monolayers to complex molecular assemblies. *Chem. Soc. Rev.*, **2011**, *40*, 2704.

89 Baranton, S., Belanger, D., Electrochemical derivatization of carbon surface by reduction of in situ generated diazonium cations. *J. Phys. Chem. B*, **2005**, *109*, 24401.

90 Baranton, S., Belanger, D., In situ generation of diazonium cations in organic electrolyte for electrochemical modification of electrode surface. *Electrochim. Acta*, **2008**, *53*, 6961.

91 Doppelt, P., Hallais, G., Pinson, J., Podvorica, F., Verneyre, S., Surface modification of conducting substrates. Existence of azo bonds in the structure of organic layers obtained from diazonium salts. *Chem. Mater.*, **2007**, *19*, 4570.

92 Menanteau, T., Levillain, E., Breton, T., Spontaneous grafting of nitrophenyl groups on carbon: Effect of radical scavenger on organic layer formation. *Langmuir*, **2014**, *30*, 7913.

93 Mesnage, A., Lefevre, X., Jegou, P., Deniau, G., Palacin, S., Spontaneous grafting of diazonium salts: Chemical mechanism on metallic surfaces. *Langmuir*, **2012**, *28*, 11776.

94 Combellas, C., Kanoufi, F., Pinson, J., Podvorica, F.I., Time-of-flight secondary ion mass spectroscopy characterization of the covalent bonding between a carbon surface and aryl groups. *Langmuir*, **2005**, *21*, 280.

95 Toupin, M., Belanger, D., Thermal stability study of aryl modified carbon black by in situ generated diazonium salt. *J. Phys. Chem. C*, **2007**, *111*, 5394.

96 Abiman, P., Wildgoose, G.G., Compton, R.G., Investigating the mechanism for the covalent chemical modification of multiwalled carbon nanotubes using aryl diazonium salts. *Int. J. Electrochem. Sci.*, **2008**, *3*, 104.

97 Lehr, J., Williamson, B.E., Downard, A.J., Spontaneous grafting of nitrophenyl groups to planar glassy carbon substrates: Evidence for two mechanisms. *J. Phys. Chem. C*, **2011**, *115*, 6629.

98 Galli, C., Radical reactions of arenediazonium ions - an easy entry into the chemistry of the aryl radical. *Chem. Rev.*, **1988**, *88*, 765.

99 Bernard, M.C., Chausse, A., Cabet-Deliry, E., Chehimi, M.M., Pinson, J., Podvorica, F., Vautrin-Ul, C., Organic layers bonded to industrial, coinage, and noble metals through electrochemical reduction of aryldiazonium salts. *Chem. Mater.*, **2003**, *15*, 3450.

100 Boukerma, K., Chehimi, M.M., Pinson, J., Blomfield, C., X-ray photoelectron spectroscopy evidence for the covalent bond between an iron surface and aryl groups attached by the electrochemical reduction of diazonium salts. *Langmuir*, **2003**, *19*, 6333.

101 Chausse, A., Chehimi, M.M., Karsi, N., Pinson, J., Podvorica, F., Vautrin-Ul, C., The electrochemical reduction of diazonium salts on iron electrodes. The formation of covalently bonded organic layers and their effect on corrosion. *Chem. Mater.*, **2002**, *14*, 392.

102 Delamar, M., Desarmot, G., Fagebaume, O., Hitmi, R., Pinson, J., Saveant, J.M., Modification of carbon fiber surfaces by electrochemical reduction of aryl diazonium salts: Application to carbon epoxy composites. *Carbon*, **1997**, *35*, 801.

103 deVilleneuve, C.H., Pinson, J., Bernard, M.C., Allongue, P., Electrochemical formation of close-packed phenyl layers on Si(111). *J. Phys. Chem. B*, **1997**, *101*, 2415.

104 Hurley, B.L., McCreery, R.L., Covalent bonding of organic molecules to Cu and Al alloy 2024 T3 surfaces via diazonium ion reduction. *J. Electrochem. Soc.*, **2004**, *151*, B252.

105 Itoh, T., McCreery, R.L., In situ Raman spectroelectrochemistry of electron transfer between glassy carbon and a chemisorbed nitroazobenzene monolayer. *J. Am. Chem. Soc.*, **2002**, *124*, 10894.

106 Laforgue, A., Addou, T., Belanger, D., Characterization of the deposition of organic molecules at the surface of gold by the electrochemical reduction of aryldiazonium cations. *Langmuir*, **2005**, *21*, 6855.

107 Laurentius, L., Stoyanov, S.R., Gusarov, S., Kovalenko, A., Du, R.B., Lopinski, G.P., McDermott, M.T., Diazonium-derived aryl films on gold nanoparticles: Evidence for a carbon-gold covalent bond. *ACS Nano*, **2011**, *5*, 4219.

108 Atmane, Y.A., Sicard, L., Lamouri, A., Pinson, J., Sicard, M., Masson, C., Nowak, S., Decorse, P., Piquemal, J.Y., Galtayries, A., Mangeney, C., Functionalization of aluminum nanoparticles using a combination of aryl diazonium salt chemistry and iniferter method. *J. Phys. Chem. C*, **2013**, *117*, 26000.

109 Bell, K.J., Brooksby, P.A., Polson, M.I.J., Downard, A.J., Evidence for covalent bonding of aryl groups to MnO_2 nanorods from diazonium-based grafting. *Chem. Commun.*, **2014**, *50*, 13687.

110 Cui, B., Gu, J.Y., Chen, T., Yan, H.J., Wang, D., Wan, L.J., Solution effect on diazonium-modified Au(111): Reactions and structures. *Langmuir*, **2013**, *29*, 2955.

111 Jayasundara, D.R., Cullen, R.J., Colavita, P.E., In situ and real time characterization of spontaneous grafting of aryldiazonium salts at carbon surfaces. *Chem. Mater.*, **2013**, *25*, 1144.

112 Lehr, J., Williamson, B.E., Flavel, B.S., Downard, A.J., Reaction of gold substrates with diazonium salts in acidic solution at open-circuit potential. *Langmuir*, **2009**, *25*, 13503.

113 Ma, H.F., Lee, L., Brooksby, P.A., Brown, S.A., Fraser, S.J., Gordon, K.C., Leroux, Y.R., Hapiot, P., Downard, A.J., Scanning tunneling and atomic force microscopy evidence for covalent and noncovalent interactions between aryl films and highly ordered pyrolytic graphite. *J. Phys. Chem. C*, **2014**, *118*, 5820.

114 Brooksby, P.A., Downard, A.J., Electrochemical and atomic force microscopy study of carbon surface modification via diazonium reduction in aqueous and acetonitrile solutions. *Langmuir*, **2004**, *20*, 5038.

115 Fontaine, O., Ghilane, J., Martin, P., Lacroix, J.C., Randriamahazaka, H., Ionic liquid viscosity effects on the functionalization of electrode material through the electroreduction of diazonium. *Langmuir*, **2010**, *26*, 18542.

116 Ghilane, J., Martin, P., Fontaine, O., Lacroix, J.C., Randriamahazaka, H., Modification of carbon electrode in ionic liquid through the reduction of phenyl diazonium salt. Electrochemical evidence in ionic liquid. *Electrochem. Commun.*, **2008**, *10*, 1060.

117 Ronkainen, N.J., Halsall, H.B., Heineman, W.R., Electrochemical biosensors. *Chem. Soc. Rev.*, **2010**, *39*, 1747.

118 Menanteau, T., Levillain, E., Breton, T., Electrografting via diazonium chemistry: From multilayer to monolayer using radical scavenger. *Chem. Mater.*, **2013**, *25*, 2905.

119 Li, Q., Batchelor-McAuley, C., Lawrence, N.S., Hartshorne, R.S., Compton, R.G., The synthesis and characterisation of controlled thin sub-monolayer films of 2-anthraquinonyl groups on graphite surfaces. *New J. Chem.*, **2011**, *35*, 2462.

120 Kano, K., Uno, B., Surface-redox reaction-mechanism of quinones adsorbed on basal-planepyrolytic graphite-electrodes. *Anal. Chem.*, **1993**, *65*, 1088.

121 McDermott, M.T., McCreery, R.L., Scanning-tunneling-microscopy of ordered graphite and glassy-carbon surfaces - electronic control of quinone adsorption. *Langmuir*, **1994**, *10*, 4307.

122 Combellas, C., Kanoufi, F., Pinson, J., Podvorica, F.I., Sterically hindered diazonium salts for the grafting of a monolayer on metals. *J. Am. Chem. Soc.*, **2008**, *130*, 8576.

123 Mattiuzzi, A., Jabin, I., Mangeney, C., Roux, C., Reinaud, O., Santos, L., Bergamini, J.F., Hapiot, P., Lagrost, C., Electrografting of calix[4]arenediazonium salts to form versatile robust platforms for spatially controlled surface functionalization. *Nat. Commun.*, **2012**, *3*.

124 Nielsen, L.T., Vase, K.H., Dong, M.D., Besenbacher, F., Pedersen, S.U., Daasbjerg, K., Electrochemical approach for constructing a monolayer of thiophenolates from grafted multilayers of diaryl disulfides. *J. Am. Chem. Soc.*, **2007**, *129*, 1888.

125 Peng, Z.Q., Holm, A.H., Nielsen, L.T., Pedersen, S.U., Daasbjerg, K., Covalent sidewall functionalization of carbon nanotubes by a "formation-degradation" approach. *Chem. Mater.*, **2008**, *20*, 6068.

126 Malmos, K., Dong, M.D., Pillai, S., Kingshott, P., Besenbacher, F., Pedersen, S.U., Daasbjerg, K., Using a hydrazone-protected benzenediazonium salt to introduce a near-monolayer of benzaldehyde on glassy carbon surfaces. *J. Am. Chem. Soc.*, **2009**, *131*, 4928.

127 Chretien, J.M., Ghanem, M.A., Bartlett, P.N., Kilburn, J.D., Covalent tethering of organic functionality to the surface of glassy carbon electrodes by using electrochemical and solid-phase synthesis methodologies. *Chem.-Eur. J.*, **2008**, *14*, 2548.

128 Ghanem, M.A., Chretien, J.M., Kilburn, J.D., Bartlett, P.N., Electrochemical and solid-phase synthetic modification of glassy carbon electrodes with dihydroxybenzene compounds and the electrocatalytic oxidation of NADH. *Bioelectrochemistry*, **2009**, *76*, 115.

129 Kocak, I., Ghanem, M.A., Al-Mayouf, A., Alhoshan, M., Bartlett, P.N., A study of the modification of glassy carbon and edge and basal plane highly oriented pyrolytic graphite electrodes modified with anthraquinone using diazonium coupling and solid phase synthesis and their use for oxygen reduction. *J. Electroanal. Chem.*, **2013**, *706*, 25.

130 Pinczewska, A., Sosna, M., Bloodworth, S., Kilburn, J.D., Bartlett, P.N., High-throughput synthesis and electrochemical screening of a library of modified electrodes for NADH oxidation. *J. Am. Chem. Soc.*, **2012**, *134*, 18022.

131 Sosna, M., Chretien, J.M., Kilburn, J.D., Bartlett, P.N., Monolayer anthracene and anthraquinone modified electrodes as platforms for *Trametes hirsuta* laccase immobilisation. *Phys. Chem. Chem. Phys.*, **2010**, *12*, 10018.

132 Leroux, Y.R., Fei, H., Noel, J.M., Roux, C., Hapiot, P., Efficient covalent modification of a carbon surface: Use of a silyl protecting group to form an active monolayer. *J. Am. Chem. Soc.*, **2010**, *132*, 14039.

133 Leroux, Y.R., Hapiot, P., Nanostructured monolayers on carbon substrates prepared by electrografting of protected aryldiazonium salts. *Chem. Mater.*, **2013**, *25*, 489.

134 Gietter, A.A.S., Pupillo, R.C., Yap, G.P.A., Beebe, T.P., Rosenthal, J., Watson, D.A., On-surface cross-coupling methods for the construction of modified electrode assemblies with tailored morphologies. *Chem. Sci.*, **2013**, *4*, 437.

135 Barfidokht, A., Gooding, J.J., Approaches toward allowing electroanalytical devices to be used in biological fluids. *Electroanal.*, **2014**, *26*, 1182.

136 Liu, G.Z., Paddon-Row, M.N., Gooding, J.J., Protein modulation of electrochemical signals: Application to immunobiosensing. *Chem. Commun.*, **2008**, 3870.

137 Liu, G., Gooding, J.J., An interface comprising molecular wires and poly(ethylene glycol) spacer units self-assembled on carbon electrodes for studies of protein electrochemistry. *Langmuir*, **2006**, *22*, 7421.

138 Gui, A.L., Yau, H.M., Thomas, D.S., Chockalingam, M., Harper, J.B., Gooding, J.J., Using supramolecular binding motifs to provide precise control over the ratio and distribution of species in multiple component films grafted on surfaces: Demonstration using electrochemical assembly from aryl diazonium salts. *Langmuir*, **2013**, *29*, 4772.

139 Liu, G.Z., Chockalingham, M., Khor, S.M., Gui, A.L., Gooding, J.J., A comparative study of the modification of gold and glassy carbon surfaces with mixed layers of in situ generated aryl diazonium compounds. *Electroanal.*, **2010**, *22*, 918.

140 Liu, G.Z., Liu, J.Q., Bocking, T., Eggers, P.K., Gooding, J.J., The modification of glassy carbon and gold electrodes with aryl diazonium salt: The impact of the electrode materials on the rate of heterogeneous electron transfer. *Chem. Phys.*, **2005**, *319*, 136.

141 Liu, G.Z., Paddon-Row, M.N., Gooding, J.J., A molecular wire modified glassy carbon electrode for achieving direct electron transfer to native glucose oxidase. *Electrochem. Commun.*, **2007**, *9*, 2218.

142 Louault, C., D'Amours, M., Belanger, D., The electrochemical grafting of a mixture of substituted phenyl groups at a glassy carbon electrode surface. *Chemphyschem*, **2008**, *9*, 1164.

143 Santos, L., Mattiuzzi, A., Jabin, I., Vandencasteele, N., Reniers, F., Reinaud, O., Hapiot, P., Lhenry, S., Leroux, Y., Lagrost, C., One-pot electrografting of mixed monolayers with controlled composition. *J. Phys. Chem. C*, **2014**, *118*, 15919.

144 Vila, N., Belanger, D., Mixtures of functionalized aromatic groups generated from diazonium chemistry as templates towards bimetallic species supported on carbon electrode surfaces. *Electrochim. Acta*, **2012**, *85*, 538.

145 Harper, J.C., Polsky, R., Wheeler, D.R., Lopez, D.M., Arango, D.C., Brozik, S.M., A multifunctional thin film Au electrode surface formed by consecutive electrochemical reduction of aryl diazonium salts. *Langmuir*, **2009**, *25*, 3282.

146 Lee, L., Brooksby, P.A., Leroux, Y.R., Hapiot, P., Downard, A.J., Mixed monolayer organic films via sequential electrografting from aryldiazonium ion and arylhydrazine solutions. *Langmuir*, **2013**, *29*, 3133.

147 Leroux, Y.R., Hui, F., Noel, J.M., Roux, C., Downard, A.J., Hapiot, P., Design of robust binary film onto carbon surface using diazonium electrochemistry. *Langmuir*, **2011**, *27*, 11222.

148 Santos, L., Ghilane, J., Lacroix, J.C., Formation of mixed organic layers by stepwise electrochemical reduction of diazonium compounds. *J. Am. Chem. Soc.*, **2012**, *134*, 5476.

149 Alonso-Lomillo, M.A., Dominguez-Renedo, O., Hernandez-Martin, A., Arcos-Martinez, M.J., Horseradish peroxidase covalent grafting onto screen-printed carbon electrodes for levetiracetam chronoamperometric determination. *Anal. Biochem.*, **2009**, *395*, 86.

150 Alonso-Lomillo, M.A., Yardimci, C., Dominguez-Renedo, O., Arcos-Martinez, M.J., CYP450 2B4 covalently attached to carbon and gold screen printed electrodes by diazonium salt and thiols monolayers. *Anal. Chim. Acta*, **2009**, *633*, 51.

151 Dou, Y.H., Haswell, S.J., Greenman, J., Wadhawan, J., Voltammetric immunoassay for the detection of protein biomarkers. *Electroanal.*, **2012**, *24*, 264.

152 Lerner, M.B., Dailey, J., Goldsmith, B.R., Brisson, D., Johnson, A.T.C., Detecting lyme disease using antibody-functionalized single-walled carbon nanotube transistors. *Biosens. Bioelectron.*, **2013**, *45*, 163.

153 Radi, A.E., Lates, V., Marty, J.L., Mediatorless hydrogen peroxide biosensor based on horseradish peroxidase immobilized on 4-carboxyphenyl film electrografted on gold electrode. *Electroanal.*, **2008**, *20*, 2557.

154 Harper, J.C., Polsky, R., Wheeler, D.R., Dirk, S.M., Brozik, S.M., Selective immobilization of DNA and antibody probes on electrode arrays: Simultaneous electrochemical detection of DNA and protein on a single platform. *Langmuir*, **2007**, *23*, 8285.

155 Corgier, B.P., Bellon, S., Anger-Leroy, M., Blum, L.J., Marquette, C.A., Protein-diazonium adduct direct electrografting onto SPRi-biochip. *Langmuir*, **2009**, *25*, 9619.

156 Corgier, B.P., Laurent, A., Perriat, P., Blum, L.J., Marquette, C.A., A versatile method for direct and covalent immobilization of DNA and proteins on biochips. *Angew. Chem. Int. Edit.*, **2007**, *46*, 4108.

157 Corgier, B.P., Marquette, C.A., Blum, L.J., Diazonium-protein adducts for graphite electrode microarrays modification: Direct and addressed electrochemical immobilization. *J. Am. Chem. Soc.*, **2005**, *127*, 18328.

158 Corgier, B.P., Marquette, C.A., Blum, L.J., Direct electrochemical addressing of immunoglobulins: Immuno-chip on screen-printed microarray. *Biosens. Bioelectron.*, **2007**, *22*, 1522.

159 Marquette, C.A., Bouteille, F., Corgier, B.P., Degiuli, A., Blum, L.J., Disposable screen-printed chemiluminescent biochips for the simultaneous determination of four point-of-care relevant proteins. *Anal. Bioanal. Chem.*, **2009**, *393*, 1191.

160 Polsky, R., Harper, J.C., Wheeler, D.R., Dirk, S.M., Arango, D.C., Brozik, S.M., Electrically addressable diazonium-functionalized antibodies for multianalyte electrochemical sensor applications. *Biosens. Bioelectron.*, **2008**, *23*, 757.

161 Makos, M.A., Omiatek, D.M., Ewing, A.G., Heien, M.L., Development and characterization of a voltammetric carbon-fiber microelectrode pH sensor. *Langmuir*, **2010**, *26*, 10386.

162 Yang, X.H., Hall, S.B., Burrell, A.K., Officer, D.L., A pH-responsive hydroquinone-functionalised glassy carbon electrode. *Chem. Commun.*, **2001**, 2628.

163 Betelu, S., Vautrin-Ul, C., Chausse, A., Novel 4-carboxyphenyl-grafted screen-printed electrode for trace Cu(II) determination. *Electrochem. Commun.*, **2009**, *11*, 383.

164 Bouden, S., Bellakhal, N., Chausse, A., Dachraoui, M., Vautrin-Ul, C., Correlations between the grafting conditions and the copper detection by diazonium functionalized carbon screen-printed electrodes. *Electrochim. Acta*, **2014**, *125*, 149.

165 Bouden, S., Bellakhal, N., Chausse, A., Vautrin-Ul, C., Performances of carbon-based screen-printed electrodes. Modified by diazonium salts with various carboxylic functions for trace metal sensors. *Electrochem. Commun.*, **2014**, *41*, 68.

166 Ustundag, Z., Solak, A.O., EDTA modified glassy carbon electrode: Preparation and characterization. *Electrochim. Acta*, **2009**, *54*, 6426.

167 Betelu, S., Vautrin-Ul, C., Ly, J., Chausse, A., Screen-printed electrografted electrode for trace uranium analysis. *Talanta*, **2009**, *80*, 372.

168 Levesque, L., lawrence, M.F., Bourguignon, B., Leclerc, G., Drug eluting device for treating vascular diseases. PCT Int. Appl. (2002), WO2002066092 (to Angiogene Inc.)

169 Levy, Y., Tal, N., Tzemach, G., Weinberger, J., Domb, A.J., Mandler, D., Drug-eluting stent with improved durability and controllability properties, obtained via electrocoated adhesive promotion layer. *J. Biomed. Mater. Res. B*, **2009**, *91B*, 819.

170 Bureau, C., Haroun, F., Henault, E., Drug eluting stent with a biodegradable realease layer attached with an electro-grafted primer coating. European patent. (2007), EP2037981 (to Alchimedics)

171 Belmont, J.A., Bureau, C., Chehimi, M.M., Gam-Derouich, S., Pinson, J., *Patents and industrial applications of aryl diazonium salts and other coupling agents*, in *Aryl diazonium salts*, M.M. Chehimi, Editor. 2012, Wiley-VCH. pp. 309.

172 Bureau, C., Formation of organic electro-grafted films on the surface of electrically conductive or semi-conductive surfaces. PCT patent. (2007), WO2007099137 (to Alchimer)

173 http://www.alchimer.com/.

Chapter 2. Experimental

2.1 General Synthesis and Reagents

2.1.1 Reagents and solvents

Unless stated otherwise, all solvents and chemical reagents were obtained from commercial sources and used as received. For electrochemistry, acetonitrile (ACN) and ethanol (EtOH) were HPLC grade. When anhydrous solvent were required, HPLC grade solvents were dried in an alumina column drying system.[1] Milli-Q water (resistivity > 18 MΩ cm) was used to prepare all aqueous solutions and was used for all aqueous washing steps.

2.1.2 Tetrabutylammonium tetrafluoroborate

Tetrabutylammonium tetrafluoroborate ($TBABF_4$) electrolyte was prepared by mixing tetrabutylammonium hydroxide (TBAOH, 40%) and tetrafluoroboric acid (HBF_4, 48%). HBF_4 (5mL) was diluted to 25 mL with water and added, with stirring, to diluted TBAOH (20 mL diluted to 100 mL with water). The white precipitate was washed with water and filtered under vacuum. The $TBABF_4$ electrolyte was dried for 3 days in an oven at 60 °C and then for 2 days under vacuum at 80 °C. The electrolyte was stored in a desiccator.

2.1.3 Synthesis of aryldiazonium salts

Unless specified otherwise, aryldiazonium salts were synthesised using a literature method.[2] Briefly, the amine derivative (5 mmol) was dissolved in 4 mL of 25% HBF_4, the mixture was cooled in an acetone-salt-ice bath and sodium nitrite ($NaNO_2$, 5 mmol), dissolved in small amount of water, was added dropwise to the cold mixture with stirring. The precipitate formed was filtered under suction. The crude product was then purified by dissolving in a minimum amount of ACN and cooling the solution in an ice bath with gradual addition of

diethyl ether to re-precipitate the product. The product was filtered and washed with cold water and diethyl ether. The purified product was dried under vacuum and stored in the freezer in the dark.

All diazonium salts were characterised by ^{1}H NMR. In all cases the aromatic protons shifted up field compared to the aniline starting materials.

2.1.3.1 4-Acetylbenzenediazonium tetrafluoroborate ($[COCH_3\text{-}Ar\text{-}N_2]BF_4$)

Yellow precipitate (yield = 58%). ^{1}H NMR (400 MHz, CD_3CN): δ = 8.62 9d, 2H, J = 8.4 Hz), 8.37 (d, 2H, J = 9.2 Hz), 2.71 (s, 3H), ppm.

2.1.3.2 Benzenediazonium tetrafluoroborate ($[H\text{-}Ar\text{-}N_2]BF_4$)

White precipitate (yield = 57%). ^{1}H NMR (400 MHz, CD_3CN): δ = 8.49 (d, 2H, J = 8.0 Hz), 8.29 (t, 1H, J = 8.0 Hz), 7.96 (t, 2H, J = 8.0 Hz), ppm.

2.1.3.3 4-Bromobenzenediazonium tetrafluoroborate ($[Br\text{-}Ar\text{-}N_2]BF_4$)

White precipitate (yield = 53%). ^{1}H NMR (400 MHz, CD_3CN): δ = 8.36 (d, 2H, J = 9.2 Hz), 8.13 (d, 2H, J = 9.2 Hz), ppm.

2.1.3.4 4-Carboxybenzenediazonium tetrafluoroborate ($[COOH\text{-}Ar\text{-}N_2]BF_4$)

White precipitate (yield = 48%). ^{1}H NMR (400 MHz, CD_3CN): δ = 8.60 (d, 2H, J = 9.2 Hz), 8.44 (d, 2H, J = 8.8 Hz), ppm.

2.1.3.5 4-Cyanobenzenediazonium tetrafluoroborate ($[CN\text{-}Ar\text{-}N_2]BF_4$)

White precipitate (yield = 54%). ^{1}H NMR (400 MHz, CD_3CN): δ = 8.64 (d, 2H, J = 9.2 Hz), 8.27 (d, 2H, J = 9.2 Hz), ppm.

2.1.3.6 4-Ethynylbenzenediazonium tetrafluoroborate ([Eth-Ar-N_2]BF_4)

Brown precipitate (yield = 46%). ^{1}H NMR (400 MHz, CD_3CN): δ = 8.46 (d, 2H, *J* = 9.2 Hz), 7.98 (d, 2H, *J* = 8.4 Hz), 4.25 (s, 1H), ppm.

2.1.3.7 4-methylbenzenediazonium tetrafluoroborate ([CH_3-Ar-N_2]BF_4)

White precipitate (yield = 32%). ^{1}H NMR (400 MHz, CD_3CN): δ = 8.36 (d, 2H, *J* = 8.8 Hz), 7.76 (d, 2H, *J* = 8.4 Hz), 2.64 (s, 3H), ppm.

2.1.3.8 4-Nitrobenzenediazonium tetrafluroborate (NBD)

Pale yellow (yield = 62%). ^{1}H NMR (400 MHz, CD_3CN): δ = 8.81 (d, 2H, *J* = 8.8 Hz), 8.68 (d, 2H, *J* = 9.2 Hz), ppm.

2.1.3.9 4-Trifluoromethylbenzenediazonium tetrafluoroborate ([CF_3-Ar-N_2]BF_4)

White precipitate (yield = 55%). ^{1}H NMR (400 MHz, CD_3CN): δ = 8.70 (d, 2H, *J* = 8.4 Hz), 8.25 (d, 2H, *J* = 8.8 Hz), ppm.

2.1.4 Synthesis of protected aryldiazonium salts

2.1.4.1 TIPS protected ethynylbenzenediazonium salt

4-((Triisopropylsilyl)ethynyl)aniline (TIPS-Eth-Ar-NH_2) was synthesised according to a published method.[3] 4-Iodoaniline (1 g), palladium (II) acetate (20.5 mg), copper (I) iodide (8.7 mg) and triphenylphosphine (48 mg) were dissolved in freshly distilled triethylamine (10 mL). The mixture was degassed using two freeze-thaw cycles. Triisopropylsilylacetylene (1.1 mL) was then added by syringe, and the mixture was carefully degassed by boiling briefly under reduced pressure and then flushing with N_2(g). After stirring at room temperature overnight hexane was added, and the solution was filtered through Celite. The filtrate was evaporated and then purified by column chromatography on silica eluting with

dichloromethane (DCM)/pet. ether mixture by gradually increasing the polarity. Product was obtained as a yellow oil, yield = 0.95 g, 76%. ^{1}H NMR (500 MHz, DMSO-d_6): δ = 7.20 (d, 2H, *J* = 8.5 Hz), 6.61 (d, 2H, *J* = 8.5 Hz), 5.62 (s, 2H), 1.17 (s, 21H), ppm.

4-((Triisopropylsilyl)ethynyl)benzenediazonium tetrafluoroborate ([TIPS-Eth-Ar-N_2]BF_4) was synthesised by adaptation of a previously described procedure.[4] TIPS-Eth-Ar-NH_2 (0.55 g, 2 mmol) was dissolved in acetone (~10 mL) and 25% HBF_4 (15 mL) was added. After cooling in an ice bath, $NaNO_2$ (0.41 g, 6 mmol) was added to the solution, the reaction mixture was stirred overnight and then the precipitate was filtered under vacuum. The product was re-precipitated from an ACN and water mixture, and rinsed with cold diethyl ether. The pale yellow precipitate was dried under vacuum overnight and stored in the freezer in the dark. Yield = 0.15 g, 20%. ^{1}H NMR (500 MHz, $CDCl_3$): δ = 8.56 (d, 2H, J = 9.0 Hz), 7.74 (d, 2H, J = 8.5 Hz), 1.14 (m, 21H), ppm.

2.1.4.2 Fm protected carboxybenzenediazonium salt

4-(((*tert*-butoxy)carbonyl)amino)benzoic acid (Boc-NH-Ar-COOH) was synthesised by the following method:[5] 4-aminobenzoic acid (3.0 g, 0.022 mol) was dissolved in 75 mL dioxane/water (2 : 1) mixture. Triethylamine (4.5 mL, 0.032 mol) was then added to the mixture followed by Boc_2O (7.5 mL, 0.032 mol). The reaction was stirred overnight at room temperature. Excess solvent was evaporated under vacuum, and 3 M HCl was added dropwise to the residue to obtain a white precipitate, which was collected by filtration, washed with water and dried under vacuum (yield = 4.54 g, 88%). ^{1}H NMR (400 MHz, DMSO-d_6): δ = 7.82 (d, 2H, *J* = 8.8 Hz), 7.54 (d, 2H, *J* = 8.8 Hz), 1.48 (s, 9H), ppm.

9-H-Fluoren-9-ylmethyl 4-(((*tert*-butoxy)carbonyl)amino)benzoate (Boc-NH-Ar-COO-Fm) was prepared by the following Steglich esterification method.[6] Boc-NH-Ar-COOH (4.0

g, 0.020 mol), 4-dimethylaminopyridine (DMAP, 80 mg) and 9-fluorenylmethanol (FmOH, 4.0 g, 0.020 mol) were dissolved in anhydrous dimethylformamide (DMF, 10 mL). The reaction mixture was stirred and cooled in an ice-bath followed by the addition of N,N′-dicyclohexylcarbodiimide (DCC, 2.7 g, 0.013 mol). The reaction was stirred for a further 5 min in the ice-bath followed by 3 h at room temperature. Precipitated urea was removed by filtration, and the filtrate was evaporated under vacuum. The residue was then taken up in DCM and washed twice with 0.5 M HCl, followed by saturated $NaHCO_3$, and dried over $MgSO_4$. The solvent was removed under vacuum and the desired product was obtained by column chromatography on silica, eluted with DCM. Product was obtained as a colourless oil, yield = 2.53 g, 48%. ^{1}H NMR (400 MHz, $CDCl_3$): δ = 8.03 (d, 2H, *J* = 8.4 Hz), 7.79 (d, 2H, *J* = 7.2 Hz), 7.65 (d, 2H, *J* = 7.6 Hz), 7.47 (d, 2H, *J* = 8.8 Hz), 7.41 (t, 2H, *J* = 7.2 Hz), 7.32 (t, 2H, *J* = 7.2 Hz), 4.59 (d, 2H, *J* = 7.2 Hz), 4.38 (t, 1H, *J* = 7.6 Hz), 1.26 (s, 9H), ppm.

9-H-Fluoren-9-ylmethyl 4-aminobenzoate (Fm-COO-Ar-NH_2) was obtained by the deprotection of the Boc group of Boc-NH-Ar-COO-Fm by using trifluoroacetic acid (TFA).[7] Boc-NH-Ar-COO-Fm (2.5 g, 6 mmol) was dissolved in DCM (15 mL) followed by addition of TFA (10 mL), and the reaction mixture was stirred for 1 h at room temperature. Excess reagent was removed under vacuum, and sat. $NaHCO_3$ was added dropwise to neutralise the solution. The white precipitate was collected by filtration and impurities were removed by washing with hexane. ^{1}H NMR (400 MHz, $CDCl_3$): δ = 7.93 (d, 2H, *J* = 8.4 Hz), 7.79 (d, 2H, *J* = 7.2 Hz), 7.66 (d, 2H, *J* = 7.2 Hz), 7.41 (t, 2H, *J* = 7.2 Hz), 7.32 (t, 2H, *J* = 7.6 Hz), 6.70 (d, 2H, *J* = 8 Hz), 4.55 (d, 2H, *J* = 7.2 Hz), 4.37 (t, 1H, *J* = 7.2 Hz), ppm.

4-((9-H-Fluoren-9-ylmethoxy)carbonyl)benzene-1-diazonium tetrafluoroborate ([Fm-COO-Ar-N_2]BF_4) was synthesised by dissolving NH_2-Ar-COO-Fm (0.15 g, 0.45 mmol) in dry ACN and the reaction was stirred at -40 °C followed by the addition of $NOBF_4$ (65 mg,

0.55 mmol). The reaction was further stirred for 2 h at -40 °C and the solvent was evaporated under vacuum. The precipitate was re-dissolved in a small amount of ACN and re-precipitated by addition of cold diethyl ether. The yellow precipitate was collected and dried under vacuum and stored in the freezer and in the dark (yield = 0.18 g, 93%). ^{1}H NMR (500 MHz, CD_3CN): δ = 8.57 (d, 2H, *J* = 9 Hz), 8.34 (d, 2H, *J* = 9 Hz), 7.90 (d, 2H, *J* = 7.5 Hz), 7.73 (d, 2H, *J* = 7.5 Hz), 7.48 (t, 2H, *J* = 7.5 Hz), 7.40 (t, 2H, *J* = 7.5 Hz), 4.81 (d, 2H, *J* = 6.5 Hz), 4.48 (t, 1H, *J* = 6.5), ppm.

2.1.4.3 Boc protected aminobenzenediazonium salt

***tert*-butyl N-(4-aminophenyl)carbamate (Boc-NH-Ar-NH_2)** was prepared by mixing Boc_2O and *p*-phenylenediamine. *p*-Phenylenediamine (5.0 g, 0.046 mol) was dissolved in DCM and degassed under N_2(g) and the reaction was cooled in a salt-ice bath. Boc_2O (5 mL, 0.02 mol) was then added dropwise to the cold mixture and the reaction was stirred overnight under N_2(g). The product was purified by column chromatography on silica eluted with pet. ether/EtOAc (2 : 1) to afford a light brown solid (4.1 g, 98% yield. ^{1}H NMR (500 MHz, $CDCl_3$): δ = 7.11 (d, 2H, *J* = 7 Hz), 6.62 (d, 2H, *J* = 6.5 Hz), 6.25 (b, 1H, NHBoc), 3.52 (b, 2H, NH_2), 1.49 (s, 9H, $C(CH_3)_3$), ppm.

4-(((*tert*-butoxy)carbonyl)amino)benzene-1-diazonium tetrafluoroborate ([Boc-NH-Ar-N_2]BF_4) was synthesised by dissolving Boc-NH-Ar-NH_2 (0.4 g, 2 mmol) in dry ACN, cooling the solution to -40 °C followed by the addition of $NOBF_4$ (0.28 g, 2.4 mmol). The reaction was stirred for 2 h at -40 °C and the solvent was evaporated under vacuum. The precipitate was re-dissolved in ACN and re-precipitated by addition of cold diethyl ether. The orange precipitate was collected and dried under vacuum and stored in the freezer and in the

dark (yield = 0.25 g, 41%). ^{1}H NMR (400MHz, CD_3CN): δ = 8.36 (d, 2H, *J* = 10 Hz), 7.94 (d, 2H, *J* = 10 Hz), 1.58 (s, 9H), ppm.

2.1.4.4 Boc protected (aminomethyl)benzenediazonium salt

***tert*-butyl *N*-(4-aminomethylphenyl)carbamate (Boc-NH-CH_2-Ar-NH_2)** was prepared according to a literature procedure.[8] Briefly, 4-aminomethylphenylamine (1.5 g, 0.012 mol) and Boc_2O (3.2 mL, 0.014 mol) was dissolved in tetrahydrofuran (THF) and stirred for 2 h at room temperature. The solvent was evaporated under vacuum and the residue was purified by column chromatography on silica with pet. ether/EtOAc (3 : 2) as the eluent. Product was obtained as a yellow solid, yield = 2.5 g, 92%. ^{1}H NMR (400 MHz, $CDCl_3$) δ = 7.07 (d, 2H, *J* = 7.6 Hz), 6.64 (d, 2H, *J* = 8.4 Hz), 4.74 (b, 1H, NHBoc), 4.18 (d, 2H, *J* = 5.6 Hz), CH_2NH), 3.64 (s, 2H, NH_2), 1.45 (s, 9H, $C(CH_3)_3$) ppm.

4-(((*tert*-butoxy)carbonyl)aminomethyl)benzene-1-diazonium tetrafluoroborate ([Boc-NH-CH_2-Ar-N_2]BF_4) was synthesised following the literature procedure.[9] Boc-NH-CH_2-Ar-NH_2 (1.67 g, 7.5 mmol) was dissolved in HBF_4 (40%, 1.65 mL, 7.5 mmol) and water (10 mL) and cooled in a salt-ice bath. To the cold solution, $NaNO_2$ (0.55 g, 8.0 mmol) dissolved in water (2 mL) was added dropwise with stirring. The reaction was carried out under N_2(g). After 1 h, the cold reaction mixture was filtered and washed with diethyl ether and dried under vacuum to give the diazonium salt as an orange solid (yield = 1.7 g, 69%). ^{1}H NMR (400 MHz, CD_3CN) δ = 8.44 (d, 2H, *J* = 8.8 Hz), 7.81 (d, 2H, *J* = 9.2 Hz), 6.06 (b, 1H, NHBoc), 4.46 (d, 2H, *J* = 6.4 Hz), 1.45 (s, 9H), ppm.

2.1.4.5 Fmoc protected aminobenzenediazonium salt

9H-fluoren-9-ylmethyl N-(4-aminophenyl)carbamate (Fmoc-NH-Ar-NH_2) was synthesised in two steps. Firstly, Boc-NH-Ar-NH_2 (1g, 5 mmol) and 9-

fluorenylmethoxycarbonyl chloride (Fmoc-Cl, 1.24 g, 5 mmol) was dissolved in DCM, followed by the addition of N,N-diisopropylethylamine (DIPEA, 4.2 mL, 25 mmol).[10] The reaction was stirred overnight at room temperature. The white precipitate, Fmoc-NH-Ar-NH-Boc, was collected by filtration and dried under vacuum. Fmoc-NH-Ar-NH_2 was obtained by deprotecting the Boc group of Fmoc-NH-Ar-NH-Boc in 10 mL TFA/DCM (1 : 1). The reaction was stirred for 1 h followed by addition of saturated $NaHCO_3$ to neutralise the solution. The precipitate was collected under filtration and washed with pet. ether to afford a yellow solid (yield = 1.5 g, 96 %). ^{1}H NMR (300 MHz, acetone) δ = 7.90 (d, 2H, *J* = 9 Hz), 7.75 (d, 2H, *J* = 9 Hz), 7.68 (d, 2H, *J* = 9 Hz), 7.44 (t, 2H, *J* = 9 Hz), 7.38 (t, 2H, *J* = 9 Hz), 7.33 (d, 2H, *J* = 9 Hz), 4.55 (d, 2H, *J* = 6 Hz), 4.32 (t, 1H, *J* = 6 Hz) ppm.

4-(((9H-fluoren-9-ylmethoxy)carbonyl)amino)benzene-1-diazonium tetrafluoroborate ([Fmoc-NH-Ar-N_2]BF_4) was synthesised using the same method as the preparation of [Boc-NH-Me-Ar-N_2]BF_4 with a slight modification. Fmoc-NH-Ar-NH_2 was dissolved in a small amount of acetone before the addition of HBF_4. The product was a yellow solid (yield = 39%). ^{1}H NMR (400 MHz, DMSO-d_6) δ = 8.62 (d, 2H, *J* = 9.2 Hz), 8.02 (d, 2H, *J* = 7.2 Hz), 7.96 (d, 2H, *J* = 9.2 Hz), 7.84 (d, 2H, *J* = 7.6 Hz), 7.53 (t, 2H, *J* = 6.8 Hz), 7.46 (t, 2H, *J* = 6.8 Hz), 4.76 (d, 2H, *J* = 6.4 Hz), 4.47 (t, 1H, *J* = 6 Hz) ppm.

2.1.4.6 Fmoc protected (aminomethyl)benzenediazonium salt

9H-Fluoren-9-ylmethyl N-((4-nitrophenyl)methyl)carbamate (Fmoc-NH-CH_2-Ar-NO_2) was synthesised according to the literature method.[10] Briefly, 4-nitrobenzylamine hydrochloride (0.2 g, 1 mmol, Fmoc-Cl (0.26 g, 1 mmol) and DIPEA (0.87 mL, 5 mmol) in DCM (20 mL) were reacted for 2 h at room temperature. Excess solvent was evaporated under vacuum to afford a white precipitate with 83% yield (0.3 g). ^{1}H NMR (400 MHz, $CDCl_3$) δ = 8.17 (d, 2H, *J* = 8.4 Hz), 7.77 (d, 2H, *J* = 7.6 Hz), 7.58 (d, 2H, *J* = 7.6 Hz), 7.42

(d, 2H, *J* = 7.2 Hz), 7.37 (t, 2H, *J* = 6.8 Hz), 7.31 (t, 2H, *J* = 6.8 Hz), 5.15 (b, 1H, NHFmoc), 4.53 (d, 2H, *J* = 6.4 Hz), 4.45 (d, 2H, *J* = 5.6), 4.21 (t, 1H, *J* = 5.6 Hz) ppm.

9H-Fluoren-9-ylmethyl N-((4-aminophenyl)methyl)carbamate (Fmoc-NH-CH_2-Ar-NH_2) was prepared by reducing Fmoc-NH-CH_2-Ar-NO_2 (0.1 g) in the presence of H_2 and Pd/C (50 mg, 10% Pd) in MeOH for 3 h at room temperature.[10] Pd/C was separated by filtration through Celite and the filtrate was evaporated under vacuum. The white precipitate was dried under vacuum (yield = 0.1 g, 92%). ^{1}H NMR (400 MHz, $CDCl_3$) δ = 7.75 (d, 2H, *J* = 7.6 Hz), 7.58 (d, 2H, *J* = 7.6 Hz), 7.38 (t, 2H, *J* = 6.8 Hz), 7.29 (t, 2H, *J* = 6.8 Hz), 7.06 (d, 2H, *J* = 8 Hz), 6.64 (d, 2H, *J* = 7.6 Hz), 4.93 (b, 1H, NHFmoc), 4.42 (d, 2H, *J* = 7.6 Hz), 4.25 (d, 2H, *J* = 5.6 Hz), 4.22 (t, 1H, *J* = 5.6 Hz), 3.65 (b, 2H, NH_2) ppm.

4-((((9H-Fluoren-9-ylmethoxy)carbonyl)amino)methyl)benzene-1-diazonium tetrafluoroborate ([Fmoc-NH-CH_2-Ar-N_2]BF_4) was synthesised using the HBF_4/$NaNO_2$ diazonium synthesis method as for [Boc-NH-CH_2-Ar-N_2]BF_4. The product was a yellow solid (yield = 56 %). ^{1}H NMR (400 MHz, CD_3CN) δ = 8.41 (d, 2H, *J* = 8 Hz), 7.87 (d, 2H, *J* = 8 Hz), 7.73 (d, 2H, *J* = 8.4 Hz), 7.68 (d, 2H, *J* = 7.6 Hz), 7.46 (t, 2H, *J* = 7.6 Hz), 7.37 (t, 2H, *J* = 7.2 Hz), 6.37 (b, 1H, NHFmoc), 4.48 (m, 4H), 4.27 (t, 1H, *J* = 5.6 Hz), ppm.

2.1.5 Synthesis of ferrocene derivatives

2.1.5.1 Azidomethyl ferrocene

Azidomethyl ferrocene ($FcCH_2N_3$) was synthesised according to a published procedure.[11] Hydroxymethyl ferrocene ($FcCH_2OH$) (50 mg) and sodium azide (6 eq.) were dissolved in glacial acetic acid (3 mL) and stirred at 50 °C for 3 h. DCM (50 mL) was added to the reaction mixture and the organic phase was washed with saturated $NaHCO_3$ (3 × 50 mL), dried over Na_2SO_4, filtered and evaporated under vacuum. The product was purified by

column chromatography on silica (EtOAc/hexane 1:4) to afford a yellow oil (yield = 78%). ^{1}H NMR (500 MHz, $CDCl_3$): δ = 4.23 (m, 2H, H_{Cp}), 4.19 (m, 2H, H_{Cp}), 4.17 (m, 5H, H_{Cp}), 4.11 (s, 2H, CH_2N_3), ppm.

2.1.5.2 Aminomethyl ferrocene

Aminomethyl ferrocene ($FcCH_2NH_2$) was synthesised according to a literature procedure.[12] Ferrocene carboxaldehyde (1.00 g, 4.7 mmol), sodium hydroxide (1.10 g, 27.5 mmol) and hydroxylamine hydrochloride (0.65 g, 9.3 mmol) were refluxed in EtOH (50 mL) for 3 h. The mixture was left to cool to room temperature before water was added. The product was extracted with DCM (3 × 100 mL) and dried over Na_2SO_4. The solvent was evaporated under vacuum to give ferrocenecarbaldehyde oxime as an orange solid.

Ferocenecarbaldehyde oxime (0.40 g, 1.7 mmol) in anhydrous THF (10 mL) was added dropwise to $LiAlH_4$ (0.35 g, 9.2 mmol) in anhydrous THF (10 mL). The mixture was refluxed for 6 h under N_2(g). After cooling, water was cautiously added to the mixture and extracted by diethyl ether (3 × 100 mL). The organic layer was dried over Na_2SO_4 and evaporated under vacuum to give $FcCH_2NH_2$ as a brown oil. $FcCH_2NH_2$ was stored in the freezer. ^{1}H NMR (500 MHz, $CDCl_3$) δ = 4.16 (m, 2H, H_{Cp}), 4.13 (s, 5H, H_{Cp}), 4.10 (m, 2H, H_{Cp}), 3.54 (s, 2H, CH_2), ppm.

2.1.6 Synthesis of 2-azidoanthraquinone

2-Azidoanthraquinone (AQ-N_3) was synthesised by adaptation of the published method.[13] 2-Aminoanthraquinone (1 mmol) was dissolved in DMF (14 mL) and sodium azide (3 eq.) was dissolved in water (3 mL). The two solutions were mixed together and stirred at room temperature. *Tert*-butyl nitrite (12 eq.) was then added to the mixture and the reaction was further stirred for 48 h. Water (10 mL) was added to the reaction mixture and extracted with

EtOAc (3 × 25 mL). The combined ethyl acetate layer was dried over Na_2SO_4 and solvent was removed by evaporation under vacuum. The product was purified by column chromatography on silica (EtOAc/pet. ether 4:1) giving a yellow solid. Yield = 57%. ^{1}H NMR (400 MHz, DMSO-d_6) δ = 8.20 – 8.24 (m, 3H), 7.92 – 7.96 (m, 4H), ppm.

2.1.7 Phosphate buffer solution

Phosphate buffer (PB) pH 7, was prepared using $NaH_2PO_4.2H_2O$ and Na_2HPO_4 to give a combined concentration of 0.1 M. The amount of each reagent was estimated using the Handerson-Hasselbach equation (eq. 2.1), where pK_a corresponds to the acidic proton of the acid base pair in use, in this case 6.86, $[A^-]$ is the concentration of the base component, HPO_4^{2-}, and [HA] is the concentration of the acidic component, $H_2PO_4^-$. The pH was measured with a pH meter and used as prepared.

$$pH = pK_a + \log ([A^-]/[HA]) \qquad \text{eq. 2.1}$$

2.2 Instruments

2.2.1 Nuclear magnetic resonance

^{1}H NMR spectra were obtained using Agilent 400-MR and Varian 500 INOVA instruments operating at 400 and 500 MHz, respectively. All samples were dissolved in commercially available deuterated solvents. Spectra were referenced to the solvent peak: $CDCl_3$, 7.26 ppm; CD_3CN, 2.0 ppm; DMSO-d_6, 2.6 ppm.

2.2.2 pH meter

pH was measured using an EDT instruments GP 353 ATC pH meter.

2.2.3 Electrochemistry

Electrochemical measurements were performed using an Ecochemie Autolab PGSTAT302 or PGSTAT302N potentiostat/galvanostat interfaced to PC computer system and controlled by Autolab General Purpose Electrochemical System (GPES) software version 4.9.

2.2.4 Atomic force microscopy

Atomic force microscopy (AFM) images were obtained using a Nanoscope Dimension TM3100 microscope integrated with a Nanoscope IIIa controller (Digital Instruments, Veeco). All measurements were performed in ambient air conditions in noncontact tapping mode using silicon cantilevers. Budget Sensors Tap300Al-G series cantilevers were used for topographical imaging.

2.3 Electrochemical Methods

2.3.1 Electrodes

2.3.1.1 Glassy carbon (GC)

GC disk electrodes were fabricated in the Mechanical Workshop of the Department of Chemistry, University of Canterbury. Short (~5 mm) GC plugs were cut from a 3 mm diameter cylindrical GC rod. Each plug was embedded in a tight fitting Teflon tube with one flat end and the other inside the Teflon and in contact with a brass rod (Figure 2.1a). The brass rod extended from the Teflon and acted as the electrical contact for the electrode. The Teflon ensures that only the flat surface of the GC is in contact with the solution.

GC plates, 15 mm × 15 mm, were cut from a GC slab, 3 mm thick (Figure 2.1b). The two different cell setups for use with GC disk and GC, HOPG and PPF plates are described in the following section 2.3.2. GC electrodes were cleaned by hand polishing with a slurry of 1 μm alumina powder (Leco Corporation) on a piece of lecloth (Leco Corporation) until there were

no visible markings or scratches. After polishing, the electrodes were sonicated in Milli-Q water for 5 min to ensure elimination of the alumina from the surface. This procedure was repeated after each set of experiments.

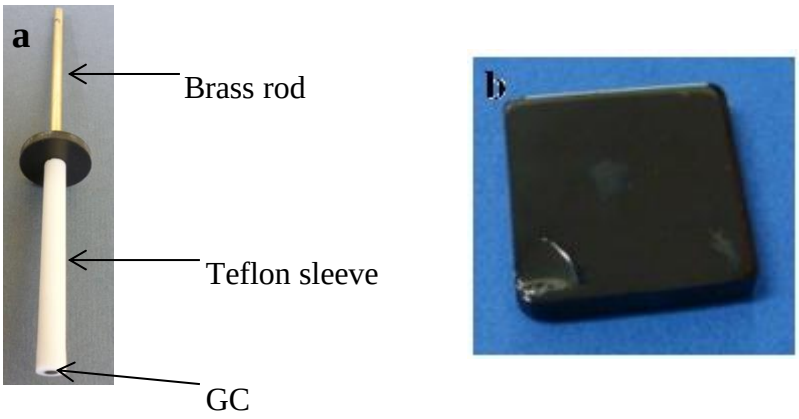

Figure 2.1 Photographs of GC: a) disk; b) plate.

2.3.1.2 Pyrolysed photoresist films (PPFs)

A silicon <100> wafer was coated with a layer of AZ1518 photoresist to protect the surface prior to cutting into 15 mm × 15 mm square chips. The protective photoresist film was removed from the silicon squares by sonication in acetone, methanol and isopropanol for 1 min each and dried with N_2(g). The photoresist AZ-P460 (Clariant) was spin-coated onto the clean silicon chips at 4000 rpm for 35 s. The photoresist-covered chips were soft-baked at 100 °C for 7 min on a hot plate and cooled to room temperature prior to application of a second layer of photoresist at 4000 rpm for 35 s. The photoresist-coated chips were then placed in a furnace within a quartz tube, and forming gas (95% nitrogen and 5% hydrogen) was flowed (2.5 L min^{-1}) through the tube during the heating phases of pyrolysis. The furnace was slowly heated up to 1125 °C over several hours and maintained at 1125 °C for 1 h. The chips were allowed to cool to room temperature under a 0.5 L min^{-1} stream of forming gas before the samples were removed from the furnace and stored under vacuum. PPF was

sonicated in ACN for 30 s prior to modification. Only PPF samples with sheet resistances < 30 Ω □$^{-1}$ were used for film deposition experiments.

2.3.1.3 Highly ordered pyrolytic graphite (HOPG)

HOPG substrates (Grade SPI-1) were obtained from SPI supplies. Between each experiment, a fresh HOPG surface was prepared by using adhesive tape to remove the top most graphite layers.

2.3.2 Cell setup

Two types of electrochemical cells were used in this thesis work: either a standard pear shaped glass cell (Figure 2.2a) or a pear shaped glass cell with a hole in the base (Figure 2.2b). For the standard glass cell, inlets at the top of the cell were used to introduce the GC disk working electrode, Pt counter electrode and reference electrode. A fourth inlet was also available for N_2(g) purging of solutions. Modification of GC plate, PPF and HOPG was carried out using the cell with a hole in the base. The working electrode (GC plate, PPF or HOPG) was positioned between the metal base holder and the glass cell. A Viton or Kalrez O-ring was placed between the electrode surface and the glass cell to provide a seal to prevent leakage of solution. The area of the working electrode exposed to solution was defined by the size of O-ring used. A strip of copper was placed onto the electrode to maintain electrical contact, and the setup was then secured by four metal springs attached to the cell and metal base holder. The Pt counter electrode, reference electrode and gas inlet were introduced from the top of the cell.

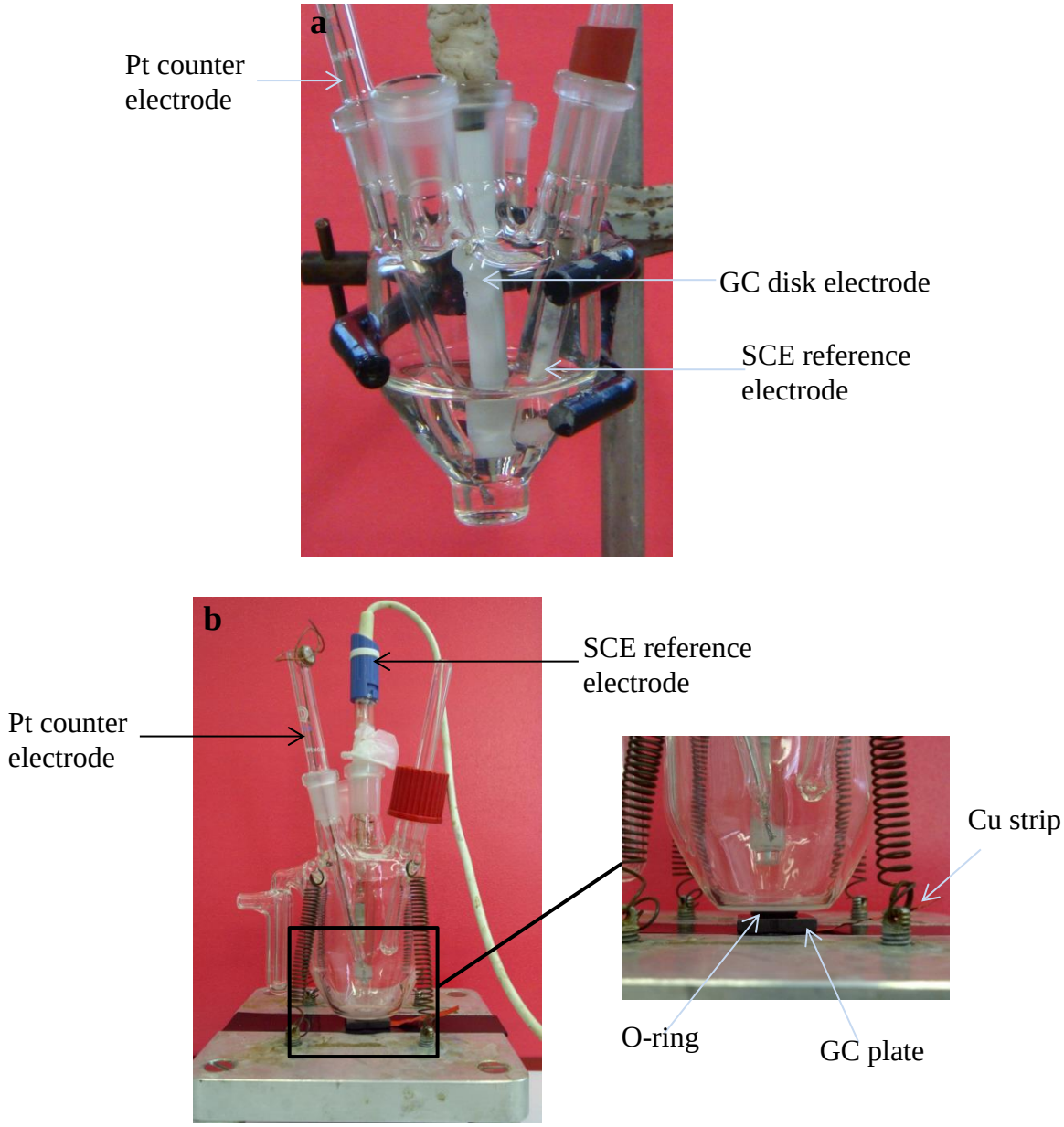

Figure 2.2 Photograph of the electrochemical cell setup used for experiments involving: a) GC disks; b) plate electrodes such as GC plate, PPF and HOPG.

2.3.3 Reference electrodes

A saturated calomel reference electrode (SCE) was used for all aqueous solutions and a calomel electrode (CE) with 1 M LiCl was used for non-aqueous solutions, unless specified otherwise.

2.4 Surface Modification Procedures

2.4.1 Electrochemical modification

The conditions used for electrografting from aryldiazonium salt and arylhydrazine solutions can be found in the experimental section of each chapter.

2.4.2 Non-electrochemical reactions on electrodes

Unless specified otherwise in the experimental section of each chapter, the reactions below were used to couple functional molecules to the bare or modified electrode surfaces. The subsequent washing procedures are described in the experimental section of each chapter.

2.4.2.1 Click reaction of $FcCH_2N_3$ and AQ-N_3 with H-Eth-Ar modified electrodes

Electrodes modified with ethynyl functionality were immersed in a stirred 5 mL solution of $FcCH_2N_3$ or AQ-N_3 (1 mg) in THF, and $CuSO_4$ (2.5 mL, 10 mM) was added. After 15 min flushing with N_2(g), a solution of 10 mM L-ascorbic acid and 15 mg of $NaHCO_3$ in 2.5 mL of water was added dropwise to the solution. The mixture was stirred for a further 3 h under N_2(g).

2.4.2.2 Oxalyl chloride activation

Acid chloride coupling reactions were carried out based on the published method,[14] as described below.

2.4.2.2.1 Activation of GC surfaces and reaction with amine derivatives

The GC electrode (modified or freshly polished) was placed in a sealed reaction vessel and heated under reflux in anhydrous DCM (6 mL) with $(COCl)_2$ (25 μL) and pyridine (8 μL) for 1 h under N_2(g). All volatiles were removed under vacuum followed by the introduction of the amine containing compound (10 mg) in anhydrous DCM (6 mL) with triethylamine

(Et_3N, ~50 μL) under N_2(g). The reaction was stirred for 5 min in an ice bath and then at room temperature overnight. A N_2(g) atmosphere was maintained throughout the reaction.

2.4.2.2.2 Activation of carboxylic acid derivatives and reactions with GC

The carboxylic acid derivative (10 mg) was placed in a sealed reaction vessel under a N_2(g) atmosphere. Anhydrous DCM (6 mL) was introduced followed by $(COCl)_2$ (25 μL) and pyridine (8 μL). After reflux for 1 h, all volatile compounds were removed under vacuum. Anhydrous DCM (6 mL) was introduced into the reaction vessel to re-dissolve the activated compound. GC electrodes were then carefully and quickly inserted into the reaction vessel (minimising exposure of the solution to air) followed by the addition of Et_3N (~ 50 μL). The reaction was stirred in an ice-bath for 5 min and then at room temperature overnight. A N_2(g) atmosphere was maintained throughout the reaction.

2.4.2.3 EDC + HOBt activated amide bond formation reactions

EDC + HOBt activated coupling reactions were conducted by stirring the modified electrodes overnight at room temperature in 5 mL of DMF containing 11 mM of EDC, 20 mM DIPEA, 11 mM HOBt and 10 mM of the amine or carboxylic acid compound.

2.4.2.4 HBTU activated amide bond formation reactions

The HBTU coupling method was performed by stirring the modified electrode overnight at room temperature in 5 mL of DMF containing 12 mM of HBTU, 20 mM of DIPEA and 10 mM of the amine or carboxylic acid compound. A N_2(g) atmosphere was maintained throughout the reaction.

2.5 Atomic Force Microscopy Depth Profiling Technique

Depth profiling experiments were performed at PPF surfaces following previously described procedures.[15] A chip that has three silicon cantilevers of different lengths (MikroMasch CSC37/AIBS) was utilised for the depth profiling 'scratching' technique. In this technique, the AFM laser is focused on the shortest cantilever while the camera visual system is aligned to the longest cantilever. As the shortest tip is engaged with the surface, the longest tip digs into the surface film (Figure 2.3). When the short tip is repeatedly scanned over a 10 μm × 2.5 μm area, the longest tip scratches the surface film away. After scratching, the cantilever is disengaged and replaced with a new cantilever (Budget Sensors Tap300Al-G). The scratch is imaged by scanning orthogonally to the scratch direction in tapping mode. The depth of the scratch was determined from the AFM images using Nanoscope Analysis Version 1.20 software. A 'box' was positioned over the AFM images using the step height calculation tool to give an average line profile (Figure 2.4). The box size was selected to include the maximum amount of the scratch area, while avoiding inclusion of large amounts of scratching debris. For each surface, at least two scratches were made and at least 8 transverse cross sections were chosen from the corresponding images, yielding at least eight average line profiles. Each line profile gave two film thicknesses: one from the step on the right side of the scratched section and the other from the left. Thus, the reported film thickness for each sample is the mean of at least 16 values, and the uncertainty is the standard deviation of the mean.

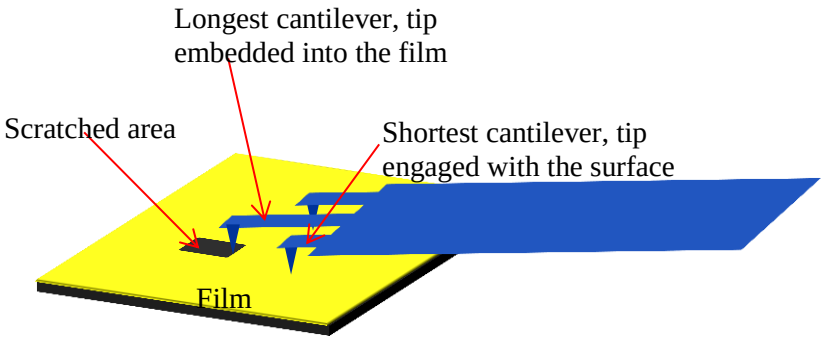

Figure 2.3 Cartoon depiction of the AFM depth profiling technique showing the shortest cantilever tip engaged with the surface in noncontact tapping mode while longest cantilever tip is physically digging into the film creating a trench.

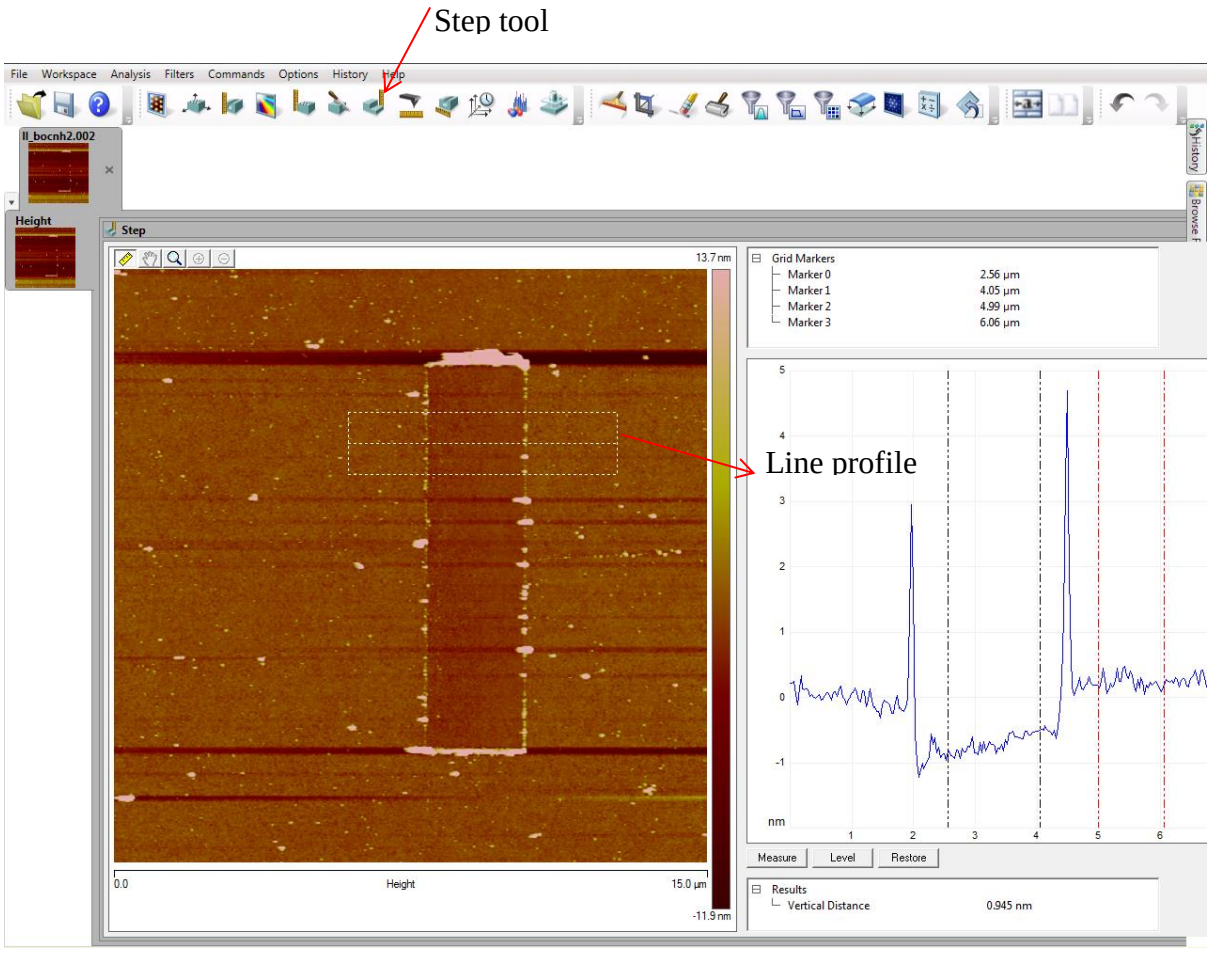

Figure 2.4 Image showing the determination of film thickness using the step tool option from Nanoscope Analysis software.

2.6 Integration of Voltammetric Peak Area (*Linkfit*)

Surface concentration, Γ (mol cm^{-2}), of electroactive species were determined from cyclic voltammetry (CV) using equation 2.2, where Q is the charge (C) obtained from the voltammetric peak area (V. A) divided by the scan rate, ν (V s^{-1}) (equation 2.3), n is the number of electrons in the redox process, F is the Faraday constant (96485 C mol^{-1}) and A is the geometric area of the working electrode (cm^2).

$$\Gamma = \frac{Q}{nFA} \qquad \text{eq. 2.2}$$

$$Q = \frac{peak\ area}{\nu} \qquad \text{eq. 2.3}$$

The voltammetric peak areas were determined by correcting the baseline using a third-order polynomial and integrating the area under the peak using Linkfit 4.1 software (John S. Loring, Copyright 1996-2000). For voltammetry that consists of two closely-spaced peaks, such as the CVs shown in Chapter 4, Figure 4.13 and Chapter 6, Figure 6.12, a mixed Lorentzian-Gaussian algorithm was fitted to the experimental CV. Figure 2.5 shows an example of curve-fitting two closely-spaced peaks.

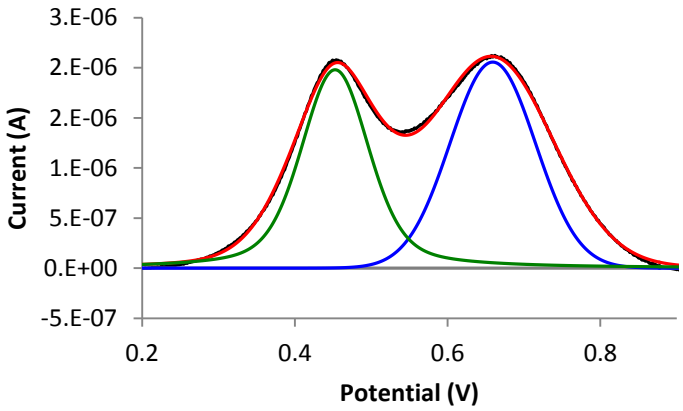

Figure 2.5 A plot showing how a voltammogram is fitted after the baseline correction was performed. Black line: voltammogram obtained from GC surface modified with two ferrocenyl groups immobilised through different linkages (Figure 4.13, Chapter 4); red line: the fitted curve; green line: fitted peak 1; blue line: fitted peak 2.

Surface concentrations of surface-bound nitrophenyl (NP) groups was calculated assuming the reactions shown in equations 2.4 – 2.6 and equations 2.7 and 2.8 as described below. Figure 2.6 shows the typical CV for surface immobilised NP groups obtained in 0.1 M H_2SO_4. The irreversible reduction peak at $E_{p,c}$ ~ -0.6 V corresponds to the reduction of NP groups to aminophenyl (equation 2.4) and hydroxyaminophenyl (equation 2.5) groups. The reversible redox couple at $E_{½}$ ~ 0.3 V corresponds to the hydroxyaminophenyl/nitrosophenyl redox couple (equation 2.6).[16]

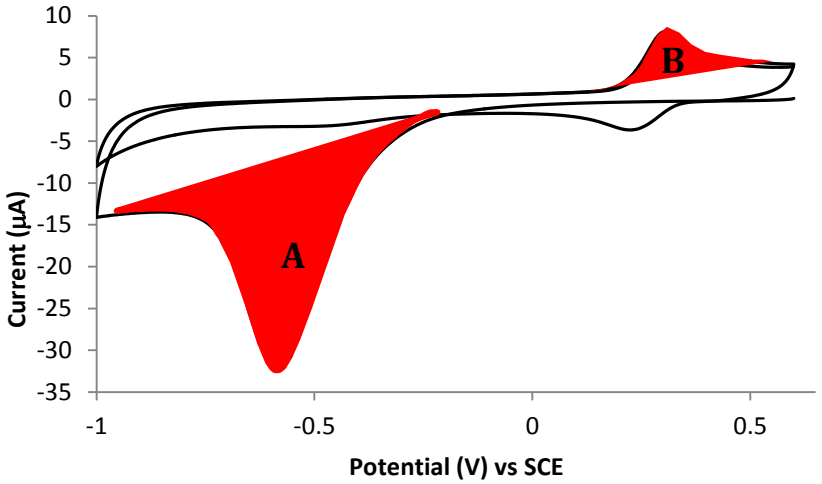

Figure 2.6 CV showing the first scan of GC modified with NP groups obtained in 0.1 M H_2SO_4 at a scan rate of 100 mV s^{-1}.

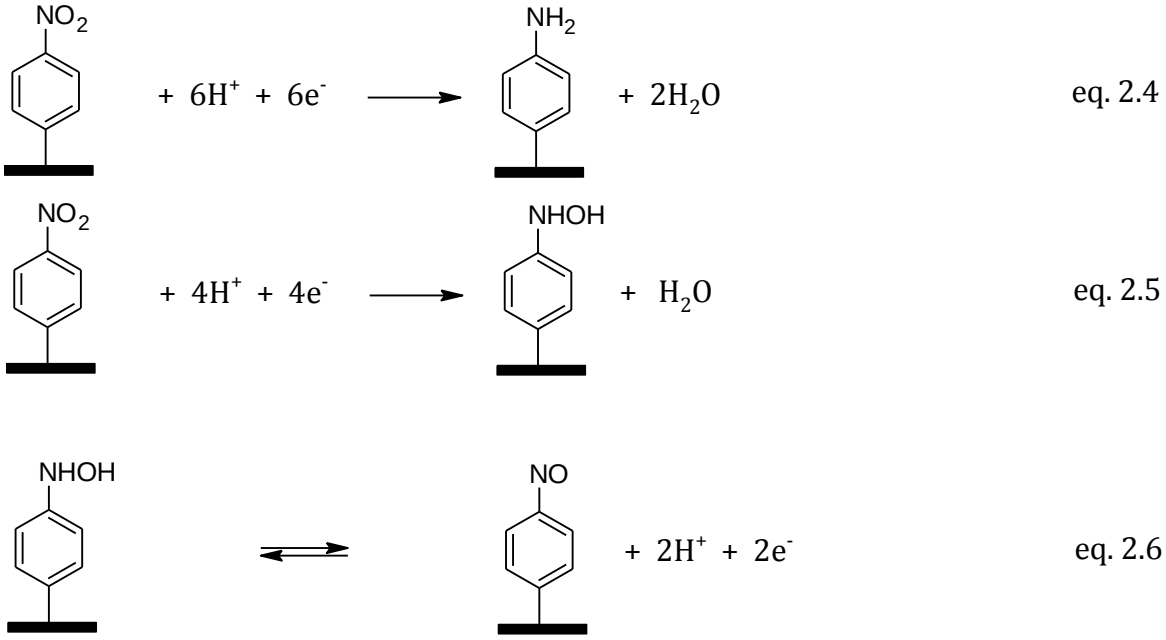

From equations 2.2 and 2.3:

$$\Gamma = \frac{peak\ area}{n\nu FA} \qquad \text{eq. 2.7}$$

Considering the stoichiometry of equations 2.4 – 2.6, the surface concentration of NP groups is calculated as:

$$\Gamma_{NP} = \frac{Area\ A + Area\ B}{6\nu FA} \qquad \text{eq. 2.8}$$

2.7 Estimation of Molecule Dimensions (*Avogadro*)

Avogadro 1.1.1 freeware[17] was used to calculate the dimension of molecules. Typically, two or three reasonable conformations of the structures were drawn, the lowest energy conformation was chosen and the dimension was measured using the tools provided by the software. The diameter, *d*, of the molecule was estimated by assuming there is a free rotation between the aryl ring and the rest of the molecule. For example, Figure 2.7 shows the dimension of the Fmoc-NH-CH_2-Ar molecule assuming a free rotation along the aryl-carbon axis.

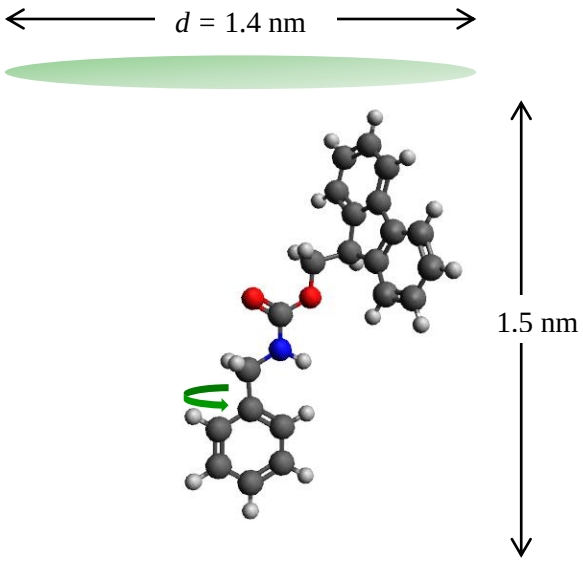

Figure 2.7 Molecular dimension and structure of Fmoc-NH-CH_2-Ar estimated using *Avogadro* 1.1.1 freeware.

2.8 References

1 Pangborn, A.B., Giardello, M.A., Grubbs, R.H., Rosen, R.K., Timmers, F.J., Safe and convenient procedure for solvent purification. *Organometallics*, **1996**, *15*, 1518.

2 Dunker, M.F.W., Starkey, E.B., Jenkins, G.L., The preparation of some organic mercurials from diazonium borofluorides. *J. Am. Chem. Soc.*, **1936**, *58*, 2308.

3 Anderson, S., Phenylene ethynylene pentamers for organic electroluminescence. *Chem.-Eur. J.*, **2001**, *7*, 4706.

4 Leroux, Y.R., Fei, H., Noel, J.M., Roux, C., Hapiot, P., Efficient covalent modification of a carbon surface: Use of a silyl protecting group to form an active monolayer. *J. Am. Chem. Soc.*, **2010**, *132*, 14039.

5 Mu, F.R., Coffing, S.L., Riese, D.J., Geahlen, R.L., Verdier-Pinard, P., Hamel, E., Johnson, J., Cushman, M., Design, synthesis, and biological evaluation of a series of lavendustin A analogues that inhibit EGFR and syk tyrosine kinases, as well as tubulin polymerization. *J. Med. Chem.*, **2001**, *44*, 441.

6 Neises, B., Steglich, W., Simple method for the esterification of carboxylic acids. *Angew. Chem. Int. Edit.*, **1978**, *17*, 522.

7 Shendage, D.M., Frohlich, R., Haufe, G., Highly efficient stereoconservative amidation and deamidation of alpha-amino acids. *Org. Lett.*, **2004**, *6*, 3675.

8 Lee, J., Kang, M., Shin, M., Kim, J.M., Kang, S.U., Lim, J.O., Choi, H.K., Suh, Y.G., Park, H.G., Oh, U., Kim, H.D., Park, Y.H., Ha, H.J., Kim, Y.H., Toth, A., Wang, Y., Tran, R., Pearce, L.V., Lundberg, D.J., Blumberg, P.M., N-(3-acyloxy-2-benzylpropyl)-n '- 4-(methylsulfonylamino)benzyl thiourea analogues: Novel potent and high affinity antagonists and partial antagonists of the vanilloid receptor. *J. Med. Chem.*, **2003**, *46*, 3116.

9 Chretien, J.M., Ghanem, M.A., Bartlett, P.N., Kilburn, J.D., Covalent tethering of organic functionality to the surface of glassy carbon electrodes by using electrochemical and solid-phase synthesis methodologies. *Chem.-Eur. J.*, **2008**, *14*, 2548.

10 Ulysse, L., Chmielewski, J., The synthesis of a light-switchable amino-acid for inclusion into conformationally mobile peptides. *Bioorg. Med. Chem. Lett.*, **1994**, *4*, 2145.

11 Casas-Solvas, J.M., Ortiz-Salmeron, E., Gimenez-Martinez, J.J., Garcia-Fuentes, L., Capitan-Vallvey, L.F., Santoyo-Gonzalez, F., Vargas-Berenguel, A., Ferrocene-carbohydrate conjugates as electrochemical probes for molecular recognition studies. *Chem.-Eur. J.*, **2009**, *15*, 710.

12 Baramee, A., Coppin, A., Mortuaire, M., Pelinski, L., Tomavo, S., Brocard, J., Synthesis and in vitro activities of ferrocenic aminohydroxynaphthoquinones against *Toxoplasma gondii* and *Plasmodium falciparum*. *Bioorg. Med. Chem.*, **2006**, *14*, 1294.

13 Das, J., Patil, S.N., Awasthi, R., Narasimhulu, C.P., Trehan, S., An easy access to aryl azides from aryl amines under neutral conditions. *Synthesis-Stuttgart*, **2005**, 1801.

14 Noel, J.M., Sjoberg, B., Marsac, R., Zigah, D., Bergamini, J.F., Wang, A.F., Rigaut, S., Hapiot, P., Lagrost, C., Flexible strategy for immobilizing redox-active compounds using in situ generation of diazonium salts. Investigations of the blocking and catalytic properties of the layers. *Langmuir*, **2009**, *25*, 12742.

15 Brooksby, P.A., Downard, A.J., Electrochemical and atomic force microscopy study of carbon surface modification via diazonium reduction in aqueous and acetonitrile solutions. *Langmuir*, **2004**, *20*, 5038.

16 Yu, S.S.C., Tan, E.S.Q., Jane, R.T., Downard, A.J., An electrochemical and XPS study of reduction of nitrophenyl films covalently grafted to planar carbon surfaces. *Langmuir*, **2007**, *23*, 11074.

17 Hanwell, M.D., Curtis, D.E., Lonie, D.C., Vandermeersch, T., Zurek, E., Hutchison, G.R., Avogadro: An advanced semantic chemical editor, visualization, and analysis platform. *J. Cheminf.*, **2012**, *4*.

Chapter 3. Coupling Reactions Directly on Glassy Carbon

3.1 Introduction

As discussed in Chapter 1, there is a lack of direct experimental evidence on the structure of glassy carbon (GC), however it is generally described as network of randomly intertwined ribbons of graphitic planes.[1-7] GC is considered to present mainly edge-plane sites that can react with air and water resulting in a surface terminated with a variety of surface oxides, such as carbonyl, hydroxyl and carboxylate functional groups.[8, 9] Examples of surface oxides that form at a graphitic edge are shown schematically in Figure 1.2 (Chapter 1). As described in Chapter 1, the surface oxide coverage and type of functional group can vary depending on the pre-treatment of the GC electrodes.[10-17] Polishing, the method of electrode preparation used in this work, has been reported to give a surface O/C ratio between 0.08 – 0.33.[8, 13-20] Use of different polishing materials and techniques, and also different suppliers of GC may account for the wide range of reported O/C ratios. Moreover, the methods used to quantify surface O and O/C ratio may lead to different values. When X-ray photoelectron spectroscopy (XPS) is used to measure the O/C ratio, the amount of bulk carbon sampled will depend on the angle of incidence of the X-ray beam. This information is usually not reported, but will have an impact on the measured O/C ratio. Furthermore, when surface functionalities are estimated by coupling with tags, low yields of coupling reactions will result in low estimates. Table 3.1 summarises data on surface oxides at polished GC.

Table 3.1 Summary of O/C ratio at polished GC and the method of detection used.

Entry No.	Surface oxide functional groups	GC source and polishing method	Reagent used for tagging[a]	Detection method	O/C ratio	Ref
1	Total oxygen	GC (grade 30s, Tokai Mfg. Tokyo) polished with 0.3 μm followed by 0.05 μm alumina/H_2O slurry and rinsed with H_2O in between	None	XPS	0.084	10
2	Total oxygen	GC (Atomergic Chemetals (V10-50)) polished with 1 μm alumina/H_2O and 1 μm diamond paste, sonicated in H_2O for 30 s in between	None	XPS	0.33	13
3	Hydroxyl			XPS (curve-fit, 286.2 eV)	0.20	
4	Carbonyl			XPS (curve-fit, 287.7 eV)	0.07	
5	Carboxyl			XPS (curve-fit, 289.1 eV)	0.07	
6	Total oxygen	GC (Normar Industries & Electrosynthesis Co., manufactured by Le Carbone) without polishing	None	XPS	0.12	18
7	Total oxygen	GC polished with 0.3 μm followed by 0.05 μm alumina/H_2O and sonicated in H_2O for 1 min after each step	None	XPS	0.12	18
8	Hydroxyl			XPS (curve-fit, 285.7 eV)	0.024	
9	Carbonyl			XPS (Curve-fit, 287.1 eV)	0.008	
10	Total oxygen	GC polished with 6 μm, 1 μm and 0.25 μm diamond paste followed by 0.3 μm and 0.05 μm alumina/H_2O. GC was sonicated for 1 min in methanol after diamond paste polishing and in H_2O after alumina polishing	None	XPS	0.17	18
11	Hydroxyl			XPS (curve-fit, 285.8 eV)	0.060	
12	Carbonyl			XPS (curve-fit, 287.6 eV)	0.012	
13	Hydroxyl	GC (GLCP-10, Electrosynthesis Co. Inc.) polished with 6 μm followed by 1 μm diamond paste. Sonicated in H_2O, ethyl ether and H_2O for 5 min each	TAA[b]	XPS[c]	0.0451 & 0.0994 (2 samples)	19
14	Hydroxyl	GC polished with 6 μm and 1 μm diamond paste followed by soxhlet extraction in methanol for 8 h	TAA[b]	XPS[c]	0.0124 & 0.0125 (2 samples)	
15	Carbonyl	GC (GLCP-10, Electrosynthesis Co. Inc.) polished with 6 μm followed by 1 μm diamond paste and sonicated in H_2O, ethyl ether and H_2O for 5 min each	PFPH[d]	XPS[e]	0.014 – 0.022	20

16	Total oxygen	GC (Atomergic, grade V10) polished with 1.0 μm followed by 0.05 μm alumina/H_2O and sonicated for 2 min in H_2O	None	XPS	0.27	14
17	Hydroxyl			XPS (curve-fit, 285.8 eV)	0.068	
18	Carboxyl			XPS (curve-fit, 288.7 eV)	0.019	
19	Carbonyl	GC-20 (Tokai, Japan) or GC-20s (Bioanalytical systems) polished with 1.0 μm, 0.3 μm, 0.05 μm alumina/H_2O followed by sonication in H_2O	DNPH[f]	Raman	0.012	11
20	Total oxygen	GC-20 (Tokai, Japan or Bioanalytical System Inc.) polised with alumina/cyclohexane	None	XPS	0.04	15
21	Total oxygen	GC was polished with with alumina/H_2O	None	XPS	0.14	
22	Carbonyl		DNPH[f]	Raman	0.012	
23	Hydroxyl		DNBC[g]	XPS	0.0096	
24	Total oxygen	GC-20 (Tokai, Japan) polished with 1.0 μm, 0.3 μm and 0.05 μm alumina/H_2O followed by sonication in H_2O for 10 min, and heated to 575 ^oC under N_2(g).	None	XPS	0.12	16
25	Hydroxyl		DNBC[g]	XPS	0.009	
26	Hydroxyl		FMA[h]	Raman	0.008	
27	Total oxygen	GC polished with 0.3 μm followed by 0.05 μm alumina/H_2O and sonicated in H_2O and EtOH	None	XPS	0.13	17

[a]Reagents, that are either Raman active or have a distinguishable signal for XPS analysis (such as N, F, etc.), were used to react with specific oxide groups on the GC surface to determine the amount of specific oxide functionalities.

[b]TAA = titanium diisopropoxide bis(2,4-pentanedionate), reagent used to react with hydroxyl groups through coordination of Ti with surface hydroxyl groups

[c]Quantitation of surface hydroxyl group was determined from the equation below:

$$\%\ FG = \frac{\%\ T}{N_T\ (100 - \%\ T\ [\frac{N_A}{N_T}])}$$

% FG is the percent of hydroxyl functional group on the surface ([moles of functional group/total surface moles] × 100).

% T is the percent atomic of the elemental tag (Ti)on the derivatised surface.

N_T is the number of tag atoms per mole of derivatised functional group (N_T = 1)

N_A is the net number of atoms added per mole of the original functional group to the surface by the derivatisation reaction (N_A = 5)

[d]PFPH = pentafluorophenylhydrazine, reagent used to react with carbonyl group as depicted below:

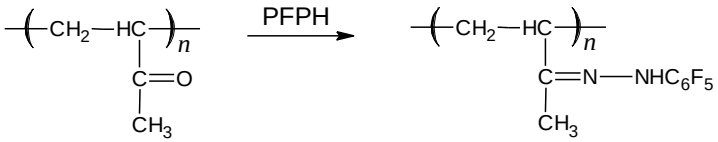

[e]The range of values arises from the different ratio obtained from the N 1s and F 1s to C 1s spectrum from XPS data

[f]DNPH = 2,4-dinitrophenylhydrazine, reagent used to react with carbonyl group

[g]DNBC = dinitrobenzoylchloride, reagent used to react with hydroxyl group

[h]FMA = fluorescein mixed anhydride, reagent used to react with hydroxyl group

As detailed in Table 3.1, attachment of organic molecules via surface oxygen functionalities can be achieved by using a reagent that will react specifically with a particular functional group. For example, Entries 13 and 14 of Table 3.1 show that titanium diisopropoxide bis(2,4-pentanedionate) (TAA) can be used to determine the concentration of surface hydroxyl groups;[19] it was shown that this reagent is specific for hydroxyl groups in the presence of carboxylic acid and carbonyl groups.[21] However, different cleaning steps after polishing resulted in different hydroxyl concentrations: cleaning by sonication resulted in an irreproducible O/C ratio (0.0451 and 0.0994), from two repeat experiments, while cleaning by soxhlet extraction in methanol resulted in a reproducible O/C ratio (0.0124 and 0.0125) from two different experiments. Clearly, the hydroxyl content of GC cleaned by sonication is higher than when cleaned by soxhlet extraction, presumably due to hydroxyl-containing polishing residues not being removed by sonication. Reaction of the hydrazine containing compounds 2,4-dinitrophenylhydrazine and pentafluorophenylhydrazine (DNPH and PFPH) with surface carbonyl groups has also been used to estimate the amount of carbonyl groups on the surface, with values varying from 0.012 to 0.022 (Table 3.1, Entries 15, 19, and 22).[11, 15, 16, 20]

The data in Table 3.1 shows that most commonly, when individual oxides are quantified, hydroxyl groups are present at significantly higher concentration than carbonyl or carboxyl groups. An exception is shown in Table 3.1, Entries 22 and 23.[15] From Raman (carbonyl) and XPS (hydroxyl) measurement, concentrations of 0.90 and 0.48 ($\times 10^{-10}$ mol cm^{-2}) were found for surface carbonyl and hydroxyl, respectively.[15] This method gives higher carbonyl groups compared to hydroxyl groups. This unexpected finding may arise due to different yields for the tagging reactions and therefore the values may not accurately reflect the amount of surface oxide groups. Furthermore, estimation of specific surface oxide concentrations using tagging usually gives very low O/C ratios, the sum of which do not match total O/C ratio. For

instance, Table 3.1, Entries 22 and 23 lists the O/C ratios of 0.14, 0.012, and 0.0096 for total oxygen, carbonyl and hydroxyl, respectively. The sum of O/C ratios from carbonyl and hydroxyl groups only represents 2% of the 14% total oxygen and while the remaining 12% may be due to other oxygen-containing functionalities such as carboxyl or ether, it is more likely that non-quantitative reactions of the surface oxides with the tagging reagents give low estimations of individual surface oxides.

In addition to the reagents mentioned in Table 3.1, cyanuric chloride has been used by Yacynych and co-workers[22, 23] as a linking agent to attach hydroxymethyl ferrocene ($FcCH_2OH$) and glucose oxidase to pyrolytic graphite. Cyanuric chloride reacts with hydroxyl groups on the surface to generate reactive chloride-containing groups that can further react with a nucleophilic compound as depicted in Scheme 3.1.[22] Firstly, the pyrolytic graphite was activated by radiofrequency oxygen plasma to increase the surface oxide content and then the surface was treated with $LiAlH_4$ to convert most of the oxides to hydroxyl groups. This surface was then reacted with cyanuric chloride followed by $FcCH_2OH$[22] (or glucose oxidase).[23] Ferrocene surface concentration, estimated from cyclic voltammetry, was 2.1×10^{-10} mol cm^{-2}.[22] The theoretical calculated surface concentration for a hexagonally close-packed monolayer of Fc groups on a flat surface is 4.5×10^{-10} mol cm^{-2} (assuming that the Fc headgroup is a sphere of 6.6 Å in diameter),[24] and hence the Fc surface concentration was ~47% of a close-packed monolayer.

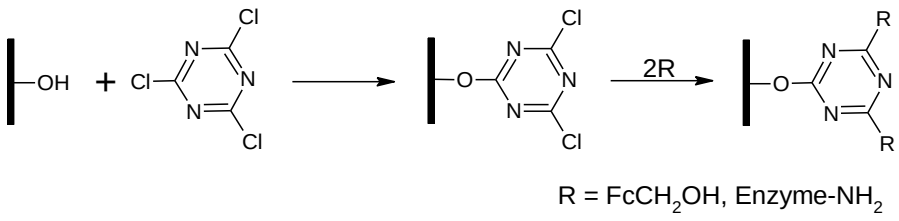

Scheme 3.1 Reaction scheme employing cyanuric chloride as a linking agent. Adapted from reference 22.

Another example is the work of Miller and co-workers,[25, 26] where thionyl chloride was used to convert carboxylic acids on the surface to more reactive acid chlorides followed by reaction with a chiral amino acid to obtain an amide-linked chiral surface. Before modification with thionyl chloride, graphite rods were baked in air at 160 °C for 36 h to introduce acidic groups.[26] After modification with thionyl chloride and subsequent reaction with (S)-(–)-phenylanaline methyl ester, the modified electrode, (S)-(–)-C_{el}PheM, was used as a cathode in aqueous solution to carry out reduction of ketones to produce chiral alcohols. Amide coupling using carbodiimide as the activating agent has also been used to couple glucose oxidase[27] or xanthine oxidase[28] to oxidised graphite electrodes.

Reaction of organosilanes with carbon surface oxides has been reported by Elliot and Murray.[29] The reaction is represented in Scheme 3.2. Silanes incorporating chloride or nitrogen were used so that XPS analysis could identify N 1s, Cl 2p and Si 2p signals after modification. Modification was successful, however no quantitative estimation of surface coverage was reported.[29] Reaction of GC with 2,4-dinitrophenylhydrazine (DNPH) was also investigated by the authors,[29] and analysis of this surface was carried out using XPS and electrochemistry. However, CVs of the modified GC were poorly defined and surface concentrations were not calculated.[29]

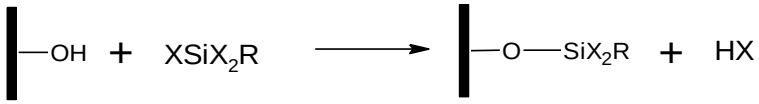

Scheme 3.2 An example of reaction of surface oxide with organosilane. X = Cl, OMe or OEt. Adapted from reference 29.

Only a limited number of methods permit the spontaneous attachment of an organic layer to a carbon surface. In this context, spontaneous is used to describe reactions that occur at room temperature in ambient light and in the absence of an activating procedure. The reaction of aryldiazonium reactions with conducting substrates has been discussed in Chapter 1. Less

commonly studied is the reaction of amines directly with carbon substrates.[30-41] A systematic study has been reported by Gallardo and co-workers;[32] the spontaneous attachment of several primary amines to GC surfaces was achieved by immersion of GC in solutions of amines in acetonitrile at room temperature. Amine compounds bearing an electroactive nitrophenyl (NP) group (3-nitrobenzylamine, 4-nitrobenzylamine and 4-nitrophenylethylamine) were used to measure the surface concentrations of the attached species by cyclic voltammetry. The surface concentration of NP groups increased as the immersion time and the concentration of the amine increased. The surface concentration for samples immersed in a 20 mM solution of amine for 3 h ranged from 6.9 – 7.9 × 10^{-10} mol cm^{-2}, while immersion in 10 mM solutions for 3 and 6 h gave concentrations of 3.8 – 5.0 × 10^{-10} mol cm^{-2} and 6.0 – 7.7 × 10^{-10} mol cm^{-2}, respectively. The calculated surface concentration for a close-packed monolayer of NP groups is 12 × 10^{-10} mol cm^{-2},[42] and hence assuming a typical roughness factor of 2 for a polished GC,[43-45] the experimental NP surface concentration of ~ 8 × 10^{-10} mol cm^{-2} corresponds to ~40% of a close-packed monolayer. The spontaneous attachment of amine to GC was proposed to occur via two reaction pathways:[32] First, a Michael-type reaction between the amine and electron-deficient double bonds on the surface (Scheme 3.3) was considered. This is similar to the mechanism proposed by Buttry and co-workers[31] for the reaction of amine with carbon fibres. However, Gallardo and co-workers[32] found that the yield of the reaction increased after oxidation of the GC surface and tentatively suggested that a second mechanism involved attack of nitrogen on oxidised carbons.[32] Although not explicitly mentioned by the authors, the formation of imines through reaction of amines with aldehyde and ketone functionalities is a possible pathway.[39, 46] However, another explanation is that oxidising the GC surface will not only increase hydroxyl groups but also electron-withdrawing carbonyl and carboxyl groups.[10, 13, 14, 47] These groups will promote the Michael-

type reaction as shown in Scheme 3.3. To date, the Michael-type addition reaction has been used to immobilise porphyrins[33, 34], quinones,[41] gold nanoparticles[30] and ferrocene.[40]

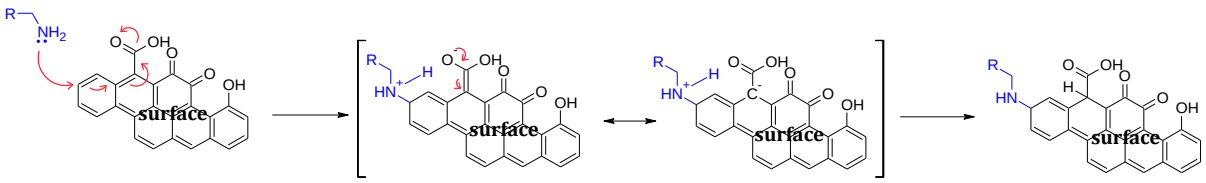

Scheme 3.3 Proposed mechanism for the reaction of amine with GC surface via Michael-type addition reaction.

In this Chapter, the attachment of organic groups to GC surfaces by non-electrochemical methods is described. Electroactive compounds (ferrocenyl (Fc) and NP) were attached to GC either by direct immersion of the freshly polished GC in a solution of the compound of interest, or by chemical activation of the GC surface prior to modification. Cyclic voltammetry was used to quantify the surface concentration of the eletroactive species. The reactions studied were selected because they form the 'blanks' for the grafting work described in later Chapters. To assess coupling reactions occurring at grafted tether layers, it is first necessary to establish the importance of reactions occurring directly at the GC surface.

3.2 Experimental

All chemical reagents and materials are detailed in Chapter 2. Aminomethyl ferrocene ($FcCH_2NH_2$) was synthesised according to a literature method,[48] which is briefly described in Section 2.1.5.2. The general procedure for activation of carboxylic acid groups with oxalyl chloride ($(COCl)_2$) is described in Section 2.4.2.2. Amide coupling reactions involving EDC + HOBt and HBTU are described in Section 2.4.2.3 and 2.4.2.4, respectively.

After coupling reactions, GC electrodes were sonicated in acetonitrile (ACN) for 5 min, unless specified otherwise.

Reaction at GC with $(COCl)_2$ followed by reaction with water. GC was activated with $(COCl)_2$ as described in Section 2.4.2.2. After reflux for 1 h, the GC electrode was removed from the reaction vessel and immersed in Milli-Q water for 30 min and dried with a stream of N_2(g).

Spontaneous reaction. Freshly polished GC electrodes were stirred in a 10 mM solution of the amine compound overnight. The solvents used are described in the text. After reaction, the GC electrode was sonicated in ACN for 5 min.

Direct reaction of GC with $FcCH_2NH_2$ with applied potential. Freshly polished GC electrodes were immersed in a 10 mM solution of $FcCH_2NH_2$ in DMF containing 0.1 M $TBABF_4$ as an electrolyte. A Pt mesh auxiliary electrode and Ag wire pseudoreference electrode were introduced to the cell and the selected potential (-0.8 V or 0.2 V) was applied to the GC electrode overnight. The reaction at -0.8 V was performed under an N_2 atmosphere.

Hydrolysis. Hydrolysis experiments were carried out by sonication of the modified GC electrodes in a solution of 0.15 M KOH(aq) for 25 min. After sonication, electrodes were rinsed with H_2O and dried with a stream of N_2(g).

Electrochemistry. All experiments described in this Chapter were carried out using GC rods (area = 0.071 cm^2) as the working electrode, Pt mesh as the counter electrode and SCE as the reference electrode for aqueous solutions and CE (1 M LiCl) for non-aqueous solutions. Unless specified otherwise, electrochemistry of Fc coupled GC was investigated in 0. 1 M $LiClO_4$-EtOH at a scan rate of 200 mV s^{-1}, and NP modified GC was investigated in 0.1 M H_2SO_4 at a scan rate of 100 mV s^{-1}. The surface concentration of immobilised Fc was determined by averaging the areas under the anodic and cathodic peaks from the third voltammetric cycle, unless specified otherwise. The surface concentration of immobilised NP

groups was estimated from the first cycle using the NP reduction and the hydroxyaminophenyl oxidation peak areas and the number of electrons involved in each redox process.[49] Voltammetric peak area analysis was performed using Linkfit software.[50] When more than one sample was analysed, the reported surface concentrations are the mean values based on the number of samples indicated in the text. When two surface concentrations were averaged, the uncertainties indicate the range of values. When three or more surface concentrations were averaged, the reported uncertainties are standard deviations of the means. The details of surface concentration calculations are explained in Chapter 2.

3.3 Results and Discussion

Table 3.2 summarises the methods used to attach Fc and NP groups to GC via activating agents, and the corresponding surface concentrations of immobilised electro-active Fc and NP groups. The surface concentrations of attached Fc and NP groups were determined from cyclic voltammograms obtained in 0.1 M $LiClO_4$-EtOH and 0.1 M H_2SO_4, respectively.

Table 3.2 Reaction of $FcCH_2NH_2$ and 4-nitrobenzylamine hydrochloride (NBA.HCl) with GC electrodes using the methods listed, and surface concentrations of electro-active ferrocene and nitrophenyl attached to the GC surface.

Expt.	Nature of GC	Activation of GC	Modifying species	Reaction Solvent	$E_{½}$ (Fc/Fc$^+$) (V)	$\Gamma_{Fc\ or\ NP}$ (10^{-10} mol cm^{-2})	n^a
I	Polished	$(COCl)_2$	$FcCH_2NH_2$	DCM	0.39	2.2 ± 0.6	4
II	Polished	$(COCl)_2$	NBA.HCl	DCM	n/a	2.5 ± 0.4	5
III	Polished	$(COCl)_2$	$FcCH_2OH$	DCM	-	-	2
IV	Polished	$(COCl)_2$	FcCOOH	DCM	-	-	2
V	Polished	EDC + HOBt	$FcCH_2NH_2$	DMF	0.40	1.8 ± 0.2	3
VI	Polished	EDC + HOBt	NBA.HCl	DMF	n/a	1.5 ± 0.5	4
VII	Polished	HBTU	$FcCH_2NH_2$	DMF	0.39	1.3 ± 0.2	5
VIII	Polished	HBTU	NBA.HCl	DMF	n/a	1.1 ± 0.2	3
IX^b	GC + $(COCl)_2$ + H_2O	EDC + HOBt	$FcCH_2NH_2$	DMF	0.39	1.3 ± 0.5	3
X^b	GC + $(COCl)_2$	EDC + HOBt	NBA.HCl	DMF	n/a	2.0 ± 0.3	3

	+ H_2O

[a] *n* is the number of samples analysed

[b] Freshly polished GC was activated in $(COCl)_2$ and reacted with water before it was used for further coupling reactions

3.3.1 Reactions with GC activated with $(COCl)_2$ (Experiments I – IV, Table 3.2)

Scheme 3.4 shows the expected reaction when GC is activated with $(COCl)_2$ and reacted with different nucleophiles. Similar to thionyl chloride, $(COCl)_2$ is capable of converting carboxylic acid functionalities to a more reactive acid chloride functional group. GC, freshly polished with alumina slurry, was activated with $(COCl)_2$ by refluxing in anhydrous DCM for 1 h in the presence of pyridine. The activated GC was then reacted with $FcCH_2NH_2$, NBA.HCl, $FcCH_2OH$, or FcCOOH overnight in DCM solution containing Et_3N as described in Section 2.3.1.2. Figure 3.1 shows CVs of GC surfaces following these reactions. As can be seen in Figure 3.1a black line, a clearly-defined redox response is obtained in 0.1 M $LiClO_4$-EtOH for an activated GC electrode reacted with $FcCH_2NH_2$. The potential is consistent with a Fc group with an electron donating substituent (Scheme 3.4a). The small peak-to-peak separation (ΔE_p = 12 mV, scan rate = 200 mV s^{-1}) is evidence of a surface-coupled species.[51] From the area under the cyclic voltammetric peak and eq. 2.1 (Chapter 2), the surface concentration of Fc was calculated to be $(2.2 \pm 0.6) \times 10^{-10}$ mol cm^{-2} (Table 3.2, Experiment I). An ideal close-packed monolayer of Fc on a flat surface has a calculated surface concentration of 4.5×10^{-10} mol cm^{-2},[24] and assuming the typical GC surface roughness factor of 2,[43-45] there is about 24% of a monolayer coverage of Fc on the surface. Clearly, the concentration of Fc groups is lower than that of an ideal close-packed monolayer as expected for a reaction occurring only at surface oxide functionalities on the GC surface.

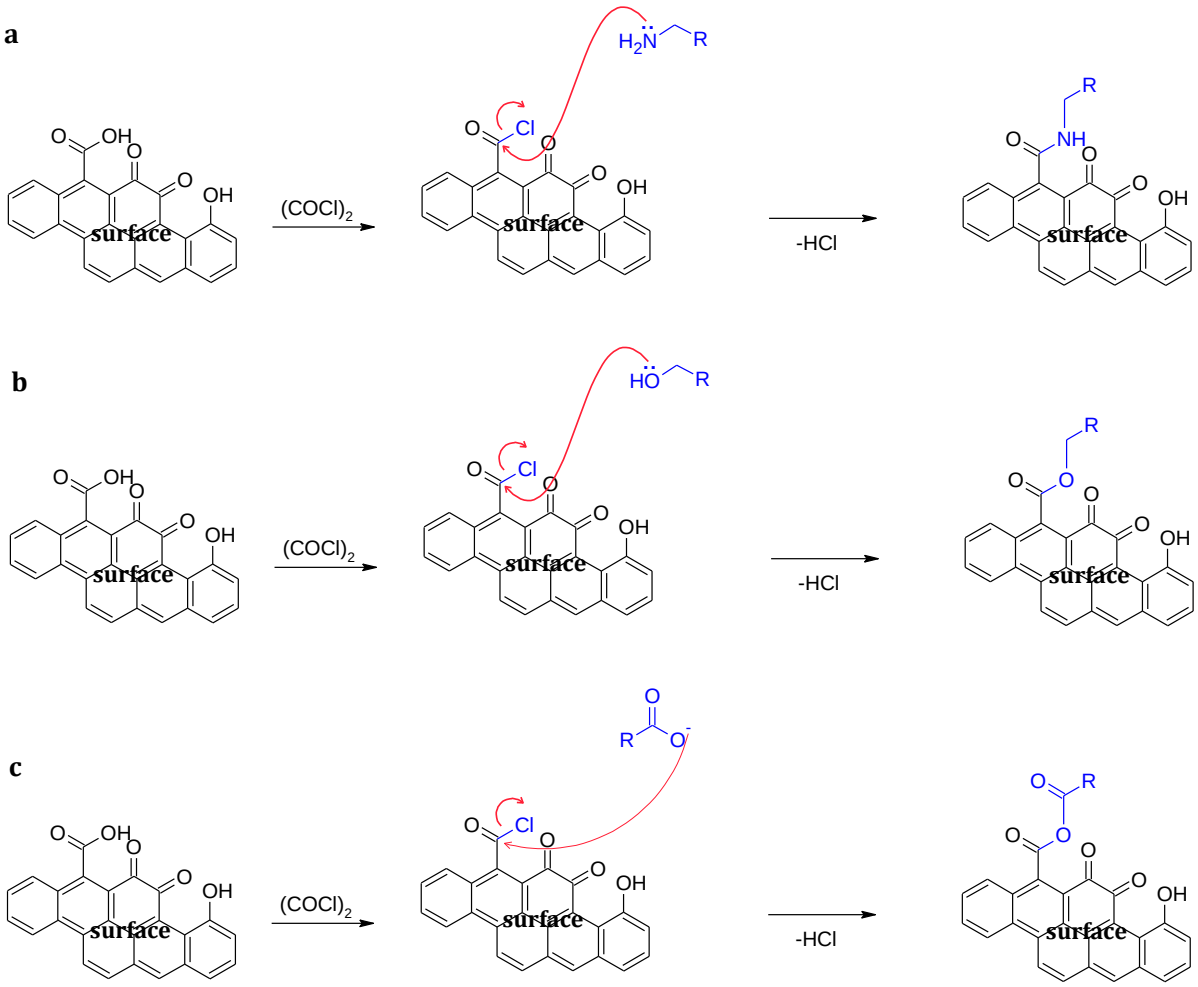

Scheme 3.4 Proposed pathway for reaction of GC activated with $(COCl)_2$ with: a) $FcCH_2NH_2$ or NBA (Table 3.2, Experiment I and II); b) $FcCH_2OH$ (Experiment III); and c) FcCOOH (Experiment IV).

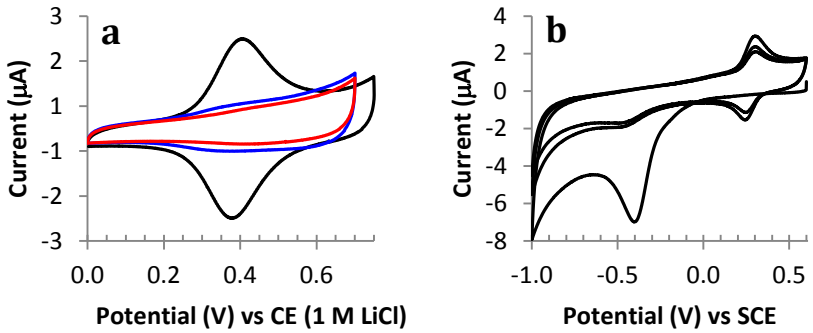

Figure 3.1 a) CVs of GC electrode activated with $(COCl)_2$ and reacted with $FcCH_2NH_2$ (black line), $FcCH_2OH$ (red line) and FcCOOH (blue line). CVs obtained in 0.1 M $LiClO_4$-EtOH at a scan rate of 200 mV s^{-1}; b) three repeat scans of GC electrode activated with $(COCl)_2$ and reacted with NBA.HCl. CVs obtained in 0.1 M H_2SO_4 at a scan rate of 100 mV s^{-1}.

Figure 3.1b shows CVs obtained at an activated GC electrode after reaction with NBA.HCl in the presence of base (Table 3.2, Experiment II). The modified surface shows the expected irreversible reduction peak at E_p ~ -0.4 V arising due to the simultaneous six-electron reduction of NP group to aminophenyl groups and a four-electron reduction to hydroxyaminophenyl groups in 0.1 M H_2SO_4.[49] The hydroxyaminophenyl groups are oxidised to nitrosophenyl groups at $E_{½}$ ~ 0.3 V and the chemically reversible hydroxyaminophenyl/nitrosophenyl couple can be seen on subsequent scans.[49] (The equations for NP reduction processes can be found in Chapter 2.) From the areas under the cyclic voltammetric peaks and the number of electrons involved in each redox process, the surface concentration of NP groups was estimated to be $(2.5 \pm 0.4) \times 10^{-10}$ mol cm^{-2} (Table 3.2, Experiment II). The calculated surface concentration of an ideal close-packed monolayer of NP groups on a flat surface is 12×10^{-10} mol cm^{-2}.[42] Accounting for a typical roughness factor of 2 for a polished GC,[43-45] the surface concentration of NP groups is about 10% of a close-packed monolayer.

Coupling of $(2.2 \pm 0.6) \times 10^{-10}$ mol cm^{-2} Fc and $(2.5 \pm 0.4) \times 10^{-10}$ mol cm^{-2} of NP groups to the surface suggests that the surface concentration of carboxylates on polished GC is ~ 2.4×10^{-10} mol cm^{-2}. To assess how this values compares with O/C ratios determined by XPS (GC plates has total O/C = 0.07) and the values reported by other authors (Table 3.1), the surface concentration of C atoms on GC is required. This was estimated by assuming that GC is a 100% graphite edge-plane surface consisting equal amounts of armchair and zig-zag edges. The calculated distance between C atoms for each type of edge is shown in Figure 3.2., giving an average (assuming an equal amount of armchair and zig-zag plane) of 4.4×10^7 C atoms per cm. Assuming the spacing between graphite sheets is 3.48 Å for GC,[8] the surface concentration of C atoms is estimated to be ~ 22×10^{-10} mol cm^{-2} for a flat surface. The C

atom density for a graphene sheet is 63 × 10^{-10} mol cm^{-2},[52] therefore the estimated concentration of C atoms for GC that consists only of edge-plane C seems reasonable. Thus, by taking into account the roughness factor of GC and assuming there are ~ 44 × 10^{-10} mol cm^{-2} of surface C atoms, a surface concentration of ~ 2.4 × 10^{-10} mol cm^{-2} for carboxylates indicates that ~ 5% of C atoms bear a carboxylate group. As there are 2 O atoms for each carboxylate, this equates to an O/C ratio of 0.1. This is higher than the total O/C ratio found in this work (0.07), but is in the range of reported values for total O/C ratios at polished GC. The discrepancy between the total O/C value and the carboxylate O value may be due to different GC being used in each experiment (GC plates vs GC disks). The carboxylate group values found in this experiment is similar to the value of 0.07 for carboxyl groups reported by Cabaniss and co-workers[13] (Table 3.1, Entry 5). The other value reported for carboxyl groups (Table 3.1, Entry 18) is lower (0.019),[14] but considering the assumptions made in calculating surface concentrations of C atoms on GC, and the surface roughness, and experimental uncertainty, this is reasonable agreement.

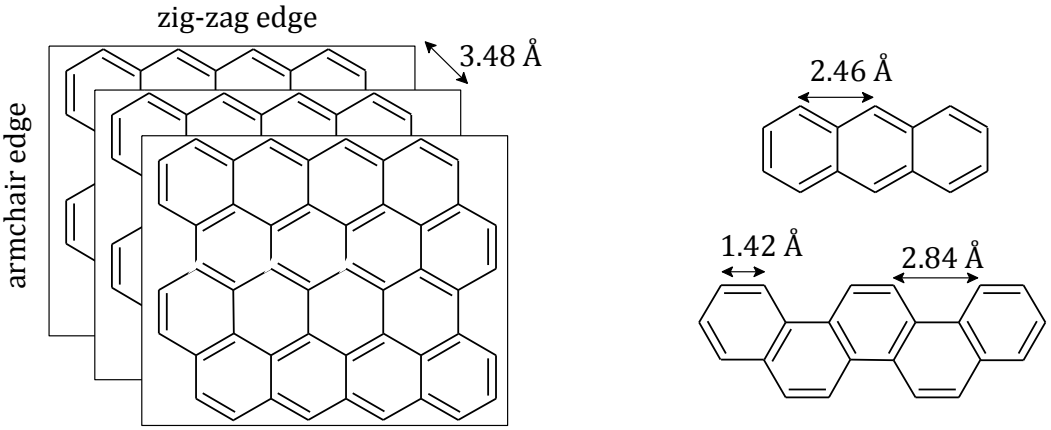

Figure 3.2 C–C atom distance for armchair and zig-zag edges and the intersheet distance of graphite.

When the reaction of $FcCH_2OH$ with activated GC was carried out, no ferrocene/ferrocenium (Fc/Fc^+) redox couple was observed at the treated electrode (Figure 3.1a, red line). This may be due to the fact that –OH is less nucleophilic than a $–NH_2$ group, and therefore, $FcCH_2OH$

does not undergo nucleophilic addition. It is also possible that the reaction does occur but that the ester linkage formed via attack of the surface carboxyl groups (Scheme 3.4b) has decomposed (hydrolysed) before investigation by CV. However, as shown later (Section 3.3.4), ester links are sufficiently stable for the time required to carry out the investigation. Hence, it is unlikely that the reaction of $FcCH_2OH$ with $(COCl)_2$-activated GC has occurred. The reaction of FcCOOH with $(COCl)_2$-activated GC was also attempted. Figure 3.1a blue line, shows that only a trace amount of Fc was immobilised on the surface. FcCOOH is less nucleophilic than $FcCH_2OH$, and hence the trace amount of Fc seen after reaction with FcCOOH is tentatively assigned to physisorption of FcCOOH onto the GC surface, rather than a covalently coupled species (Scheme 3.4c). Considering the successful immobilisation of $FcCH_2NH_2$ and NBA.HCl but the lack of reaction of $FcCH_2OH$ and FcCOOH, it is possible that coupling of the amine derivatives did not in fact proceed through amide bond formation, but through other mechanism, such as a Michael-type addition reaction (discussed later, Section 3.3.3).

3.3.2 Reactions with GC using different amide coupling reagents (Experiments V – X, Table 3.2)

To further investigate whether reactions of amines at $(COCl)_2$-activated GC proceed via amide bond formation, two separate experiments were conducted using different amide coupling reagents (Table 3.2, Experiments V–VIII). Scheme 3.5 shows the expected reaction products. Freshly polished GC electrodes were reacted with $FcCH_2NH_2$ and NBA.HCl either in the presence of EDC + HOBt (Experiments V & VI) or HBTU (Experiments VII & VIII) in DMF overnight. Figure 3.3 shows the CVs of surface-attached Fc obtained via reaction of freshly polished GC with $FcCH_2NH_2$ using EDC + HOBt (black line) and HBTU (blue line) as the coupling agents. From the area under the Fc voltammetric peaks, surface

concentrations of (1.8 ± 0.2) and (1.3 ± 0.2) × 10^{-10} mol cm^{-2} were estimated for Fc coupled using EDC + HOBt and HBTU, respectively (Table 3.2, Experiments V & VII). The Fc concentration obtained from the HBTU method is lower than for the EDC + HOBt method, which in turn is lower than the $(COCl)_2$ method. The higher reaction yield for the $(COCl)_2$ method is expected if the reactions involve amide bond formation, since this reagent gives a cleaner reaction compared to the other two coupling reagents, which usually result in urea as a by-product.[53] However, the different Fc concentrations found for the HBTU and EDC + HOBt methods is surprising since both these amide coupling reagents undergo similar mechanisms (Scheme 3.5). Clearly the different activating agents give different yields. This may indicate that these reactions proceed through different pathways. Moreover, reaction of GC with NBA.HCl using EDC + HOBt and HBTU resulted in surface concentrations of (1.5 ± 0.5) and (1.1 ± 0.2) × 10^{-10} mol cm^{-2}, respectively (Table 3.2, Experiment VI and VIII), which match the Fc results where the surface concentrations decrease in the order of $(COCl)_2$ > EDC + HOBt > HBTU.

To investigate the possibility that $(COCl)_2$ activation increases the carboxylic acid content of polished GC, GC was activated with $(COCl)_2$ and then reacted with water to convert the acid chlorides back to carboxylic acid groups. These surfaces were then reacted with $FcCH_2NH_2$ and NBA.HCl using EDC + HOBt as coupling agents (Table 3.2, Experiment IX and X). Figure 3.3 red line illustrates the CV of surface coupled Fc arising from the reaction of $FcCH_2NH_2$ with $(COCl)_2$ activated, then deactivated, GC. The Fc surface concentration estimated from this CV is (1.3 ± 0.5) × 10^{-10} cm^{-2} (Table 3.2, Experiment IX), which is lower than the surface concentration obtained using EDC + HOBt without prior $(COCl)_2$ activation (Table 3.2, Experiment V). One possibility to account for the lower concentration obtained for the water treated $(COCl)_2$-activated GC is that during handling the activated electrode and

reaction with water, the surface has reacted with adventitious impurities that do not result in carboxylic acid functionalities. Thus the concentration of remaining carboxylic acid functionalities could be less than on the initial polished GC surface. However, considering the uncertainties, these concentrations are similar within experimental error.

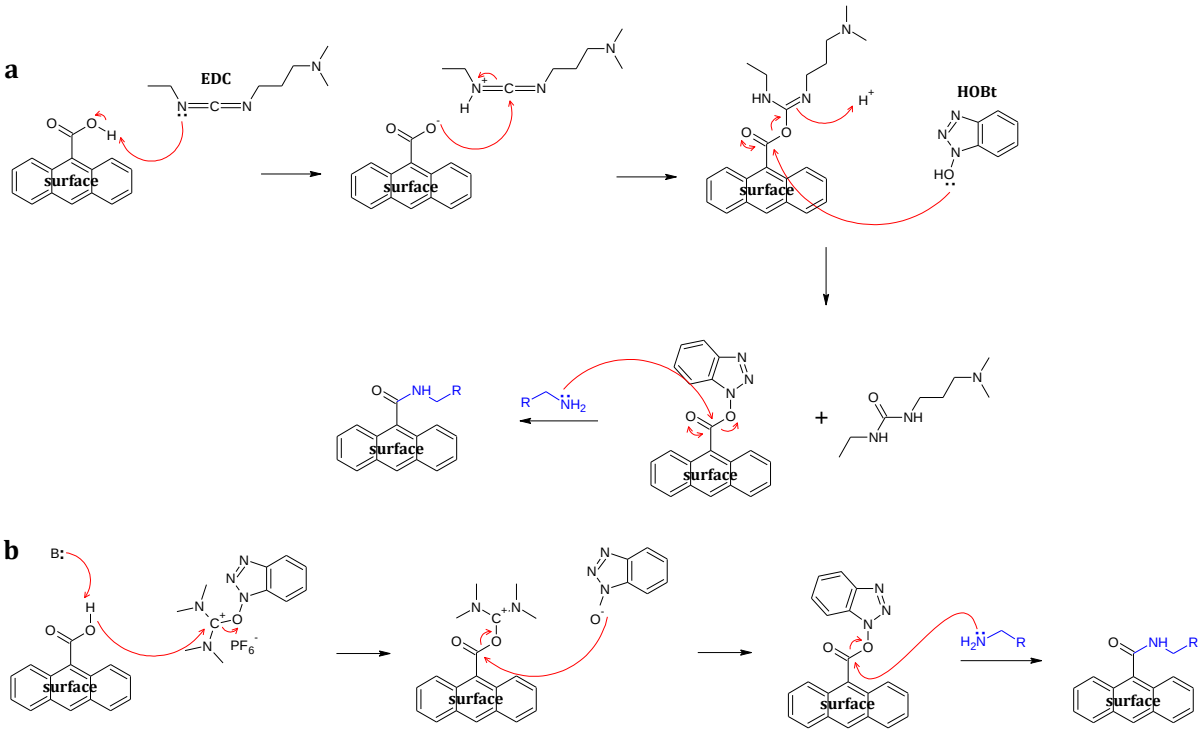

Scheme 3.5 Proposed mechanism for reaction of GC with $FcCH_2NH_2$ or NBA.HCl using: a) EDC + HOBt (Table 3.2, Experiment V & VI); and b) HBTU (Experiment VII & VIII).

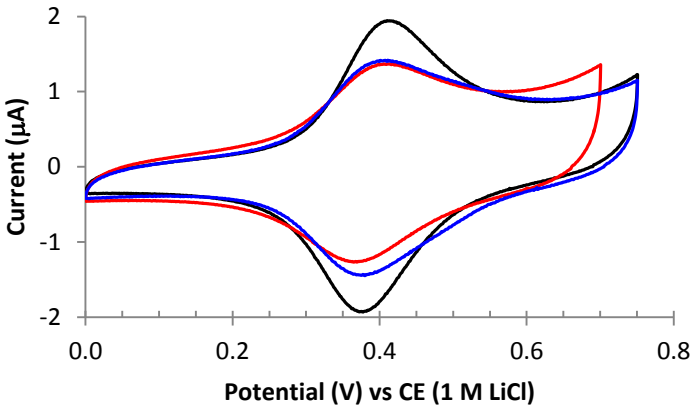

Figure 3.3 CVs obtained in 0.1 M $LiClO_4$-EtOH after reaction of $FcCH_2NH_2$ with: freshly polished GC using EDC + HOBt (black line); freshly polished GC using HBTU (blue line); and GC activated with $(COCl)_2$ and then reacted with water followed by coupling reaction using EDC + HOBt (red line). Scan rate of 200 mV s^{-1}.

The reaction of water-treated $(COCl)_2$-activated GC with NBA.HCl in the presence of EDC + HOBt resulted in a NP surface concentration of $(2.0 \pm 0.3) \times 10^{-10}$ mol cm^{-2} (Table 3.2, Experiment X). Clearly, this value is greater than for the reaction of polished GC with NBA.HCl in the presence of EDC + HOBt (Table 3.2, Experiment VI), which is the opposite trend to the Fc results. However, all of these values are similar within experimental error and these experiments provide no evidence for an increase in surface carboxylic acid groups after activation with $(COCl)_2$.

3.3.3 Reactions of amines directly at polished GC

As discussed in Section 3.1, reaction of amine containing compounds with bare GC via a Michael-type reaction pathway has been reported.[32] The results described above cannot rule out the possibility that a Michael-type mechanism is also part of, or solely, the reaction pathway for reactions employing carboxylic acid activating agents. To examine this possibility, further experiments were undertaken involving the reaction of $FcCH_2NH_2$ directly with polished GC. Table 3.3 lists the conditions used to directly attach Fc groups to GC, and the corresponding surface concentrations of immobilised Fc groups. The spontaneous attachment of primary amines to GC electrode reported by Gallardo and co-workers[32] were conducted in ACN as the solvent. In the present work, the reactions of GC with $FcCH_2NH_2$ were also undertaken in DCM and DMF, the same solvents used for the amide bond coupling reactions. Figure 3.4 shows the CVs of Fc immobilised by immersion of freshly polished GC in 10 mM solutions of $FcCH_2NH_2$ overnight at room temperature. The surface concentrations of Fc groups determined from the area under the CV peaks are (6.2 ± 0.9), (2.6 ± 0.2), and $(2.2 \pm 0.4) \times 10^{-10}$ mol cm^{-2} for reactions undertaken in ACN, DMF and DCM, respectively (Table 3.3, Experiments I–III). The Fc concentration for the reaction undertaken in ACN is similar to that found by Gallardo and co-workers[32] ($(6.0 - 7.7) \times 10^{-10}$ mol cm^{-2} for 6 h

immersion), which is higher than the theoretical calculated monolayer value on a flat surface (4.5×10^{-10} mol cm^{-2}).[24] However, considering the surface roughness factor of GC ~2,[43-45] the Fc concentration obtained in ACN is within monolayer coverage.

It is apparent that, the spontaneous reaction of amine with GC is dependent on the solvent, with ACN yielding the highest surface concentration. This can be attributed to differences in solvation of the amines and also because DMF and DCM are less acidic than ACN, which means that in ACN, the aliphatic amines are stronger bases. Hence, ACN will promote the Michael-type addition mechanism and the observed solvent dependency is good evidence for a Michael-type reaction.

Table 3.3 Reaction of $FcCH_2NH_2$ directly with freshly polished GC electrodes in different solvents and applied potentials as listed, and the corresponding surface concentrations of electro-active ferrocene attached to the GC surface.

Expt.	Activation of GC	Applied potential (V)	Reaction Solvent	$E_{½}$ (V)	Γ_{Fc} (10^{-10} mol cm^{-2})	n^a
I	-	-	ACN	0.38	6.2 ± 0.9	5
II	-	-	DMF	0.39	2.6 ± 0.2	6
III	-	-	DCM	0.41	2.2 ± 0.4	4
IV	-	-0.8	DMF	0.38	0.6 ± 0.2	2
V	-	+0.2	DMF	0.39	3.7 ± 0.4	2

[a] *n* is the number of samples analysed

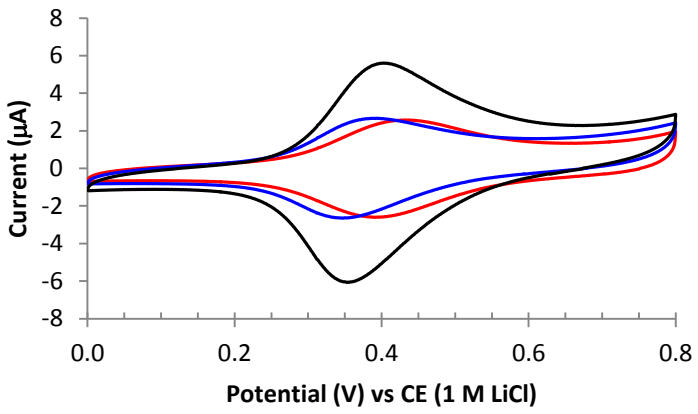

Figure 3.4 CVs obtained in 0.1 M $LiClO_4$-EtOH after direct reaction of GC with $FcCH_2NH_2$ in: ACN (black line); DMF (blue line); and DCM (red line). Scan rate of 200 mV s^{-1}.

As shown in Scheme 3.3 Michael-type addition involves the attack of amine derivatives at the double bond of GC with electron delocalisation across the aromatic GC network. To find further evidence to support the proposal of a Michael-type addition mechanism, reactions of amines with GC were carried out under conditions where the electron accepting nature of GC was enhanced or decreased. For this purpose, a potential was applied to the GC electrode during the reaction. Figure 3.5, black line, is a CV obtained after the GC electrode was immersed (for ~ 16 h) in a 10 mM solution of $FcCH_2NH_2$ in DMF at open circuit potential (OCP ~ 0 V vs Ag wire). Six repeat experiments gave a surface concentration of $(2.6 \pm 0.2) \times 10^{-10}$ mol cm^{-2} (Table 3.3, Experiment II). When the experiment was repeated but with a potential of -0.8 V (vs Ag wire) applied to the GC electrode, the CV shown in blue (Figure 3.5) was obtained. The average surface concentration of two repeat experiments was $(0.6 \pm 0.2) \times 10^{-10}$ mol cm^{-2} (Table 3.3, Experiment IV). Moreover, repeat experiments with an applied potential of 0.2 V resulted in the CV shown in red (Figure 3.5) and an average surface concentration of $(3.7 \pm 0.4) \times 10^{-10}$ mol cm^{-2} was obtained (Table 3.3, Experiment V). Note that for these experiments under an applied potential, 0.1 M $TBABF_4$ was added to the reaction solutions. For the reaction carried out at -0.8 V, the solvent was degassed with N_2 prior to application of the potential and N_2 atmosphere was maintained throughout the experiment. The applied potential of 0.2 V was chosen to be prior to the onset potential for the Fc oxidation in 0.1 M $TBABF_4$-DMF solution ($E_{½}$ = 0.55 V vs Ag wire).

These results show that the amount of Fc immobilised on the surface is strongly dependent on the applied potential during the reaction. This dependency is consistent with the reaction proceeding via a Michael-type addition. At -0.8 V the ability of the GC electrode to delocalise electrons is expected to be significantly decreased compared to at OCP and the yield of the reaction decreases accordingly. On the other hand, the electron delocalisation

ability of the electrode should be greater at 0.2 V than at OCP and the expected increase in reaction yield with $FcCH_2NH_2$ is observed. However, promoting or decreasing the electron accepting nature of the GC will not only support the Michael-type reaction, but all nucleophilic addition reactions.

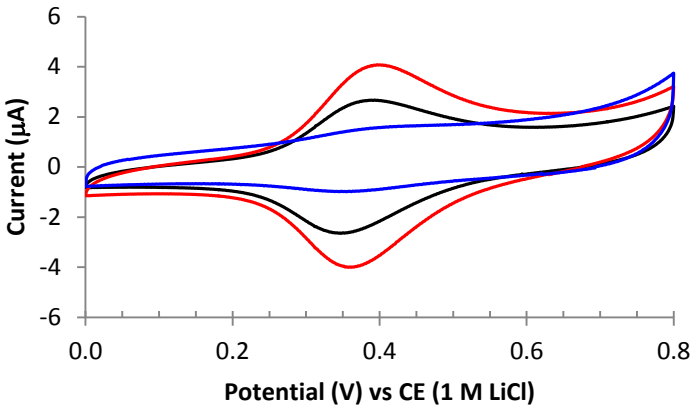

Figure 3.5 CVs obtained in 0.1 M $LiClO_4$-EtOH after direct reaction of GC with $FcCH_2NH_2$ in DMF: without applied potential (black line); applied -0.8 V (blue line); and applied +0.2 V (red line). Scan rate of 200 mV s^{-1}.

Another possible pathway for the spontaneous reaction of amines with surface oxides on GC is the spontaneous formation of imines.[39] This reaction has been proposed to account for the immobilisation of thionine on oxidised GC (via the aldehyde group).[39] While this reaction pathway cannot be completely discounted for the reactions described in this work, the stability of the resulted surfaces (Section 3.3.4) suggests that imines are unlikely to be the major component, since imine linkages are known to be unstable towards hydrolysis. Furthermore, if the reaction of $FcCH_2NH_2$ with surface aldehydes and ketones proceeds quantitatively and hence their concentration is in the range of $(2.2 – 6.2) \times 10^{-10}$ mol cm^{-2}, this corresponds to an O/C ratio of 0.05 (estimated from reactions performed in DMF and DCM) – 0.14 (estimated from reactions performed in ACN). XPS analysis of polished GC plates gave a total O/C ratio of 0.07 and hence the amount of Fc grafted to GC by direct reaction in ACN solution is significantly greater than that expected based only on reactions

with surface aldehydes or ketones. For the reaction carried out in DMF and DCM, it is possible that reaction proceed via imine formation, but this is unlikely. XPS measurement of GC reveals that in the majority or reports, hydroxyl groups account for a large proportion of surface oxygen on polished GC (Table 3.1), and therefore aldehydes and ketones are expected to be present in small amount, and hence these results are consistent with Michael-type addition as the major or sole reaction responsible for immobilisation of FC groups by direct reaction of $FcCH_2NH_2$ with polished GC.

Considering the facile reaction between amines and GC via a Michael-type reaction mechanism and following the same reasoning as above (~0.1 O/C ratio obtained from reaction in the presence of amide activating agent), it seems likely that this Michael-type reaction occurs during the amide coupling reactions described in Section 3.3.1 and 3.3.2. For reaction of amine containing compounds with GC in the presence of an activating agent (HBTU, EDC + HOBt, or $(COCl)_2$), amide bonds are expected to be the linking group between the modifier and the surface as depicted in Schemes 3.4 and 3.5. On the other hand, for a Michael-type addition reaction, covalent bonds between the amine nitrogen and the GC surface carbon to form a N–C linkage is expected (Scheme 3.3). These different linkages might be expected to give different Fc redox potential ($E_{½}$ values), however, the electron donating $–CH_2$ groups directly adjacent to the Fc will have a major influence on $E_{½}$ for the Fc/Fc^+ couple. This is confirmed by the $E_{½}$ values in Table 3.2 and Table 3.3 which are all close to 0.4 V. However, while the $E_{½}$ values are all similar, they vary by up to 30 mV which is outside the estimated experimental uncertainty (± 10 mV). Close examination of the proposed surface structure and the CVs does not reveal any trends or explanation for these values. Hence, on the basis of the results described for reaction between GC and amines in the presence and absence of activating agents, it is not possible to determine to what extent

Michael-type addition and imine formation occur simultaneously with amide coupling (for reactions undertaken in the presence of activating agents), or even if amide coupling occurs at all.

3.3.4 Reactions of activated carboxylate derivatives of Fc with polished GC

The reactions of polished GC with 4-nitrobenzoic acid (NO_2-Ar-COOH), FcCOOH and $FcCH_2COOH$ after activation of the carboxylic acid derivatives with $(COCl)_2$ were examined (Table 3.4, Experiment I and III). Figure 3.6a shows the CVs of GC reacted with $(COCl)_2$-activated NO_2-Ar-COOH (Table 3.4, Experiment I), and Figures 3.6b and 3.6c show well-defined CVs of immobilised Fc obtained after reaction of bare GC with $(COCl)_2$-activated FcCOOH and $FcCH_2COOH$, respectively. The NP modified electrode shows the expected irreversible reduction of NP groups at $E_{p,c}$ ~ -0.35 V, and a reversible hydroxyaminophenyl/nitrosophenyl couple at $E_{½}$ ~ 0.3 V. From the area under the voltammetric peaks, the surface concentrations of NP groups were determined to be $2.4 \pm 0.2 \times 10^{-10}$ mol cm^{-2} (Table 3.4, Experiment I), and the surface concentrations of Fc groups are calculated to be (1.6 ± 0.2) and $(2.4 \pm 0.4) \times 10^{-10}$ mol cm^{-2} for FcCOOH and $FcCH_2COOH$, respectively (Table 3.4, Experiment II and III). Similar concentrations were obtained for immobilised NP and Fc groups (via $FcCH_2COOH$), while a lower value was obtained from FcCOOH coupling. This lower value may be due to greater steric hindrance for FcCOOH compared to $FcCH_2COOH$ when reacted with GC. As expected, the Fc that is directly attached to carboxylic acid substituent (FcCOOH, Figure 3.6b) has a higher $E_{½}$ (i.e. is more difficult to oxidise) than the Fc that has an electron donating $–CH_2$ group linking to the acid ($FcCH_2COOH$, Figure 3.6c).

Table 3.4 Reaction of $(COCl)_2$ activated carboxylic acid derivatives with polished GC electrodes, and the corresponding surface concentrations of electro-active species attached to the GC surface. Also, the effect of KOH on the surface concentration of Fc groups immobilised by different methods.

Expt.	Nature of GC	Modifying Species	KOH treatment	$E_{½}$ (Fc/Fc$^+$) (V)	Γ_{Fc} (10^{-10} mol cm^{-2})	n^a
I	Polished	NO_2-Ar-COOH + $(COCl)_2$	No	-	2.4 ± 0.2	2
II	Polished	FcCOOH + $(COCl)_2$	No	0.66	1.6 ± 0.2	2
III	Polished	$FcCH_2COOH$ + $(COCl)_2$	No	0.40	2.4 ± 0.4	3
IV	Polished	$FcCH_2COOH$ + $(COCl)_2$	Yes	0.45	0.3 ± 0.1	2
V[b]	Polished	$FcCH_2NH_2$	Yes	0.42	1.2 ± 0.1	2
VI[c]	Activated with $(COCl)_2$	$FcCH_2NH_2$	Yes	0.40	1.4 ± 0.1	2
VII[d]	Grafted with Boc-NH-CH_2-Ar-N_2^+	$FcCH_2COOH$ + HBTU	No	0.31	4.0 ± 0.4	4
VIII[d]	Grafted with Boc-NH-CH_2-Ar-N_2^+	$FcCH_2COOH$ + HBTU	Yes	0.31	3.3 ± 0.7	2

[a] *n* is the number of samples analysed

[b] Reaction conditions are the same as Table 3.3, Experiment III

[c] Reaction conditions are the same as Table 3.2, Experiment I

[d] GC was first grafted with Boc-NH-CH_2-Ar-N_2^+ followed by deprotection in 4 M HCl-MeOH and coupling reaction with $FcCH_2COOH$ using HBTU as the coupling agent(Chapter 6)

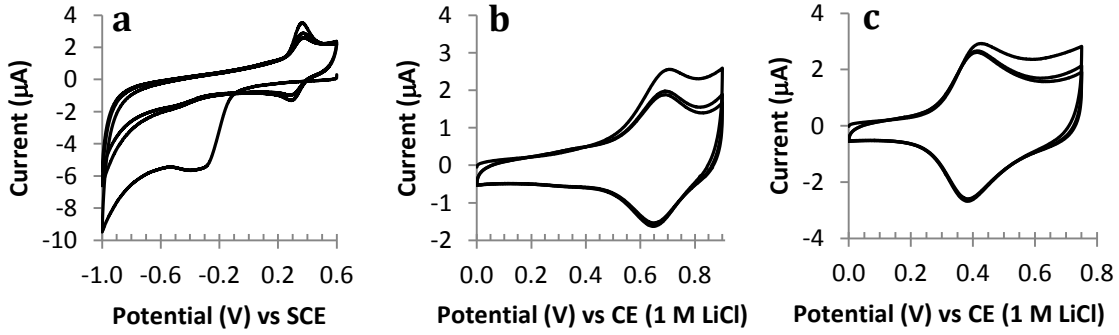

Figure 3.6 Three consecutive CV scans obtained in: a) 0.1 M H_2SO_4 at a scan rate of 100 mV^{-1}, b, c) 0.1 M $LiClO_4$-EtOH at a scan rate of 200 mV s^{-1}, at GC electrodes after reaction with $(COCl)_2$-activated: a) NO_2-Ar-COOH, b) FcCOOH, and c) $FcCH_2COOH$.

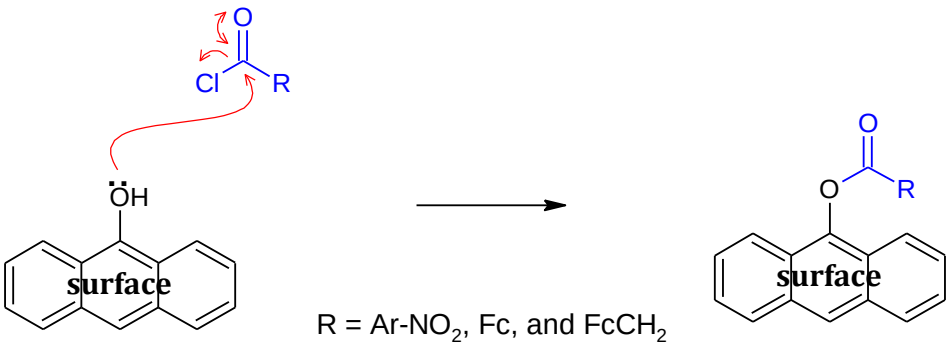

Scheme 3.6 Proposed mechanism for reaction of GC with $(COCl)_2$-activated carboxylic acid derivatives (Table 3.4, Experiment I – III).

The mechanism for the reaction between activated carboxylate derivatives and GC is unknown, but it is likely that a surface hydroxyl group attacks the carbonyl group of the carboxylic acid derivatives to give an ester linkage (Scheme 3.6). To test this hypothesis, a hydrolysis reaction was carried out on the modified electrode. Ester linkages readily hydrolyse in the presence of acid or base.[54, 55] Thus, after the GC electrode was modified with $(COCl)_2$-activated $FcCH_2COOH$, it was subjected to sonication in 0.15 M KOH solution for 25 min. Figure 3.7 shows the CVs of surface attached Fc before (black line) and after (red line) sonication in KOH solution. Figure 3.7a shows that after treatment in KOH, the amount of Fc remaining on the surface is very small. The calculated surface concentration after sonication in 0.15 M KOH is $(0.3 \pm 0.1) \times 10^{-10}$ mol cm^{-2} (Table 3.4, Experiment IV), which corresponds to a 88% decrease in surface concentration. This observation is consistent with the existence of an ester linkage that is readily hydrolysed by KOH. For comparison, two further experiments were undertaken. GC was modified by activation with $(COCl)_2$ followed by reaction with $FcCH_2NH_2$ and also by direct reaction of polished GC with $FcCH_2NH_2$ in DCM. The modified electrodes were sonicated for 25 min in 0.15 M KOH solution. As seen in Figures 3.7b and 3.7c, the decrease in peak current after sonication in KOH (red line) is significantly less than in Figure 3.7a. For the modified electrodes shown in Figure 3.7b and 3.7c, the surface concentration after KOH treatment was determined to be (1.2 ± 0.1) and (1.4

$\pm$ 0.1) $\times$ 10^{-10} mol cm^{-2} (Table 3.4, Experiment V and VI), which corresponds to a (45 $\pm$ 5)% and (49 $\pm$ 5)% decrease in surface concentration for the reaction of GC directly with $FcCH_2NH_2$ and the reaction of GC with $FcCH_2NH_2$ in the presence of $(COCl)_2$, respectively. Note, the percentage decrease is calculated from the ratio of the Fc surface concentration before and after treatment in KOH of the same modified electrodes. This clearly indicates that the linkage formed from the reaction of bare GC with $(COCl)_2$ activated $FcCH_2COOH$ is different to the linkages formed from the direct reaction of bare GC with $FcCH_2NH_2$ and from the reaction of GC with $FcCH_2NH_2$ in the presence of $(COCl)_2$ and supports the formation of an ester linkage in the former reaction.

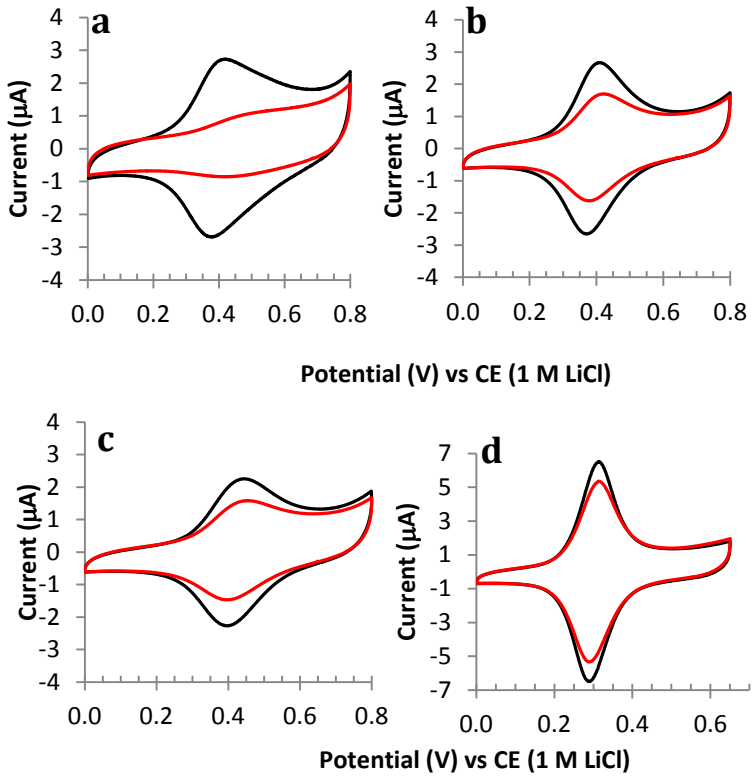

Figure 3.7 CVs obtained in 0.1 M $LiClO_4$-EtOH of: a) bare GC reacted with $(COCl)_2$ activated $FcCH_2COOH$; b) GC activated with $(COCl)_2$ reacted with $FcCH_2NH_2$; c) bare GC immersed in a DCM solution of $FcCH_2NH_2$; and d) GC was grafted with Boc-NH-CH_2-Ar layer followed by deprotection of the Boc group and coupling reaction with $FcCH_2COOH$. Black line: modified GC before treatment in KOH; red line: modified GC after sonication in 0.15 M KOH for 25 min. Scan rate was 200 mV s^{-1}.

The origin of the decrease in surface concentration after treatment in KOH for electrodes modified by reaction of $FcCH_2NH_2$ directly with GC and with $(COCl)_2$-activated GC (Figure 3.7b and 3.7c) was investigated further. Despite being more stable than an ester, amide linkages are also known to undergo hydrolysis reactions.[56] A further experiment was conducted to investigate the stability of amide linkages upon sonication in KOH solution. A GC electrode was first modified with a Boc-protected aminomethylphenyl film (Boc-NH-CH_2-Ar-GC, Chapter 6), followed by deprotection of the Boc-groups and coupling of $FcCH_2COOH$ to the aminomethylphenyl surface (NH_2-CH_2-Ar-GC) to yield Fc immobilised via amide linkages (Scheme 6.2). This surface can be assumed to have Fc immobilised onto the GC surface by amide linkages only. (As in a blank experiment, only a small amount of Fc was detected after reaction of $FcCH_2COOH$ with bare GC under the same conditions, see Chapter 6.) Figure 3.7d shows that after treatment in KOH solution (red line) there was a 22% decrease in surface concentration of Fc groups (Table 3.4, Experiment VII and VIII). This indicates that the amide linkage has good stability upon sonication in KOH solution.

Considering this result, the ~50% decrease in Fc concentration after sonication of the electrode prepared by reaction of $FcCH_2NH_2$ with $(COCl)_2$-activated GC is unlikely to be due solely to hydrolysis of amide linkages. There are two possible explanations for the decrease in Fc surface concentration after sonication in KOH for this surface. First, Fc might be lost by hydrolysis at an amide link plus removal of physisorbed material and/or removal of Fc attached to the surface by a Michael-type addition reaction. A second possibility is that there is only a small amount of Fc, if any, attached via an amide link and Fc is in fact mostly or solely attached through direct reaction with the GC surface (the Michael-type addition pathway). The very similar stability of the two types of surface ($FcCH_2NH_2$ attached by direct reaction and after activation of GC with $(COCl)_2$) after KOH treatment support the

second suggestion. It is not clear why the Michael-type addition product would be less stable than the amide linkage. However, my observations throughout the course of this thesis work indicate that the shorter the link between the Fc groups and GC, the less stable the Fc. Hence, the instability may not due to the link between the Fc and the surface, but due to the Fc moiety itself.

3.4 Conclusion

GC readily reacts directly with amine derivatives as reported previously.[32] The observed solvent dependency and requirement for electron delocalisation support the conclusion of earlier works that a Michael-type addition mechanism is responsible for the reaction. The more basic ACN yields the highest surface concentration ($(6.2 \pm 0.9) \times 10^{-10}$ mol cm^{-2}), and a negative potential applied to the GC led to only trace amounts of immobilised Fc. GC activated with $(COCl)_2$ also reacts readily with amine derivatives. The results obtained from surface concentration calculations, $E_{½}$ measurement, and hydrolysis experiments indicate that reaction with and without $(COCl)_2$ as activating agent result in modified GC with similar properties. This suggests that the Michael-type addition pathway may be responsible for both reactions. In addition, Fc can be attached to GC via the reaction of polished GC with $(COCl)_2$-activated carboxylic acid derivatives, most likely via the formation of ester linkages. An important characteristic of these different methods for modification of GC is that multilayer coatings are not formed. Surface concentrations are consistent with monolayers or sub-monolayers. As expected, because these reactions can only occur directly on the GC surface and coupling onto already immobilised molecules should not be possible. This property is useful for fabrication of mixed layers using these reactions to fill the spaces in a prior grafted sparse monolayer. These methods for forming mixed layers are described in

Chapters 4 and 6. The reactions described in this Chapter are also the blanks for coupling reaction to monolayers grafted from aryldiazonium salts as described in Chapters 5 and 6.

3.5 References

1 Jenkins, G.M., Kawamura, K., Structure of glassy carbon. *Nature*, **1971**, *231*, 175.

2 Jenkins, G.M., Kawamura, K., Ban, L.L., Formation and structure of polymeric carbons. *P. Roy. Soc. Lond. A. Mat.*, **1972**, *327*, 501.

3 Harris, P.J.F., Fullerene-related structure of commercial glassy carbons. *Philos. Mag.*, **2004**, *84*, 3159.

4 Harris, P.J.F., New perspectives on the structure of graphitic carbons. *Crit. Rev. Solid State*, **2005**, *30*, 235.

5 Pesin, L.A., Structure and properties of glass-like carbon. *J. Mater. Sci.*, **2002**, *37*, 1.

6 Pesin, L.A., Baitinger, E.M., A new structural model of glass-like carbon. *Carbon*, **2002**, *40*, 295.

7 Brown, N.M.D., You, H.X., Surface-structure of a glassy-carbon - scanning tunneling microscopy study. *J. Mater. Chem.*, **1991**, *1*, 469.

8 McCreery, R.L., Advanced carbon electrode materials for molecular electrochemistry. *Chem. Rev.*, **2008**, *108*, 2646.

9 Wildgoose, G.G., Abiman, P., Compton, R.G., Characterising chemical functionality on carbon surfaces. *J. Mater. Chem.*, **2009**, *19*, 4875.

10 Engstrom, R.C., Strasser, V.A., Characterization of electrochemically pretreated glassy-carbon electrodes. *Anal. Chem.*, **1984**, *56*, 136.

11 Fryling, M.A., Zhao, J., McCreery, R.L., Resonance Raman observation of surface carbonyl groups on carbon electrodes following dinitrophenylhydrazine derivatization. *Anal. Chem.*, **1995**, *67*, 967.

12 Kiema, G.K., Aktay, M., McDermott, M.T., Preparation of reproducible glassy carbon electrodes by removal of polishing impurities. *J. Electroanal. Chem.*, **2003**, *540*, 7.

13 Cabaniss, G.E., Diamantis, A.A., Murphy, W.R., Linton, R.W., Meyer, T.J., Electrocatalysis of proton-coupled electron-transfer reactions at glassy-carbon electrodes. *J. Am. Chem. Soc.*, **1985**, *107*, 1845.

14 Sundberg, K.M., Smyrl, W.H., Atanasoska, L., Atanasoski, R., Surface modification and oxygen reduction on glassy-carbon in chloride media. *J. Electrochem. Soc.*, **1989**, *136*, 434.

15 Chen, P.H., McCreery, R.L., Control of electron transfer kinetics at glassy carbon electrodes by specific surface modification. *Anal. Chem.*, **1996**, *68*, 3958.

16 Ray, K.R., McCreery, R.L., Characterization of the surface carbonyl and hydroxyl coverage on glassy carbon electrodes using Raman spectroscopy. *J. Electroanal. Chem.*, **1999**, *469*, 150.

17 Zhao, Q.L., Zhang, Z.L., Bao, L., Pang, D.W., Surface structure-related electrochemical behaviors of glassy carbon electrodes. *Electrochem. Commun.*, **2008**, *10*, 181.

18 Kamau, G.N., Willis, W.S., Rusling, J.F., Electrochemical and electron spectroscopic studies of highly polished glassy-carbon electrodes. *Anal. Chem.*, **1985**, *57*, 545.

19 Collier, W.G., Tougas, T.P., Determination of surface hydroxyl-groups on glassy-carbon with X-ray photoelectron-spectroscopy preceded by chemical derivatization. *Anal. Chem.*, **1987**, *59*, 396.

20 Tougas, T.P., Collier, W.G., Determination of surface carbonyl groups on glassy-carbon with X-ray photoelectron-spectroscopy preceded by derivatization with pentafluorophenylhydrazine. *Anal. Chem.*, **1987**, *59*, 2269.

21 Briggs, D., Kendall, C.R., Derivatization of discharge-treated LDPE: An extension of XPS analysis and a probe of specific interactions in adhesion. *Int. J. Adhes. Adhes.*, **1982**, *2*, 13.

22 Yacynych, A.M., Kuwana, T., Cyanuric chloride as a general linking agent for modified electrodes: Attachment of redox groups to pyrolytic graphite. *Anal. Chem.*, **1978**, *50*, 640.

23 Ianniello, R.M., Yacynych, A.M., Immobilized enzyme chemically modified electrode as an amperometric sensor. *Anal. Chem.*, **1981**, *53*, 2090.

24 Chidsey, C.E.D., Bertozzi, C.R., Putvinski, T.M., Mujsce, A.M., Coadsorption of ferrocene-terminated and unsubstituted alkanethiols on gold - electroactive self-assembled monolayers. *J. Am. Chem. Soc.*, **1990**, *112*, 4301.

25 Firth, B.E., Miller, L.L., Mitani, M., Rogers, T., Lennox, J., Murray, R.W., Anodic and cathodic reactions on a chemically modified edge surface of graphite. *J. Am. Chem. Soc.*, **1976**, *98*, 8271.

26 Watkins, B.F., Behling, J.R., Kariv, E., Miller, L.L., Chiral electrode. *J. Am. Chem. Soc.*, **1975**, *97*, 3549.

27 Bourdillon, C., Bourgeois, J.P., Thomas, D., Covalent linkage of glucose-oxidase on modified glassy-carbon electrodes - kinetic phenomena. *J. Am. Chem. Soc.*, **1980**, *102*, 4231.

28 Ianniello, R.M., Lindsay, T.J., Yacynych, A.M., Immobilized xanthine-oxidase chemically modified electrode as a dual analytical sensor. *Anal. Chem.*, **1982**, *54*, 1980.

29 Elliott, C.M., Murray, R.W., Chemically modified carbon electrodes. *Anal. Chem.*, **1976**, *48*, 1247.

30 Kesavan, S., Abraham John, S., Spontaneous grafting: A novel approach to graft diazonium cations on gold nanoparticles in aqueous medium and their self-assembly on electrodes. *J. Colloid. Interf. Sci.*, **2014**, *428*, 84.

31 Buttry, D.A., Peng, J.C.M., Donnet, J.B., Rebouillat, S., Immobilization of amines at carbon fiber surfaces. *Carbon*, **1999**, *37*, 1929.

32 Gallardo, I., Pinson, J., Vila, N., Spontaneous attachment of amines to carbon and metallic surfaces. *J. Phys. Chem. B*, **2006**, *110*, 19521.

33 Jeevagan, A.J., John, S.A., Electrochemical sensor for guanine using a self-assembled monolayer of 1,8,15,22-tetraaminophthalocyanatonickel(II) on glassy carbon electrode. *Anal. Biochem.*, **2012**, *424*, 21.

34 Sivanesan, A., John, S.A., Adsorption thermodynamics and kinetics study for the self-assembly of 1,8,15,22-tetraaminophthalocyanatocobalt(II) on glassy carbon surface. *Electrochim. Acta*, **2009**, *54*, 7458.

35 Wildgoose, G.G., Hyde, M.E., Lawrence, N.S., Leventis, H.C., Jiang, L., Jones, T.G.J., Compton, R.G., 4-nitrobenzylamine partially intercalated into graphite powder and multiwalled carbon nanotubes: Characterization using X-ray photoelectron spectroscopy and in situ atomic force microscopy. *Langmuir*, **2005**, *21*, 4584.

36 Zawadzki, J., Infrared studies on the adsorption of normal-butylamine on carbon-films. *Carbon*, **1988**, *26*, 183.

37 Muthukumar, P., John, S.A., Effect of amine substituted at *ortho* and *para* positions on the electrochemical and electrocatalytic properties of cobalt porphyrins self-assembled on glassy carbon surface. *Electrochim. Acta*, **2014**, *115*, 197.

38 Jeevagan, A.J., John, S.A., Electrochemical determination of caffeine in the presence of paracetamol using a self-assembled monolayer of non-peripheral amine substituted copper(II) phthalocyanine. *Electrochim. Acta*, **2012**, *77*, 137.

39 Xu, X.Y., Feng, Y., Li, J.J., Li, F., Yu, H.J., A novel protocol for covalent immobilization of thionine on glassy carbon electrode and its application in hydrogen peroxide biosensor. *Biosens. Bioelectron.*, **2010**, *25*, 2324.

40 Gautier, C., Ghodbane, O., Wayner, D.D.M., Belanger, D., Modification of glassy carbon electrodes by 4-chloromethylphenyl units and D-glucosaminic acid. *Electrochim. Acta*, **2009**, *54*, 6327.

41 Smith, R.D.L., Pickup, P.G., Novel electroactive surface functionality from the coupling of an aryl diamine to carbon black. *Electrochem. Commun.*, **2009**, *11*, 10.

42 Liu, Y.C., McCreery, R.L., Reactions of organic monolayers on carbon surfaces observed with unenhanced Raman-spectroscopy. *J. Am. Chem. Soc.*, **1995**, *117*, 11254.

43 McDermott, M.T., Kneten, K., McCreery, R.L., Anthraquinonedisulfonate adsorption, electron-transfer kinetics, and capacitance on ordered graphite-electrodes - the important role of surface-defects. *J. Phys. Chem.*, **1992**, *96*, 3124.

44 McDermott, M.T., McDermott, C.A., McCreery, R.L., Scanning tunneling microscopy of carbon surfaces - relationships between electrode-kinetics, capacitance, and morphology for glassy-carbon electrodes. *Anal. Chem.*, **1993**, *65*, 937.

45 Pontikos, N.M., McCreery, R.L., Microstructural and morphological-changes induced in glassy-carbon electrodes by laser irradiation. *J. Electroanal. Chem.*, **1992**, *324*, 229.

46 He, Z., Bhattacharyya, S., Leavy, M.C., Cleland, W.E., Sabapathy, R.C., Hussey, C.L., A voltammetric investigation of the reactions between surface-confined amines and quinones on gold electrodes: Evidence for imine formation. *J. Electroanal. Chem.*, **1998**, *458*, 7.

47 Kepley, L.J., Bard, A.J., Ellipsometric, electrochemical, and elemental characterization of the surface phase produced on glassy-carbon electrodes by electrochemical activation. *Anal. Chem.*, **1988**, *60*, 1459.

48 Baramee, A., Coppin, A., Mortuaire, M., Pelinski, L., Tomavo, S., Brocard, J., Synthesis and in vitro activities of ferrocenic aminohydroxynaphthoquinones against *Toxoplasma gondii* and *Plasmodium falciparum*. *Bioorg. Med. Chem.*, **2006**, *14*, 1294.

49 Yu, S.S.C., Tan, E.S.Q., Jane, R.T., Downard, A.J., An electrochemical and XPS study of reduction of nitrophenyl films covalently grafted to planar carbon surfaces. *Langmuir*, **2007**, *23*, 11074.

50 Loring, J.S., *Linkfit*. **2000**, Ph.D. Dissertation, University of California, Davis: University of California, Davis.

51 Bard, A.J., Faulkner, L.R., *Electrochemical methods fundamentals and applications*. Second ed. **2001**: John Wiley & Sons, Inc.

52 Jung, N., Crowther, A.C., Kim, N., Kim, P., Brus, L., Raman enhancement on graphene: Adsorbed and intercalated molecular species. *ACS Nano*, **2010**, *4*, 7005.

53 Montalbetti, C., Falque, V., Amide bond formation and peptide coupling. *Tetrahedron*, **2005**, *61*, 10827.

54 Newling, W.B.S., Hinshelwood, C.N., The kinetics of the acid and the alkaline hydrolysis of esters. *J. Chem. Soc.*, **1936**, 1357.

55 Stefanidis, D., Jencks, W.P., General base catalysis of ester hydrolysis. *J. Am. Chem. Soc.*, **1993**, *115*, 6045.

56 Marlier, J.F., Multiple isotope effects on the acyl group transfer reactions of amides and esters. *Accounts Chem. Res.*, **2001**, *34*, 283.

Chapter 4. Preparation of Ethynyl Terminated Monolayers and Mixed Monolayers

4.1 Introduction

As described in Chapter 1, grafting via aryldiazonium salts usually leads to disordered multilayers.[1-5] The mechanism for the formation of multilayers is shown in Scheme 1.2, Chapter 1; it involves the attack of an aryl radial on the already grafted aryl layers. As mentioned in Chapter 1, a protection-deprotection strategy has been developed to prevent the formation of multilayers;[6-10] bulky protecting groups on the aryl diazonium derivatives prevent the attack of an aryl radical on the already grafted layer, and subsequent removal of the protecting groups reveals a monolayer of reactive functional groups that can be used for further coupling reactions (Scheme 1.9, Chapter 1).

The work of Leroux and co-workers[6] has demonstrated the use of the triisopropylsilyl (TIPS) protecting group on ethynylbenzenediazonium salt to yield a monolayer film. Electrografting of 4-((triisopropylsilyl)ethynylbenzenediazonium salt ([TIPS-Eth-Ar-N_2]BF_4 followed by the deprotection of the TIPS group with tetrabutylammonium fluoride (TBAF) results in a monolayer of phenylethynylene groups (H-Eth-Ar). The formation of the H-Eth-Ar monolayer was demonstrated by a successful click reaction with azidomethylferrocene ($FcCH_2N_3$, Scheme 4.1).

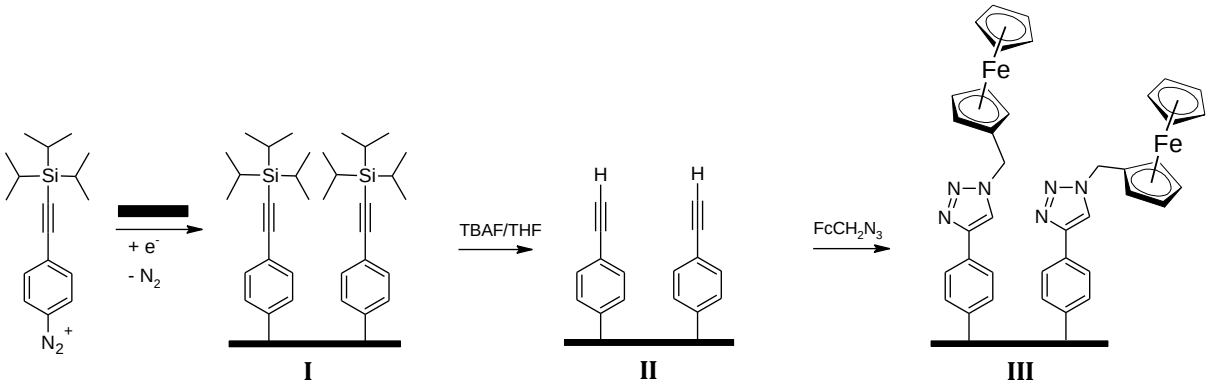

Scheme 4.1 Strategy for the preparation of a monolayer bearing an Eth functionality that can be further used for attachment of an azido derivative (ferrocene) via click chemistry.

As detailed in Chapter 1, preparation of mixed layers can be achieved by a sequential grafting of two different aryldiazonium salts;[11-13] grafting of the first aryldiazonium salt usually contains bulky groups, which can be subsequently removed to create pinholes in the film for grafting of a second aryldiazonium salt (Schemes 1.11 and 1.12, Chapter 1). Leroux and co-workers[11] have prepared a mixed film by grafting a layer of TIPS-Eth-Ar followed by attachment of nitrophenyl (NP) groups, using 4-nitrobenzenediazonium salt (NBD) as the second modifier. Their strategy is shown in Scheme 4.2. Two approaches were investigated: in the first strategy, TIPS-Eth-Ar-GC surface was first deprotected in TBAF/THF, to reveal the H-Eth-Ar-GC surface, followed by grafting of NP groups (Scheme 4.2a). However, this approach led to the formation of multilayers and eliminated the reactivity of the H-Eth-Ar layer toward click chemistry. During the grafting of the NP groups, the NP radicals are assumed to attack both the aryl ring of the already grafted H-Eth-Ar layer and the Eth moiety itself, which prevents further click reactions. Another approach is to preserve the reactivity of the Eth groups by grafting the NP groups on the protected TIPS-Eth-Ar-GC surface (Scheme 4.2b). The surface concentration of ferrocenyl (Fc) groups after the click reaction was found to be similar to the single-component monolayer but a multilayer of NP groups was detected.

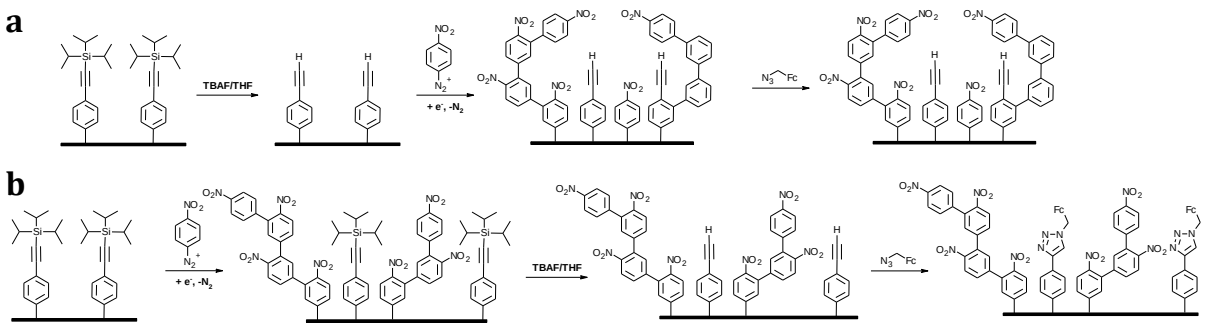

Scheme 4.2 Strategies for the preparation of a mixed layer employed by Leroux and co-workers:[11] a) TIPS-Eth-Ar-GC surface was first deprotected followed by grafting of NBD and then click chemistry, b) TIPS-Eth-Ar-GC surface was grafted with NBD followed by deprotection and then click chemistry.

In this Chapter, the strategies of Leroux and co-workers[6, 11] described above have been studied and further developed, with the aim of preparing mixed monolayers with controlled composition. The electrografting of [TIPS-Eth-Ar-N_2]BF_4 and the preparation of mixed monolayer films using [TIPS-Eth-Ar-N_2]BF_4 are discussed. NP and Fc were chosen as the film components because their redox activity is well understood and allows an estimation of their surface concentrations.

4.2 Experimental

All chemical reagents and materials are described in Chapter 2. Azidomethyl ferrocene ($FcCH_2N_3$) was synthesised following a literature method,[14] which is briefly explained in Chapter 2, Section 2.1.5.1. [TIPS-Eth-Ar-N_2]BF_4 was synthesised by adaptation of a published report[6] which is described in Section 2.1.4.1. The synthesis of NBD and ethynylbenzenediazonium tetrafluoroborate, [H-Eth-Ar-N_2]BF_4, is outlined in Section 2.1.3. PPF preparation is detailed in Section 2.3.1.2. The AFM technique for measurement of film thickness is described in Section 2.5.

All experiments in this chapter were undertaken using a GC disk (area = 0.071 cm^2) as the working electrode, except for AFM experiments for which PPF was used. Pt mesh was the counter electrode and SCE was the reference electrode for aqueous solutions and CE (1 M LiCl) for non-aqueous solutions.

Electrografting. TIPS-Eth-Ar groups were electrografted to GC and PPF from a solution of 5 mM [TIPS-Eth-Ar-N_2]BF_4 in 0.1 M $TBABF_4$-ACN using five cycles between 0.60 and -0.75 V at a scan rate of 50 mV s^{-1}. The modified electrode (TIPS-Eth-Ar-GC) was rinsed with acetone, sonicated in ACN for 5 min, and dried with a stream of N_2(g). TIPS was cleaved from the layer by immersing the modified electrode in a stirred solution of 0.05 M TBAF-THF for 20 min[6] giving the deprotected monolayer, H-Eth-Ar-GC. Electrodes were carefully rinsed with THF and acetone after deprotection. Multilayer films of H-Eth-Ar groups were electrografted to GC from a solution of 1 mM [H-Eth-Ar-N_2]BF_4 in 0.1 M $TBABF_4$-ACN using two cycles between 0.60 and -0.50 V at a scan rate of 200 mV s^{-1}. The electrode was rinsed with acetone, sonicated in ACN for 5 min, and dried with a stream of N_2(g). Electroreduction of NBD was carried out in a solution of NBD in 0.1 M $TBABF_4$-ACN, while electrooxidation of 4-nitrophenylhydrazine (NPH) was carried out in a solution of NPH in 0.1 M KH_2PO_4 (aq, pH 4.5). The concentration of NBD and NPH, potential limits and number of cyclic scans used are described in the Results and Discussion section. After grafting of NBD, electrodes were rinsed with acetone, sonicated in ACN for 2 min, and dried with a stream of N_2(g). After modification with NPH, electrodes were rinsed with water, sonicated in ACN for 2 min, and dried with a stream of N_2(g).

Mixed layer preparation by sequential electrografting. The first modifier, [TIPS-Eth-Ar-N_2]BF_4, was electrografted to the surface and deprotected using the method described above. NP groups were electrografted from solutions of either 0.01 mM NBD in 0.1 M $TBABF_4$-

ACN using three cycles between 0.6 and 0.2 V at a scan rate of 100 mV s^{-1}, or 0.5 mM NPH in 0.1 M KH_2PO_4 (aq, pH 4.5) using one cycle between -0.2 and 0.5 V at a scan rate of 100 mV s^{-1}. After modification in NBD, the electrodes were rinsed with acetone, sonicated in ACN for 2 min, and dried with a stream of N_2(g). After modification in NPH, the electrodes were rinsed with water, sonicated in ACN for 2 min, and dried with a stream of N_2(g).

Mixed layer preparation by electrografting followed by direct reaction of the second modifier with GC. A TIPS-Eth-Ar-GC surface was prepared using the method described above. NP groups were coupled directly to the GC surface either by reaction with 4-nitrobenzylamine hydrochloride (NBA.HCl, 10 mM) in the presence of HBTU (12 mM) and DIPEA (20 mM) in DMF (5 mL) overnight (as described in Chapter 2, Section 2.3.1.4) or by activating the GC surface with oxalyl chloride ($(COCl)_2$) prior to reaction with NBA.HCl (as described in Chapter 2, Section 2.3.1.2.1). Alternatively, Fc was coupled to the GC surface as the second modifier by reaction of H-Eth-Ar-GC with $(COCl)_2$ activated FcCOOH; the activation of FcCOOH is described in Chapter 2, Section 2.3.1.2.2. After these coupling reactions, the electrodes were sonicated in ACN for 5 min, and dried with a stream of N_2(g).

Click reaction on H-Eth-Ar-GC surfaces. $FcCH_2N_3$ was clicked to H-Eth-Ar-GC surfaces by the method outlined in Chapter 2, Section 2.3.1.1. The resulting Fc-coupled electrodes were rinsed by stirring in EDTA-Na_2 for 10 min, to remove copper residues, and were then stirred in THF for 20 min and dried with a stream of N_2(g). For the mixed layer prepared by electrografting followed by direct reaction with GC, the electrodes were rinsed with EDTA-Na_2 for 10 min and sonicated in THF for 2 min followed by ACN for 3 min and dried with stream of N_2(g) after click reaction.

Electrochemistry. Cyclic voltammograms (CVs) of immobilised Fc and NP groups were obtained in 0.1 M $LiClO_4$-EtOH at a scan rate of 200 mV s^{-1} and 0.1 M H_2SO_4 at a scan rate of 100 mV s^{-1}, respectively, unless specified otherwise. For mixed films, the voltammetry of Fc groups was recorded prior to reduction of NP groups. The surface concentration of immobilised Fc was determined by averaging the areas under the anodic and cathodic peaks from the second voltammetric cycle, unless stated otherwise. The surface concentration of immobilised NP groups was estimated from the first cycle using the NP reduction and the hydroxyaminophenyl oxidation peak areas and the number of electrons involved in each redox process[15] as described in Chapter 2, Section 2.5.

4.3 Results and Discussion

4.3.1 Preparation and characterisation of modified electrodes using redox probe voltammetry and click chemistry

The TIPS protected diazonium salt was synthesised by the method of Leroux and co-workers[6] (Chapter 2, Section 2.2.4.1). GC electrodes were modified with a TIPS protected film by recording cyclic voltammetric scans in a 5 mM solution of [TIPS-Eth-Ar-N_2]BF_4 in ACN using 0.1 M $TBABF_4$ as the electrolyte. Figure 4.1 shows a typical CV of [TIPS-Eth-Ar-N_2]BF_4; the irreversible reduction peaks of the diazonium ion are present in the 1st scan ($E_{p,c}$ = 0.2 V and 0 V), and disappear on the subsequent scans. This response is typical of aryldiazonium ions and is consistent with the formation of grafted layers that restrict further electrochemical reduction by inhibiting electron transfer from the electrode surface to the diazonium ion in solution. Note that the appearance of two reduction peaks in the first scan has been reported for many diazonium ion derivatives.[2, 16-19] However, their origin remains unclear. Chapter 7 describes an investigation of this phenomenon.

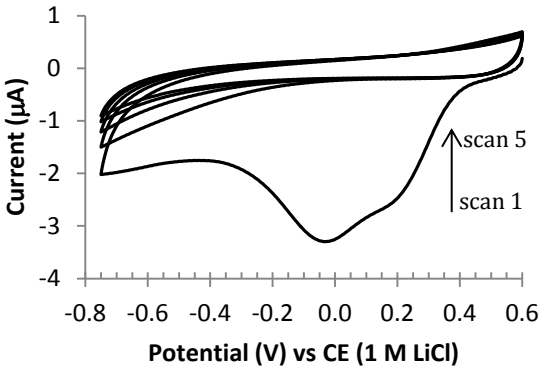

Figure 4.1 Five consecutive scans at a bare GC electrode in a solution of 5 mM [TIPS-Eth-Ar-N_2]BF_4 in 0.1 M $TBABF_4$-ACN. Scan rate = 50 mV s^{-1}.

The blocking properties of the grafted TIPS-Eth-Ar-GC surface (structure I, Scheme 4.1) were characterised by voltammetry of dopamine, ferrocyanide and ferrocene as redox probes. The use of solution based redox probes is based on the effects of insulating surface layers on electron transfer rates for redox species in solution as described by equation 4.1,[20] where k^0 is the standard heterogeneous rate constant, β is a tunnelling parameter which depends on the nature of the blocking layer, and x is the thickness of the blocking layer.

$$k(x) = k^0(x = 0) \exp(-\beta x) \qquad \text{eq. 4.1}$$

As seen from equation 4.1, the rate constant for electron transfer is dependent on the thickness of the blocking film; as the thickness of the film increases, the rate of electron transfer will decrease. As the rate of electron transfer between the electrode and the redox probe decreases, the peak-to-peak separation (ΔE_p) of a CV will increase and the peak current will decrease.[21, 22] Hence, as the surface film becomes more blocking (thicker), the ΔE_p value becomes larger, and the currents lower.

Dopamine is an example of an inner-sphere redox probe.[23-26] In an inner-sphere reaction, there is a strong interaction of reactant, intermediates, or products with the electrode surface.[23] Thus, such reactions involve specific adsorption of the reactants, intermediates, or

products on the electrode surface.[23] For dopamine, the rate of electron transfer is not only affected by the ability of dopamine to adsorb on the electrode surface but the amount of surface oxide available for hydrogen bonding to dopamine may also influence the observed kinetics.[26] The rate of electron transfer is observed to increase (ΔE_p decreases) as adsorption sites and surface oxide content increases.[26] Ferrocyanide is also an inner-sphere redox probe, however its response is not sensitive to the presence of surface oxide.[24] Ferrocene is an example of an outer-sphere redox probe, where the reactants, intermediates, and products do not interact strongly with the electrode surface and electron transfer occurs by tunnelling.[23]

Figure 4.2 shows CVs obtained in solutions of dopamine, ferrocyanide and ferrocene at polished GC, TIPS-Eth-Ar-GC, and the modified electrode after deprotection. After modification of the GC electrode with TIPS-Eth-Ar groups (structure I, Scheme 4.1), the redox responses of dopamine and ferrocyanide are strongly blocked (blue lines, Figures 4.2a and 4.2b, respectively), with no peak in the expected potential range and only very low current. On the other hand, the response of ferrocene is much less affected (Figure 4.2c). Very low background currents for the dopamine and ferrocyanide CVs suggest that solvents and/or ions cannot penetrate through the layer and therefore dopamine and ferrocyanide cannot access the surface. Because dopamine and ferrocyanide are both inner-sphere redox species and tunnelling across the layer is not possible, no response is obtained for these species. The CVs of ferrocene are obtained in $TBABF_4$-ACN, in which the film may be more porous in the aqueous solvent used for dopamine and ferrocyanide voltammetry. Therefore ferrocene may be able to diffuse through the hydrophobic film and access the surface. The CV of Figure 4.2c, blue line, has a distinctly sigmoidal shape, consistent with ferrocene undergoing electron transfer at pinholes in the film.[20] Furthermore, ferrocene is an outer-sphere redox probe and tunnelling across the film is also expected to contribute to the ferrocene redox response.

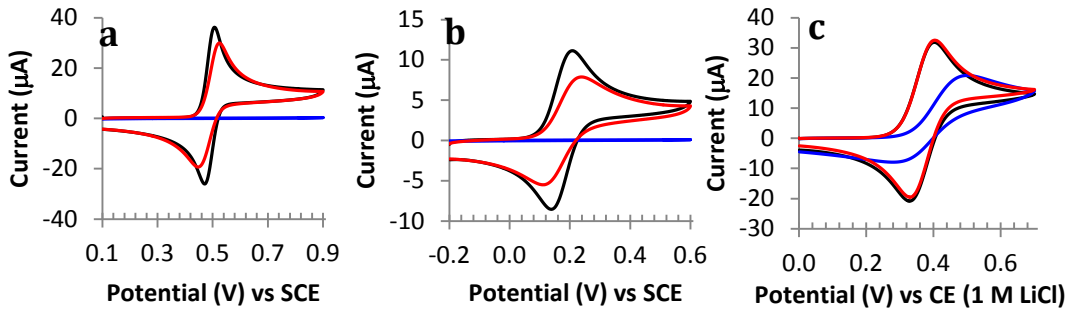

Figure 4.2 CVs obtained in a solution of: a) 1 mM dopamine in 0.1 M H_2SO_4; b) 1 mM ferrocyanide in 0.1 M PB (pH 6.9); and c) 1 mM ferrocene in 0.1 M $TBABF_4$-ACN at scan rate = 100 mV s^{-1}. Bare GC: black line, TIPS-Eth-Ar-GC: blue line, and H-Eth-Ar-GC: red line.

After deprotection of the modified surface in 0.05 M TBAF-THF for 20 min (structure II, Scheme 4.1), the response for all of the redox probes is close to that of bare GC (Figure 4.2, red lines). The CV obtained in dopamine solution at H-Eth-Ar-GC (Figure 4.2a, red line), suggests that there are surface sites available for dopamine adsorption. This is consistent with the expected creation of pin-holes by removal of TIPS groups. Similarly, the response of ferrocyanide at H-Eth-Ar-GC indicates that direct interaction with the surface is possible. The ferrocene response is the same as at the unmodified GC surface, indicating that under the experimental conditions, there is no detectable effect in the rate of electron transfer. Hence, these results are consistent with generation of a highly porous and presumably thinner layer after deprotection.

The CVs for ferrocyanide and ferrocene shown in Figures 4.2b and 4.2c, respectively, are similar to those reported by Leroux and co-workers[6, 7] (ferricyanide was used in their work) for the same modified surfaces. In their work, the response of ferrocene was very significantly blocked at the TIPs-Eth-Ar-GC surface, presumably due to the grafting of a thicker film than in the present work, through the use of a higher concentration of diazonium ion for grafting. However, after deprotection, Leroux and co-workers also found no retardation of the ferrocene response, similar to the present work.

The reactivity of the expected H-Eth-Ar terminated layer after deprotection (structure II, Scheme 4.1) was tested by performing a "click" reaction, a copper(I)-catalysed Huisgen 1,3-dipolar cycloaddition.[27, 28] $FcCH_2N_3$ was clicked onto the deprotected H-Eth-Ar monolayer using the method described in Chapter 2, Section 2.3.1.1. The CV of the expected Fc functionalised surface (structure III, Scheme 4.1) was investigated in EtOH solution containing $LiClO_4$ as the electrolyte. CVs of the Fc modified surface (Figure 4.3a) show a well-defined ferrocene/ferrocenium (Fc/Fc^+) redox couple at $E_{½}$ = 0.44 V with ΔE_p = 23 mV, close to expected ideal value of 0 V for surface immobilised species.[20] In addition, the CVs of the ferrocene modified electrode obtained at scan rates of 50 – 500 mV s^{-1} (Figure 4.3b) show the expected linear relationship between peak current and scan rate[20, 29] (Figure 4.3c), indicating that there are no kinetic limitations under these conditions. These results are consistent with a surface coupled species. By integrating the area under the Fc redox peaks of 15 modified electrodes, the average surface concentration of immobilised Fc groups was (2.4 ± 0.3) × 10^{-10} mol cm^{-2}. The calculated surface concentration of hexagonal close-packed TIPS-Eth-Ar groups on a flat surface is 2.3 × 10^{-10} mol cm^{-2}.[7] This calculation assumes the TIPS group is a sphere with diameter of 0.92 nm. Hence assuming a GC surface roughness factor of 2[30] and a quantitative yield for the click reaction, the observed surface concentration of Fc indicates that ~50% of a compact monolayer of TIPS-Eth-Ar is grafted to the GC surface. Interestingly, Leroux and co-workers[6] reported a surface concentration of 4.4 × 10^{-10} mol cm^{-2} for Fc clicked to a deprotected TIPS-Eth-Ar layer. Considering surface roughness, this is not inconsistent with monolayer coverage. On the other hand, Leroux and co-workers[6] appeared to make one measurement only and did not indicate the reliability of their result and hence it is not possible to make meaningful comparisons with this work.

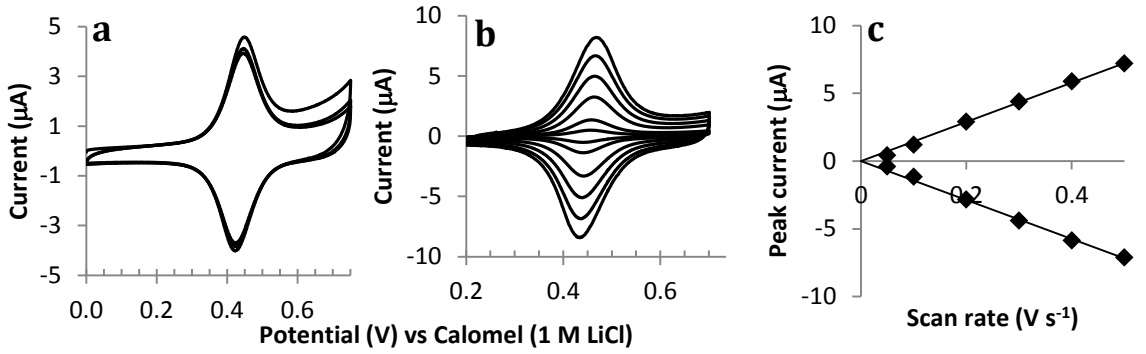

Figure 4.3 CVs obtained in 0.1 M $LiClO_4$-EtOH of a GC electrode modified with an H-Eth-Ar monolayer and coupled with Fc; a) three consecutive scans at 200 mV s^{-1}; b) repeat scans at scan rates ranging from 50 – 500 mV s^{-1}; and c) plot of peak currents against the scan rate.

To compare the properties of H-Eth-Ar monolayers and multilayers, an H-Eth-Ar^{multi} film was grafted to GC from the corresponding non-protected aryldiazonium salt. The grafting was carried out by two cyclic voltammetic scans of the freshly polished GC electrode in a solution of 1 mM [H-Eth-Ar-N_2]BF_4 in 0.1 M TBABF_4-ACN at a scan rate of 200 mV s^{-1}. Figure 4.4 shows the CV of the electrografting, where on the first scan irreversible reduction of the diazonium ion is observed, and only very low current is seen on the second scan as expected for the formation of blocking layers. The blocking properties of the film were investigated with the redox probes, dopamine, ferrocyanide and ferrocene. As can be seen from Figure 4.5, after modification with H-Eth-Ar^{multi} films, the electrode blocks the response of all redox probes (blue lines) and upon immersion of the modified electrode in 0.05 M TBAF-THF solution, there is no significant change in the blocking behaviour (red lines). (The films were immersed in 0.05 M TBAF-THF to replicate the treatment of the TIPS-protected surface.)

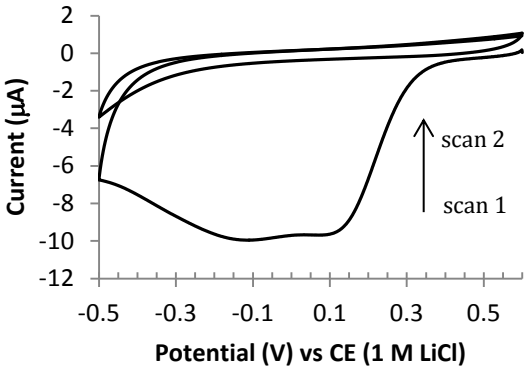

Figure 4.4 Two consecutive scans at a bare GC electrode in a solution of 1 mM [H-Eth-Ar-N_2]BF_4 in 0.1 M TBABF_4-ACN. Scan rate = 200 mV s^{-1}.

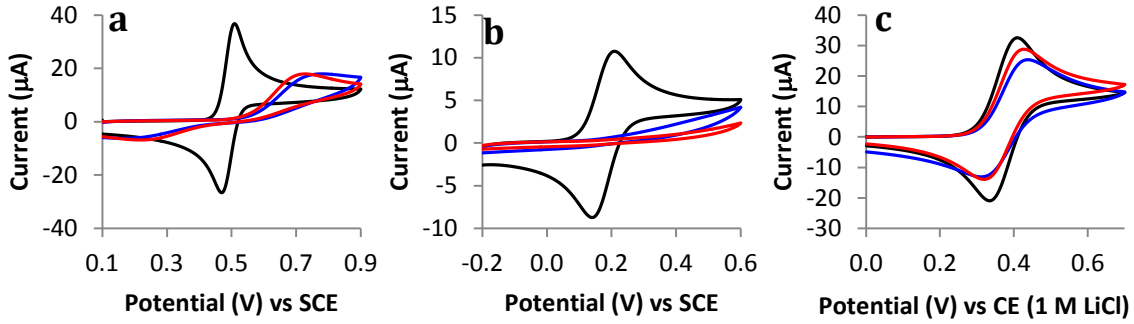

Figure 4.5 CVs obtained in a solution of: a) 1 mM dopamine in 0.1 M H_2SO_4; b) 1 mM ferrocyanide in 0.1 M PB (pH 6.9); and c) 1 mM ferrocene in 0.1 M TBABF_4-ACN at scan rate = 100 mV s^{-1}. Bare GC: black line, H-Eth-Ar^{multi}-GC: blue line, and H-Eth-Ar^{multi}-GC immersed in 0.05 M TBAF-THF for 20 min: red line.

Figure 4.5a (blue line) shows the response of dopamine after modification of GC with a H-Eth-Ar^{multi} film. A small dopamine redox couple is observed with ΔE_p = 450 mV. This is different to the response obtained at the TIPS-Eth-Ar-GC surface (Figure 4.2a, blue line), where a very blocking behaviour was observed. This indicates that at the H-Eth-Ar^{multi} film, dopamine can access some of the GC surface, presumably due to a loosely packed multilayer structure that allows solvent and ion penetration of the film. Immersion of the H-Eth-Ar^{multi}-GC electrode in TBAF-THF (Figure 4.5a, red line) does not cause any significant difference, as expected. Figure 4.5b shows that the H-Eth-Ar^{multi} film blocks the response of ferrrocyanide more than that of dopamine. This may be because ferrocyanide is larger and more hydrophilic than dopamine and therefore cannot penetrate the hydrophobic multilayer.

Hence the film prevents electron transfer between ferrocyanide and the electrode. The ferrocene CV (Figure 4.5c) obtained at the H-Eth-Ar^{multi}-GC surface has ΔE_p = 127 mV (blue line), smaller than that at the TIPS-Eth-Ar-GC surface (ΔE_p = 143 mV, Figure 4.2c). The smaller ΔE_p value corresponds to a less blocking film; either the H-Eth-Ar^{multi} film is not as thick as the TIPS film and electron tunnelling is still possible or the film is more porous allowing ferrocene to permeate the layer. Upon immersion of the H-Eth-Ar^{multi}-GC electrode in TBAF-THF (red line), the peak current increases slightly and ΔE_p = 110 mV. However, the ΔE_p is still larger than at bare GC (75 mV, black line). The faster rate of electron transfer after immersion in TBAF-THF may be due to the removal of physisorbed impurities making the film more porous.

Ferrocene was clicked onto this H-Eth-Ar^{multi}-GC surface using the same procedure as for monolayer films. Figure 4.6 shows the CV of the H-Eth-Ar^{multi} film Fc/Fc$^+$ redox couple with $E_{½}$ = 0.44 V and ΔE_p = 47 mV. The $E_{½}$ value is the same as for Fc clicked to the monolayer H-Eth-Ar film, but the ΔE_p value is significantly greater. This is consistent with a thicker film, which decreases the electron transfer rate. The average surface concentration of Fc groups attached to this H-Eth-Ar^{multi} film is $(1.6 \pm 0.2) \times 10^{-10}$ mol cm^{-2} (n = 3), which is less than the value found for the deprotected monolayer film ($(2.4 \pm 0.3) \times 10^{-10}$ mol cm^{-2}). The lower surface concentration of clicked Fc suggests that the number of accessible H-Eth groups is lower for the multilayer than monolayer film. It is likely that only H-Eth groups on the outer layer of the multilayer film undergo the click reaction, and that the disorganisation of the layer may introduce steric hindrance, limiting the reactivity to the click reaction. Another possibility is that some of the coupled Fc groups in the multilayer film are electro-inactive and so cannot be quantified by CV.[31, 32]

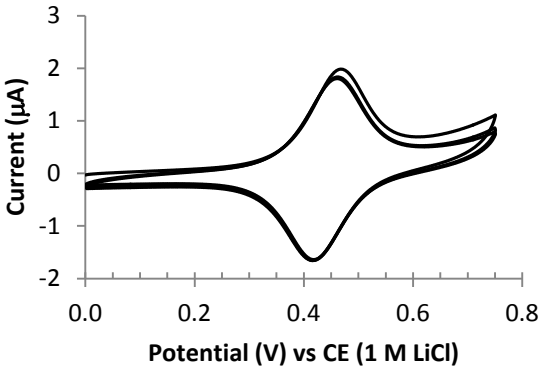

Figure 4.6 CVs obtained in 0.1 M $LiClO_4$-EtOH of a GC electrode modified with an H-Eth-Ar^{multi} film and coupled with Fc at 200 mV s^{-1}.

During the voltammetric investigation of Fc groups clicked to deprotected monolayer H-Eth-GC surfaces, an interesting solvent and electrolyte dependency was noted. The $E_{½}$ for the Fc/Fc^+ couple was seen to be dependent on the solvent and electrolyte (Figure 4.7). Such shifts have been noted in other studies and are attributed to the ability of the electrolyte anion to ion-pair with, and stabilise, the Fc^+ centre.[33-39] Hydrophobic anions, such as PF_6^-, ClO_4^-, and BF_4^-, pair more effectively with Fc^+ ion than hydrophilic anions such as NO_3^-, Cl^-, SO_4^{2-}, and F^-.[35, 38] As a consequence, Fc is thermodynamically easier to oxidise in the presence of hydrophobic anions giving a less positive $E_{½}$. The reported ordering of $E_{½}$ for Fc/Fc^+ couples is: $PF_6^- < ClO_4^- < BF_4^- < NO_3^- < Cl^- < SO_4^{2-} < F^- < NH_2SO_3^-$.[38] As seen in Figure 4.7a and Table 4.1, in agreement with this ordering, the CVs obtained in EtOH and ACN with $LiClO_4$ as the electrolyte (black and red lines, respectively) have a less positive $E_{½}$ (0.44 V) compared to those obtained with $TBABF_4$ (blue and green lines, $E_{½}$ = 0.47 V). Similar results were observed for the thicker H-Eth-Ar^{multi}-GC film prepared from the non-protected diazonium ion (Figure 4.7b). CVs obtained in ACN with $LiClO_4$ as the electrolyte have an $E_{½}$ = 0.43 (red line), while in $TBABF_4$ electrolyte solution, $E_{½}$ = 0.48 V (green line). These results are consistent with the tighter ion pairing of Fc^+ with ClO_4^- than with BF_4^-. A dependency of $E_{½}$ for Fc/Fc^+ couples on the solvent has also been reported,[39-42] arising from

the interaction of the solvent with Fc and Fc^+ centres. For example, the increase in H-bond donor ability of the solvent causes the $E_{½}$ to shift to a less positive potential.[39-41] This is because the H-bond donor ability provides greater stability to Fc^+ than Fc.[40, 41] As seen in Figure 4.7a and Table 4.1, the CVs obtained in the highest H-bond donor solvent, H_2O, (purple line), have the least positive $E_{½}$ (0.35 V). However, $E_{½}$ values obtained in EtOH and ACN are the same, even though the H-bond donor ability of EtOH is higher than that of ACN. This may be because the $E_{½}$ values shown here do not take into account the liquid junction potential between the working and reference electrodes in the different electrolyte/solvent systems. Differences in liquid junction potentials in EtOH and ACN may outweigh the effects of solvent on the $E_{½}$ of the Fc/Fc^+ redox couple.

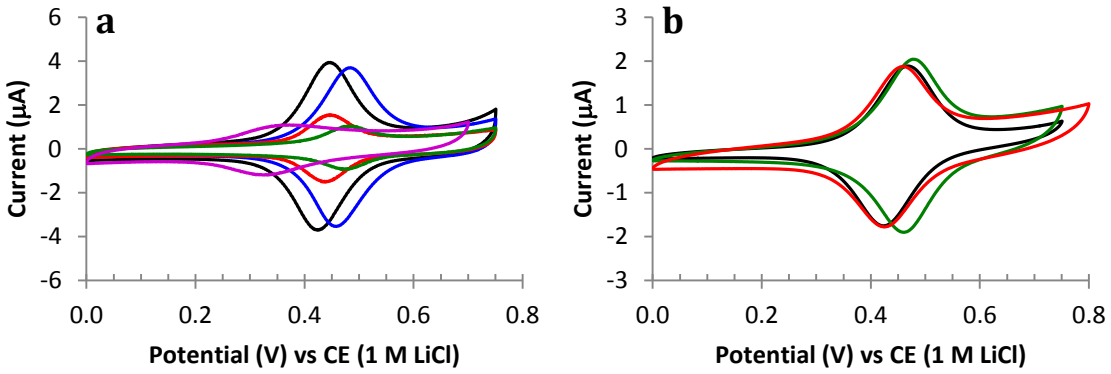

Figure 4.7 CVs of a GC electrode modified with a H-Eth-Ar film and coupled with Fc: a) deprotected monolayer, and b) multilayer. CVs obtained in: 0.1 M $LiClO_4$-EtOH (black line); 0.1 M $TBABF_4$-EtOH (blue line); 0.1 M $LiClO_4$-ACN (red line); 0.1 M $TBABF_4$-ACN (green line) and 0.1 M $LiClO_4$-H_2O (purple line). Scan rate = 200 mV s^{-1}.

Table 4.1 $E_{½}$ and apparent concentration of surface immobilised Fc via reaction of $FcCH_2N_3$ with a deprotected monolayer of H-Eth-Ar.

Solvent	Electrolyte	$E_{½}$ (V) vs CE (1 M LiCl)	Apparent Γ_{Fc} (10^{-10} mol cm^{-2})
EtOH	$LiClO_4$	0.44	2.7
EtOH	$TBABF_4$	0.47	2.5
ACN	$LiClO_4$	0.44	1.3

ACN	$TBABF_4$	0.47	0.8
H_2O	$LiClO_4$	0.43	1.0

More unusual than shifts in $E_{½}$ values, the peak currents (and peak areas) for Fc attached to the monolayer are also strongly dependent on the solvent and, to a lesser extent, the electrolyte. The data in Table 4.1 shows that the calculated surface concentration of Fc in the same film can range from 0.8 to 2.7 × 10^{-10} mol cm^{-2}, depending on the solvent and electrolyte used to obtained the CVs. These changes in apparent surface concentration were reversible although the Fc response was not stable to prolonged scanning (scanning 50× in $LiClO_4$-EtOH decreased the apparent Fc concentration by 35%). This solvent dependency was only seen in the monolayer film prepared from the deprotected diazonium derivative (Figure 4.7a), but not for Fc coupled to the multilayer analogue (Figure 4.7b). Interestingly, a similar strong dependency on solvent was also observed for Fc coupled to a monolayer film through amide bonds (Chapter 5). Figure 4.7a and Table 4.1 show that the electrolyte also affects the peak areas and apparent surface concentration in ACN; the response is larger in the presence of $LiClO_4$ (red line) than $TBABF_4$ (green line). However, the electrolyte ($LiClO_4$ or $TBABF_4$) has no influence on the response in EtOH (black and blue line, respectively). The factors underlying these observations are unknown, and were not investigated further in this work. However, it appears that the close proximity of the attached Fc to the underlying GC substrate is a key factor. This suggests that the phenomenon arises due to the effect of the electrical double layer.

There is one reported[38] observation of variable peak areas for CVs of a Fc-terminated monolayer obtained in 0.01 M sodium phosphate buffer (pH 7.0) in the presence of added sodium salts of different anions at a concentration of 0.1 M. The Fc-terminated monolayer was prepared by self-assembly of $Fc(CH_2)_4COO(CH_2)_9SH$ on a Au surface. Similar Fc/Fc^+

peak areas were obtained in the presence of the hydrophobic anions PF_6^-, ClO_4^-, BF_4^-, and NO_3^-, while the Fc/Fc^+ peak areas decreased significantly in the presence of the hydrophilic anions Cl^-, SO_4^{2-}, F^- and $NH_2SO_3^-$.[38] The authors noted this phenomenon but offered no explanation. However, this behaviour is somewhat different to that found in the present work. In that work, all voltammetry was conducted in aqueous solution and the effect of different solvents was not investigated. This contrasts with the presence work where the influence of solvent was investigated and there was limited investigation on the effect of anions on the Fc response. In aqueous solution, only $LiClO_4$ was used as electrolyte. Hence, it is not clear whether the variable peak areas for CVs of Fc clicked to monolayers of H-Eth-Ar groups have the same origin as the effects described in the earlier work.

Other reports of variable peak currents and peak areas for CVs of immobilised Fc groups clearly have origins different to those seen here. Brett and co-workers[43] reported an example where the peak currents of Fc species were dependent on temperature. The peak currents of a $FcCOO(CH_2)_{11}SH$ self-assembled monolayer (SAM) on Au were constant from 5 to 30 °C, however as the temperature increased above 30 °C, the peak currents decreased consistently. This effect was irreversible, presumably due to the loss of Fc groups at high temperature.[43] Pressure has also been reported to influence the apparent electrochemically-determined surface concentration of Fc groups in SAMs of $Fc(CH_2)_{11}SH$.[44] Under high pressure, the apparent surface concentration of Fc groups decreased, and upon release of the pressure, the surface concentration of Fc groups returned to its initial value.[44] This effect was attributed to the steric requirements of the oxidation step because the incorporation of counter ions to stabilise the Fc^+ centre is more difficult at high pressure, due to the volume expansion required for formation of Fc^+ and incorporation of the counter ions.[44]

The variability in apparent surface concentration of Fc groups illustrated in Figure 4.7 and Table 4.1 demonstrates that it is important to choose the 'right' solvent/electrolyte system to investigate surface coupled Fc for the determination of surface concentration. It is assumed here that the surface concentrations of Fc groups calculated from CVs obtained in $LiClO_4$-EtOH correspond to the actual concentrations, but this assumption was not independently verified.

4.3.2 Formation of mixed layers

4.3.2.1 Formation of mixed layers via sequential electrografting from aryldiazonium ion and arylhydrazine solutions

The work in this section has been published in reference 13. The aim of the work was to prepare mixed monolayer films using a similar route to that of Leroux and co-workers[11] (described in the Introduction) but with more controlled grafting of a second modifier using NBD and NPH. Three different routes to form a mixed layer were explored, as shown in Scheme 4.3.

For the three routes shown in Scheme 4.3, the key step is limiting grafting of the second modifier to a monolayer that fills in the gaps created by the first layer. NPH was chosen as a second modifier because it has been shown that grafting via the oxidation of arylhydrazine usually results in monolayers (or near monolayers) of covalently attached films when the grafting is carried out in aqueous solution at pH $\leq$ 7.[45, 46] NBD was also employed as the second modifier because it is electro-active which allows estimation of its surface concentration. A multilayer film of NP groups attached to PPF has been shown to have (2.5 $\pm$ 0.5) $\times$ 10^{-10} mol cm^{-2} of NP groups per slice of film corresponding to monolayer thickness (a 'monolayer equivalent').[2] GC has a greater surface roughness than PPF and thus, to avoid the formation of multilayer mixed component films, in initial experiments grafting conditions

were optimised at bare GC to give surface concentrations of NP groups that did not exceed ~2 × 10^{-10} mol cm^{-2}. Table 4.2 lists the electrochemical conditions used to graft NP groups using both NBD and NPH on a bare GC electrode and the corresponding surface concentrations. The surface concentrations, Γ, of grafted NP groups were determined from CVs obtained in 0.1 M H_2SO_4 at a scan rate of 100 mV s^{-1}.

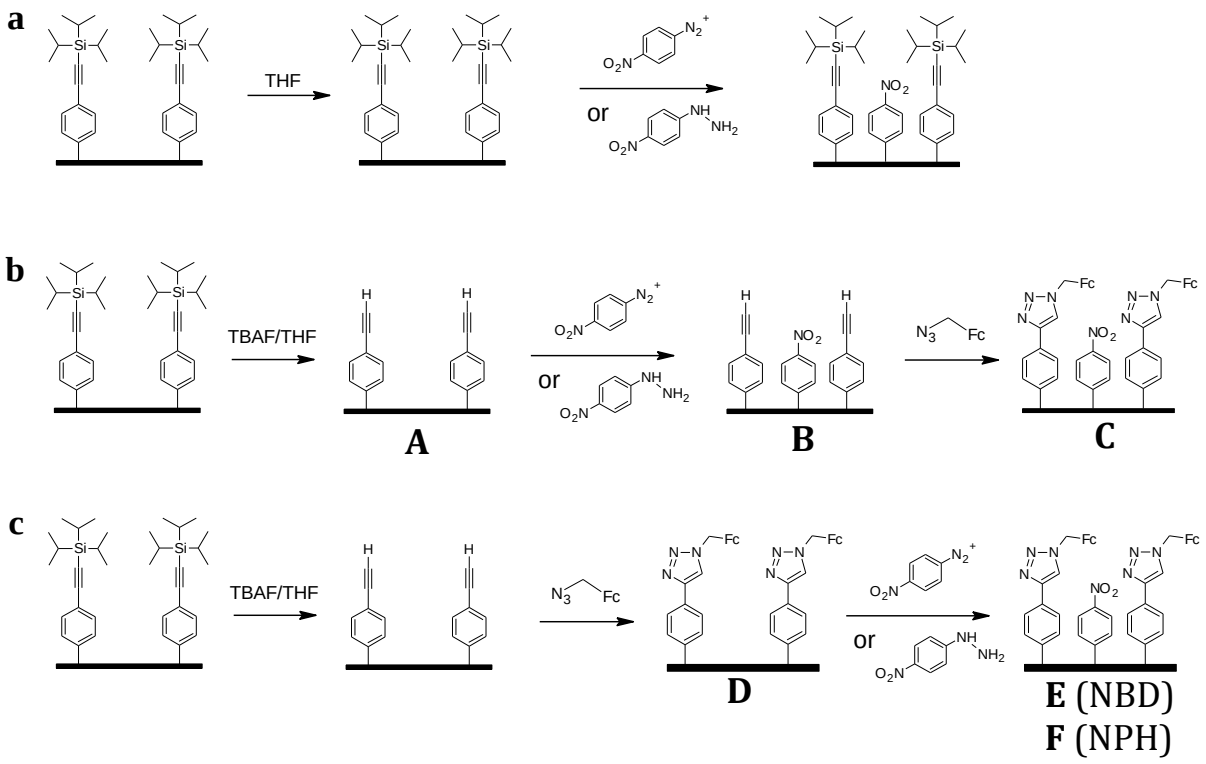

Scheme 4.3 Strategies for the preparation of mixed monolayer films from a TIPS-Eth-Ar layer using a sequential grafting of two different modifiers; a) NBD or NPH is grafted to TIPS-Eth-Ar-GC surface without deprotection of the TIPS group; b) NBD or NPH is grafted to the deprotected H-Eth-Ar-GC surface, and c) Fc is coupled to the deprotected H-Eth-Ar-GC surface prior to grafting the second modifier (NBD or NPH).

Table 4.2 Electrografting conditions on bare GC using NBD or NPH and the corresponding surface concentration of the electro-active NP group.

Expt.	**Grafting condition**[a]	Γ_{NP}[b] **(10^{-10} mol cm^{-2})**
I	1 mM NBD, 3× from 0.6 to -0.2 V	14.9
II	1 mM NBD, 1× from 0.6 to -0.2 V	16.9

III	1 mM NBD, 3× from 0.6 to 0.2 V	17.2
IV	1 mM NBD, 1× from 0.6 to 0.2 V	13.9
V	0.1 mM NBD, 3× from 0.6 to 0.2 V	10.2
VI	0.1 mM NBD, 1× from 0.6 to 0.2 V	6.7
VII	0.05 mM NBD, 3× from 0.6 to 0.2 V	6.9
VIII	0.05 mM NBD, 1× from 0.6 to 0.2 V	5.2
IX	0.01 mM NBD, 3× from 0.6 to 0.2 V	1.9 ± 0.4 (n = 5)
X	1 mM NPH, 5× from -0.2 to 0.8 V	9.6
XI	1 mM NPH, 3× from -0.2 to 0.5 V	4.9
XII	1 mM NPH, 1× from -0.05 to 0.5 V	3.9
XIII	0.5 mM NPH, 1× from -0.2 to 0.5 V	1.5 ± 0.2 (n = 6)
XIV	0.1 mM NPH, 3× from -0.05 to 0.5 V	4.0
XV	0.1 mM NPH, 1× from -0.05 to 0.5 V	2.6
XVI	0.1 mM NPH, 3× from -0.05 to 0.25 V	1.6
XVII	0.1 mM NPH, 1× from -0.05 to 0.25 V	1.0

[a]Concentration of modifier and the number of cyclic scans between the potentials indicated, starting at the first potential listed. All scans were carried out at 100 mV s^{-1}. NBD was grafted in 0.1 M $TBABF_4$-ACN. NPH was grafted in 0.1 M KH_2PO_4(aq), pH 4.5.

[b]Unless indicated otherwise, the number of repeat samples, n, was one.

Figure 4.8a shows a typical CV for NBD using the conditions described in the first entry of Table 4.2. The first scan shows the typical irreversible reduction of diazonium ions; the origin of the two reduction peaks will be discussed in Chapter 7. This grafting condition gives rise to a high NP concentration (14.9×10^{-10} mol cm^{-2}), which clearly corresponds to a multilayer. By decreasing the concentration of the diazonium salt, increasing the lower potential limit and decreasing the number of cycles, the surface concentration of NP groups could be decreased (Table 4.2, Experiments II to IX). For NBD grafting, a very low solution concentration of NBD (0.01 mM), and 3 cycles potential over a relatively small potential window (0.6 V to 0.2 V), gives the surface concentration closest to a monolayer equivalent (Experiment IX). Thus, this grafting condition was subsequently used for the preparation of mixed films using NBD. (Note that the contribution from spontaneous grafting was minimised by performing the electrografting immediately after contact of the GC electrode with the diazonium ion solution.)

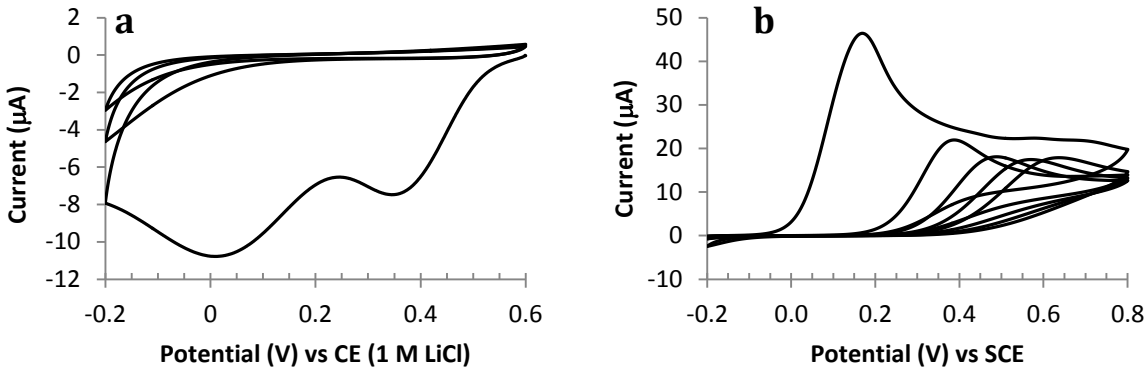

Figure 4.8 Grafting conducted at a bare GC electrode in a solution of a) 1 mM NBD in 0.1 M $TBABF_4$-ACN and b) 1 mM NPH in 0.1 M KH_2PO_4(aq), pH 4.5. Scan rate = 100 mV s^{-1}.

Grafting of NP groups using NPH proceeds by a three-electron oxidation of the arylhydrazine to give an aryl radical that subsequently reacts with the substrate to give a covalent bond[45] as depicted in Scheme 4.4. Grafting using the conditions listed in Table 4.2, Experiment X, shows a well-defined irreversible oxidation peak at 0.17 V; the peak diminishes and moves to more positive potentials on repeat scans (Figure 4.8b). This behaviour is similar to that reported by Daasbjerg and co-workers,[45, 46] although they found an oxidation peak potential at $E_{p,a}$ = 0.33 V. Those workers obtained CVs in a 2 mM solution of NPH at a scan rate of 200 mV s^{-1}. Use of a higher solution concentration and faster scan rate than for the CVs shown in Figure 4.8b is expected to give a more positive peak potential; faster grafting of a blocking film in the higher concentration of NPH solution and the effect of a higher scan rate on the kinetically limited redox process will both contribute to this effect. Note that as the pH increases, $E_{p,a}$ for oxidation of NPH shifts to more negative potentials. The pH used in this experiment (pH 4.5) differs by only half a pH unit from that used by Daasbjerg and co-workers[45, 46] (pH 5) and is expected to lead to a ~30 mV shift in $E_{½}$ (and $E_{p,a}$) in the positive direction. However, this is not observed; the oxidation peak potential is shifted by 160 mV in the negative direction, and thus the different oxidation potential observed is not due to the pH used. Grafting of 5 mM NPH by scanning 1 cycle from -0.2 V to 0.5 V, Table 4.1, Experiment XIII, was chosen for the preparation of mixed films using

NPH as the second modifier because these conditions give the concentration of NP groups closest to a monolayer equivalent.

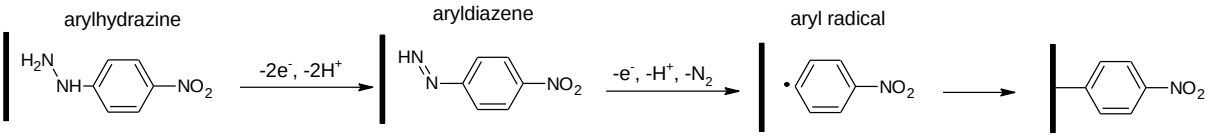

Scheme 4.4 Proposed reaction for oxidation of arylhydrazine, adapted from reference 45

Table 4.3 summarises the results of mixed film preparation using the routes shown in Scheme 4.3. In the first route (Scheme 4.3a), NP groups were grafted to a protected TIPS-Eth-Ar-GC surface. Firstly, the TIPS-Eth-Ar-GC modified electrode was immersed in stirred THF solution for 20 min to remove any physisorbed oligomers[11] followed by grafting of the NP groups and then removal of the TIPS protecting group. The modified surface was then investigated in 0.1 M H_2SO_4 for estimation of NP surface concentration. Table 4.3 Experiments I and II show that only small concentrations of NP groups were grafted under these conditions; this is attributed to the shielding of the electrode surface by the bulky TIPS protecting groups. Although an advantage of this strategy is that removal of the TIPS groups after the immobilisation of the second modifier will remove any NP groups attached to the TIPS groups, the low surface concentration of NP groups demonstrate that this strategy can only be used for the formation of mixed monolayers with a very low concentration of one component.

Table 4.3 Conditions for preparation of mixed films by routes shown in Scheme 4.3 and the corresponding surface concentration of electro-active Fc and NP groups.

Expt.	Route	Grafting conditions[a]	Γ_{Fc} (10^{-10} mol cm^{-2})	Γ_{NP} (10^{-10} mol cm^{-2})	n^b
I	4.3a	0.01 mM NBD, 3× from 0.6 to 0.2 V	n/a	0.4 ± 0.2	3
II	4.3a	0.5 mM NPH, 1× from -0.2 to 0.5 V	n/a	0.6 ± 0.1	3
III	4.3b	0.01 mM NBD, 3× from 0.6 to 0.2 V	1.6 ± 0.1	0.9 ± 0.5	3
IV	4.3b	Blank: condition same as III but in the absence of NBD	2.0 ± 0.2	n/a	2

V	4.3b	0.5 mM NPH, 1× from -0.2 to 0.5 V	1.8 ± 0.5	1.3 ± 0.8	3
VI	4.3b	Blank: condition same as V but in the absence of NPH	2.1 ± 0.4	n/a	2
VII	4.3c	0.01 mM NBD, 3× from 0.6 to 0.2 V	1.5 ± 0.1	1.6 ± 0.3	3
VIII	4.3c	Blank: condition the same as VII but in the absence of NBD	1.3 ± 0.1	n/a	2
IX	4.3c	0.5 mM NPH, 1× from -0.2 to 0.5 V	1.6 ± 0.2	1.8 ± 0.6	3
X	4.3c	Blank: condition same as IX but in the absence of NPH	1.9 ± 0.1	n/a	2

[a]Concentration of modifier and the number of cyclic scans between the potentials indicated, starting at the first potential listed.

[b]*n* is the number of samples analysed.

An alternative strategy was investigated, where the TIPS groups was removed prior to grafting of the second modifier (Scheme 4.3b). To check the reactivity and accessibility of the H-Eth-Ar moieties after grafting of NP groups, a click reaction using $FcCH_2N_3$ was carried out. Figure 4.9a shows the usual well-defined Fc/Fc^+ redox couple of the mixed film obtained in 0.1 M $LiClO_4$-EtOH and Figure 4.9b shows the expected irreversible reduction of NP groups to aminophenyl and hydroxyaminophenyl groups. The chemically reversible hydroxyaminophenyl/nitrosophenyl couple ($E_{½}$ ~ 0.3 V) can be seen on subsequent scans. From the areas under the cyclic voltammetric peaks, the surface concentrations of Fc and NP groups were calculated, giving (1.6 ± 0.1) and (0.9 ± 0.5) × 10^{-10} mol cm^{-2} for Fc and NP, respectively (Table 4.3, Experiment III). The surface concentration of Fc groups is lower compared to Fc clicked to a single-component deprotected TIPS-Eth-Ar-GC surface ((2.4 ± 0.3) × 10^{-10} mol cm^{-2}) as described in the previous section. This suggests that the reactivity or the accessibility of the H-Eth-Ar groups has been decreased by the grafting of NP groups. It is possible that H-Eth-Ar groups react with radicals produced during the reduction of NBD, which decreases the amount of H-Eth-Ar groups available for the following click reaction. In addition or alternatively, after grafting of NP groups to the surface, the H-Eth-Ar groups may become sterically hindered for the subsequent click reaction. The surface concentration of NP

groups is also low compared to NBD grafting to bare GC under the same conditions ((1.9 ± 0.4) × 10^{-10} mol cm^{-2}, Table 4.2, Experiment IX). This indicates that grafting of NBD on the already modified electrode has a lower yield, maybe due to fewer surface sites available for the grafting. A blank reaction, where a TIPS-Eth-GC surface was treated to the same series of steps as in the experiment above but in the absence of NBD was also carried out; the surface concentration of Fc groups was (2.0 ± 0.2) × 10^{-10} mol cm^{-2} (Table 4.3 Experiment IV), which is similar to the concentration of Fc clicked to a single-component film of deprotected TIPS-Eth-Ar-GC surface ((2.4 ± 0.3) × 10^{-10} mol cm^{-2}). This finding suggests that the conditions of modifying procedure do not affect the reactivity and/or accessibility of the H-Eth-Ar moieties toward click reaction, but the grafting of the second modifier is responsible for the lower Fc yield obtained.

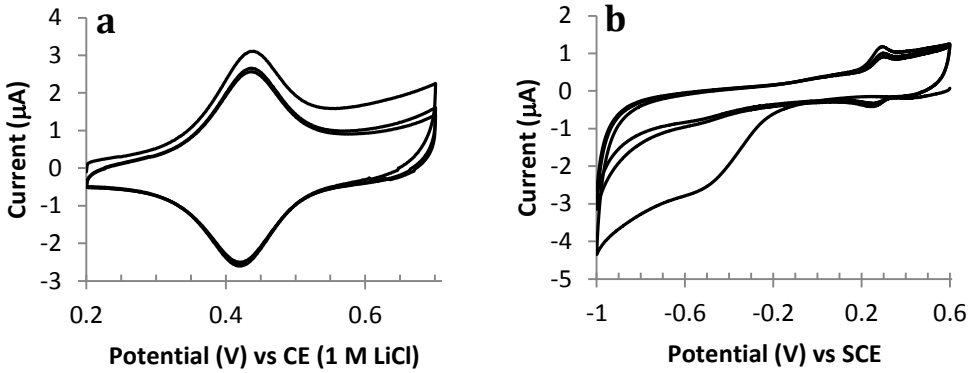

Figure 4.9 Repeat CVs of a GC electrode modified by route 4.3b using the conditions shown in Table 4.2, Experiment III. Scans were performed in: a) 0.1 M $LiClO_4$-EtOH at a scan rate of 200 mV s^{-1} and b) 0.1 M H_2SO_4 at a scan rate of 100 mV s^{-1}.

Due to the low concentration of NP groups and poor reproducibility (in Experiment III), grafting of the second modifier using NPH instead of NBD was investigated. Figure 4.10 shows that the mixed film prepared using NPH as the second modifier via route 4.3b exhibits well-defined CVs for both redox centres. The surface concentrations of Fc and NP groups are (1.8 ± 0.5) and (1.3 ± 0.8) × 10^{-10} mol cm^{-2}, respectively (Table 4.3, Experiment V). The concentration of Fc and NP groups are similar, within experimental error, to the single-

component groups grafted on bare GC under the same conditions ((2.4 ± 0.3) and (1.5 ± 0.2) × 10^{-10} mol cm^{-2}, respectively). The blank experiment, in which a TIPS-Eth-GC film was treated to the same steps as when grafting NPH but in the absence of NPH, gives a Fc surface concentration of (2.1 ± 0.4) × 10^{-10} mol cm^{-2} (Table 4.3, Experiment VI), which is the same as the Fc concentration obtained on a monolayer H-Eth-Ar-GC surface. This indicates that the conditions used for grafting of NPH and grafting of NPH itself do not affect the reactivity and/or accessibility of H-Eth-Ar groups towards click chemistry. However, although the average surface concentrations of Fc and NP groups are those expected for a mixed monolayer, this method gives even poorer reproducibility than the previous method, and hence a different strategy was attempted.

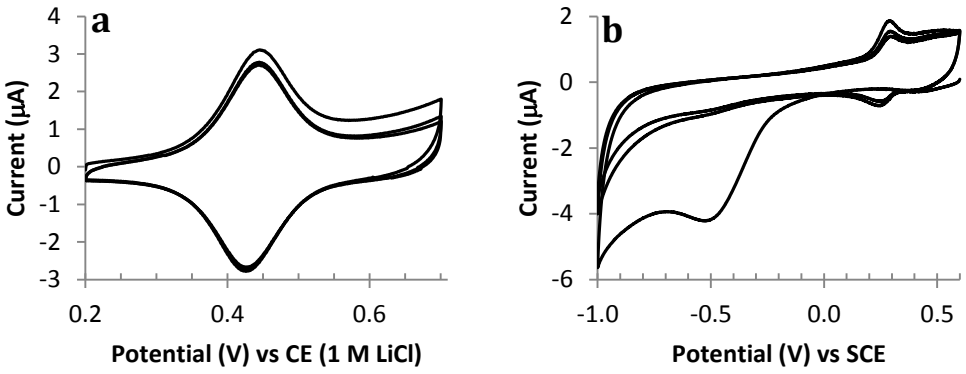

Figure 4.10 Repeat CVs of a GC electrode modified by route 4.3b using the conditions shown in Table 4.2, Expt. III. Scans were performed in: a) 0.1 M $LiClO_4$-EtOH at a scan rate of 200 mV s^{-1} and b) 0.1 M H_2SO_4 at a scan rate of 100 mV s^{-1}.

Scheme 4.3c shows the third strategy investigated for preparation of mixed monolayers. In this route, the click reaction of H-Eth-Ar-GC with $FcCH_2N_3$ was performed prior to grafting the second modifier. The aim was to eliminate the possibility of radical attack on the H-Eth-Ar-GC groups during the second grafting step. Table 4.3 Experiment VII describes the results of preparing mixed layers by this route using NBD under the same grafting conditions as for route 4.3b. This gives a similar Fc concentration ((1.5 ± 0.1) × 10^{-10} mol cm^{-2}) compared to that found using the route 4.3b strategy (Table 4.2, Experiment III), but a much higher NP

concentration ((1.6 ± 0.3) × 10^{-10} mol cm^{-2}) and a smaller experimental variability. Similar surface concentrations of Fc and NP ((1.6 ± 0.2) and (1.8 ± 0.6) × 10^{-10} mol cm^{-2}, respectively) are also obtained when NP groups are grafted from NPH (Table 4.3, Experiment IX). The NP concentrations of these mixed films are the same as the NP concentration found for a single-component film. However, the Fc concentrations of these mixed films are lower than the Fc concentration found for a single-component film. Blank experiments were carried out to account for this finding. Table 4.3 Experiment VIII and X list the surface concentration of Fc obtained when the TIPS-Eth-Ar-GC surface was treated to the same series of steps as in Experiments VII and IX but in the absence of NBD and NPH, respectively. The surface concentrations of Fc groups were (1.3 ± 0.1) and (1.9 ± 0.1) × 10^{-10} mol cm^{-2} for the NBD and NPH blanks, respectively. This compares with (2.4 ± 0.3) × 10^{-10} mol cm^{-2} for Fc clicked to a TIPS-Eth-Ar-GC surface without blank treatment and suggests that some Fc moieties are cleaved during the series of steps carried out in route 4.3c. Taking into account these blank experiments, the Fc concentrations of the mixed films obtained from route 4.3c are the maximum expected. Thus route 4.3c gives films with surface concentrations of Fc and NP groups consistent with a mixed monolayer.

Although films with very similar compositions were generated for experiments carried out with NBD and NPH using route 4.3c, the second grafting is more reproducible using NBD than NPH. This is surprising because when grafting from NBD solution, spontaneous grafting at open circuit potential is expected to contribute to the layer to an unknown extent.[47] On the other hand, NPH does not undergo spontaneous grafting at GC.[45]

Even though experiments carried out via route 4.3c resulted in surface concentrations of electro-active Fc and NP groups consistent with a monolayer structure, these results do not eliminate the possibility that NP groups have coupled to the Fc (or the already grafted first

layer) or form oligomeric strands, anchored to the surface or the first grafted layer. AFM depth profiling experiments were conducted to measure the thickness of these mixed layers. The AFM depth profiling technique involves removing a small section of film by scratching with an AFM tip (Figure 4.11a) and then measuring the depth of the scratched area (Figure 4.11b) using non-contact AFM as described in Chapter 2. PPF was used as the substrate, instead of GC, due to the lower surface roughness of PPF compared to GC. Average thickness of modified films at various stages of preparation by routes 4.3b and 4.3c (Scheme 4.3) are listed in Table 4.4. All of the measured film thicknesses (except for B) are lower than the calculated monolayer film thickness. The lower than expected thickness may be due to the interaction of the AFM tip with the underlying film. There is no evidence for multilayer formation suggesting that under these conditions, grafting of NP groups occurs within the layers (most likely to the PPF surface) rather than on top of the pre-existing layers. Hence, grafting of the second modifier does not result in multilayer formation.

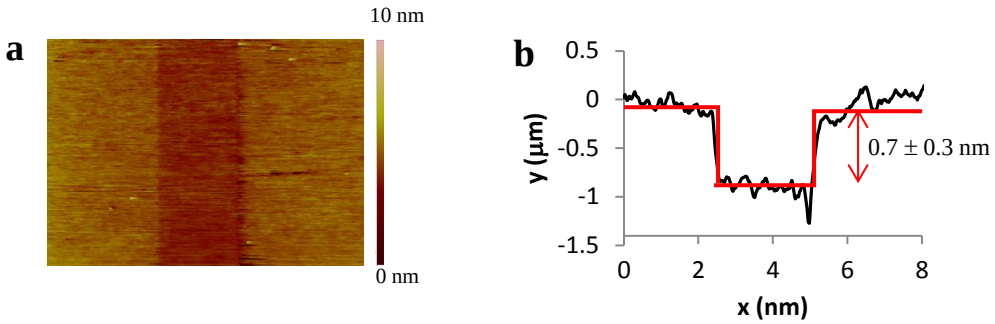

Figure 4.11 a) AFM topography images and b) depth profiles data of film structure B (Scheme 4.3).

Table 4.4 Thickness of films on PPF at various stages of modification (Scheme 4.3)

Film structure (Scheme 4.3)	Average film thickness (nm)	Calculated height[a] (nm)
A	0.4 ± 0.3	0.7
B[b]	0.7 ± 0.3	0.7
C[b]	0.8 ± 0.4	1.4
D	0.9 ± 0.3	1.4
E	0.8 ± 0.2	1.4
F	0.7 ± 0.2	1.4

[a]Molecule height was estimated using *Avogadro* freeware
[b]NP groups grafted from NPH.

4.3.2.2 *Formation of mixed monolayers via filling up void space using reactions with bare GC*

As demonstrated in Chapter 3, the reaction of primary alkyl amines and $(COCl)_2$ activated carboxylic acid compounds with bare GC results in surface grafting. Thus, another strategy to prepare a mixed monolayer is to take advantage of the reactivity of bare GC towards amine and carboxylic acid compounds as the second modifier to fill the void space created by the cleavage of the TIPS group (Scheme 4.5). An advantage of this procedure is that the second modifier can only react with the bare GC surface and not with the already grafted layer, and therefore the possibility of multilayer formation is avoided. Two routes were briefly investigated using this strategy. In the first route (Scheme 4.5, route a), after the deprotection of TIPS to obtain a H-Eth-Ar-GC surface, NBA.HCl was reacted with the modified surface using the HBTU method (HBTU activates carboxylic acid functionalities on the GC surface for amide coupling reactions), or carboxylic acid groups on the GC surface were first activated with $(COCl)_2$ and then reacted with NBA.HCl. The reactivity of the H-Eth-Ar group was then tested using the click reaction with $FcCH_2N_3$. In the second route, Fc was clicked to the H-Eth-Ar-GC surface prior to reaction of activated FcCOOH with GC (Scheme 4.5, route b). FcCOOH was chosen because the $E_{½}$ of the Fc/Fc^+ redox couple when attached to bare GC surface is 0.66 V, which is different to that of the $FcCH_2N_3$ clicked onto the H-Eth-Ar-GC surface ($E_{½}$ = 0.44 V). Hence, it was possible to distinguish between the two Fc moieties. Furthermore, for a surface with only Fc modifiers, the electrochemical investigation of the two different modifiers can be carried out in the same solution. For proof-of-concept studies, this is more convenient than a surface bearing NP and Fc groups, where CVs were obtained in 0.1 M $LiClO_4$-EtOH followed by 0.1 M H_2SO_4 for Fc and NP, respectively.

Table 4.5 summarises data for the mixed films prepared using the routes shown in Scheme 4.5. The preparation of the TIPS-Eth-Ar-GC surface and the deprotection of TIPS were carried out using the same method as in the earlier experiments. This surface was then reacted with NBA.HCl in the presence of HBTU and DIPEA followed by reaction with $FcCH_2N_3$. As shown in Figure 4.12, the mixed film exhibits well-defined CVs for both redox centres, with estimated surface concentrations of (1.7 ± 0.1) and $(1.1 \pm 0.1) \times 10^{-10}$ mol cm^{-2} for Fc and NP groups, respectively (Table 4.5, Experiment I). Interestingly, the concentration of NP groups coupled to the already modified GC is the same as that coupled to bare GC, $(1.1 \pm 0.2) \times 10^{-10}$ mol cm^{-2} (Chapter 3, Table 3.2 Experiment VIII). This is surprising because part of the GC surface has been covered by H-Eth-Ar groups in the mixed layer. The reason for this finding is unknown, but it is reproducible on repeat experiment. In contrast, the Fc concentration of the mixed layer is lower than that of the single-component Fc film ($(2.4 \pm 0.3) \times 10^{-10}$ mol cm^{-2}). This may be due to the steric hindrance imposed on the H-Eth-Ar groups after immobilisation of NP groups which decreases the accessibility of H-Eth-Ar groups for the click reaction.

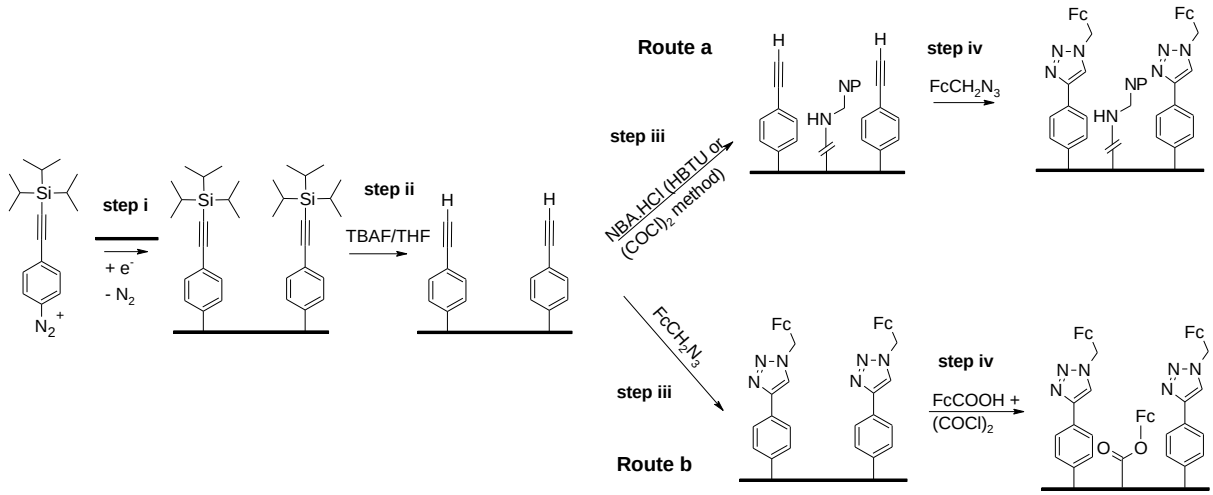

Scheme 4.5 Strategy for the preparation of mixed monolayer films from a monolayer H-Eth-Ar-GC surface using the filling-up approach; a) NBA.HCl was first coupled to the H-Eth-Ar-GC surface using either a HBTU or $(COCl)_2$ method followed by click reaction with $FcCH_2N_3$; b) $FcCH_2N_3$ was clicked to the H-Eth-Ar-GC surface prior to reaction with $(COCl)_2$-activated FcCOOH.

When a H-Eth-Ar-GC surface was activated in $(COCl)_2$ prior to reaction with NBA.HCl, the surface concentration of Fc and NP groups were (1.2 ± 0.1) and (2.4 ± 0.3) × 10^{-10} mol cm^{-2}, respectively (Table 4.5, Experiment II). Similar to the results above, this NP concentration was also in agreement with the NP concentration obtained on bare GC using $(COCl)_2$ ((2.5 ± 0.4) × 10^{-10} mol cm^{-2}, Chapter 3, Table 3.2 Experiment II), and the Fc concentration is much lower than for the single-component film. A blank experiment was carried out to test whether treatment with $(COCl)_2$ deactivates the H-Eth-Ar-GC surface for the click reaction. The H-Eth-Ar-GC surface was activated with $(COCl)_2$ and then was immersed in water to convert acid chlorides back to acid groups, Fc was then clicked to the surface. Table 4.5 Experiment III lists the Fc surface concentration ((1.8 ± 0.1) × 10^{-10} mol cm^{-2}) for the blank experiment. Clearly, the $(COCl)_2$ activation decreases the reactivity of the H-Eth-Ar groups towards click chemistry. However, the Fc surface concentration obtained in the mixed film is still lower than for the blank. These results can be accounted for if in addition to deactivation by $(COCl)_2$, the higher concentration of NP groups immobilised using $(COCl)_2$ sterically hinder the H-Eth-Ar groups towards the click reaction. This explanation is consistent with the lower NP concentration but higher Fc concentration obtained with the HBTU method. However, the total surface concentration of NP and Fc groups is greater for the $(COCl)_2$ method than for coupling using HBTU. This is most likely because HBTU is a milder coupling agent than $(COCl)_2$ as can be seen from the results above and those described in Chapter 3.

Table 4.5 Conditions for preparation of mixed films by the routes shown in Scheme 4.4 and the corresponding surface concentrations of electro-active Fc and NP groups.

Expt.	Route	2nd coupling species and method used	Γ_{NP} (10^{-10} mol cm^{-2})	Γ_{Fc} (10^{-10} mol cm^{-2})	n^a
I	4.5a	NBA.HCl + HBTU	1.1 ± 0.1	1.7 ± 0.1	2
II	4.5a	NBA.HCl + $(COCl)_2$	2.4 ± 0.3	1.2 ± 0.1	2

III[b]	4.5a	Blank	N/A	1.8 ± 0.1	2
IV	4.5b	FcCOOH + $(COCl)_2$	N/A	1.7 ± 0.1[c] 1.7 ± 0.3[d]	2

[a]*n* is the number of samples analysed

[b]Blank experiment was carried out using the same condition as Experiment II, but instead of reacting with NBA.HCl, it was reacted with H_2O for 30 min

[c]Reaction with $FcCH_2N_3$

[d]Reaction with $(COCl)_2$-activated FcCOOH

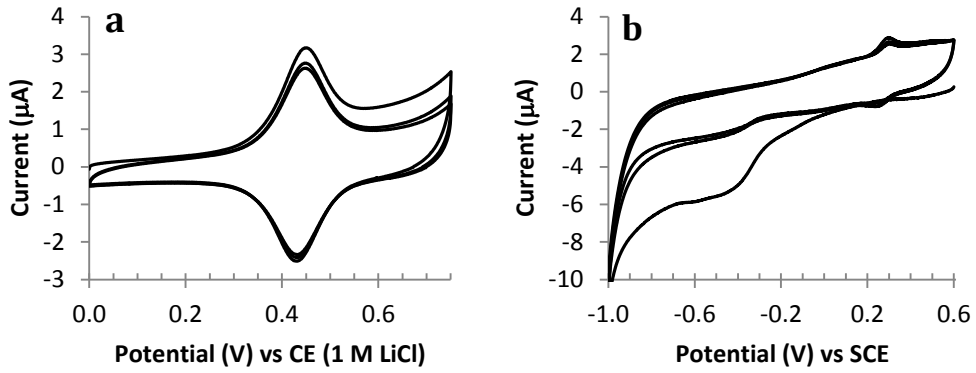

Figure 4.12 Repeat CVs of a GC electrode modified by route 4.5a using the conditions shown in Table 4.5, Experiment I. Scans were performed in: a) 0.1 M $LiClO_4$-EtOH at a scan rate of 200 mV s^{-1} and b) 0.1 M H_2SO_4 at a scan rate of 100 mV s^{-1}.

Table 4.5 Experiment IV describes experiments similar to those above but in these experiments $FcCH_2N_3$ was clicked first, followed by reaction of GC with $(COCl)_2$ activated FcCOOH (Scheme 4.5b). Figure 4.13 shows the CVs of two well-defined sequential Fc/Fc^+ redox couples. The first Fc/Fc^+ redox couple at $E_{½}$ = 0.44 V arises from the Fc clicked to the H-Eth-Ar group on the surface, while the second couple at $E_{½}$ = 0.65 V arises from the Fc coupled directly to the GC surface. The peak area of each Fc/Fc^+ couple was estimated by curve fitting the voltammetric peaks using Linkfit software[48] (Chapter 2). Each peak was integrated to obtain the corresponding area and thus the surface concentration. As can be seen from the CV (Figure 4.13), the Fc was not stable upon continuous cycling and the first scan is markedly different to the subsequent scans, therefore, data from the second scan was used for curve-fitting and subsequent calculation of the surface concentration. Table 4.5 Experiment IV shows that preparation of a mixed film using route 4.5b gives an equal amount of electro-

active Fc from the 1st and 2nd modifier, (1.7 ± 0.1) and (1.7 ± 0.3) × 10^{-10} mol cm^{-2}, respectively, with total surface concentrations consistent with monolayer films.

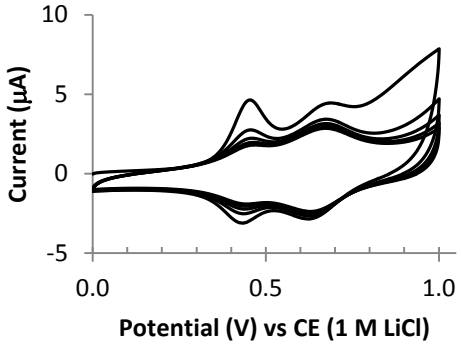

Figure 4.13 Five consecutive cycles obtained in 0.1 M $LiClO_4$-EtOH of a GC electrode modified by route 4.5b using the conditions shown in Table 4.5, Experiment III. Scan rate = 200 mV s^{-1}.

Comparing the results in Tables 4.3 and 4.5 shows that mixed monolayers can be prepared by several routes: sequential grafting using two different diazonium salts (Scheme 4.3) or by first grafting using a protected aryldiazonium salt that will create a void space upon removal of the protecting group followed by filling in the void space using reactions directly on the bare GC (Scheme 4.5). The latter strategy (Scheme 4.5) has advantages for the preparation of mixed monolayers, because there is no need to carefully control the grafting of the second modifier. Hence, the potential problem of the attack of the second modifier on the already grafted moiety is not encountered in this second approach (Scheme 4.5).

4.4 Conclusion

Preparation of monolayer terminated H-Eth-Ar groups by reduction of an aryldiazonium salt using the protection-deprotection approached has been investigated. The reactivity of the H-Eth-Ar moiety was tested using the azide-alkyne 'click' reaction with $FcCH_2N_3$ as the model azide compound. Comparison of the reactivities of monolayer and multilayer H-Eth-Ar films towards click reaction was also described. Monolayer H-Eth-Ar films give a higher concentration of electro-active Fc than multilayers which may be due to a more ordered

structure of monolayer films, which decreases steric hindrance for the click reaction. Preparation of binary layers on GC surfaces using electroreduction of [TIPS-Eth-Ar-N_2]BF_4 as the first modifier has been explored. The deprotection of the TIPS group creates pin-holes that can be filled by a second modifier either by electrografting or by chemical modification. Electrografting via aryldiazonium salts or arylhydrazine can be used in the second step to fill-in the existing H-Eth-Ar monolayer. However, grafting conditions need to be optimised to ensure that multilayers do not form and that the second modifier does not attach to the already grafted film. Alternatively, the second component can be immobilised by reaction of the bare GC with amine or carboxylic acid containing molecules. Regardless of the strategy applied, the use of TIPS as the protecting group results in a binary monolayer with approximately equal concentrations of each modifier. Direct reaction with GC is preferred for the attachment of the second component because controlled conditions are not necessary and the reaction can only result in a monolayer. Moreover, utilising the possibility of reaction of amine or carboxylic acid groups with bare GC surfaces, a lot of different functionalities can be immobilised onto the surface to form mixed layers containing more than one component. Further use of [TIPS-Eth-Ar-N_2]BF_4 for forming a binary mixed layer will be discussed in Chapters 5 and 6.

4.5 References

1 Anariba, F., DuVall, S.H., McCreery, R.L., Mono- and multilayer formation by diazonium reduction on carbon surfaces monitored with atomic force microscopy "scratching". *Anal. Chem.*, **2003**, *75*, 3837.

2 Brooksby, P.A., Downard, A.J., Electrochemical and atomic force microscopy study of carbon surface modification via diazonium reduction in aqueous and acetonitrile solutions. *Langmuir*, **2004**, *20*, 5038.

3 Doppelt, P., Hallais, G., Pinson, J., Podvorica, F., Verneyre, S., Surface modification of conducting substrates. Existence of azo bonds in the structure of organic layers obtained from diazonium salts. *Chem. Mater.*, **2007**, *19*, 4570.

4 Kariuki, J.K., McDermott, M.T., Formation of multilayers on glassy carbon electrodes via the reduction of diazonium salts. *Langmuir*, **2001**, *17*, 5947.

5 Belanger, D., Pinson, J., Electrografting: A powerful method for surface modification. *Chem. Soc. Rev.*, **2011**, *40*, 3995.

6 Leroux, Y.R., Fei, H., Noel, J.M., Roux, C., Hapiot, P., Efficient covalent modification of a carbon surface: Use of a silyl protecting group to form an active monolayer. *J. Am. Chem. Soc.*, **2010**, *132*, 14039.

7 Leroux, Y.R., Hapiot, P., Nanostructured monolayers on carbon substrates prepared by electrografting of protected aryldiazonium salts. *Chem. Mater.*, **2013**, *25*, 489.

8 Leroux, Y.R., Hui, F., Hapiot, P., A protecting-deprotecting strategy for structuring robust functional films using aryldiazonium electroreduction. *J. Electroanal. Chem.*, **2013**, *688*, 298.

9 Malmos, K., Dong, M.D., Pillai, S., Kingshott, P., Besenbacher, F., Pedersen, S.U., Daasbjerg, K., Using a hydrazone-protected benzenediazonium salt to introduce a near-monolayer of benzaldehyde on glassy carbon surfaces. *J. Am. Chem. Soc.*, **2009**, *131*, 4928.

10 Nielsen, L.T., Vase, K.H., Dong, M.D., Besenbacher, F., Pedersen, S.U., Daasbjerg, K., Electrochemical approach for constructing a monolayer of thiophenolates from grafted multilayers of diaryl disulfides. *J. Am. Chem. Soc.*, **2007**, *129*, 1888.

11 Leroux, Y.R., Hui, F., Noel, J.M., Roux, C., Downard, A.J., Hapiot, P., Design of robust binary film onto carbon surface using diazonium electrochemistry. *Langmuir*, **2011**, *27*, 11222.

12 Santos, L., Ghilane, J., Lacroix, J.C., Formation of mixed organic layers by stepwise electrochemical reduction of diazonium compounds. *J. Am. Chem. Soc.*, **2012**, *134*, 5476.

13 Lee, L., Brooksby, P.A., Leroux, Y.R., Hapiot, P., Downard, A.J., Mixed monolayer organic films via sequential electrografting from aryldiazonium ion and arylhydrazine solutions. *Langmuir*, **2013**, *29*, 3133.

14 Casas-Solvas, J.M., Ortiz-Salmeron, E., Gimenez-Martinez, J.J., Garcia-Fuentes, L., Capitan-Vallvey, L.F., Santoyo-Gonzalez, F., Vargas-Berenguel, A., Ferrocene-carbohydrate conjugates as electrochemical probes for molecular recognition studies. *Chem.-Eur. J.*, **2009**, *15*, 710.

15 Yu, S.S.C., Tan, E.S.Q., Jane, R.T., Downard, A.J., An electrochemical and XPS study of reduction of nitrophenyl films covalently grafted to planar carbon surfaces. *Langmuir*, **2007**, *23*, 11074.

16 Baranton, S., Belanger, D., Electrochemical derivatization of carbon surface by reduction of in situ generated diazonium cations. *J. Phys. Chem. B*, **2005**, *109*, 24401.

17 Baranton, S., Belanger, D., In situ generation of diazonium cations in organic electrolyte for electrochemical modification of electrode surface. *Electrochim. Acta*, **2008**, *53*, 6961.

18 Cline, K.K., Baxter, L., Lockwood, D., Saylor, R., Stalzer, A., Nonaqueous synthesis and reduction of diazonium ions (without isolation) to modify glassy carbon electrodes using mild electrografting conditions. *J. Electroanal. Chem.*, **2009**, *633*, 283.

19 Richard, W., Evrard, D., Gros, P., New insight into 4-nitrobenzene diazonium reduction process: Evidence for a grafting step distinct from NO_2 electrochemical reactivity. *J. Electroanal. Chem.*, **2012**, *685*, 109.

20 Bard, A.J., Faulkner, L.R., *Electrochemical methods fundamentals and applications*. Second ed. **2001**: John Wiley & Sons, Inc.

21 Nicholso.Rs, Theory and application of cyclic voltammetry for measurement of electrode reaction kinetics. *Anal. Chem.*, **1965**, *37*, 1351.

22 Cruickshank, A.C., Tan, E.S.Q., Brooksby, P.A., Downard, A.J., Are redox probes a useful indicator of film stability? An electrochemical, AFM and XPS study of electrografted amine films on carbon. *Electrochem. Commun.*, **2007**, *9*, 1456.

23 Bard, A.J., Inner-sphere heterogeneous electrode reactions. Electrocatalysis and photocatalysis: The challenge. *J. Am. Chem. Soc.*, **2010**, *132*, 7559.

24 Chen, P.H., McCreery, R.L., Control of electron transfer kinetics at glassy carbon electrodes by specific surface modification. *Anal. Chem.*, **1996**, *68*, 3958.

25 DuVall, S.H., McCreery, R.L., Control of catechol and hydroquinone electron-transfer kinetics on native and modified glassy carbon electrodes. *Anal. Chem.*, **1999**, *71*, 4594.

26 DuVall, S.H., McCreery, R.L., Self-catalysis by catechols and quinones during heterogeneous electron transfer at carbon electrodes. *J. Am. Chem. Soc.*, **2000**, *122*, 6759.

27 Berg, R., Straub, B.F., Advancements in the mechanistic understanding of the copper-catalyzed azide-alkyne cycloaddition. *Beilstein Journal of Organic Chemistry*, **2013**, *9*, 2715.

28 Sokolova, N.V., Nenajdenko, V.G., Recent advances in the Cu(I)-catalyzed azide-alkyne cycloaddition: Focus on functionally substituted azides and alkynes. *RSC Advances*, **2013**, *3*, 16212.

29 Laviron, E., General expression of the linear potential sweep voltammogram in the case of diffusionless electrochemical systems. *J. Electroanal. Chem.*, **1979**, *101*, 19.

30 Pontikos, N.M., McCreery, R.L., Microstructural and morphological-changes induced in glassy-carbon electrodes by laser irradiation. *J. Electroanal. Chem.*, **1992**, *324*, 229.

31 Brooksby, P.A., Downard, A.J., Multilayer nitroazobenzene films covalently attached to carbon. An AFM and electrochemical study. *J. Phys. Chem. B*, **2005**, *109*, 8791.

32 Ceccato, M., Nielsen, L.T., Iruthayaraj, J., Hinge, M., Pedersen, S.U., Daasbjerg, K., Nitrophenyl groups in diazonium-generated multilayered films: Which are electrochemically responsive? *Langmuir*, **2010**, *26*, 10812.

33 Hupp, J.T., The ferrocene assumption in redox thermodynamics - implications from optical intervalence studies of ion-pairing to ferrocenium. *Inorg. Chem.*, **1990**, *29*, 5010.

34 Ju, H.X., Leech, D., Effect of electrolytes on the electrochemical behaviour of 11-(ferrocenylcarbonyloxy)undecanethiol SAMs on gold disk electrodes. *Phys. Chem. Chem. Phys.*, **1999**, *1*, 1549.

35 Norman, L.L., Badia, A., Microcantilevers modified with ferrocene-terminated self-assembled monolayers: Effect of molecular structure and electrolyte anion on the redox-induced surface stress. *J. Phys. Chem. C*, **2011**, *115*, 1985.

36 Rowe, G.K., Creager, S.E., Redox and ion-pairing thermodynamics in self-assembled monolayers. *Langmuir*, **1991**, *7*, 2307.

37 Uosaki, K., Sato, Y., Kita, H., Electrochemical characteristics of a gold electrode modified with a self-assembled monolayer of ferrocenylalkanethiols. *Langmuir*, **1991**, *7*, 1510.

38 Valincius, G., Niaura, G., Kazakeviciene, B., Talaikyte, Z., Kazemekaite, M., Butkus, E., Razumas, V., Anion effect on mediated electron transfer through ferrocene-terminated self-assembled monolayers. *Langmuir*, **2004**, *20*, 6631.

39 Rowe, G.K., Creager, S.E., Interfacial solvation and double-layer effects on redox reactions in organized assemblies. *J. Phys. Chem.*, **1994**, *98*, 5500.

40 Baker, M.V., Kraatz, H.B., Quail, J.W., Solvent effects on the redox properties of ferrocenoyl-dipeptides. *New J. Chem.*, **2001**, *25*, 427.

41 Noviandri, I., Brown, K.N., Fleming, D.S., Gulyas, P.T., Lay, P.A., Masters, A.F., Phillips, L., The decamethylferrocenium/decamethylferrocene redox couple: A superior redox standard to the ferrocenium/ferrocene redox couple for studying solvent effects on the thermodynamics of electron transfer. *J. Phys. Chem. B*, **1999**, *103*, 6713.

42 Sahami, S., Weaver, M.J., Deficiencies of the ferricinium-ferrocene redox couple for estimating transfer energies of single ions. *Journal of Solution Chemistry*, **1981**, *10*, 199.

43 Brett, D.J.L., Williams, R., Wilde, C.P., Temperature effects on the voltammetry of ferrocene terminated self-assembled monolayers. *J. Electroanal. Chem.*, **2002**, *538*, 65.

44 Cruanes, M.T., Drickamer, H.G., Faulkner, L.R., Characterization of charge-transfer processes in self-assembled monolayers by high-pressure electrochemical techniques. *Langmuir*, **1995**, *11*, 4089.

45 Malmos, K., Iruthayaraj, J., Ogaki, R., Kingshot, P., Besenbacher, F., Pedersen, S.U., Daasbjerg, K., Grafting of thin organic films by electrooxidation of arylhydrazines. *J. Phys. Chem. C*, **2011**, *115*, 13343.

46 Malmos, K., Iruthayaraj, J., Pedersen, S.U., Daasbjerg, K., General approach for monolayer formation of covalently attached aryl groups through electrografting of arylhydrazines. *J. Am. Chem. Soc.*, **2009**, *131*, 13926.

47 Barriere, F., Downard, A.J., Covalent modification of graphitic carbon substrates by non-electrochemical methods. *J. Solid State Electr.*, **2008**, *12*, 1231.

48 Loring, J.S., *Linkfit*. **2000**, Ph.D. Dissertation, University of California, Davis: University of California, Davis.

Chapter 5. Preparation of Carboxyphenyl Monolayers and Mixed Layers

5.1 Introduction

As detailed in Chapter 1, preparation of monolayers from aryldiazonium salts can be achieved through a protection-deprotection approach (Scheme 1.9, Chapter 1). The use of the triisopropylsilyl (TIPS) protecting group on ethynylbenzenediazonium salt, [TIPS-Eth-Ar-N_2]BF_4 to yield a monolayer film terminated with ethynyl (Eth) groups has been reported by Leroux and co-workers[1-3] and also in this thesis work (Chapter 4).

In this Chapter, preparation of a carboxyphenyl (H-COO-Ar) monolayer via a protection-deprotection strategy is described.[4] Carboxylic acid groups are particularly useful for tethering a wide range of species, especially amine derivatives via amide bond coupling. An example is the immobilisation of biomolecules via the formation of amide linkages through coupling with carboxylic acid terminated films.[5-8] Another example is the assembly of metal organic frameworks (MOFs) onto the surface.[9-12] Most MOF assembly employs carboxylic acid functionalised ligands;[13-15] thus a carboxylic acid terminated surface can be used as an anchoring point for MOF assembly to provide direct bonds between the surface and the MOF.[9, 10, 12]

This chapter first describes the synthesis of the protected aryldiazonium salt, 4-((9-H-fluoren-9-ylmethoxy)carbonyl)benzene-1-diazonium tetrafluoroborate ([Fm-COO-Ar-N_2]BF_4). Grafting and deprotection of the Fm-COO-Ar layer was investigated and the resulting films were characterised by electrochemistry and atomic force microscopy (AFM). Preparation of binary mixed layers of [Fm-COO-Ar-N_2]BF_4 and [TIPS-Eth-Ar-N_2]BF_4 to give a

corresponding surface with H-COO-Ar and H-Eth-Ar groups, respectively was also investigated. Most of the work described in this Chapter has been published in reference 4.

5.2 Experimental

All chemical reagents and materials are outlined in Chapter 2. Azidomethyl ferrocene ($FcCH_2N_3$) was synthesised following a literature method[16] which is briefly described in Section 2.1.5.1. Aminomethyl ferrocene ($FcCH_2NH_2$) was synthesised according to a published method[17] which is briefly explained in Section 2.1.5.2. The syntheses of 9-H-fluoren-9-yl methyl 4-aminobenzoate (Fm-COO-Ar-NH_2) and its diazonium salt, [Fm-COO-Ar-N_2]BF_4, are detailed in Section 2.1.4.2. PPF preparation is described in Section 2.3.1.2. The AFM depth profiling technique for film thickness measurement is explained in Section 2.5.

All experiments in this chapter were undertaken using a GC disk sealed in Teflon (area = 0.071 cm^2) as the working electrode, except for AFM experiments for which PPF was used. A Pt mesh was used as counter electrode and SCE as reference electrode for aqueous solution and CE (1 M LiCl) for non-aqueous solution, unless specified otherwise.

Electrografting. Fm-COO-Ar groups were electrograted to GC and PPF from a solution of 5 mM [Fm-COO-Ar-N_2]BF_4 in 0.1 M TBABF_4-ACN using five cycles between 0.80 and -0.75 V at a scan rate of 50 mV s^{-1}. The modified electrode (Fm-COO-Ar-GC) was rinsed with acetone, sonicated in ACN for 5 min, and dried with a stream of N_2(g). Fm was removed from the layer by immersing the modified electrode in a stirred solution of 20% piperidine in DMF[18] for 40 min giving the deprotected monolayer, H-COO-Ar-GC. Electrodes were carefully rinsed with acetone and H_2O after deprotection.

Mixed layer preparation from mixed solution. Electrografting was carried out from a mixed solution of [Fm-COO-Ar-N_2]BF_4 and [TIPS-Eth-Ar-N_2]BF_4 in 0.1 M $TBABF_4$-ACN using five cycles between 0.80 and -0.75 V at a scan rate of 50 mV s^{-1}. The modified electrode was rinsed with acetone, and sonicated in ACN for 5 min, and dried with a stream of N_2(g). Fm was removed first in 20% piperidine-DMF for 40 min, followed by removal of the TIPS group in 0.05 M TBAF-THF for 20 min.[1] Modified electrodes were carefully rinsed with acetone and H_2O after each deprotection step.

Mixed layer preparation by sequential electrografting: [Fm-COO-Ar-N_2]BF_4 as first modifier. The first modifier, [Fm-COO-Ar-N_2]BF_4, was electrografted to the surface and deprotected using the same method as described above. The second modifier, [TIPS-Eth-Ar-N_2]BF_4, was electrografted to the H-COO-Ar-GC modified surface from a solution of 5 mM [TIPS-Eth-Ar-N_2]BF_4 in 0.1 M $TBABF_4$-ACN using two cycles between 0.60 and -0.75 V at a scan rate of 200 mV s^{-1}. The modified electrodes were rinsed with acetone and sonicated in ACN for 5 min after each grafting step. After removal of the protecting groups in each of the deprotection solutions, electrodes were carefully rinsed with acetone and H_2O, and dried with a stream of N_2(g).

Mixed layer preparation by sequential electrografting: [TIPS-Eth-Ar-N_2]BF_4 as first modifier. The first modifier was electrografted from a solution of 5 mM [TIPS-Eth-Ar-N_2]BF_4 in 0.1 M $TBABF_4$-ACN using five cycles between 0.60 and -0.75 V at a scan rate of 50 mV s^{-1}. The second modifier, [Fm-COO-Ar-N_2]BF_4, was electrografted to the H-Eth-Ar-GC modified surface from a solution of 5 mM [Fm-COO-Ar-N_2]BF_4 in 0.1 M $TBABF_4$-ACN using two cycles between 0.80 and -0.75 V at a scan rate of 200 mV s^{-1}. After each grafting step, the electrodes were rinsed with acetone and sonicated in ACN for 5 min. Deprotection

was carried out by stirring in the respective deprotection solution for 1 h each. Electrodes were carefully rinsed with acetone and H_2O after each deprotection step.

Amide coupling reaction on H-COO-Ar-GC surface. $(COCl)_2$-activated coupling reactions were conducted according to the method described in Section 2.4.2.2.1. After coupling by the $(COCl)_2$ method, modified electrodes were stirred in DCM for 10 min followed by sonication in EtOH for 2 min. HBTU-promoted coupling reactions were performed using the method detailed in Section 2.4.2.4. After coupling by the HBTU method, modified electrodes were sonicated in ACN for 5 min.

Coupling reactions on mixed layers. Coupling of 4-nitrobenzylamine hydrochloride (NBA.HCl) to H-COO-Ar moieties in mixed layers was carried out by the methods described above, prior to the click reaction of H-Eth-Ar groups. $FcCH_2NH_3$ was clicked to H-Eth-Ar groups by the method outlined in Chapter 2, Section 2.4.2.1. After amine coupling, electrodes were sonicated in ACN for 5 min and dried with a stream of N_2(g). After the click reaction, electrodes were stirred in EDTA-Na_2 for 20 min, and sonicated in THF and ACN for 2 and 3 min, respectively.

Electrochemistry. Cyclic voltammograms (CVs) of immobilised ferrocenyl (Fc) and nitrophenyl (NP) groups were obtained in 0.1 M $LiClO_4$-EtOH at a scan rate of 200 mV s^{-1} and 0.1 M H_2SO_4 at a scan rate of 100 mV s^{-1}, respectively. For mixed films, the voltammetry of Fc groups was recorded prior to that of NP groups. The surface concentration of immobilised Fc was determined by averaging the areas under the anodic and cathodic peaks from the third voltammetric cycle, unless stated otherwise. The surface concentration of immobilised NP groups was estimated from the first cycle using the NP reduction and the hydroxyaminophenyl oxidation peak areas and the number of electrons involved in each redox process[19] as described in Chapter 2.

5.3 Results and Discussion

5.3.1 Preparation and characterisation of carboxyphenyl monolayers

5.3.1.1 Synthesis of the protected carboxyphenyl diazonium salt precursor

The protected carboxyphenyl diazonium salt, [Fm-COO-Ar-N_2]BF_4, was synthesised in four steps as shown in Scheme 5.1. Firstly, Boc protection on the amine group of 4-aminobenzoic acid was carried out,[20] followed by a Steglich esterification[21] with 9-fluerenylmethanol (FmOH) to give the Fm-COO-Ar-NH-Boc compound. It is necessary to protect the amine group prior to the esterification step because the amine is more reactive than the hydroxyl functionality of FmOH. Without protection, the amine and carboxylic acid groups of 4-aminobenzoic acid would couple. After esterification, the Boc group was cleaved using trifluoroacetic acid (TFA)[22] to yield the Fm-COO-Ar-NH_2 aniline derivative. Finally, the desired [Fm-COO-Ar-N_2]BF_4 salt was obtained by reaction of the aniline derivatives with $NOBF_4$ at -40 °C under a N_2 atmosphere. Details of the synthesis can be found in Chapter 2.

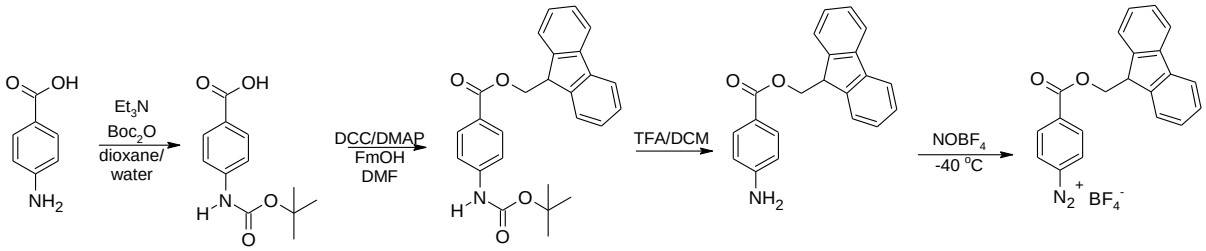

Scheme 5.1 Reaction scheme for the preparation of [Fm-COO-Ar-N_2]BF_4.

5.3.1.2 Characterisation of carboxyphenyl monolayers using redox probe voltammetry

The strategies for preparation of carboxyphenyl monolayers and subsequent coupling of amine molecules are shown in Scheme 5.2. Electrografting was carried out by scanning five cycles between 0.80 to -0.75 V at 50 mV s^{-1} in a solution of 5 mM [Fm-COO-Ar-N_2]BF_4 in 0.1 M $TBABF_4$-ACN (Figure 5.1). As expected for aryldiazonium ion grafting, irreversible

reduction peaks ($E_{p,c}$ = 0.38 V and 0.14 V) were observed on the first scan and relatively low current and featureless voltammograms in subsequent scans. (The origin of these two reduction peaks is discussed in Chapter 7.) The disappearance of the reduction peaks after one cycle indicates inhibition of electron transfer to diazonium ion in solution, consistent with the formation of a non-conducting layer.

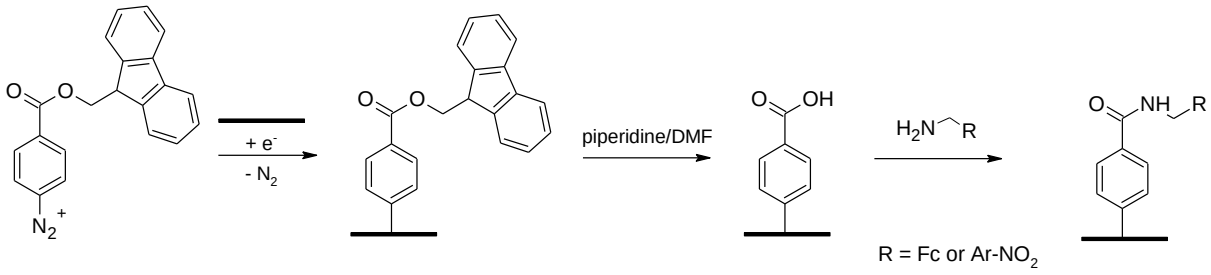

Scheme 5.2 Schematic representation for the preparation of H-COO-Ar-GC monolayer and further coupling of Fc and NP groups to the layer.

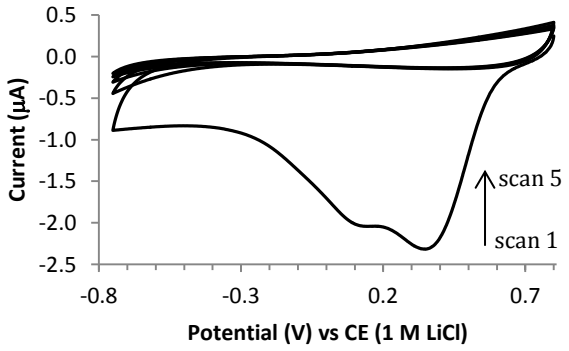

Figure 5.1 Five consecutive CV scans at a bare GC electrode in a solution of 5 mM [Fm-COO-Ar-N_2]BF_4 in 0.1 M $TBABF_4$-ACN. Scan rate = 50 mV s^{-1}.

After grafting a Fm-COO-Ar film, removal of the Fm protecting groups in 20% piperidine-DMF solution[18] was examined. Deprotection decreases the thickness of the layer and hence should decrease the effect of the layer on electron transfer rates to redox probes in solution. The effect of immersion in the deprotection solution was monitored at 20 min intervals by recording the CV of 1 mM dopamine in 0.1 M H_2SO_4 at the modified electrode. As described in Chapter 4, dopamine is an inner sphere redox probe,[23-26] and its voltammetry is surface

sensitive and also surface oxide sensitive.[24, 26] The electrode kinetics of dopamine depend on the ability of dopamine to adsorb on the electrode surface and/or to hydrogen bond (H-bond) to surface oxides.[26] Figure 5.2 shows that the Fm-COO-Ar-GC surface is totally blocking to dopamine redox activity (black line), however after stirring in 20% piperidine-DMF solution for 20 min (blue line), well-defined dopamine redox peaks are observed with a peak separation, ΔE_p, of 101 mV, but with peak currents approximately half those at the bare GC surface (red line). After 40 min stirring in the deprotection solution (green line), the peak currents are close to those for the bare GC surface, consistent with generation of catalytic sites that are accessible by dopamine, either from the void space created by the removal of Fm groups, or from H-bonding to the H-COO-Ar-GC surface. A further 20 min stirring gives little further change (yellow line). Hence it appears that the cleavage of Fm groups is essentially complete after stirring in a solution of 20% piperidine-DMF for 40 min. Therefore, for further experiments, 40 min was adopted as the standard deprotection time, unless specified otherwise.

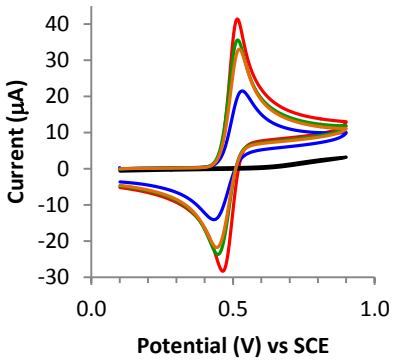

Figure 5.2 CVs obtained in a solution of 1 mM dopamine in 0.1 M H_2SO_4 at scan rate = 100 mV s^{-1}. Red line: bare GC; black line: Fm-COO-Ar-GC; blue line: Fm-COO-Ar-GC after stirring in 20% piperidine-DMF for 20 min; green line: 40 min and yellow line: 60 min.

Ferrocene and ferrocyanide were also chosen as additional redox probes to investigate the blocking properties at each stage of modification: before deprotection, after immersion of the Fm-COO-Ar modified electrode in DMF solution in the absence of piperidine, and after

subsequent immersion in the deprotection solution (Figure 5.3). Immersion in DMF in the absence of piperidine was included to demonstrate that piperidine is required to obtain the deprotected H-COO-Ar layer. After grafting and before deprotection, the voltammogram recorded in ferrocene-ACN solution (Figure 5.3a, blue line) shows only very low current over the potential range where the ferrocene redox reaction occurs at the bare electrode (black line); this is consistent with a relatively thick and non-porous layer, which significantly slows the electron transfer rate for the ferrocene/ferrocenium (Fc/Fc^{+}) redox couple. After immersion of the modified surface in DMF solution for 40 min, the CV obtained in ferrocene solution (green line) is less blocked towards the ferrocene redox reaction, indicating that a more porous layer is formed; this may be due to swelling of the film and/or removal of physisorbed impurities. Subsequently, after deprotection in 20 % piperidine-DMF solution for 40 min (red line), the CV is very similar to that obtained at bare GC, suggesting that a thin layer that has no detectable influence on the ferrocene electron transfer is obtained. Similar results were obtained with dopamine in aqueous H_2SO_4 solution (Figure 5.3b).

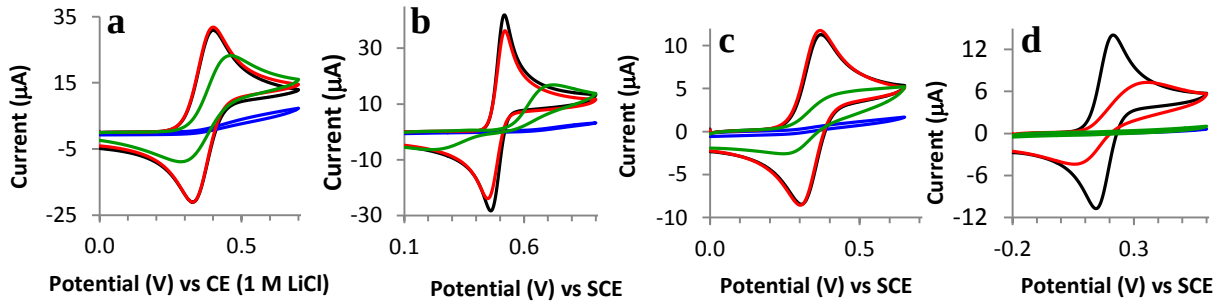

Figure 5.3 CVs of bare GC (black line), Fm-COO-Ar-GC before deprotection (blue line), after immersion in DMF for 40 min (green line), and after deprotection in piperidine for 40 min (red line), in a solution of: a) 1 mM ferrocene in 0.1 M $TBABF_4$-ACN; b) 1 mM dopamine in 0.1 M H_2SO_4; c) 1 mM ferrocyanide in 0.1 M HCl (pH 1.2); and d) 1 mM ferrocyanide in 0.1 M PB (pH 6.9). Scan rate = 100 mV s^{-1}.

The electrochemistry of ferrocyanide at different pH (1.2 and 6.9) was examined because the deprotected surface, H-COO-Ar-GC, is pH sensitive. A multilayer H-COO-Ar film has a pK_a

of 2.8 – 3.3,[27] and hence at pH 1.2 and 6.9, the deprotected film is expected to be largely protonated (neutral) and deprotonated (negatively charged), respectively. The CVs obtained for ferrocyanide in aqueous solution at pH 1.2 and 6.9 are shown in Figures 5.3c and 5.3d, respectively. The results observed for ferrocyanide at pH 1.2 are similar to those found for dopamine and ferrocene. However, at pH 6.9 the deprotected surface, H-COO-Ar-GC (red line), shows a low current for the ferrocyanide redox couple compared to that at bare GC, and the ΔE_p of 279 mV is large compared to that at bare GC (ΔE_p = 65 mV). This result is consistent with a H-COO-Ar-GC surface that has acid-base properties. At pH 6.9, the surface is deprotonated, and negatively charged; electrostatic repulsion between the negatively charged surface and the negatively charged ferri/ferrocyanide redox species is expected and this slows the electron transfer rate compared to that at the neutral deprotected surface (pH 1.2). The fact that the CV obtained at pH 1.2 is similar to that at bare GG suggests that the electrochemistry is not affected by the presence of the grafted layer, hence indicating as expected, that only a very thin layer is present. Moreover, because ferrocyanide is an inner sphere redox species, this indicates that ferrocyanide can interact directly with the GC surface, presumably at the voids created by deprotection of Fm groups.

5.3.1.3 Characterisation of carboxyphenyl monolayers using amide coupling reactions

The reactivity of the H-COO-Ar monolayer was tested by performing amide coupling reactions with amine derivatives. NBA and $FcCH_2NH_2$ were coupled to the H-COO-Ar monolayer, to give a surface modified with NP and Fc groups, respectively. NP and Fc were chosen because they are electro-active and allow the electrochemical estimation of their surface concentration. Coupling reactions were carried out using two different activating agents: $(COCl)_2$ and HBTU. Figures 5.4a and 5.4b show CVs obtained in 0.1 M H_2SO_4 for H-COO-Ar film after reaction with NBA.HCl using the $(COCl)_2$ and HBTU methods,

respectively. Both CVs show the irreversible reduction of NP groups to aminophenyl and hydroxyaminophenyl groups at ~0.5 V, and the chemically reversible hydroxyaminophenyl/nitrosophenyl couple centred at ~0.25 V. From the peak areas in the first cyclic scan, the estimated surface concentration of immobilised NP groups for the $(COCl)_2$ and HBTU method were (4.1 ± 0.7) (n = 5) and (3.0 ± 0.8) (n = 3) × 10^{-10} mol cm^{-2}, respectively. Although these surface concentration values have relatively large uncertainties, in all amide coupling reactions throughout this thesis work, $(COCl)_2$-activation gave higher coupling yields than HBTU, and the same is presumably the case here. As explained in Chapter 3, this may be due to the cleaner product obtained using $(COCl)_2$ method compared to the HBTU coupling reagents, which usually results in urea as a by-product.[28]

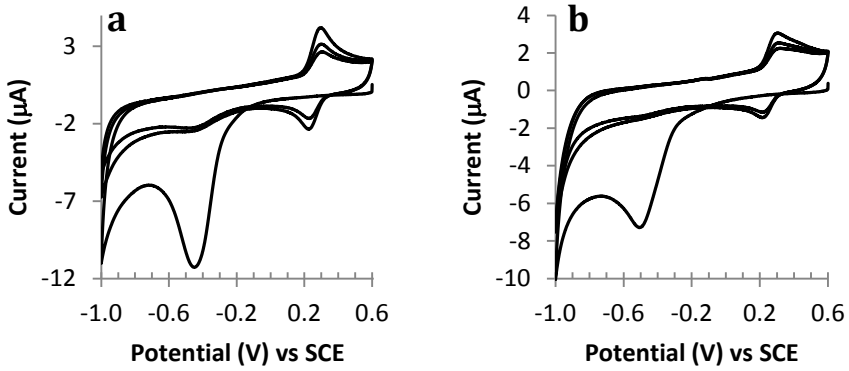

Figure 5.4 Three consecutive CVs scans obtained in 0.1 M H_2SO_4 of GC electrodes modified with H-COO-Ar monolayers followed by coupling of NP group using: a) $(COCl)_2$ method; and b) HBTU method. Scan rate = 100 mV s^{-1}.

CVs obtained in 0.1 M $LiClO_4$-EtOH for H-COO-Ar films reacted with $FcCH_2NH_2$ using the $(COCl)_2$ and HBTU methods are shown in Figures 5.5a and 5.5b, respectively. A well-defined Fc/Fc^+ redox couple is observed for both methods, with $E_{½}$ = 0.36 V and ΔE_p = 30 mV and 25 mV for the $(COCl)_2$ and HBTU methods, respectively. These are typical CVs for surface attached molecules.[29] The calculated Fc surface concentrations for these two methods are (4.3 ± 0.5) (n = 3) and (2.8 ± 0.7) (n = 3) × 10^{-10} mol cm^{-2}, respectively. The amounts of

NP and Fc immobilised on the surface can be compared with the theoretical maximum concentration of each group in a monolayer. Based on the size of each moiety, the calculated surface concentrations of NP and Fc on a flat surface are 12×10^{-10} and 4.5×10^{-10} mol cm^{-2}, respectively.[30, 31] Assuming the typical GC surface roughness factor of 2,[32-34] it is clear that the amounts of NP and Fc groups immobilised on H-COO-Ar-GC are not limited by the size of the groups. Hence, it can be assumed that the measured surface concentrations of NP and Fc moieties reflect the surface concentration of H-COO-Ar groups in the monolayer. Although the $(COCl)_2$ method gives consistently higher values, considering the experimental uncertainty, all of these values are close to each other. Thus, the surface concentration of carboxylic acid groups is ~ 3.5×10^{-10} mol cm^{-2}.

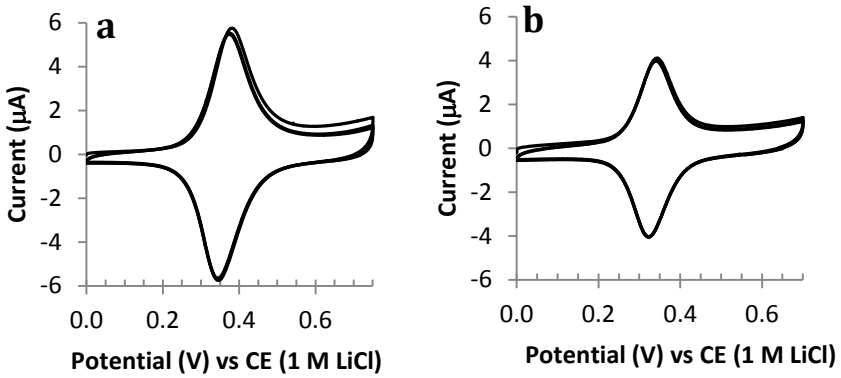

Figure 5.5 Three consecutive CVs scans obtained in 0.1 M $LiClO_4$-EtOH of a GC electrode modified with a H-COO-Ar monolayer followed by coupling of Fc group using: a) $(COCl)_2$ method; and b) HBTU method. Scan rate = 200 mV s^{-1}.

The theoretical maximum surface concentration of H-COO-Ar groups grafted to a surface by this protection-deprotection approach was estimated by assuming that the density of grafted groups is governed by the size of the Fm protecting group. Assuming that the protected aryl moieties are arranged in a hexagonal close packed monolayer (giving 90 % coverage of the surface), the surface concentration, Γ, in mol cm^{-2} can be calculated using the following

equation (eq. 5.1), where *d* is the diameter, in nm, of the disk representing the protecting group, and N_A is Avogadro's number (6.022×10^{23} mol^{-1}).

$$\Gamma = \frac{0.907}{\pi\left(\frac{d}{2}\right)^2} \times \frac{1}{N_A}$$

$$\Gamma = \frac{1.92 \times 10^{-10}}{d^2} \qquad \text{eq. 5.1}$$

The diameter, *d*, was evaluated from the conformation of the Fm-COO-Ar molecule using *Avogadro* 1.1.1 freeware (Figure 5.6). By assuming there is a free rotation of the Fm protecting group along the aryl-carboxy axis, *d* = 1.1 nm, and hence the theoretical maximum surface concentration of H-COO-Ar on an ideal flat surface is 1.7×10^{-10} mol cm^{-2}.

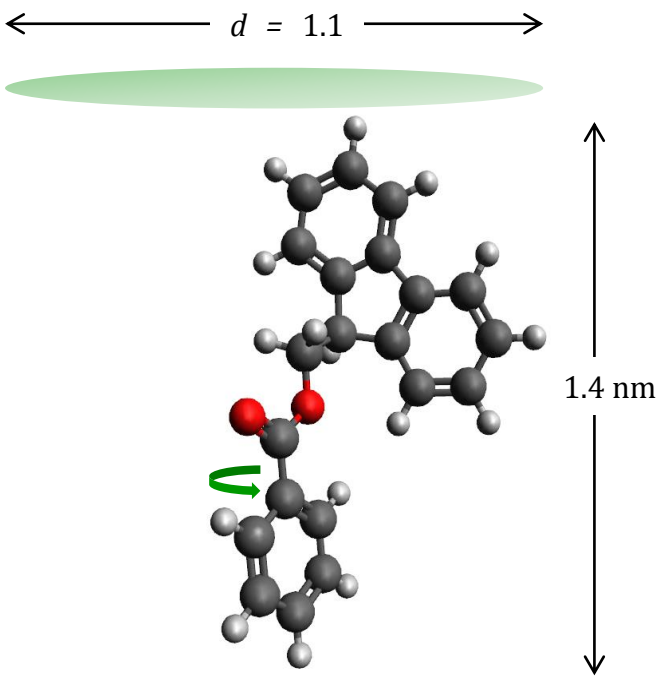

Figure 5.6 Molecular dimension and structure of Fm-COO-Ar estimated using *Avogadro* 1.1.1 freeware.

Comparing the theoretical calculated surface concentration (1.7×10^{-10} mol cm^{-2}) and the experimental (~ 3.5×10^{-10} mol cm^{-2}) value, clearly, the concentration of H-COO-Ar groups

obtained experimentally is higher than the calculated value. However, by taking into consideration the typical roughness factor of GC of about 2,[32-34] the experimental value is close to the calculated value. Furthermore, as described in Chapter 3, direct reaction of bare GC with amine derivatives is possible.[35-41] The surface concentration of NP groups coupled to bare GC using the $(COCl)_2$ and HBTU methods was found to be (2.5 ± 0.4) (n = 5) and (1.1 ± 0.2) (n = 3) × 10^{-10} mol cm^{-2}, respectively. The surface concentration of Fc groups coupled to bare GC using $(COCl)_2$ and HBTU was (2.2 ± 0.6) (n = 4) and (1.3 ± 0.2) (n = 5) × 10^{-10} mol cm^{-2}, respectively (Chapter 3). Thus, coupling of the amine derivatives directly to activated GC is expected to contribute to the measured surface concentrations of NP and Fc groups at the grafted H-COO-Ar monolayer surface. A further blank experiment was undertaken using the conditions for $(COCl)_2$-activated reactions but without $(COCl)_2$. For this experiment, all standard steps for preparation of the H-COO-Ar monolayer and coupling of NBA to the monolayer were carried out, but in the absence of $(COCl)_2$. It was found that only 0.4 ± 0.1 × 10^{-10} mol cm^{-2} (n = 2) of NP groups were immobilised when no $(COCl)_2$ was added, suggesting that in the presence of $(COCl)_2$, the reaction proceeds via the formation of an amide bond, as shown in Scheme 5.2. The small amount of immobilised NP groups is unexpected, since the reaction of bare GC with $FcCH_2NH_2$ in DCM resulted in a surface concentration of 2.4 ± 0.3 × 10^{-10} mol cm^{-2} (n = 3, Chapter 3). That reaction was assumed to proceed via a Michael-type addition mechanism. Hence, it appears that in the presence of the H-COO-Ar monolayer, the accessibility of the GC surface is limited. Although the contribution of Fc coupled directly to GC through amide bonds is unknown, the low yield of the Michael-type reaction at H-COO-Ar-GC surface implying poor accessibility to the surface, suggests that amide bond formation directly at GC is unlikely to be a major contribution to coupled Fc. Thus assuming only a very minor contribution from NP and Fc

coupled directly on the GC surface, the surface concentration of coupled Fc and NP groups (~3.5 × 10^{-10} mol cm^{-2}) is assumed to match that of H-COO-Ar groups grafted from the protected aryldiazonium salt.

5.3.1.4 Effect of solvent and electrolyte on the immobilised Fc redox couple

As mentioned in Chapter 4, the electrochemical response of Fc attached to a short monolayer tether is sensitive to the solvent, and to a lesser extent, the electrolyte. Figure 5.7 shows CVs of immobilised Fc, attached via the H-COO-Ar monolayer. The CVs were obtained in EtOH and ACN with $LiClO_4$ and $TBABF_4$ as electrolytes. As can be seen, the response of this layer has similar solvent and electrolyte dependency as that of Fc attached through a triazole linkage (Chapter 4, Figure 4.7a). The highest current response is obtained in EtOH and although the electrolyte does not influence the response in EtOH, in ACN, $LiClO_4$ leads to larger Fc oxidation and reduction peaks than does $TBABF_4$. Hence, this monolayer provides another example of the strong influence of solvent and electrolyte when Fc is attached to the surface via a short linker.

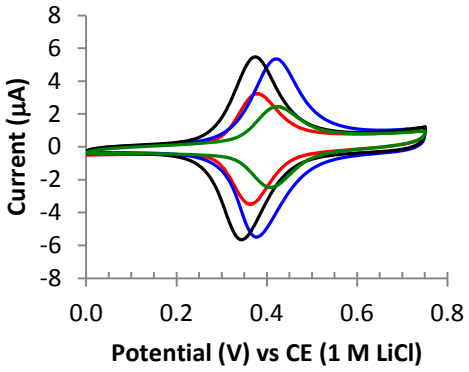

Figure 5.7 CVs of a GC electrode modified with a H-COO-Ar monolayer followed by coupling of Fc groups using the $(COCl)_2$ method. CVs obtained in: 0.1 M $LiClO_4$-EtOH (black line); 0.1 M $TBABF_4$-EtOH (blue line); 0.1 M $LiClO_4$-ACN (red line) and 0.1 M $TBABF_4$-ACN (green line). Scan rate = 200 mV s^{-1}.

5.3.1.5 *AFM film thickness measurement*

The thickness of the films grafted to PPF, before and after deprotection was measured by the AFM depth profiling technique described in Chapters 2 and 4. Figures 5.8a and 5.8b show topographic images of a scratch in a Fm-COO-Ar film (before deprotection) and H-COO-Ar film (after deprotection), respectively. Figures 5.8c and 5.8d are the corresponding depth profiles which show an average film thickness of (3.1 ± 0.3) and (0.4 ± 0.3) nm for the films before deprotection and after deprotection, respectively. The height of a Fm-COO-Ar group oriented perpendicularly on a flat surface is calculated to be ~1.4 nm (Figure 5.6) and the calculated height for a carboxyphenyl monolayer is 0.6 nm (height calculation was carried out using *Avogadro* 1.1.1 freeware). Hence the Fm-COO-Ar film is multilayered with a minimum of approximately 2-3 layers, and after deprotection, the film is consistent with a H-COO-Ar monolayer.

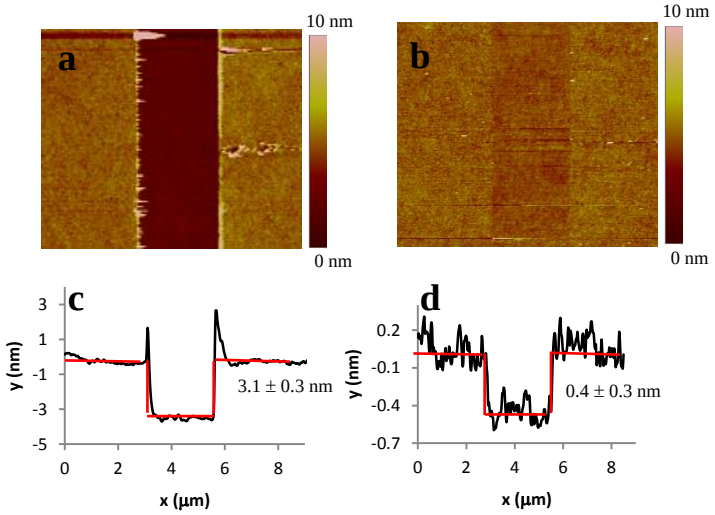

Figure 5.8 a), b) AFM topography images and c), d) depth profiles of Fm-COO-Ar modified PPF before (a & c), and after deprotection (b & d).

5.3.2 Formation of mixed layers

The availability of diazonium ions with different protected substituents gives a straightforward method for preparing mixed monolayers with two or more reactive tethers.

When the deprotected monolayer components undergo different coupling chemistry, different species can be selectively coupled to each tether. Two different strategies are demonstrated using this approach: grafting from a solution containing two different protected diazonium salts (Scheme 5.3a), and sequential grafting of two different protected diazonium salts (Schemes 5.3b and 5.3c). To demonstrate that two different functionalities are immobilised on the surface, NBA.HCl and $FcCH_2N_3$ were sequentially reacted with the surface under the conditions that promote amide coupling ($(COCl)_2$) with H-COO-Ar groups and click chemistry with H-Eth-Ar groups, respectively.

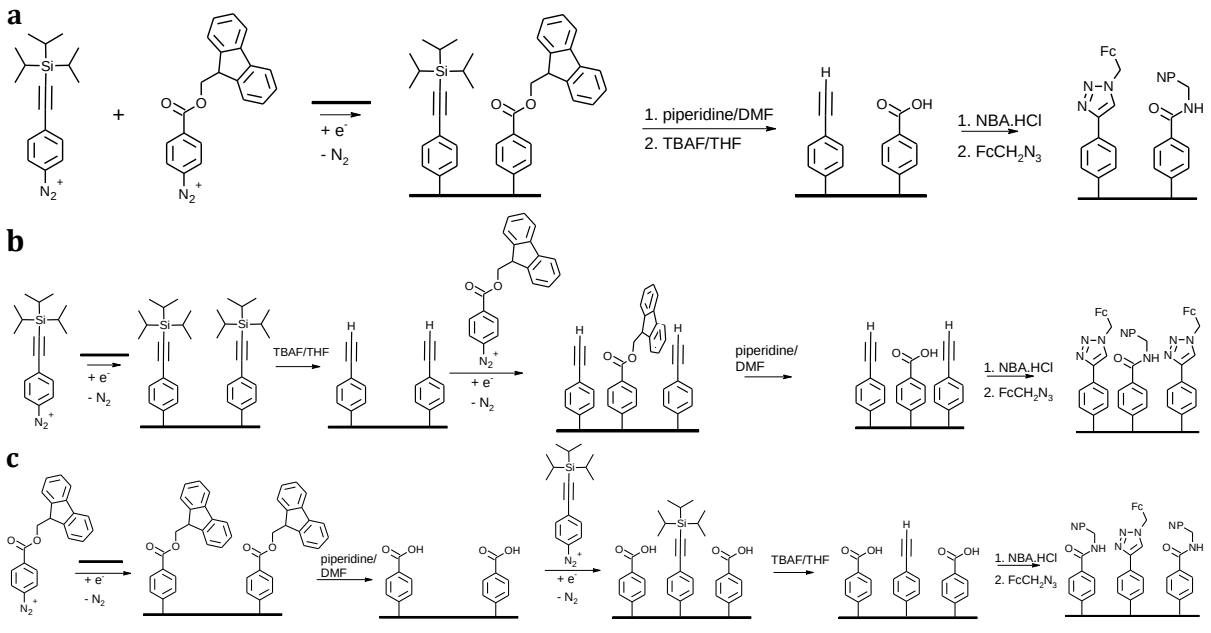

Scheme 5.3 Strategies for the preparation of mixed monolayers using $[Fm\text{-}COO\text{-}Ar\text{-}N_2]BF_4$ and $[TIPS\text{-}Eth\text{-}Ar\text{-}N_2]BF_4$.

Table 5.1 lists the modification conditions used to form the mixed films and the corresponding surface concentrations of electro-active Fc and NP groups on GC. Electrografting in a solution containing mixture of $[Fm\text{-}COO\text{-}Ar\text{-}N_2]BF_4$ and $[TIPS\text{-}Eth\text{-}Ar\text{-}N_2]BF_4$ followed by deprotection of Fm groups in 20% piperidine-DMF and deprotection of TIPS in TBAF-THF resulted in a mixed monolayer of H-Eth-Ar and H-COO-Ar groups

(Scheme 5.3a). NP and Fc groups were subsequently coupled to H-COO-Ar and H-Eth-Ar modifiers, respectively. The CVs of coupled Fc groups were investigated first by scanning in 0.1 M $LiClO_4$-EtOH, followed by CVs of NP groups in 0.1 M H_2SO_4. Table 5.1 Experiments I – III described the mixed films prepared using different concentration ratios of [TIPS-Eth-Ar-N_2]BF_4 and [Fm-COO-Ar-N_2]BF_4. As shown by the data in Table 5.1, preparation of mixed layers by this route gives films with relatively high concentrations of NP groups (and presumably H-COO-Ar groups), even after the solution concentration of [TIPS-Eth-Ar-N_2]BF_4 was increased to a 10 fold excess. Comparing the reduction potentials of Fm-COO-Ar-N_2^+ (0.37 V, Figure 5.1) and TIPS-Eth-Ar-N_2^+ (0.24 V, Figure 4.1, Chapter 4), it is clear that when grafting is carried out in the mixed solution, Fm-COO-Ar-N_2^+ is reduced and grafted at a higher rate than TIPS-Eth-Ar-N_2^+. Increasing the concentration of [TIPS-Eth-Ar-N_2]BF_4 to a 10 fold excess was not enough to compensate for the different rates of grafting.

Table 5.1 Conditions for preparation of mixed films by routes shown in Scheme 5.3 and the corresponding surface concentration of electro-active Fc and NP groups.

Expt.	Grafting conditions[a]	Amide coupling method[b]	Γ_{Fc} (10^{-10} mol cm^{-2})	Γ_{NP} (10^{-10} mol cm^{-2})	n[c]
I	Scheme 5.3a (5 mM Fm + 5 mM TIPS)	$(COCl)_2$	0.1	3.5	1
II	Scheme 5.3a (1 mM Fm + 5 mM TIPS)	$(COCl)_2$	0.2	3.5	1
III	Scheme 5.3a (1 mM Fm + 10 mM TIPS)	$(COCl)_2$	0.5	2.2	1
IV	Scheme 5.3b	$(COCl)_2$	0.2 ± 0.1	4.0 ± 0.3	2
V	Scheme 5.3b	HBTU	0.2 ± 0.1	3.0 ± 0.2	2
VI	Scheme 5.3c	$(COCl)_2$	1.1 ± 0.1	3.6 ± 0.1	2
VII	Scheme 5.3c	HBTU	1.3 ± 0.1	2.9 ± 0.2	3

[a]Fm = [Fm-COO-Ar-N_2]BF_4, TIPS = [TIPS-Eth-Ar-N_2]BF_4

[b]Coupling of NBA to H-COO-Ar-GC surface was carried out by either $(COCl)_2$ or HBTU method

[c]*n* is the number of samples analysed

Another approach is to graft the two diazonium salts sequentially (Schemes 5.3b and 5.3c). Table 5.1, Experiments IV and V, describe mixed films prepared via Scheme 5.3b. Grafting a TIPS-Eth-Ar film, removing the TIPS protecting group then grafting [Fm-COO-Ar-N_2]BF_4 to the voids in the layer followed by removal of the Fm group using piperidine gives a mixed monolayer of H-Eth-Ar and H-COO-Ar. Similarly to the mixed layer above, NBA was coupled to H-COO-Ar groups and $FcCH_2N_3$ was clicked to H-Eth-Ar groups to demonstrate that the two different functionalities are immobilised on the surface. Figure 5.9 shows CVs obtained at mixed films obtained using the route shown in Scheme 5.3b (Table 5.1, Experiments IV and V). As seen from the Table, the surface is also dominated by NP groups (and presumably H-COO-Ar groups) using this approach. The amount of NP groups attached to the surface is the same as for a single-component H-COO-Ar layer, while the amount of Fc clicked to the surface is much less than a single-component H-Eth-Ar layer ($(2.4 \pm 0.3) \times 10^{-10}$ mol cm^{-2}, Chapter 4). This may be because the voids created by removal of the TIPS groups (diameter = 0.92 nm) are not large enough to allow grafting of the Fm-COO-Ar-N_2^+ molecule (diameter = 1.1 nm), and therefore the grafting predominantly occurs at the already grafted H-Eth-Ar groups. The attack of radicals at the aryl ring of H-Eth-Ar groups may sterically hinder the click reaction and the direct attack of radicals on the H-Eth group itself may decrease the amount of H-Eth-Ar groups for click chemistry.

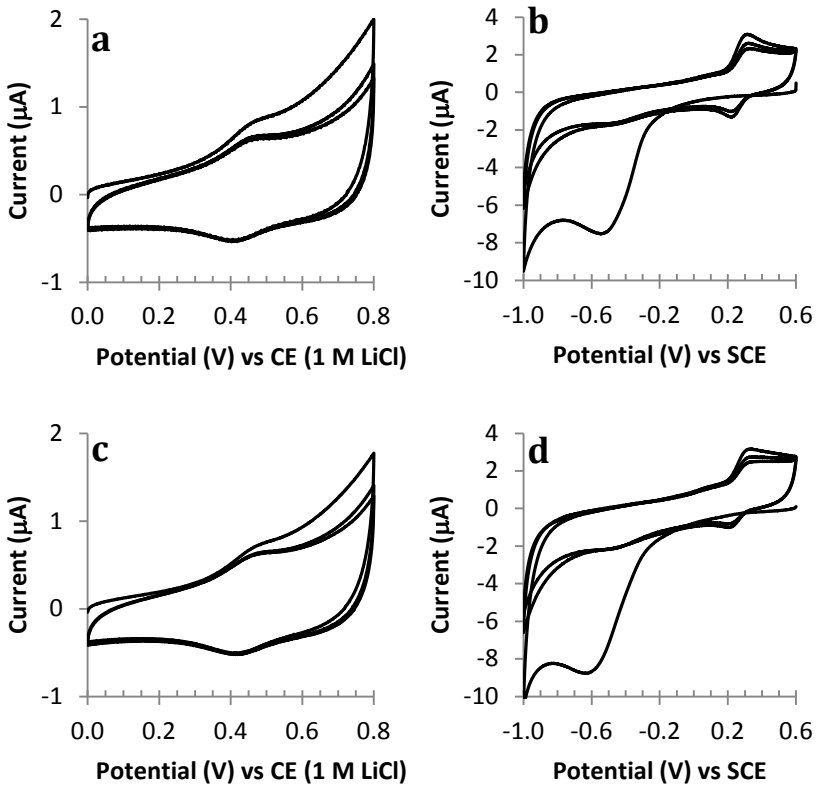

Figure 5.9 Repeat CVs for GC electrodes modified by route 5.3b using the conditions shown in Table 5.1; Experiment IV (a, b), and Experiment V (c, d). Scans were performed in: a, c) 0.1 M $LiClO_4$-EtOH at a scan rate of 200 mV s^{-1} and b, d) 0.1 M H_2SO_4 at a scan rate of 100 mV s^{-1}.

Table 5.1, Experiments VI and VII investigate the preparation of mixed layers using the route shown in Scheme 5.3c. [Fm-COO-Ar-N_2]BF_4 was electrografted first followed by the removal of the Fm groups and then electrografting of [TIPS-Eth-Ar-N_2]BF_4. After removal of the TIPS groups, coupling reactions with NBA and then $FcCH_2N_3$ were carried out (Scheme 5.3c). Figure 5.10 shows the CVs of coupled Fc and NP groups obtained in 0.1 M $LiClO_4$-EtOH and 0.1 M H_2SO_4, respectively for the films listed in Table 5.1, Experiments VI and VII. From the CVs, the surface concentrations of Fc and NP groups were (1.1 ± 0.1) and (3.6 ± 0.1) × 10^{-10} mol cm^{-2}, respectively for amide coupling carried out by the $(COCl)_2$ method (Experiment VI), while for the HBTU method, the surface concentration of Fc and NP groups were (1.3 ± 0.1) and (2.9 ± 0.2) × 10^{-10} mol cm^{-2}, respectively (Experiment VII). Clearly, the Fc concentration is higher than the previous methods. However, the NP concentration still

exceeds that of Fc using this approach. The concentration of NP groups is higher using $(COCl)_2$ than HBTU as activating agent, which is in line with the other amide coupling reactions undertaken using these reagents.

The NP concentrations for the mixed films prepared by the route shown in Scheme 5.3c are similar to the NP concentrations obtained for a single-component of H-COO-Ar layer ((4.1 ± 0.7) and $(3.0 \pm 0.8) \times 10^{-10}$ mol cm^{-2} for $(COCl)_2$ and HBTU method, respectively). However, the Fc concentrations are lower than those obtained for a single-component layer of H-Eth-Ar ($(2.4 \pm 0.3) \times 10^{-10}$ mol cm^{-2}, Chapter 4). This indicates that the grafting of [TIPS-Eth-Ar-N_2]BF_4 to the H-COO-Ar-GC surface does not affect the reactivity or accessibility of H-COO-Ar groups towards the subsequent coupling reaction. However, the low Fc concentrations suggest that grafting of TIPS-Eth-Ar-N_2]BF_4 has a low yield at the H-COO-Ar-GC surface and/or that the yield of the click reaction between $FcCH_2N_3$ and H-Eth-Ar groups in the mixed layer is low. Low yields might be expected for both processes due to steric hindrance from the already grafted H-COO-Ar layer and coupled-NP groups, respectively.

A further experiment was carried out to investigate whether the low yield of Fc groups coupled to the mixed layers prepared by route 5.3c arises due to a small amount of H-Eth-Ar coupled to the surface or due to a low yield from the click reaction. All steps for the preparation of a mixed layer by route 5.3c were carried out, except NBA was not coupled to the surface. It was found that $(2.3 \pm 0.1) \times 10^{-10}$ mol cm^{-2} (n = 2) of Fc groups were coupled to the H-Eth-Ar groups in the mixed layer. Surprisingly, this is the same as the surface concentration of Fc groups clicked to a single-component H-Eth-Ar layer. It was expected that the amount of TIPS-Eth-Ar groups grafted to the surface that is already modified with H-COO-Ar groups would be lower than that grafted to a bare GC surface. However, this was

not the case and the reason for the apparent equal amounts of grafted groups is not understood. Thus, it appears that the grafting yield of H-Eth-Ar groups is unaffected by the H-COO-Ar groups. Hence, the low Fc concentrations obtained on the mixed layer prepared through Scheme 5.3c, must be due to the steric hindrance imposed on the H-Eth-Ar groups by the coupled-NP groups.

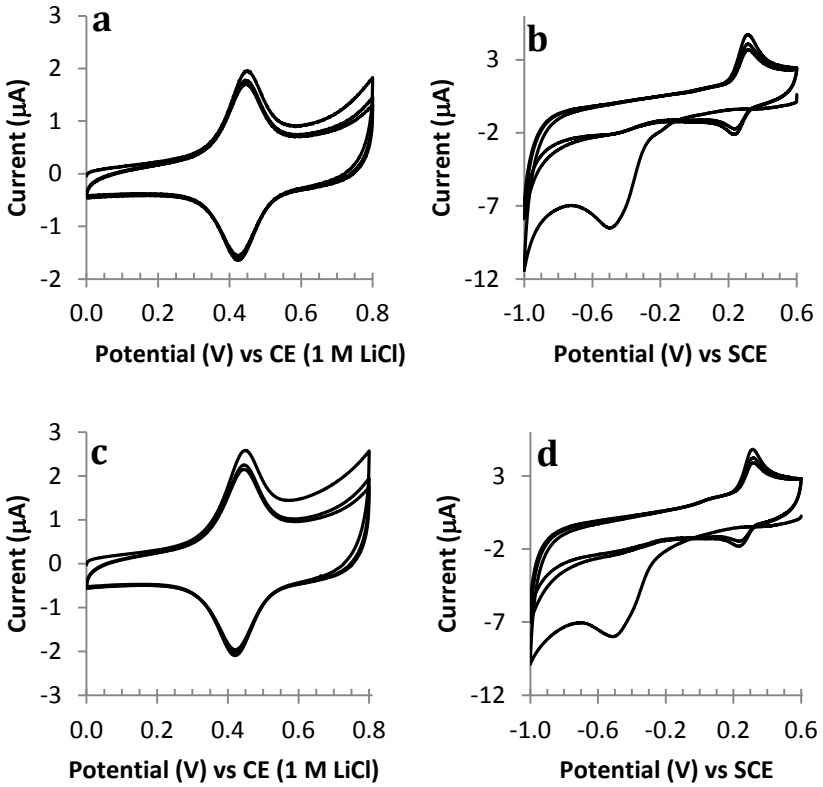

Figure 5.10 Repeat CVs or a GC electrode modified by route 5.3c using the conditions shown in Table 5.1: Experiment VI (a, b), and Experiment VII (c, d). Scans were performed in: a, c) 0.1 M $LiClO_4$-EtOH at a scan rate of 200 mV s^{-1} and b, d) 0.1 M H_2SO_4 at a scan rate of 100 mV s^{-1}.

5.4 Conclusion

Preparation of a carboxyphenyl monolayer by electrografting of a Fm protected H-COO-Ar diazonium derivative followed by deprotection of the Fm groups has been demonstrated. The reactivity and surface concentration of the H-COO-Ar moieties were investigated using an amide coupling reaction with amine derivatives containing electroactive Fc and NP groups. The surface concentration of the H-COO-Ar monolayer is estimated to be ~ 3.5×10^{-10} mol

cm^{-2}, however deducing the surface concentration of H-COO-Ar from the concentration of Fc and NP groups coupled to surface introduces an unknown uncertainty due to the contribution of reactions directly with GC. AFM film thickness measurements confirm that the film formed after deprotection is a monolayer. Preparation of mixed layers using electrografting in solutions containing two different diazonium salts ([Fm-COO-Ar-N_2]BF_4 and [TIPS-Eth-Ar-N_2]BF_4) was investigated. This method gives a film dominated by H-COO-Ar groups. Alternative strategies were also explored, in which sequential grafting was adopted. Electrografting of [TIPS-Eth-Ar-N_2]BF_4 followed by deprotection of the TIPS groups and subsequent grafting of [Fm-COO-Ar-N_2]BF_4 also gives a film that is dominated by the H-COO-Ar groups, with a ratio of 20 : 1 for reactive H-COO-Ar and H-Eth-Ar groups. The high concentration of H-COO-Ar groups is assumed to be due to the grafting of the second modifier on top of the already grafted H-Eth-Ar groups. This may be favoured because the void created by the TIPS groups (diameter = 0.92 nm) is smaller than the bulky Fm-COO-Ar-N_2^+ molecule (diameter = 1.1 nm). In contrast, when the sequence was reversed, and [Fm-COO-Ar-N_2]BF_4 was grafted first, the mixed film gives an apparent ratio of 3 : 1 for reactive H-COO-Ar and H-Eth-Ar groups. There is some uncertainty in this finding because the amount of H-COO-Ar and H-Eth-Ar groups was estimated by coupling electroactive NP and then Fc groups to H-COO-Ar and H-Eth-Ar groups, respectively. From blank experiments it was shown that the reactivity of H-Eth-Ar groups is affected by the presence of NP groups, and hence the concentration of H-Eth-Ar groups may be underestimated in the mixed monolayer. Moreover, for all of these experiments, coupling of amine derivatives directly to GC is expected to occur simultaneously with coupling to the H-COO-Ar layer and the extent of these reactions has not been quantified (and would be difficult to quantify). Therefore, the amount of NP and Fc groups may not be a true reflection of the amount of H-COO-Ar and H-Eth-Ar groups in the mixed monolayers.

Considering the three approaches investigated, the mixed solution method is the most reliable for preventing any multilayer formation. However, this method will give a sparse layer as both tether components are grafted with their protecting groups. For sequential grafting, the protecting groups were removed after the first grafting and so the voids can be filled in the second step, which leads to denser coverage. However, it appears that grafting TIPS-Eth-Ar groups first results in multilayer formation. On the other hand, grafting H-COO-Ar first does give a mixed monolayer. The dependence of the outcome on the order of grafting is assumed to originate in the different sizes of the protecting groups. If the two components that are to be included in the film can both be coupled to either H-COO-Ar or H-Eth-Ar tethers, these strategies could be tuned to enable the preparation of mixed monolayers of any component ratio.

5.5 References

1 Leroux, Y.R., Fei, H., Noel, J.M., Roux, C., Hapiot, P., Efficient covalent modification of a carbon surface: Use of a silyl protecting group to form an active monolayer. *J. Am. Chem. Soc.*, 2010, *132*, 14039.

2 Leroux, Y.R., Hapiot, P., Nanostructured monolayers on carbon substrates prepared by electrografting of protected aryldiazonium salts. *Chem. Mater.*, 2013, *25*, 489.

3 Leroux, Y.R., Hui, F., Hapiot, P., A protecting-deprotecting strategy for structuring robust functional films using aryldiazonium electroreduction. *J. Electroanal. Chem.*, 2013, *688*, 298.

4 Lee, L., Ma, H.F., Brooksby, P.A., Brown, S.A., Leroux, Y.R., Hapiot, P., Downard, A.J., Covalently anchored carboxyphenyl monolayer via aryldiazonium ion grafting: A well-defined reactive tether layer for on-surface chemistry. *Langmuir*, 2014, *30*, 7104.

5 Baffert, C., Sybirna, K., Ezanno, P., Lautier, T., Hajj, V., Meynial-Salles, I., Soucaille, P., Bottin, H., Leger, C., Covalent attachment of FeFe hydrogenases to carbon electrodes for direct electron transfer. *Anal. Chem.*, 2012, *84*, 7999.

6 Marquette, C.A., Bouteille, F., Corgier, B.P., Degiuli, A., Blum, L.J., Disposable screen-printed chemiluminescent biochips for the simultaneous determination of four point-of-care relevant proteins. *Anal. Bioanal. Chem.*, 2009, *393*, 1191.

7 Pellissier, M., Barriere, F., Downard, A.J., Leech, D., Improved stability of redox enzyme layers on glassy carbon electrodes via covalent grafting. *Electrochem. Commun.*, 2008, *10*, 835.

8 Radi, A.E., Munoz-Berbel, X., Lates, V., Marty, J.L., Label-free impedimetric immunosensor for sensitive detection of ochratoxin A. *Biosens. Bioelectron.*, 2009, *24*, 1888.

9 Balakrishnan, S., Downard, A.J., Telfer, S.G., HKUST-1 growth on glassy carbon. *J. Mater. Chem.*, 2011, *21*, 19207.

10 Betard, A., Fischer, R.A., Metal-organic framework thin films: From fundamentals to applications. *Chem. Rev.*, 2012, *112*, 1055.

11 Shekhah, O., Wang, H., Kowarik, S., Schreiber, F., Paulus, M., Tolan, M., Sternemann, C., Evers, F., Zacher, D., Fischer, R.A., Woll, C., Step-by-step route for the synthesis of metal-organic frameworks. *J. Am. Chem. Soc.*, 2007, *129*, 15118.

12 Zacher, D., Baunemann, A., Hermes, S., Fischer, R.A., Deposition of microcrystalline $Cu_3(btc)_2$ and $Zn_2(bdc)_2(dabco)$ at alumina and silica surfaces modified with patterned self assembled organic monolayers: Evidence of surface selective and oriented growth. *J. Mater. Chem.*, 2007, *17*, 2785.

13 Almeida Paz, F.A., Klinowski, J., Vilela, S.M.F., Tome, J.P.C., Cavaleiro, J.A.S., Rocha, J., Ligand design for functional metal-organic frameworks. *Chem. Soc. Rev.*, 2012, *41*, 1088.

14 Cohen, S.M., Postsynthetic methods for the functionalization of metal-organic frameworks. *Chem. Rev.*, 2012, *112*, 970.

15 Lin, Z.-J., Lu, J., Hong, M., Cao, R., Metal-organic frameworks based on flexible ligands (FL-MOFs): Structures and applications. *Chem. Soc. Rev.*, 2014.

16 Casas-Solvas, J.M., Ortiz-Salmeron, E., Gimenez-Martinez, J.J., Garcia-Fuentes, L., Capitan-Vallvey, L.F., Santoyo-Gonzalez, F., Vargas-Berenguel, A., Ferrocene-carbohydrate conjugates as electrochemical probes for molecular recognition studies. *Chem.-Eur. J.*, 2009, *15*, 710.

17 Baramee, A., Coppin, A., Mortuaire, M., Pelinski, L., Tomavo, S., Brocard, J., Synthesis and in vitro activities of ferrocenic aminohydroxynaphthoquinones against *Toxoplasma gondii* and *Plasmodium falciparum*. *Bioorg. Med. Chem.*, 2006, *14*, 1294.

18 Isidro-Llobet, A., Alvarez, M., Albericio, F., Amino acid-protecting groups. *Chem. Rev.*, 2009, *109*, 2455.

19 Yu, S.S.C., Tan, E.S.Q., Jane, R.T., Downard, A.J., An electrochemical and XPS study of reduction of nitrophenyl films covalently grafted to planar carbon surfaces. *Langmuir*, 2007, *23*, 11074.

20 Mu, F.R., Coffing, S.L., Riese, D.J., Geahlen, R.L., Verdier-Pinard, P., Hamel, E., Johnson, J., Cushman, M., Design, synthesis, and biological evaluation of a series of lavendustin A analogues that inhibit EGFR and SYK tyrosine kinases, as well as tubulin polymerization. *J. Med. Chem.*, 2001, *44*, 441.

21 Neises, B., Steglich, W., Simple method for the esterification of carboxylic acids. *Angew. Chem. Int. Edit.*, 1978, *17*, 522.

22 Shendage, D.M., Frohlich, R., Haufe, G., Highly efficient stereoconservative amidation and deamidation of alpha-amino acids. *Org. Lett.*, 2004, *6*, 3675.

23 Bard, A.J., Inner-sphere heterogeneous electrode reactions. Electrocatalysis and photocatalysis: The challenge. *J. Am. Chem. Soc.*, 2010, *132*, 7559.

24 Chen, P.H., McCreery, R.L., Control of electron transfer kinetics at glassy carbon electrodes by specific surface modification. *Anal. Chem.*, 1996, *68*, 3958.

25 DuVall, S.H., McCreery, R.L., Control of catechol and hydroquinone electron-transfer kinetics on native and modified glassy carbon electrodes. *Anal. Chem.*, 1999, *71*, 4594.

26 DuVall, S.H., McCreery, R.L., Self-catalysis by catechols and quinones during heterogeneous electron transfer at carbon electrodes. *J. Am. Chem. Soc.*, 2000, *122*, 6759.

27 Abiman, P., Crossley, A., Wildgoose, G.G., Jones, J.H., Compton, R.G., Investigating the thermodynamic causes behind the anomalously large shifts in pK_a values of benzoic acid-modified graphite and glassy carbon surfaces. *Langmuir*, 2007, *23*, 7847.

28 Montalbetti, C., Falque, V., Amide bond formation and peptide coupling. *Tetrahedron*, 2005, *61*, 10827.

29 Bard, A.J., Faulkner, L.R., *Electrochemical methods fundamentals and applications*. Second ed. 2001: John Wiley & Sons, Inc.

30 Liu, Y.C., McCreery, R.L., Reactions of organic monolayers on carbon surfaces observed with unenhanced Raman-spectroscopy. *J. Am. Chem. Soc.*, 1995, *117*, 11254.

31 Chidsey, C.E.D., Bertozzi, C.R., Putvinski, T.M., Mujsce, A.M., Coadsorption of ferrocene-terminated and unsubstituted alkanethiols on gold - electroactive self-assembled monolayers. *J. Am. Chem. Soc.*, 1990, *112*, 4301.

32 McDermott, M.T., Kneten, K., McCreery, R.L., Anthraquinonedisulfonate adsorption, electron-transfer kinetics, and capacitance on ordered graphite-electrodes - the important role of surface-defects. *J. Phys. Chem.*, 1992, *96*, 3124.

33 McDermott, M.T., McDermott, C.A., McCreery, R.L., Scanning tunneling microscopy of carbon surfaces - relationships between electrode-kinetics, capacitance, and morphology for glassy-carbon electrodes. *Anal. Chem.*, 1993, *65*, 937.

34 Pontikos, N.M., McCreery, R.L., Microstructural and morphological-changes induced in glassy-carbon electrodes by laser irradiation. *J. Electroanal. Chem.*, 1992, *324*, 229.

35 Gallardo, I., Pinson, J., Vila, N., Spontaneous attachment of amines to carbon and metallic surfaces. *J. Phys. Chem. B*, 2006, *110*, 19521.

36 Jeevagan, A.J., John, S.A., Electrochemical sensor for guanine using a self-assembled monolayer of 1,8,15,22-tetraaminophthalocyanatonickel(II) on glassy carbon electrode. *Anal. Biochem.*, 2012, *424*, 21.

37 Jeevagan, A.J., John, S.A., Electrochemical determination of caffeine in the presence of paracetamol using a self-assembled monolayer of non-peripheral amine substituted copper(II) phthalocyanine. *Electrochim. Acta*, 2012, *77*, 137.

38 Kesavan, S., Abraham John, S., Spontaneous grafting: A novel approach to graft diazonium cations on gold nanoparticles in aqueous medium and their self-assembly on electrodes. *J. Colloid. Interf. Sci.*, 2014, *428*, 84.

39 Muthukumar, P., John, S.A., Effect of amine substituted at ortho and para positions on the electrochemical and electrocatalytic properties of cobalt porphyrins self-assembled on glassy carbon surface. *Electrochim. Acta*, 2014, *115*, 197.

40 Sivanesan, A., John, S.A., Adsorption thermodynamics and kinetics study for the self-assembly of 1,8,15,22-tetraaminophthalocyanatocobalt(II) on glassy carbon surface. *Electrochim. Acta*, 2009, *54*, 7458.

41 Xu, X.Y., Feng, Y., Li, J.J., Li, F., Yu, H.J., A novel protocol for covalent immobilization of thionine on glassy carbon electrode and its application in hydrogen peroxide biosensor. *Biosens. Bioelectron.*, 2010, *25*, 2324.

Chapter 6. Preparation of Amine Functionalised Monolayer

6.1 Introduction

As explained in Chapter 1 and illustrated in the preceeding two chapters, a protection-deprotection strategy can be used to prevent the formation of multilayers when grafting is carried out using aryldiazonium salt. Preparation of monolayers containing the ethynyl functionality is achieved by the use of triisopropylsilyl (TIPS) protecting groups[1] (Chapter 4) and monolayers containing the carboxylic acid functionality can be prepared by the use of fluorenylmethyl (Fm) protecting group[2] (Chapter 5).

In this Chapter, the protection-deprotection strategy is further extended to prepare an amine functionalised monolayer. Amine-terminated layers are useful for tethering a wide range of target species, especially via formation of amide linkages.[3-13] Amines also react with aldehydes and ketones to form imines,[14, 15] and with isocyanates (or isothiocyanates) to give ureas (or thioureas).[16] An arylamine terminated surfaces can be used as a precursor for the formation of a 'sticky surface', a surface bearing diazonium ion functionality, which can then react with various target species, such as nanoparticles, carbon nanotubes and biological molecules.[17-26]

Bartlett and co-workers[6] have reported the preparation of the *tert*-butyloxycarbonyl (Boc)-protected aminomethylphenyl diazonium salt, 4-(*N*-Boc-aminomethyl)benzene diazonium tetrafluoroborate ([Boc-NH-CH_2-Ar-N_2]BF_4). After grafting of Boc-NH-CH_2-Ar groups on a GC surface the Boc group was removed to give an aminomethylphenyl layer. Anthraquinone-2-carboxylic acid was coupled to the film giving an electrochemically determined surface

coverage of $7 \pm 1 \times 10^{-10}$ mol cm^{-2} (assuming a surface roughness factor of 4).[6] The authors stated that the surface coverage is consistent with monolayer coverage of anthraquinone groups, however no film thickness measurement was undertaken. To the best of my knowledge, there are no other reports of preparation of amine-terminated monolayers via grafting aryldiazonium ions.

In this Chapter, four different amine-protected aryldiazonium salts were investigated: 4-(*N*-Boc-amino)benzene diazonium tetrafluoroborate ([Boc-NH-Ar-N_2]BF_4), [Boc-NH-CH_2-Ar-N_2]BF_4, 4-(*N*-Fmoc-amino)benzene diazonium tetrafluoroborate ([Fmoc-NH-Ar-N_2]BF_4), and 4-(*N*-Fmoc-aminomethyl)benzene diazonium tetrafluoroborate ([Fmoc-NH-CH_2-Ar-N_2]BF_4). (Fmoc is fluorenylmethyloxycarbonyl). The synthesis and electrografting of the four diazonium salts are discussed. The modified surfaces were characterised by electrochemistry, X-ray photoelectron spectroscopy (XPS) and atomic force microscopy (AFM). In addition, preparation of binary mixed layers was also investigated. Four different aryldiazonium salts were investigated to: 1) compare the effectiveness of Boc and Fmoc as protecting groups for monolayer formation; 2) compare the reactivity of the amine tethers (aromatic vs. aliphatic amine); and 3) compare the surface concentration of monolayers grafted with each protecting group.

6.2 Experimental

All chemical reagents and materials are detailed in Chapter 2. Azidomethyl ferrocene ($FcCH_2N_3$) was synthesised following a literature method,[27] which is briefly outlined in Section 2.1.5.1. Aminomethyl ferrocene ($FcCH_2NH_2$) was synthesised according to a published method,[28] which is briefly mentioned in Section 2.1.5.2. The syntheses of 4-((9-H-fluoren-9-yl-methoxy)carbonyl)benzene diazonium tetraluoroborate ([Fm-COO-Ar-N_2]BF_4), 4-((triisopropylsilyl)ethynyl)benzene diazonium tetrafluoroborate ((TIPS-Eth-Ar-N_2]BF_4),

[Boc-NH-Ar-N_2]BF_4, [Boc-NH-CH_2-Ar-N_2]BF_4, [Fmoc-NH-Ar-N_2]BF_4, and [Fmoc-NH-CH_2-Ar-N_2]BF_4 are described in Section 2.1.4. PPF preparation is described in Section 2.3.1.2. The AFM depth profiling technique for film thickness measurement is explained in Section 2.5.

All experiments in this chapter were carried out using GC disks (area = 0.071 cm^2) as the working electrode, except for AFM experiments, for which PPF was used, and XPS experiments, for which GC plates were used. Pt mesh was used as a counter electrode and SCE as reference electrode for aqueous solution and CE (1 M LiCl) for non-aqueous solution.

Electrografting. Amine-protected groups were electrografted to GC from a solution of the corresponding protected aryldiazonium salts (5 mM) in 0.1 M $TBABF_4$-ACN using five cycles between 0.60 and -0.75 V at a scan rate of 50 mV s^{-1}. The modified electrode was rinsed with acetone, sonicated in ACN for 5 min, and dried with a stream of N_2(g). Boc and Fmoc protecting groups were cleaved from the layer by immersing the modified electrode in a stirred solution of 4 M HCl-MeOH and 20% piperidine-DMF,[29] respectively. Electrodes were rinsed with acetone and H_2O after deprotection.

Amide coupling reaction on the amine functionalised surface. Oxalyl chloride ($(COCl)_2$)-activated coupling reactions were carried out according to the method described in Section 2.4.2.2.2. HBTU-activated coupling reactions were conducted using the method outlined in Section 2.4.2.4. After reaction, the modified electrodes were rinsed with acetone and sonicated in ACN for 5 min.

Mixed layer preparation by sequential electrografting: [Fmoc-NH-CH_2-Ar-N_2]BF_4 as the first modifier. Fmoc-NH-CH_2-Ar was electrografted to the surface and deprotected using the method described above. The second modifier, TIPS-Eth-Ar (or Fm-COO-Ar), was

electrografted to the NH_2-CH_2-Ar-GC modified surface from a solution of 5 mM [TIPS-Eth-Ar-N_2]BF_4 (or [Fm-COO-Ar-N_2]BF_4) in 0.1 M $TBABF_4$-ACN using two cycles between 0.60 (or 0.80 V) and -0.75 V at a scan rate of 200 mV s^{-1}. The modified electrodes were rinsed with acetone and sonicated in ACN for 5 min after each grafting step. After removal of the protecting groups in each of the deprotection solutions (Fm and Fmoc were removed in 20% piperidine-DMF, and TIPS was removed in 0.05 M TBAF-THF), electrodes were rinsed with acetone and H_2O and dried with a stream of N_2(g). Electro-active nitrophenyl (NP) and ferrocenyl (Fc) groups were coupled to the mixed layers to allow estimation of surface concentration of amine groups. NP was coupled to the NH_2-CH_2-Ar-GC surface using the HBTU coupling method in the presence of 4-aminobenzoic acid (NO_2-Ar-COOH), prior to coupling of Fc to the other modifier. Fc was coupled to H-COO-Ar-GC groups using an amide coupling reaction with $FcCH_2NH_2$ in the presence of HBTU, while for H-Eth-Ar-GC groups, Fc was immobilised on the GC by performing a click reaction with $FcCH_2N_3$ as outlined in Section 2.4.2.1. After amide coupling reactions, the modified electrodes were sonicated in ACN for 5 min. After click reactions, the modified electrodes were stirred in EDTA-Na_2 for 10 min followed by sonication in THF and ACN for 2 and 3 min, respectively.

Mixed layer preparation by sequential electrografting: [Fmoc-NH-CH_2-Ar-N_2]BF_4 as the second modifier. The first modifier, TIPS-Eth-Ar (or Fm-COO-Ar), was electrografted from a solution of 5 mM [TIPS-Eth-Ar-N_2]BF_4 (or [Fm-COO-Ar-N_2]BF_4) in 0.1 M $TBABF_4$-ACN using five cycles between 0.60 (or 0.80 V) and -0.75 V at a scan rate of 50 mV s^{-1}, followed by deprotection in TBAF-THF (or piperidine-DMF). The second modifier, Fmoc-NH-CH_2-Ar, was electrografted to the H-Eth-Ar-GC (or H-COO-Ar-GC) modified surface from a solution of 5 mM [Fmoc-NH-CH_2-Ar-N_2]BF_4 in 0.1 M $TBABF_4$-ACN using two cycles between 0.60 and -0.75 V at a scan rate of 200 mV s^{-1}. After each grafting step, the

electrodes were rinsed with acetone and sonicated in ACN for 5 min. Deprotection was carried out by stirring in the respective deprotection solutions, and electrodes were carefully rinsed with acetone and H_2O after each deprotection step. Coupling of NP and Fc was carried out as described above.

Mixed layer preparation by electrografting followed by direct reaction of the second modifier with GC. An Fmoc-NH-CH_2-Ar-GC surface was prepared using the method as described above. Fc groups were coupled directly to the GC surface either by reaction of $FcCH_2NH_2$ with GC in the presence of HBTU or by reaction of $(COCl)_2$-activated FcCOOH with GC. After the coupling reactions, the electrodes were sonicated in ACN for 5 min, and dried with a stream of N_2(g).

Mixed layer preparation for O_2 reduction studies:

Mixed layer consisting of H-Eth-Ar and NH_2-CH_2-Ar groups (Scheme 6.7a). Fmoc-NH-CH_2-Ar groups were immobilised on the surface using the method as described above. Fmoc groups were then deprotected in 20% piperidine-DMF for 2.5 h. NH_2-CH_2-Ar-GC modified electrodes were then electrografted with TIPS-Eth-Ar groups by scanning two cycles between 0.60 and -0.75 V at a scan rate of 200 mV s^{-1} in a solution of 5 mM [TIPS-Eth-Ar-N_2]BF_4 in 0.1 M $TBABF_4$-ACN. The TIPS group was then deprotected in 0.05 M TBAF-THF for 1 h. After each grafting step, the electrodes were rinsed with acetone and sonicated in ACN for 5 min, and after each deprotection step, the electrodes were rinsed with acetone and sonicated in ACN for 2 min. The modified electrodes were then reacted with 2-azidoanthraquinone (AQ-N_3) using the method described in Chapter 2, Section 2.4.2.1 or the NH_2-CH_2-Ar groups were first reacted with trifluoroacetic anhydride (TFAA, 10%) in THF overnight with stirring, prior to the click reaction. After TFAA coupling reaction, the electrodes were

sonicated in ACN for 5 min, and after the click reaction, the electrodes were stirred in EDTA-Na_2 solution for 10 min followed by sonication in ACN for 5 min.

Mixed layer consisting of H-Eth-Ar and H-COO-Ar groups (Scheme 6.7b). GC electrodes were scanned five cycles from 0.60 to -0.75 V at a scan rate of 50 mV s^{-1} in a solution of 5 mM [Fm-COO-Ar-N_2]BF_4 in 0.1 M TBABF_4-ACN. Fm groups were deprotected in 20% piperidine-DMF by stirring for 1 h. TIPS-Eth-Ar groups were then grafted by scanning two cycles between 0.60 and -0.75 V at a scan rate of 200 mV s^{-1} in a solution of 5 mM [TIPS-Eth-Ar-N_2]BF_4 in 0.1 M TBABF_4-ACN. TIPS groups were deprotected in 0.05 M TBAF-THF for 1 h. After each grafting step, the electrodes were rinsed with acetone and sonicated in ACN for 5 min, and after each deprotection step, the electrodes were rinsed with acetone and sonicated in ACN for 2 min. An amide coupling reaction with the H-COO-Ar surface was carried out using the HBTU method as described in Chapter 2, Section 2.4.2.4. Electrodes were sonicated with ACN for 5 min after the coupling reaction. Click reaction of AQ-N_3 with the modified surface was carried out using the method described in Chapter 2, Section 2.4.2.1. Electrodes were stirred in EDTA-Na_2 for 10 min and sonicated in ACN for 5 min after click reaction.

Mixed layer consisting of H-Eth-Ar and direct reaction of amine derivatives with GC surface (Scheme 6.7c). GC electrodes were scanned in a solution of 5 mM [TIPS-Eth-Ar-N_2]BF_4 in 0.1 M TBABF_4-ACN for five cycles from 0.60 to -0.75 V at 50 mV s^{-1}. After grafting, the electrodes were rinsed with acetone and sonicated in ACN for 5 min. TIPS groups were deprotected in 0.05 M TBAF-THF for 1 h. After deprotection, electrodes were rinsed with acetone and sonicated in ACN for 2 min. H-Eth-Ar-GC was then stirred in the amine derivative solution (10 mM) in ACN overnight. Electrodes were sonicated in ACN for 5 min after coupling. AQ was clicked to the surface using the method outlined in Chapter 2, Section

2.4.2.1. Electrodes were stirred in EDTA-Na_2 for 10 min and sonicated in ACN for 5 min after the click reaction.

Electrochemistry. Cyclic voltammograms (CVs) of immobilised Fc and NP groups were obtained in 0.1 M $LiClO_4$-EtOH at a scan rate of 200 mV s^{-1} and in 0.1 M H_2SO_4 at a scan rate of 100 mV s^{-1}, respectively. For mixed films, the voltammetry of Fc groups was recorded prior to that of NP groups. Unless stated otherwise, CVs of immobilised AQ groups were obtained in 0.1 M PB, pH 7.1 at a scan rate of 100 mV s^{-1} in the absence of O_2 (the solution was flushed with N_2(g)). The surface concentration of immobilised Fc was determined by averaging the area under the anodic and cathodic peaks from the third voltammetric cycle. The surface concentration of immobilised AQ was dertermined by averaging the area under the anodic and cathodic peaks from the second voltammetric cycle. The surface concentration of immobilised NP groups was estimated from the first voltammetric cycle using the NP reduction and the hydroxyaminophenyl oxidation peak areas and the number of electrons involved in each redox process[30] as described in Chapter 2. For the O_2 reduction study, the 0.1 M PB, pH 7.1 solution was saturated with O_2 by flushing with O_2 gas for at least 5 min prior to recording the CV.

XPS. XPS analysis was carried out by Dr. Colin Doyle, Department of Chemical and Materials Engineering at University of Auckland. XPS data were obtained using a Kratos Axis Ultra DLD spectrometer equipped with a monochromatic Al Kα energy source operating at 150 W. Wide scans were recorded with a step size of 1 eV and pass energy of 160 eV, and high resolution scans were carried out with a step size of 0.1 eV and a pass energy of 20 eV. Peak positions were referenced to aromatic carbon at 284.7 eV. Data treatment and peak-fitting procedures were performed using Casa XPS software (version 2.3.16).

6.3 Results and Discussion

6.3.1 Preparation and characterisation of amine functionalised monolayers

6.3.1.1 Synthesis of the protected amine functionalised aryldiazonium salts

Two different protecting groups were employed, namely Boc and Fmoc, and two different arylamines were used, aminophenyl and aminomethylphenyl, to prepare the amine functionalised aryldiazonium salts. Syntheses of the four protected aryldiazonium salts are summarised in Scheme 6.1. The Boc-protected diazonium salts were synthesised in a straightforward two step synthesis.[6] Firstly, one of the amine groups of the diamine was protected with a Boc group to obtain the Boc-protected amine (Schemes 6.1a and 6.1c, step i).[31] The second step involves the conversion of the other amine group into the diazonium ion by addition of nitrosonium tetrafluoroborate in ACN at -40 °C or by addition of aqueous sodium nitrate and tetrafluoroboric acid at 0 °C as depicted in Schemes 6.1a and 6.1c (step ii) to give [Boc-NH-Ar-N_2]BF_4 and [Boc-NH-CH_2-Ar-N_2]BF_4, respectively. The Fmoc-protected aminophenyl diazonium salt was synthesised in four steps (Scheme 6.1b). The first step is the protection of one of the amine groups of *p*-phenylenediamine with a Boc group (Scheme 6.1a, step i), this is then followed by reaction with 9-fluorenylmethyl chloroformate (Fmoc-Cl) to obtain the Boc- and Fmoc-protected *p*-phenylenediamine (Scheme 6.1b, step ii).[32] Boc group was removed by reaction with trifluoroacetic acid (TFA), to obtain the Fmoc-protected diamine, Fmoc-NH-Ar-NH_2 (Scheme 6.1b, step iii). In step iv, the diazonium ion was synthesised using the usual diazotisation method by sodium nitrite with tetrafluoroboric acid at 0 °C. The Fmoc-protected aminomethylphenyl diazonium salt was prepared in three steps from 4-nitrobenzylamine hydrochloride (Scheme 6.1d).[32] The first step of the synthesis involved the protection of the amine group with Fmoc using the same method as for the Fmoc-protected aminophenyl above (Scheme 6.1d, step i). The nitro group was then reduced

to amine group using palladium on carbon in the presence of hydrogen gas to obtain the Fmoc-protected amine, Fmoc-NH-CH_2-Ar-NH_2 (step ii). Finally, Fmoc-NH-CH_2-Ar-NH_2 was converted to the diazonium ion by addition of sodium nitrite and tetrafluoroboric acid at 0 °C (step iii). Details for these synthesis steps can be found in Chapter 2.

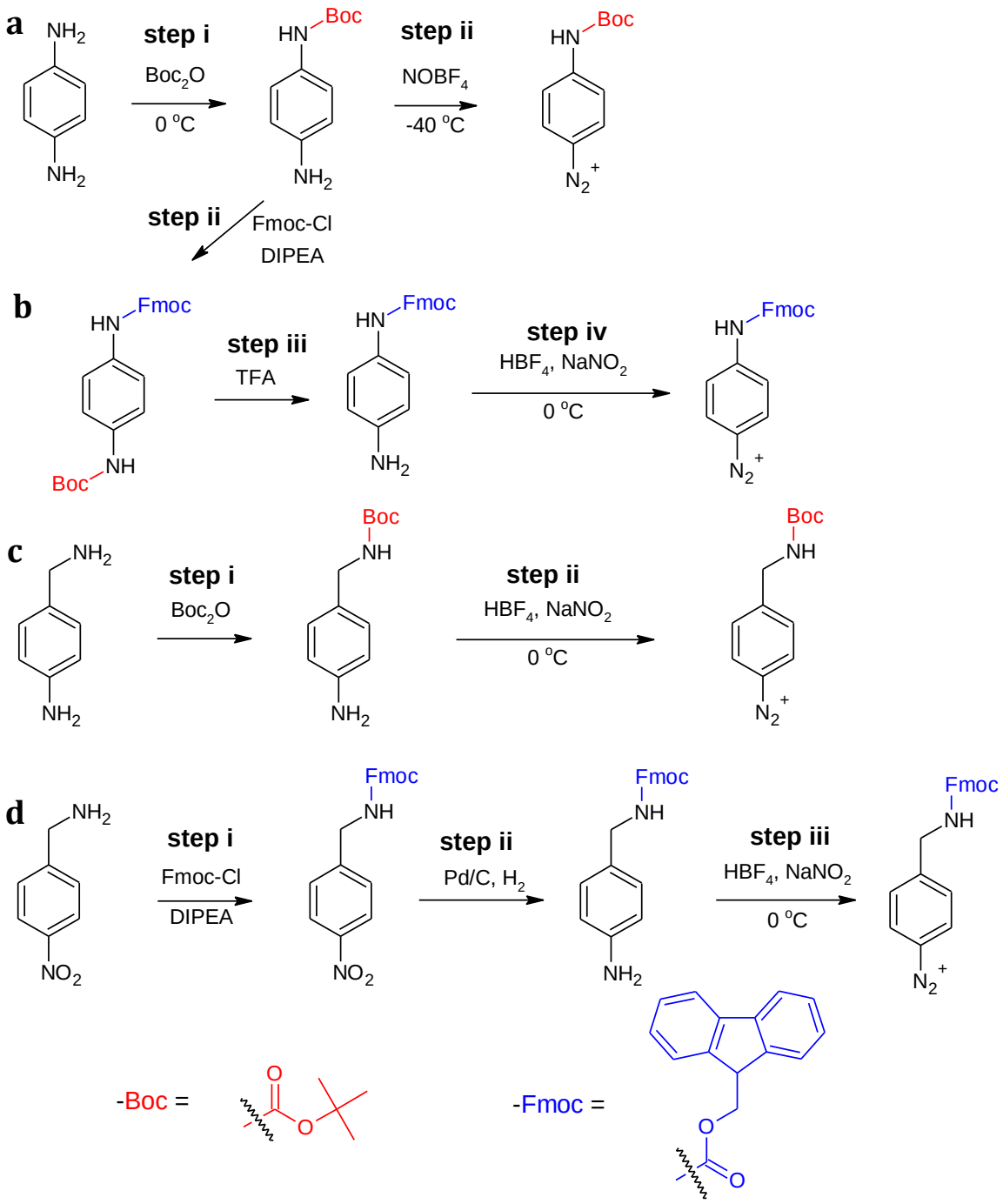

Scheme 6.1 Reaction scheme for the preparation of: a) [Boc-NH-Ar-N_2]BF_4, b) [Fmoc-NH-Ar-N_2]BF_4, c) [Boc-NH-CH_2-Ar-N_2]BF_4, and d) [Fmoc-NH-CH_2-Ar-N_2]BF_4.

6.3.1.2 Characterisation of the modified electrodes using redox probe electrochemistry

Scheme 6.2 shows the sequence of steps for electrografting protected amine-terminated diazonium salts, cleavage of the protecting groups and subsequent coupling reactions with carboxylic acid derivatives. Electrografting was performed by scanning five cycles between 0.60 and -0.75 at 50 mV s^{-1} in a solution of 0.1 M $TBABF_4$-ACN containing 5 mM of the protected aryldiazonium salt. Typical electrografting CVs carried out in Boc- and Fmoc-protected aryldiazonium salts are shown in Figures 6.1. In both cases, the one-electron irreversible reduction of aryldiazonium salt is observed on the first scan and on the subsequent scans, only featureless voltammograms with relatively low current can be seen. The disappearance of the reduction peaks after one scan is consistent with the formation of non-conducting grafted layers, which inhibit further electron transfer to aryldiazonium ion in solution. (Note, as seen on all four CVs the first scan gives rise to two reduction peaks, this phenomenon will be discussed in Chapter 7.)

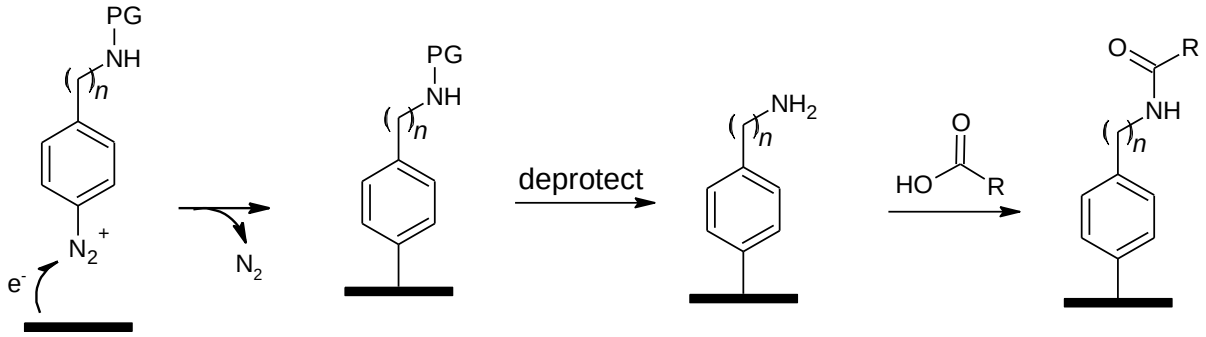

PG = protecting group (Boc or Fmoc)
n = 0 or 1

-R = -Fc, $-CH_2Fc$, or $-Ar-NO_2$

Scheme 6.2 Schematic representation for the preparation of amine functionalised monolayers by electrografting followed by deprotection of the protecting group and further amide coupling reactions.

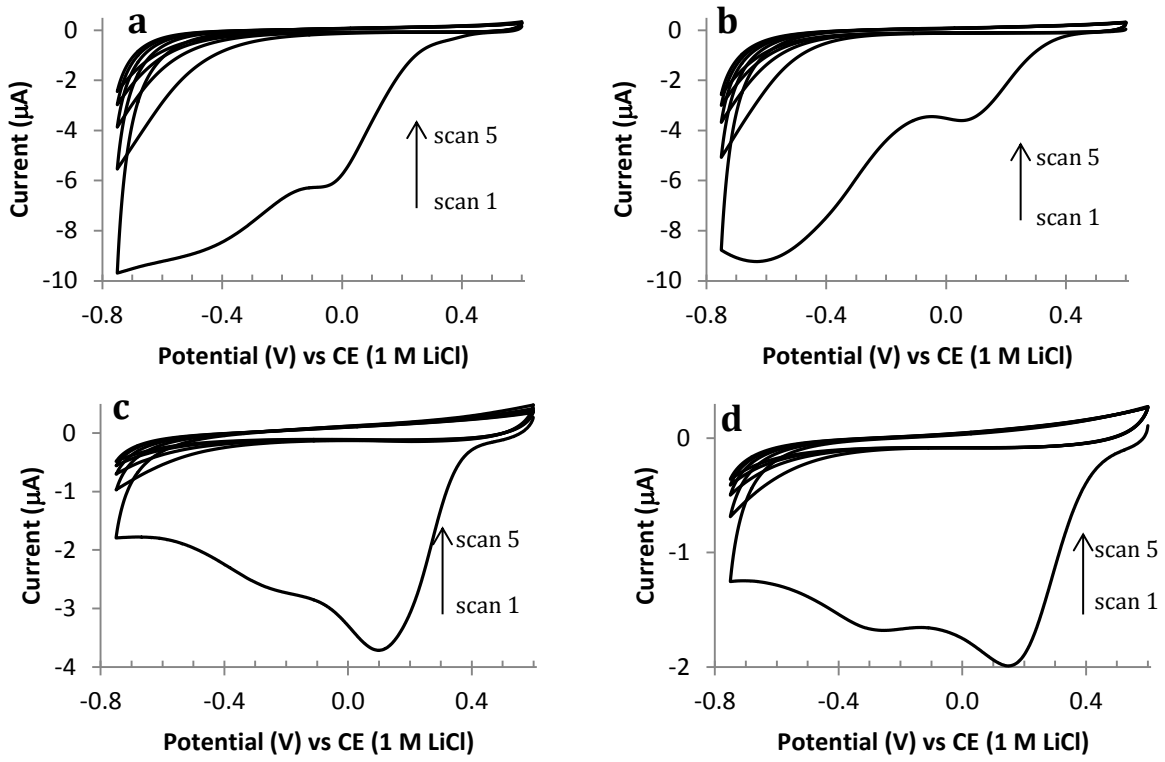

Figure 6.1 Five consecutive CV scans at a bare GC electrode in a solution of 5 mM: a) [Boc-NH-Ar-N_2]BF_4, b) [Boc-NH-CH_2-Ar-N_2]BF_4, c) [Fmoc-NH-Ar-N_2]BF_4, and d) [Fmoc-NH-CH_2-Ar-N_2]BF_4 in 0.1 M $TBABF_4$-ACN. Scan rate = 50 mV s^{-1}.

Similar to previous studies using solution redox probe voltammetry (Chapters 4 and 5), dopamine, ferrocyanide and ferrocene were used to monitor the blocking properties of the grafted films at each stage of modification. Removal of the Boc-protecting group was carried out in acidic solution (4 M HCl-MeOH), while the Fmoc-protecting group was removed in basic solution (20% piperidine-DMF).[29] Dopamine, an inner sphere redox probe,[33-36] was chosen to monitor the effect of immersion time in the deprotection solution. CVs were recorded at a scan rate of 100 mV s^{-1} in a solution of 1 mM dopamine in 0.1 M H_2SO_4 at 20 min intervals for the Boc-protected amines and at 20 min intervals for the first 40 min and then at 40 min intervals thereafter for the Fmoc-protected amines.

Figure 6.2 shows a plot of dopamine redox peak-to-peak separation (ΔE_p) against deprotection time. The presence of a film will decrease the rate of electron transfer between

the electrode and the redox probe, which will give rise to an increase in ΔE_p; the more blocking the surface film is towards electron transfer to the redox probes, the larger the ΔE_p value (Chapter 4). For all four modified surfaces, there is no evidence of dopamine redox chemistry at the modified electrode before deprotection, i.e. ΔE_p > 900 mV. This is consistent with a lack of accessible catalytic surface sites for dopamine electron transfer. As seen from Figure 6.2, as the deprotection time increases, ΔE_p decreases and reaches a constant ΔE_p of ~180 mV after 60 min for the two Boc-protected amines and 120 min for the Fmoc-NH-CH_2-Ar film. For the Fmoc-NH-Ar film (green), similar ΔE_p was observed at every interval, demonstrates that deprotection is complete by 20 min. The decrease in ΔE_p is consistent with the removal of the deprotecting groups after stirring of the modified electrodes in the deprotection solution. Unless stated otherwise, the standard deprotection time for Boc and Fmoc were 1.5 and 2 h, respectively.

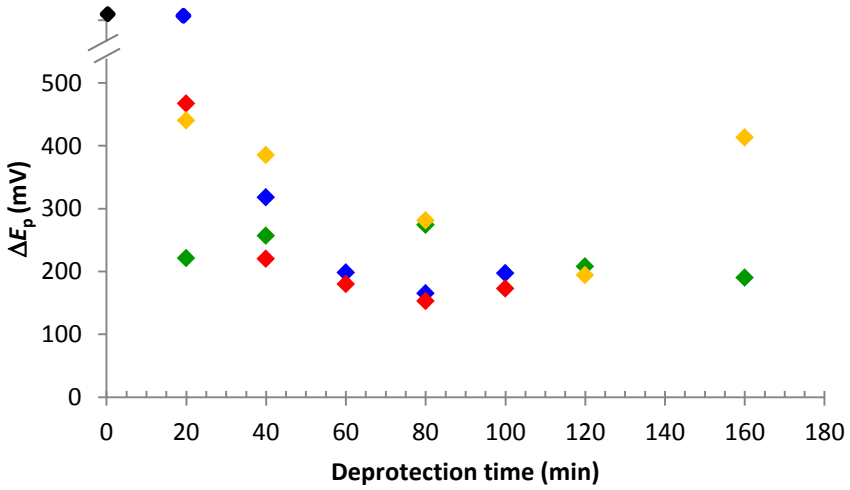

Figure 6.2 Plot of ΔE_p versus deprotection time of dopamine redox probe. Boc-NH-Ar-GC: blue; Boc-NH-CH_2-Ar-GC: red; Fmoc-NH-Ar-GC: green; Fmoc-NH-CH_2-Ar-GC: yellow. Black point represents all of the modified surfaces before deprotection. ΔE_p values were measured in 1 mM dopamine in 0.1 M H_2SO_4. Scan rate = 100 mV s^{-1}.

To further investigate the modified surfaces at each stage of preparation and to confirm the role of the deprotection reagent, CVs were obtained of dopamine in 0.1 M H_2SO_4,

ferrocyanide in 0.1 M PB pH 6.9 solution, and ferrocene in 0.1 M $TBABF_4$-ACN, before deprotection, after immersion of the modified electrode in MeOH or DMF solution in the absence of the deprotection agent, and after immersion in the deprotection solution. Immersion in MeOH and DMF in the absence of HCl and piperidine was included to demonstrate that HCl and piperidine are required to obtain the deprotected layer. The CVs are shown in Figure 6.3.

As described above, CVs recorded in dopamine solution at all electrodes after grafting and before deprotection (Figures 6.3a–d, blue line) are featureless with very low currents over the potential range where the dopamine redox reaction occurs at the bare GC electrode (black line). After immersion of the Boc-NH-Ar-GC and Boc-NH-CH_2-Ar-GC surfaces in MeOH for 1.5 h (Figures 6.3a and 6.3b), and the Fmoc-NH-Ar-GC surface in DMF for 2 h (Figure 6.3c) in the absence of deprotection agent, the CVs obtained (green line) show little change. In contrast, after immersion in DMF for 2 h, the CV of dopamine at the Fmoc-NH-CH_2-Ar-GC electrode shows oxidation and reduction peaks with low current and ΔE_p = 455 mV (Figure 3.6d). These observations indicate that the Fmoc-NH-CH_2-Ar film becomes sufficiently more porous after immersion in DMF, than the Fmoc-NH-Ar, Boc-NH-CH_2-Ar and Boc-NH-Ar films after immersion in blank deprotection solutions. The increase in porosity of the Fmoc-NH-CH_2-Ar film is presumably due to swelling of the film and/or removal of physisorbed impurities during stirring in DMF solution. It is not clear why this occurs to a significant extent for the Fmoc-NH-CH_2-Ar than other films but may be due to the greater hydrophobicity of this modifier which promotes physisorption during grafting and the larger size of Fmoc-NH-CH_2-Ar moieties leads to bigger pores created upon removal of physisorbed materials.

After deprotection in 4 M HCl-MeOH for 1.5 h for the Boc-protected amines (Figures 6.3a and 6.3b) and for 2 h in 20% piperidine-DMF for the Fmoc-protected amines (Figures 6.3c and 6.3d), well-defined dopamine redox peaks (red line) are observed. The dopamine responses after deprotection of these films have ΔE_p ~ 180 mV, which is large compared to that obtained at bare GC (ΔE_p ~ 60 mV) and at the Fm-COO-Ar and TIPS-Eth-Ar films after deprotection (ΔE_p = 70 mV, Chapter 5 and 80 mV, Chapter 4, respectively). Amine functionality are expected to have acid-base properties, where the pK_a for aniline and benzylamine are 4.9 and 9.3 respectively.[37] The protonation constant of a chemical species in solution can be different from the one on a solid support,[38, 39] However, even if there is a significant change in pK_a of the amines after grafting, in 0.1 M H_2SO_4, all of the deprotected amine surfaces are expected to be protonated (positively charged). Therefore, the larger ΔE_p values obtained for dopamine at the amine films is not unexpected because there will be electrostatic repulsion between the amine films and the redox probe, whereas H-COO-Ar and H-Eth-Ar films are neutral and there will be no repulsion effects. The lower ΔE_p observed for H-COO-Ar film than H-Eth-Ar film is presumably due to the larger pores created by the Fm groups than TIPS groups after deprotection.

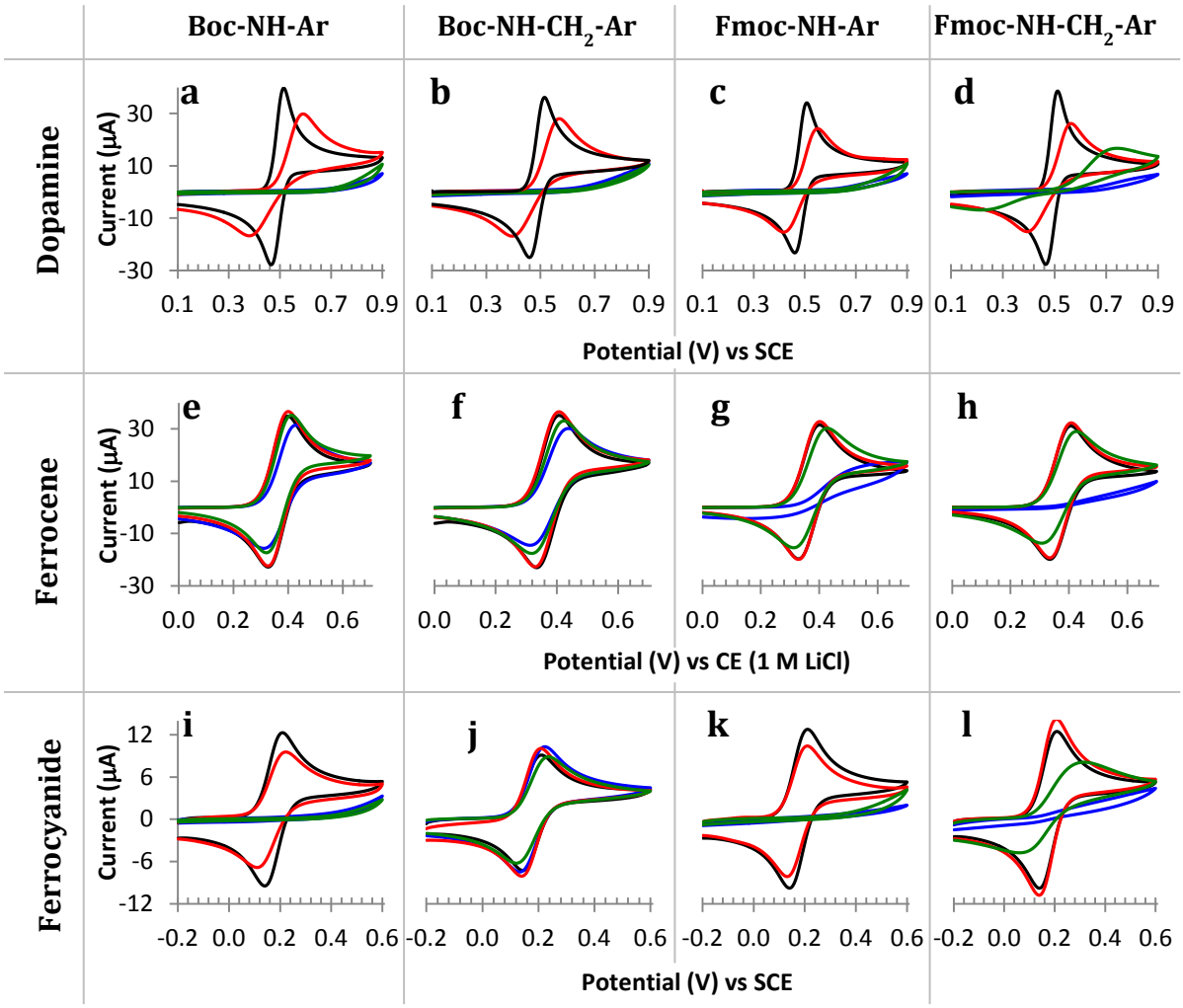

Figure 6.3 CVs of bare GC (black line), and protected aryl-layers before deprotection (blue line), after immersion in MeOH (for Boc-protected) or DMF (for Fmoc-protected) (green line), after immersion in deprotection solution (red line), obtained in a solution of: 1 mM dopamine in 0.1 M H_2SO_4 (a, b, c, d); 1 mM ferrocene in 0.1 M $TBABF_4$-ACN (e, f, g, h); 1 mM ferrocyanide in 0.1 M PB, pH, 6.9 (i, j, k ,l). GC was modified with: [Boc-NH-Ar-N_2]BF_4 (a, e, i); [Boc-NH-CH_2-Ar-N_2]BF_4 (b, f, j); [Fmoc-NH-Ar-N_2]BF_4 (c, g, k); [Fmoc-NH-CH_2-Ar-N_2]BF_4 (d, h, l). Scan rate = 100 mV s^{-1}.

Ferrocene as an outer sphere redox probe, is less sensitive to the electrode surface than are dopamine and ferrocyanide.[33] The CVs recorded in ferrocene-ACN solution at each stage of modification are shown in Figures 6.3e–h. After grafting and before deprotection (blue line), the Boc-protected amines (Figures 6.3e and 6.3f) only exert a small blocking effect on the voltammetry of ferrocene. In contrast, the Fmoc-protected amine films (Figures 6.3g and 6.3h), strongly block the ferrocene response; only very low currents are obtained. These

results are consistent with Boc-protected layers that are thinner and/or more porous than the Fmoc-protected layers. Film thickness measurements (described in Section 6.3.1.3) confirm that the Fmoc-protected layers are indeed multilayers. This behaviour is similar to that of the Fm-COO-Ar-GC surface (Chapter 5) and TIPS-Eth-Ar-GC surface (Chapter 4): a very blocking effect is exerted by the Fm-COO-Ar-GC surface, but for the TIPS group, which is similar to the Boc group, the ferrocene response is less blocked.

Immersion of the modified surfaces in MeOH for the Boc-protected amine layers (Figures 6.3e and 6.3f, green line) does not have a significant effect on the ferrocene response. This is not surprising because even before this step, the redox response is similar to that at bare GC. On the other hand, immersion of the Fmoc-protected amines in DMF (Figures 6.3g and 6.3h, green line) has a dramatic effect on the ferrocene redox response. The peak currents and ΔE_p values are close to those of bare GC. This may suggest that most of the Fmoc-protected amines are physisorbed (maybe through π-π stacking) onto the surface and are removed during stirring in DMF for 2 h. However, for the dopamine response discussed above, there is very little change for the Fmoc-NH-Ar film, and only a low current response with a large ΔE_p at the Fmoc-NH-CH_2-Ar film after immersion in DMF. These different responses of ferrocene to that of dopamine may be due to two factors. Ferrocene is an outer sphere redox probe and tunnelling across the film is expected. Moreover, the films are expected to be more porous in ACN, the solvent used for ferrocene voltammetry, than in the aqueous solvent used for dopamine. Therefore, ferrocene may be able to diffuse through the hydrophobic film and access the surface.

After removal of the protecting groups in the respective deprotection solutions (red line), all of the ferrocene CVs obtained at the four modified surfaces are similar to that of bare GC as expected for sparse, thin monolayer films.

Ferrocyanide in PB, pH 6.9 solution, was chosen as an additional redox probe to investigate the blocking properties at each stage of the modification (Figures 6.3i–l). With the exception of the Boc-NH-CH_2-Ar-GC surface (discussed below), the ferrocyanide redox responses at all of the surfaces are similar to those of dopamine at the same surface, before and after immersion in the blank deprotection solvent. This is expected as both are inner sphere redox species. However, after deprotection (red line), the ferrocyanide redox response is similar to that at bare GC, whereas the response of dopamine shows that the modified surfaces still have some blocking property. This difference is likely due to the acid-base properties of the amine tether layer as described above. For dopamine, where acidic solution was used, all of the four deprotected amine surfaces are expected to be protonated and therefore repel the positively charged dopamine. On the other hand, at pH 7, the NH_2-Ar films (Figures 6.3i and 6.3k) are expected to be neutral, while the NH_2-CH_2-Ar films (Figures 6.3j and 6.3l) are expected to be positively charged. Therefore, electrostatic attraction is expected between ferrocyanide and the NH_2-CH_2-Ar films. Hence, the ferrocyanide response after deprotection of the Fmoc-NH-CH_2-Ar film is similar to that of bare GC whereas for Boc-NH-Ar and Fmoc-NH-Ar films a small decrease in current is observed compared to bare GC. As expected, the ferrocyanide response is opposite to that obtained at the deprotected Fm-COO-Ar-GC surface (Chapter 5). At pH 7, the H-COO-Ar film will be deprotonated and therefore will repel the negatively charged ferrocyanide and a blocking response is obtained after deprotection.

The ferrocyanide redox response at the Boc-NH-CH_2-Ar-GC surface at each stage of modification is shown in Figure 6.3j. Surprisingly, similar CVs were obtained before and after deprotection. These results are reproducible for repeat modification experiments. The non-blocked response obtained after grafting and before deprotection (blue line) might suggest that the Boc-NH-CH_2-Ar groups are not grafted on the surface, or that a very thin or

very porous film was grafted. However, the dopamine redox response at the same surface (Figure 6.3, green line), clearly shows a strong blocking effect. These results are tentatively explained by protonation of the amide nitrogen. Although protonation of amide in solution would not be expected (pK_a of amide in DMSO is around 20)[40], it may be protonated on a surface. pK_a of a chemical species on a solid support can be different from the one in solution.[38, 39] For example, the pK_a of protonated bis(3-aminopropyl) terminated polyethylene glycol on graphite powder is shifted to two pK_a units lower than in solution.[39] The XPS results (Section 6.3.1.5), also suggest that the amide nitrogen may be protonated. If this is the case, the negatively charged ferrocyanide would be attracted to the positively charged surface leading to a non-blocked response. On the other hand, for the Fmoc-NH-CH_2-Ar groups, the blocking effect of the bulky and hydrophobic Fmoc groups may dominate over the effect of a positively charged amide, and hence the response of ferrocyanide is blocked at that surface.

6.3.1.3 Film thickness measurement by AFM

The CVs of redox probes described in Section 6.3.1.2 above are in qualitative agreement with the changes expected on deprotection of the grafted layers. To further confirm that the films formed after removal of the protecting groups are monolayers, film thickness measurements were carried out by the AFM depth profiling technique (Chapters 2 and 4). For these experiments, films were grafted to PPF, using the same conditions as for GC. Table 6.1 lists the average thicknesses of the grafted films before and after removal of the protecting groups and also the theoretical calculated film thicknesses. As can be seen from the data, with the exception of the Boc-NH-Ar film, the average thicknesses of all the films before deprotection are consistent with a multilayer structure with at least 2 layers. The Boc-NH-Ar film appears to be a monolayer. After deprotection, with the exception of the Boc-NH-CH_2-Ar layer, the average film thickness for all of the films is 0.4 ± 0.3 nm, consistent with a monolayer. After

deprotection of the Boc-NH-CH_2-Ar layer, an average film thickness of 1.0 ± 0.3 nm was obtained. Even though this thickness is higher than the other films after deprotection, considering the experimental uncertainty, the measured thickness is not inconsistent with a monolayer.

Table 6.1 Thickness of grafted films on PPF before and after deprotection.

Type of surfaces	Before deprotection (nm)		After deprotection (nm)	
	Average film thickness	Calculated height[a]	Average film thickness	Calculated height[a]
Boc-NH-Ar-PPF	1.0 ± 0.2	1.1	0.4 ± 0.3	0.6
Boc-NH-CH_2-Ar-PPF	1.9 ± 0.4	1.2	1.0 ± 0.3	0.7
Fmoc-NH-Ar-PPF	2.8 ± 0.5	1.4	0.4 ± 0.3	0.6
Fmoc-NH-CH_2-Ar-PPF	2.1 ± 0.4	1.5	0.4 ± 0.3	0.7

[a]Molecule height was estimated using *Avogadro* (Chapter 2)

Multilayer films form by the attack of aryl radicals on the already grafted modifiers[41] (Scheme 1.2, Chapter 1). As seen in Scheme 6.1, the Boc protecting group incorporates *t*-butyl groups and the Fmoc protecting group incorporates the aromatic fluorenyl group. Attack of aryl radicals on the aromatic Fmoc group is more likely than on the non-aromatic Boc group. Consistent with this reasoning, film thickness measurements and redox probe voltammetry (Section 6.3.1.2), show that before deprotection the Fmoc-protected films are multilayers, while the Boc-NH-Ar film is a monolayer. Consideration of the same data indicates that the Boc-NH-CH_2-Ar film is a multilayer. This may be because the orientation of the protecting group does not efficiently protect the aryl ring from radical attack. In studies of protected Eth-Ar-N_2^+ derivatives, it has been shown that a bulky protecting group (eg. TIPS) at one *meta* position is capable of preventing multilayer formation. However, with a small protecting group (eg. trimethylsilyl (TMS)) at a *meta* position, multilayer formation was observed.[42] On the other hand, a TMS group in the *para* position prevents multilayer

formation.[43] This suggests that the Boc group, which cannot be positioned directly over the *para* position on the aryl ring, is not bulky enough to prevent multilayer formation (Figure 6.4). The reason that a monolayer is formed for Boc-NH-Ar films may be due to the steric hindrance imposed on the aryl ring by the closeness of Boc groups to the aryl ring.

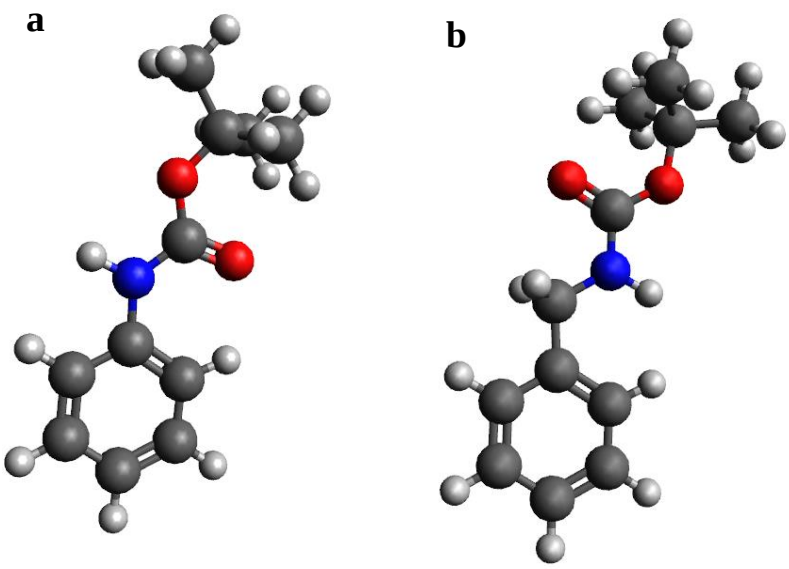

Figure 6.4 Optimised structure of: a) Boc-NH-Ar, and b) Boc-NH-CH_2-Ar.

For the Fmoc-protected films, deprotection removes any film growth originating from radical attack on Fmoc groups, leaving monolayer films, NH_2-Ar and NH_2-CH_2-Ar. Boc-NH-Ar is a monolayer film and removal of the Boc group gives a monolayer NH_2-Ar film. However, for Boc-NH-CH_2-Ar, if multilayer growth results from radical attack at the aryl ring, deprotection does not remove the additional film and the deprotected film is not a monolayer. The higher surface concentrations of NP and Fc groups (see Section 6.3.1.4) coupled to the deprotected Boc-NH-CH_2-Ar films is consistent with a multilayer film, which from the surface concentration and film thickness measurements incorporates approximately two layers.

6.3.1.4 *Reactions of amine-terminated layers with carboxylic acid derivatives*

The four deprotected amine layers were reacted with NO_2-Ar-COOH, ferrocene carboxylic acid (FcCOOH) and ferrocene acetic acid ($FcCH_2COOH$) using $(COCl)_2$ and HBTU as activating agents. Surface concentrations of all electroactive groups were determined from CVs of the modified surfaces giving the data in Table 6.2. This data can be analysed to estimate the surface concentrations of each amine monolayer, to compare the reactivity of each amine modifier and to compare the reactivity of the two ferrocene derivatives.

6.3.1.4.1 Assessing the contribution to surface concentrations from reactions with bare GC

In order to determine the surface concentration of amine groups on each modified surface, electroactive NP and Fc groups were coupled to the surface. Using these concentrations to infer the concentrations of amine groups requires knowledge of the concentration of the blank (electroactive groups immobilised on bare GC) and on the coupling yield. To gain information about these factors, surface concentrations of NP and Fc groups immobilised at each layer using $(COCl)_2$ and HBTU were compared. Table 6.2 shows that coupling of all four amine tethers with the three carboxylic acid derivatives using $(COCl)_2$ always yielded higher surface concentrations than when HBTU was used as the activating agent. In fact, this was found for all the amide coupling reactions carried out in this thesis work (Chapters 3 and 5). However, the blank experiments, where bare GC electrodes were reacted with the $(COCl)_2$-activated carboxylic acid derivatives, resulted in a significant amount of electroactive species coupled to the surface (Table 6.2 and Chapter 3). This suggests that the surface concentrations obtained from coupling the modified surfaces with carboxylic acid derivatives using $(COCl)_2$ as the activating agent may include a significant contribution from the reaction with bare GC. Hence the surface concentrations of electroactive groups obtained

using $(COCl)_2$ as the activation method are likely to over-estimate the amount of amine on the surface. In contrast, when HBTU was employed as the coupling agents, the blank experiments showed that only trace amounts of electroactive species were coupled directly to GC. Coupling reactions using HBTU are typically not quantitative: yields of peptide coupling using uronium reagents (eg. HBTU) can range from 28 to 96%.[44, 45] Hence, the values obtained from the HBTU method are likely to underestimate the surface concentration of amines.

Further insight into the importance of the blank reactions at modified surfaces (that is, reaction of $(COCl)_2$-activated Fc derivatives directly at GC for surfaces modified with deprotected amine films) can be assessed by analysing $E_{½}$ values for immobilised Fc groups (Table 6.2). Figure 6.5a shows CVs of Fc immobilised via HBTU activation of FcCOOH. No Fc is coupled to bare GC under these conditions and hence the responses with $E_{½}$ ~0.54V originate from Fc coupled to the amine layer via an amide linkage. Figure 6.5b shows CVs for the same Fc derivative activated with $(COCl)_2$ and reacted with amine-terminated layers and bare GC. For surfaces initially grafted with Boc-NH-Ar, Fmoc-NH-Ar, and Fmoc-NH-CH_2-Ar, $E_{½}$ of the immobilised Fc is ~0.6 V and the peaks are broad suggesting overlapping peaks. $(COCl)_2$-activated FcCOOH coupled directly to bare GC has $E_{½}$ ~0.66 V and hence the broad peaks are assumed to result from substantial amounts of Fc coupled to both the tether layer and to GC. For the multilayer film prepared from deprotection of the Boc-NH-CH_2-Ar layer, Fc coupled to the film, with $E_{½}$ ~0.54 V is the main component, but there is also a shoulder indicating a relatively small amount of Fc coupled directly to GC.

Table 6.2 Conditions for amide coupling reactions carried out with different amine functionalised surfaces, the corresponding $E_{½}$ values and surface concentrations of electroactive Fc and NP groups, and the calculated theoretical surface concentrations.[a]

Type of surface initially[b]	Amide coupling method	Γ_{NP} (10^{-10} mol cm^{-2})	Γ_{Fc} (FcCOOH) (10^{-10} mol cm^{-2})	$E_{½}$ (FcCOOH) (V)	Γ_{Fc} ($FcCH_2COOH$) (10^{-10} mol cm^{-2})	$E_{½}$ ($FcCH_2COOH$) (V)	Γ_{Cal}[c] (10^{-10} mol cm^{-2})
Boc-NH-Ar-GC	$(COCl)_2$	3.0 ± 0.1	3.3 ± 0.1	0.60	2.5 ± 0.2	0.36	3.5
	HBTU	1.2 ± 0.1	Trace	-	0.9 ± 0.1	0.37	
Boc-NH-CH_2-Ar-GC	$(COCl)_2$	5.4 ± 0.3	4.5 ± 0.1	0.54	4.1 ± 0.4 (n = 4)	0.35	2.0
	HBTU	3.8 ± 0.3	1.5 ± 0.1	0.54	3.9 ± 0.1	0.33	
Fmoc-NH-Ar-GC	$(COCl)_2$	3.0 ± 0.2	2.9 ± 0.2	0.61	2.3 ± 0.2	0.36	1.4
	HBTU	0.8 ± 0.1	Trace	-	0.5 ± 0.1	0.36	
Fmoc-NH-CH_2-Ar-GC	$(COCl)_2$	3.2 ± 0.6	2.5 ± 0.2	0.64	1.7 ± 0.3	0.37	1.0
	HBTU	2.1 ± 0.2	0.6 ± 0.3 (n = 3)	0.54	1.4 ± 0.1	0.34	
Bare GC (blank)	$(COCl)_2$	2.4 ± 0.2	1.6 ± 0.2	0.66	2.4 ± 0.4 (n = 3)	0.40	n/a
	HBTU	Trace	Trace	-	0.5 ± 0.3	0.44	

[a]Unless indicated otherwise, the number of repeat samples, n, was two

[b]Surface shown is the initial surface before deprotection. Amide coupling reaction was performed on the deprotected surface, $ArNH_2$ or $ArCH_2NH_2$

[c]Surface concentration was calculated based on eq. 5.1 (Chapter 5). The diameter of the protecting groups were determined using *Avogadro*

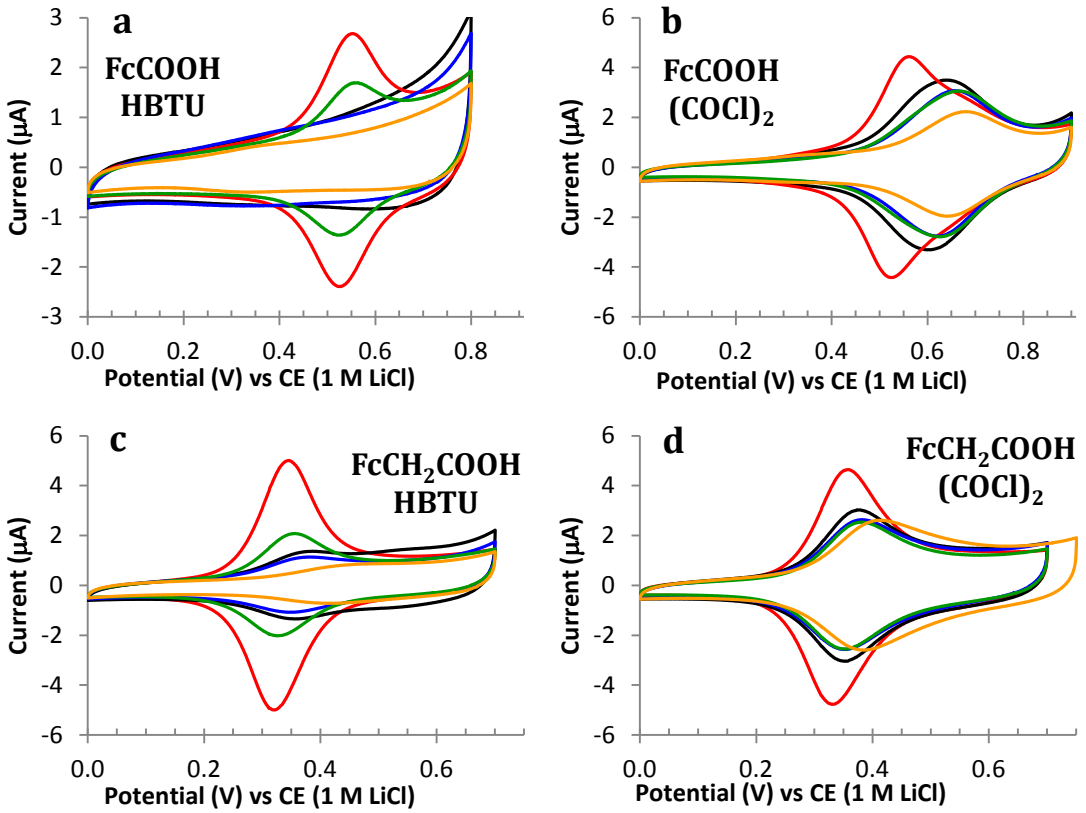

Figure 6.5 CVs showing the 3rd scan obtained in 0.1 M $LiClO_4$-EtOH at a scan rate of 200 mV s^{-1} after reaction of amine modified GC with: FcCOOH (a, b), and $FcCH_2COOH$ (c, d). HBTU as activating agent (a, c), and $(COCl)_2$ as the activating agent (b, d). Black line: Boc-NH-Ar-GC; red line: Boc-NH-CH_2-Ar-GC; blue line: Fmoc-NH-Ar-GC; green line: Fmoc-NH-CH_2-Ar-GC; yellow line: bare GC.

Figure 6.5c shows CVs of $FcCH_2COOH$ immobilised on amine-modified and bare GC using HBTU as the activating agent. The response ($E_{½}$ ~0.33V) obtained at the deprotected multilayer Boc-NH-CH_2-Ar film after reaction with $FcCH_2COOH$ is assumed to be due to Fc coupled via an amide linkage to the film. The Fc responses of the other modified surfaces have similar $E_{½}$ values indicating the response originates mainly from amide linked Fc centres. There may be a small contribution from Fc immobilised directly on GC ($E_{½}$ ~0.44V). Comparison with the response of Fc immobilised on GC by reaction of $(COCl)_2$-activated $FcCH_2COOH$ (Figure 6.5d, yellow line) reveals that the $E_{½}$ values of the Fc immobilised in the two blank experiments are different ($E_{½}$ ~0.44 and ~0.40 V for the reactions activated by

HBTU and $(COCl)_2$ respectively). This is most likely due to two different layers being formed: covalently attached Fc for the reaction with $(COCl)_2$-activated $FcCH_2COOH$ and a physisorbed species after reaction with HBTU-activated $FcCH_2COOH$. Figure 6.5d shows that reaction of $(COCl)_2$-activated $FcCH_2COOH$ with the deprotected films prepared from Boc-NH-Ar, Boc-NH-CH_2-Ar, Fmoc-NH-Ar and Fmoc-NH-CH_2-Ar layers give Fc modified surfaces with $E_{½}$ values 20-40 mV positive of that for $FcCH_2COOH$ immobilised via an amide linkage ($E_{½}$ ~0.33V). The small spacing between the $E_{½}$ values for amide-linked and ester-linked (directly to the GC) $FcCH_2$ groups ($E_{½}$ ~0.33 V and ~0.40 V, respectively) prevents estimation of the contributions of two modes of attachment for $(COCl)_2$-activated $FcCH_2COOH$ reacted with deprotected Boc-NH-Ar, Boc-NH-CH_2-Ar, Fmoc-NH-Ar, and Fmoc-NH-CH_2-Ar layers, however considering the amount of Fc obtained from the blank experiments, direct reaction with GC is likely to be significant.

6.3.1.4.2 Estimation of surface concentrations of the amine layers and comparison of reactivity of amines

From the above discussion, estimation of surface concentrations of amine groups is not straight forward. It is assumed that surface concentrations obtained from reactions with acid derivatives by HBTU method give the most reliable estimates, albeit almost certainly underestimates. Considering the HBTU data, the amount of NP and two Fc groups attached to the deprotected amine films follow the order: Boc-NH-CH_2-Ar > Fmoc-NH-CH_2-Ar > Boc-NH-Ar ≥ Fmoc-NH-Ar. For all coupling reactions, the surface concentration of each electroactive group coupled to deprotected Boc-NH-CH_2-Ar-GC surface is at least twice that coupled to the deprotected Fmoc-NH-CH_2-Ar-GC surface. This supports the conclusion from film thickness measurements that the deprotected Boc-NH-CH_2-Ar film is a multilayer with

approximately two layers. Comparing the remaining layers, which all have thickness corresponding to a monolayer, coupling at the deprotected Fm-NH-CH_2-Ar film gives the highest concentration of surface immobilised NP and Fc groups. Considering that Fmoc-NH-CH_2-Ar-N_2^+ is the largest of the protected amine diazonium ions, it seems unlikely that its surface concentration is highest. Hence, it is assumed that the reactivity of the NH_2-CH_2-Ar film must be greater than that of the NH_2-Ar films. This is not surprising because aromatic amine is less nucleophilic compared to aliphatic amine.

Considering reactions at the deprotected Fmoc-NH-CH_2-Ar layer, the surface concentrations of NP groups are greater than Fc groups. For none of the groups (NP, Fc or $FcCH_2$) is the surface concentration close to that calculated for a close-packed monolayer ((12, 4.5, or 4.5) $\times 10^{-10}$ mol cm^{-2}, respectively),[46, 47] hence the size of the coupled group does not limit the amount coupled. The voltammetry of Fc groups gives a more reliable estimate of surface concentration than does voltammetry of NP films due to the irreversible reduction of NP moieties and the difficulties of baseline correction. Assuming that the coupling of $FcCH_2COOH$ to the deprotected Fmoc-NH-CH_2-Ar-GC surface proceeds near quantitatively using the HBTU method, the surface concentration of amine groups on this surface is approximately 1.4×10^{-10} mol cm^{-2}. Thus, assuming that the grafting efficiency of the other modifiers, Boc-NH-Ar-N_2^+ and Fmoc-NH-Ar-N_2^+, is the same, and considering that Boc-NH-Ar and Fmoc-NH-Ar are smaller than Fmoc-NH-CH_2-Ar, the surface concentration of amine moieties obtained after deprotection of Boc-NH-Ar and Fmoc-NH-Ar layers are assumed to be at least 1.4×10^{-10} mol cm^{-2}. The theoretical calculated maximum surface concentration of Fmoc-NH-CH_2-Ar on a flat surface is $\sim 1 \times 10^{-10}$ mol cm^{-2} (calculated based on the diameter of the protecting group using equation 5.1, Chapter 5), and a typical GC surface roughness is

2,[48, 49] confirming that the experimental concentration is consistent with a monolayer coverage.

6.3.1.4.3 Comparison of reactivity of Fc derivatives

The data in Table 6.2 shows that the surface concentration of FcCOOH is lower than the surface concentration of $FcCH_2COOH$ after coupling to the deprotected layers using HBTU as the activating agent but that the opposite is true when $(COCl)_2$ is used. The lower yield obtained for FcCOOH coupling using HBTU is likely to be because FcCOOH is sterically and electronically more difficult to activate compared to $FcCH_2COOH$. The lower yield obtained for $FcCH_2COOH$ than FcCOOH using $(COCl)_2$-activation may be explained by the relative stabilities of the Fc derivatives to activation by $(COCl)_2$. When activating the Fc derivatives with $(COCl)_2$ under reflux for 1 h, there was no observable colour change for FcCOOH, but the colour changed from yellow to greenish blue for $FcCH_2COOH$, indicating oxidation of Fc to Fc^+ for the $FcCH_2COOH$ moieties. This change in oxidation state may promote decomposition of the Fc derivative or lead to a lower yield for the subsequent coupling reaction, thereby giving a lower surface concentration for the $FcCH_2COOH$ than FcCOOH derivative when using the $(COCl)_2$ method. However, when reaction was undertaken directly with the bare GC using $(COCl)_2$-activation, $FcCH_2COOH$ gave a higher yield than FcCOOH. The reason for this is may be due to steric difficulties when coupling the shorter FcCOOH directly to the surface. A second factor may be the proximity of the Fc to the GC surface. A general observation in this work is that the shorter the link between a Fc and the GC surface, the less stable is the Fc groups.

6.3.1.5 Film characterisation by XPS

Due to the lower reactivity of the aromatic amine compared to the aliphatic amine towards amide bond coupling in the presence of HBTU, and the formation of multilayers from Boc-NH-CH_2-Ar-N_2^+ grafting, Fmoc-NH-CH_2-Ar-N_2^+ is the most suitable diazonium ion for forming amine terminated monolayers. Films formed by grafting Fmoc-NH-CH_2-Ar-N_2^+ were further investigated using XPS. Table 6.3 lists the atomic percentages of C, O, N and Fe at each stage of Fmoc-NH-CH_2-Ar-GC modification. Because four separate GC plates were used to prepare the samples and the oxygen content may differ between the plates, no significance can be attributed to differences in O content. It was noted that in two separate measurements of bare GC plates, a small amount of N was detected. A small amount of N on bare GC has also been reported by Menanteau and co-workers,[50] but the authors gave no explanation regarding its origin. Trace N presumably comes from impurities during the GC manufacturing process. After modification of the GC surface with Fmoc-NH-CH_2-Ar groups, an increase in N content is detected, which is in accordance with the expected structure of Fmoc-NH-CH_2-Ar. Moreover, it is proposed that grafting via reduction of aryldiazonium ions sometimes leads to formation of azo bond between the surface and the modifier,[50-52] and therefore this increase in N may come from azo linkages as well. After deprotection of Fmoc groups, the amount of N is lower than for the protected film but this small difference may be attributed to sample-to-sample variation. When the deprotected surface was coupled with $FcCH_2COOH$ in the presence of HBTU, the N content does not change significantly, as expected. However, the amount of Fe on the surface is very low (0.17%). Assuming that the Fe : N ratio (0.07) represents the reaction yield, this gives a yield of 7%. However, from the electrochemical measurements of Fc surface concentrations, the yield of reaction is close to 75% (from the ratio of the experimental value to the calculated theoretical value). Hence, the low Fe : N ratio in XPS is assumed to be due to factors such as lack of stability of the Fc

groups over the time between preparing the samples and collecting the XPS data (approximately 2 weeks), loss of Fe during XPS measurement or because the N content is substantially due to azo groups, not amines. On the latter point, if every aryl groups was attached to the surface via an azo link and thus had 3 Ns, the theoretical Fe : N ratio would be 0.33, much higher than that observed. Hence, the presence of azo groups cannot fully explain the low Fe : N ratio.

Table 6.3 Atomic percentages of C, O, N and Fc on modified GC surfaces obtained from XPS survey spectra.

Type of surfaces	%C	%O	%N	%Fe[a]
Bare GC	91.67	7.70	0.62	-
Fmoc-NH-CH_2-Ar-GC	87.25	9.63	3.12	-
NH_2-CH_2-Ar-GC	90.36	7.35	2.29	-
Fc-CH_2-CONH-CH_2-Ar-GC	89.14	8.21	2.48	0.17

[a]Calculated from Fe 2p peak at 708 eV

The high resolution N 1s spectra of the four samples are shown in Figure 6.6. The spectrum of bare GC shows only a single peak at 399.8 eV, while the signals at the modified GC samples can be fitted with a main peak at 400.2 eV and a low intensity peak at 402.5 eV. Peaks close to 400 eV have been assigned to atmospheric nitrogen, amine (–NH_2), azo (–N=N–), and amide (–NH–C=O),[30, 50, 53-63] while peaks close to 402 eV have been assigned to protonated amine (–NH_3^+).[59, 60] There are no significant differences between the modified surfaces, even though the protected and Fc coupled surfaces are expected to have amide nitrogen, while the deprotected surface has amine nitrogen. However, because azo, amine and amide N have very similar binding energies, it is very difficult to distinguish between them. Surprisingly, the peak at higher binding energy usually assigned to a protonated nitrogen species is observed on all of the modified surfaces. It is expected that the deprotected NH_2-

CH_2-Ar film may be protonated since it has a pK_a of ~ 9.3. However, as explained earlier (Section 6.3.2) amides usually do not have acid-base properties in water; pK_a of amide in DMSO is around 20.[40] The CVs of the ferrocyanide redox probe at Boc-NH-CH_2-Ar films show a behaviour that is consistent with the presence of a positively charged film (Section 6.3.1.2). Therefore, it is assumed that the amides are protonated in this condition. The binding energy of the two N of diazonium ions are reported to be 403.8 and 405.1 eV.[56, 62] There are no peaks at these binding energies on any of the modified surfaces indicating that no diazonium ions are adsorbed on the surface, as expected for covalent bonding between the surface and the aryl ring.

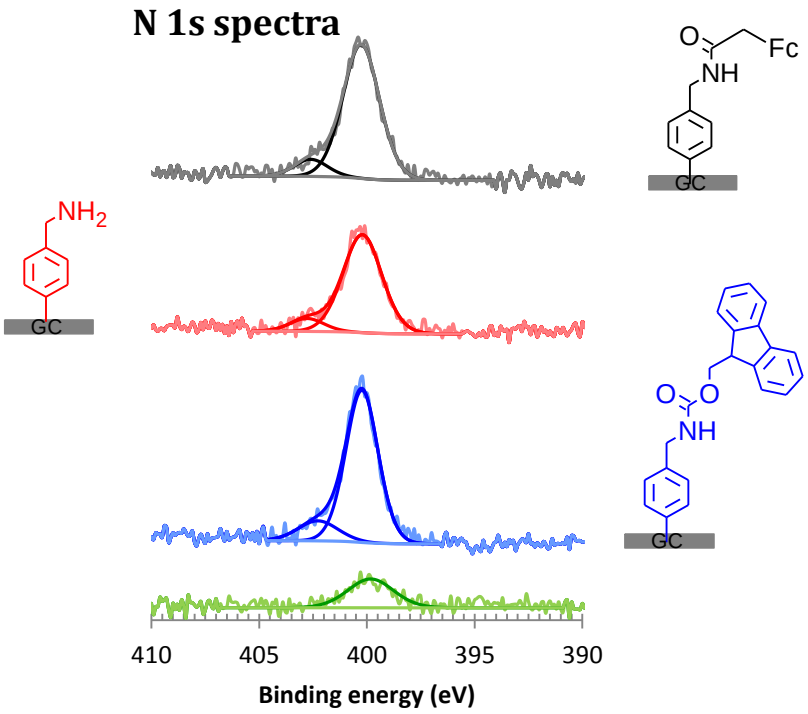

Figure 6.6 XPS N 1s core-level spectra of bare GC (green line), Fmoc-NH-CH_2-Ar-GC (blue line), NH_2-CH_2-Ar-GC (red line) and Fc-CH_2-CONH-CH_2-Ar-GC (black line).

6.3.2 Formation of mixed layers

Similar to the work described in Chapters 4 and 5, formation of binary mixed monolayers using [Fmoc-NH-CH_2-Ar-N_2]BF_4 was briefly investigated using two approaches: sequential grafting of two protected diazonium salts (Scheme 6.3) and grafting of protected diazonium

salts followed by removal of the protecting groups and filling of the void-space using direct reactions with the GC surface (Scheme 6.4).

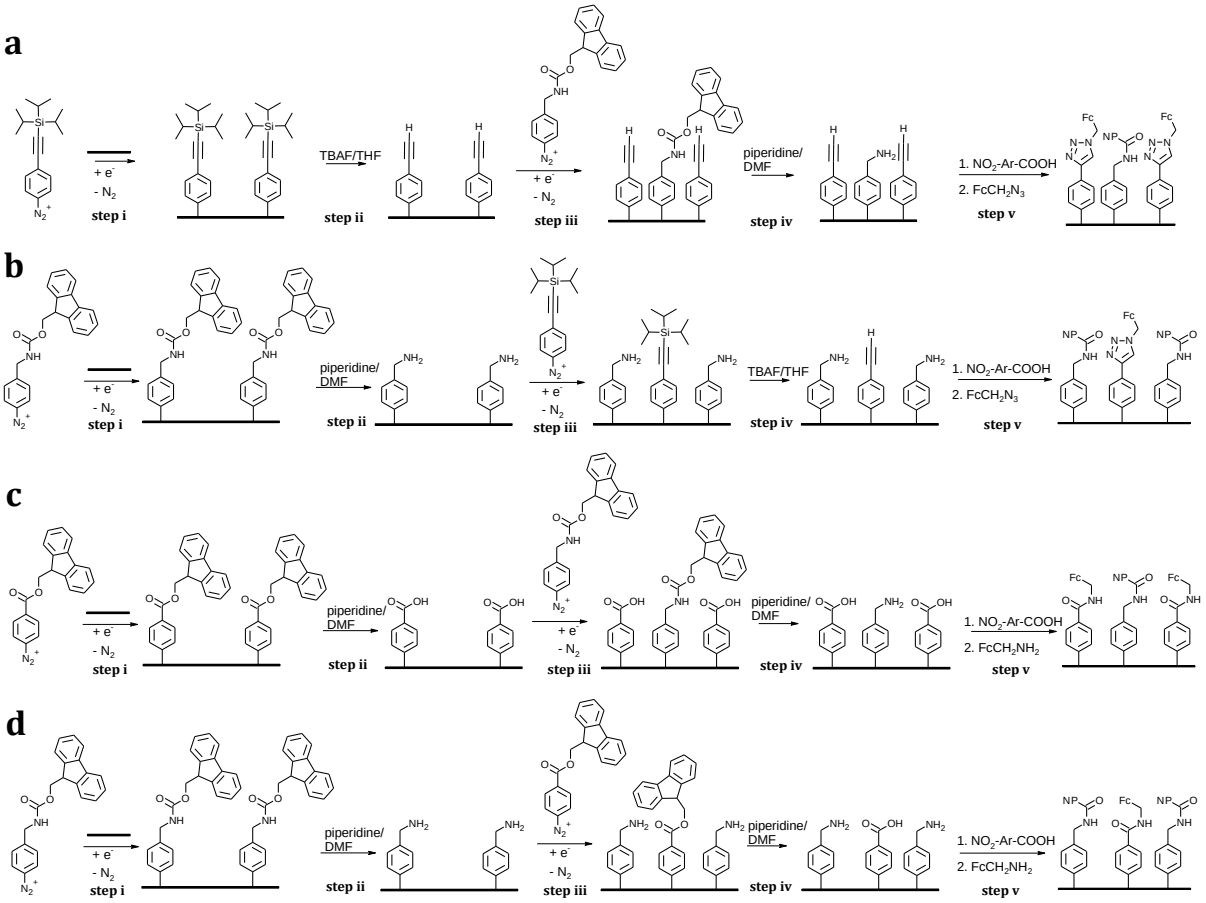

Scheme 6.3 Strategies for the preparation of mixed layers using sequential grafting of [Fmoc-NH-CH_2-ArN_2]BF_4, [TIPS-Eth-Ar-N_2]BF_4 and [Fm-COO-Ar-N_2]BF_4.

6.3.2.1 Formation of mixed layer via sequential electrografting

Scheme 6.3 shows the routes for the preparation of mixed layers by sequential grafting of two protected aryldiazonium salts. Mixed layers containing amine and ethynyl or carboxylic acid functionalities were prepared by using [Fmoc-NH-CH_2-Ar-N_2]BF_4 and [TIPS-Eth-Ar-N_2]BF_4 or [Fm-COO-Ar-N_2]BF_4, respectively (Scheme 6.3). The amounts of amine groups and ethynyl (or carboxylic acid) groups grafted on the GC surface were estimated by coupling electro-active NP and Fc to the amine and ethynyl (or carboxylic acid) moieties, respectively.

Amide coupling reactions of surface attached amine with NO_2-Ar-COOH using HBTU as the activating agent was carried out to immobilise electro-active NP groups followed by a click reaction of $FcCH_2N_3$ with the ethynyl groups or amide coupling reaction of $FcCH_2NH_2$ with the carboxylic acid groups in the presence of HBTU (Scheme 6.3, step v).

Table 6.4 lists the modification conditions used to form the mixed films and the corresponding surface concentrations of electro-active Fc and NP groups. Grafting a TIPS-Eth-Ar film, removing the TIPS protecting group then grafting [Fmoc-NH-CH_2-Ar-N_2]BF_4 to the voids in the layer and removal of the Fmoc group using piperidine gives a mixed layer of H-Eth-Ar and NH_2-CH_2-Ar groups (Scheme 6.3a). After coupling NP and Fc groups to the surface, the CVs shown in Figure 6.7 were obtained. From the CVs, surface concentrations of (0.2 ± 0.1) and $(1.6 \pm 0.1) \times 10^{-10}$ mol cm^{-2} were obtained for Fc and NP groups, respectively (Table 6.4, Experiment I). The NP concentration is slightly lower than the NP concentration obtained for a single-component NH_2-CH_2-Ar layer $(2.1 \pm 0.2) \times 10^{-10}$ mol cm^{-2} (Table 6.2), which may be because the H-Eth-Ar layer sterically hinders amide coupling at NH_2-CH_2-Ar groups. However, a very low concentration of Fc was observed on this mixed layer, indicating a low concentration of reactive H-Eth-Ar-groups. This may be because the spaces created by removal of the TIPS groups (diameter = 0.92 nm) are not large enough to allow grafting of the Fmoc-NH-CH_2-Ar-N_2^+ molecule (diameter = 1.4 nm) to the GC surface, and instead grafting may predominantly occur at the already grafted H-Eth-Ar groups. Similar observations were made for grafting of Fm-COO-Ar-N_2^+ groups on a H-Eth-Ar-GG surface (Chapter 5).

Table 6.4 Conditions for preparation of mixed films by the routes shown in Scheme 6.3 and the corresponding surface concentration of electro-active Fc and NP groups. (The surface concentrations are averaged values of two repeat experiments and the uncertainties indicate the range of values obtained.)

Expt.	Route	Γ_{Fc} (10^{-10} mol cm^{-2})	Γ_{NP} (10^{-10} mol cm^{-2})
I	6.3a	0.2 ± 0.1	1.6 ± 0.1
II	6.3b	1.6 ± 0.1	0.9 ± 0.1
III	6.3c	2.4 ± 0.3	1.1 ± 0.1
IV	6.3d	2.0 ± 0.1	0.9 ± 0.1

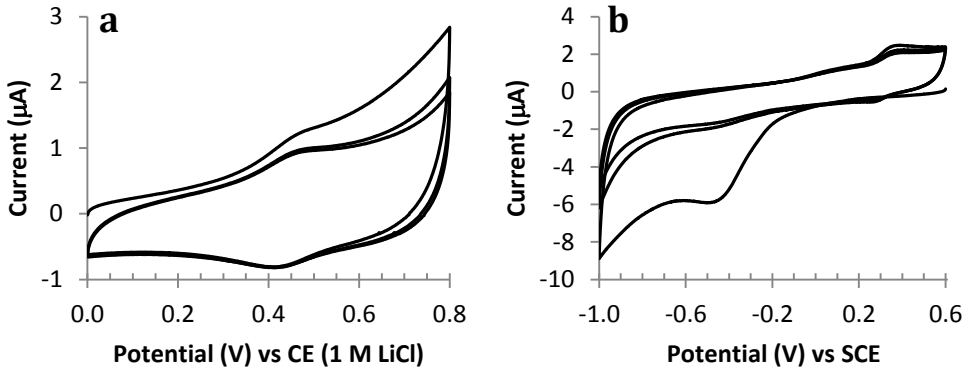

Figure 6.7 Repeat CVs of a GC electrode modified by route 6.3a. Scans were carried out in: a) 0.1 M $LiClO_4$-EtOH at a scan rate of 200 mV s^{-1} and b) 0.1 M H_2SO_4 at a scan rate of 100 mV s^{-1}.

A mixed layer consisting of NH_2-CH_2-Ar and H-Eth-Ar groups can also be prepared by the alternative procedure of grafting the bigger [Fmoc-NH-CH_2-Ar-N_2]BF_4 first followed by the removal of Fmoc groups and grafting of [TIPS-Eth-Ar-N_2]BF_4 (Scheme 6.3b). After coupling Fc and NP groups using the same method as above, this strategy gives Fc and NP surface concentrations of (1.6 ± 0.1) and (0.9 ± 0.1) × 10^{-10} mol cm^{-2}, respectively (Figure 6.8 and Table 6.4, Experiment II). A lower concentration of NP than Fc groups was obtained, and the concentration of NP groups is only half that of a single-component layer. This may indicate that grafting of TIPS-Eth-Ar-N_2^+ occurs at the already grafted NH_2-CH_2-Ar groups, and therefore the subsequent coupling of NO_2-Ar-COOH groups is limited due to steric hindrance

imposed by the H-Eth-Ar groups. The concentration of Fc groups clicked to the mixed layer was also low compared to that for Fc clicked to single-component H-Eth-Ar-GC surfaces ((2.4 ± 0.3) × 10^{-10} mol cm^{-2}, Chapter 4). The low Fc concentration may be due to steric hindrance of the click reaction by the coupled NP groups. Similar results were noted for the mixed layer of H-COO-Ar and H-Eth-Ar groups (Chapter 5, Scheme 5.3c).

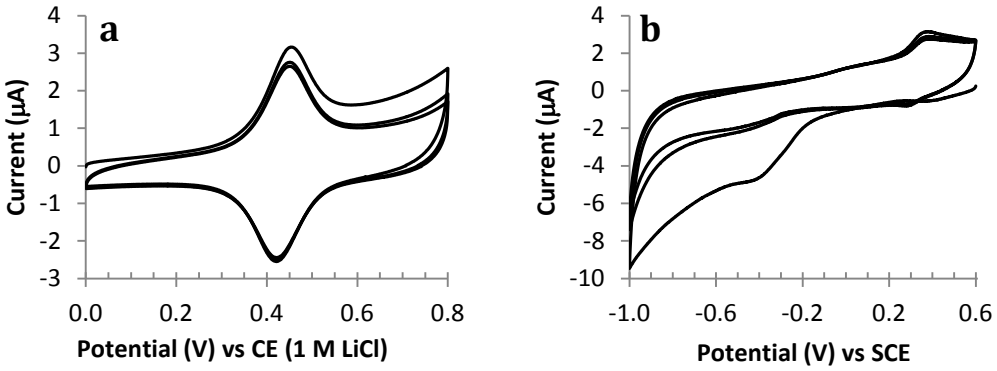

Figure 6.8 Repeat CVs of a GC electrode modified by route 6.3b. Scans were carried out in: a) 0.1 M $LiClO_4$-EtOH at a scan rate of 200 mV s^{-1} and b) 0.1 M H_2SO_4 at a scan rate of 100 mV s^{-1}.

A binary mixed layer consisting of H-COO-Ar and NH_2-CH_2-Ar groups can be prepared using [Fm-COO-Ar-N_2]BF_4 and [Fmoc-NH_2-CH_2-Ar-N_2]BF_4 as shown in Schemes 6.3c and 6.3d. Grafting of Fm-COO-Ar-N_2^+ followed by the removal of the Fm group and subsequent grafting of Fmoc-NH_2-CH_2-Ar-N_2^+ and removal of the Fmoc group resulted in a layer containing H-COO-Ar and NH_2-CH_2-Ar groups. Coupling of NO_2-Ar-COOH to the NH_2-CH_2-Ar moiety in the presence of HBTU followed by coupling of $FcCH_2NH_2$ to H-COO-Ar groups (using HBTU) resulted in a surface with immobilised NP and Fc groups. Figure 6.9 shows the CVs of the surface coupled Fc and NP groups obtained using the route shown in Scheme 6.3c. From the area under the CV peaks and the number of electrons involved in each redox process, surface concentrations of (2.4 ± 0.3) and (1.1 ± 0.1) × 10^{-10} mol cm^{-2} were estimated for Fc and NP, respectively. The amount of Fc attached to the H-COO-Ar groups of the mixed layer is similar to that attached to a single-component H-COO-Ar layer ((2.8 ±

0.7) × 10^{-10} mol cm^{-2}, Chapter 5), indicating that the reactivity of H-COO-Ar is not affected by the second film component. On the other hand, the amount of NP groups attached to the mixed film is lower than the amount of NP attached to a single-component NH_2-CH_2-Ar film ((2.1 ± 0.2) × 10^{-10} mol cm^{-2}, Table 6.2). The lower amount of NP in the mixed layer is probably due to the steric hindrance for the coupling reaction created by the H-COO-Ar groups, similar to that proposed for the mixed layer of H-Eth-Ar and NH_2-CH_2-Ar prepared by route 6.3a above. The lower surface concentration of NP groups immobilised by the route shown in Scheme 6.3c than Scheme 6.3a supports the earlier suggestion that in route 6.3a most of the NH_2-CH_2-Ar groups were actually grafted on the already grafted H-Eth-Ar groups, thus avoiding problems of steric crowding.

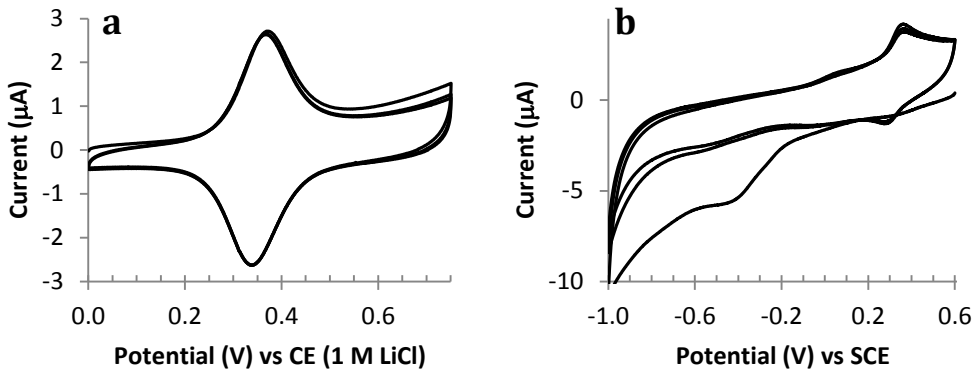

Figure 6.9 Repeat CVs of a GC electrode modified by route 6.3c. Scans were carried out in: a) 0.1 M $LiClO_4$-EtOH at a scan rate of 200 mV s^{-1} and b) 0.1 M H_2SO_4 at a scan rate of 100 mV s^{-1}.

Table 6.4, Experiment IV describes the results of preparation of mixed layers using the route shown in Scheme 6.3d. In this case, Fmoc-NH-CH_2-Ar-N_2^+ was grafted first followed by the removal of the Fmoc groups and then Fm-COO-Ar-N_2^+ was grafted. After removal of the Fmoc groups, coupling reactions similar to route 6.3c above were carried out. Figure 6.10 shows the CVs of immobilised Fc and NP groups obtained by route 6.3d. From the CVs, the surface concentrations of Fc and NP groups were estimated to be (2.0 ± 0.1) and (0.9 ± 0.1) × 10^{-10} mol cm^{-2}, respectively (Table 6.4, Experiment IV). The Fc concentration was similar to

that obtained using the previous route (Experiment III), but the NP concentration was lower. As suggested for the H-Eth-Ar and NH_2-CH_2-Ar mixed layer prepared by the route shown in Scheme 6.3b, the low NP concentration may be due to blocking of NH_2-CH_2-Ar groups by grafting of Fmoc-COO-Ar groups on top of the layer, or may be due to a low yield for the coupling reaction between NO_2-Ar-COOH and NH_2-CH_2-Ar groups as a result of steric hindrance.

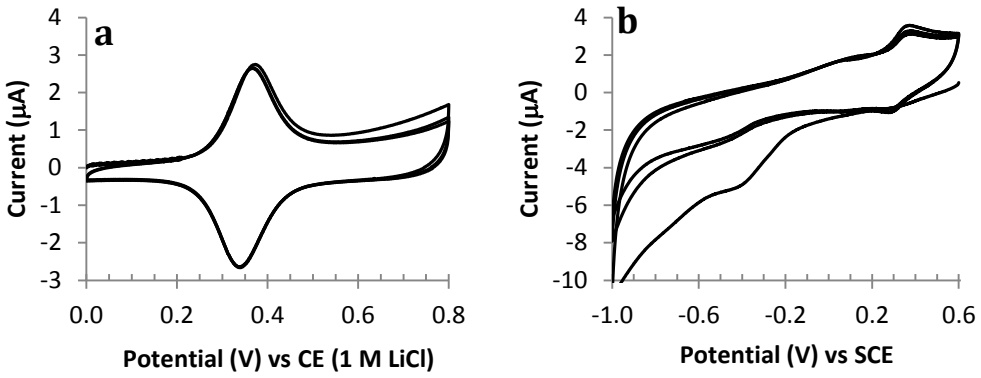

Figure 6.10 Repeat CVs of a GC electrode modified by route 6.3d. Scans were carried out in: a) 0.1 M $LiClO_4$-EtOH at a scan rate of 200 mV s^{-1} and b) 0.1 M H_2SO_4 at a scan rate of 100 mV s^{-1}.

It is clear that for sequential grafting using aryldiazonium salts, it is not possible to completely exclude the possibility of the second modifier grafting on the already grafted layer. Therefore, the preparation of binary monolayers using direct reaction of bare GC with amine or carboxylic acid derivative to immobilise the second modifier was briefly investigated. This is described in the following section.

6.3.2.2 Formation of mixed monolayers via filling up void spaces using reaction with bare GC

As described in Chapter 4, another strategy to prepare a mixed monolayer is to react the bare GC, created by the removal of the protecting groups, directly with amine or carboxylic acid derivatives (Scheme 6.4). An advantage of this procedure is the reaction of the second modifier is only possible with the bare GC surface and not with the already grafted layer, and

therefore multilayer formation is avoided. After grafting of Fmoc-NH-CH_2-Ar-N_2^+ followed by deprotection of Fmoc groups, a NH_2-CH_2-Ar layer was obtained. NP or Fc groups were then coupled to the layer using the HBTU coupling method. The resulting NP modified surface was then reacted with $FcCH_2NH_2$ in the presence of HBTU to obtain a surface consisting of a mixture of NP and Fc functionalities (Scheme 6.4a), while for the Fc coupled surface, a reaction was carried out with $(COCl)_2$-activated FcCOOH to obtain a surface containing two Fc groups with different redox potentials (Scheme 6.4b).

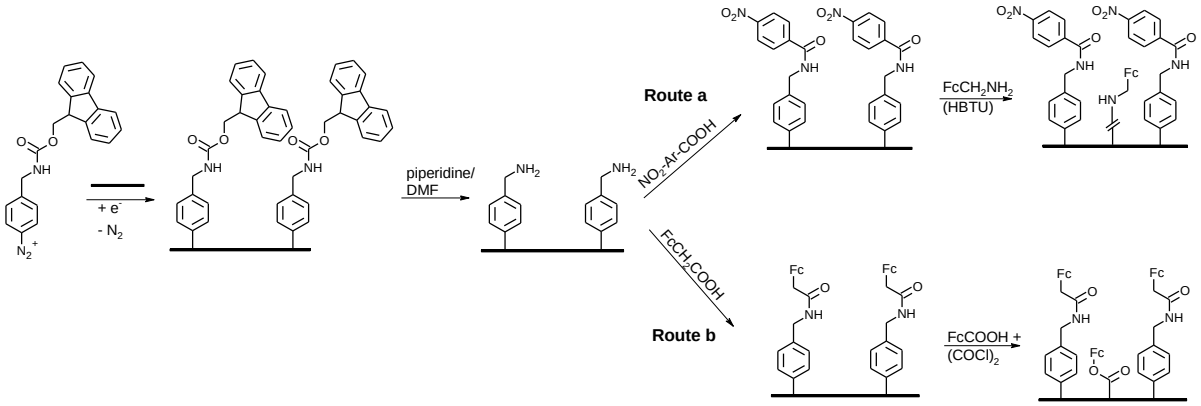

Scheme 6.4 Strategy for the preparation of mixed monolayer films from a monolayer NH_2-CH_2-Ar-GC surface using the filling-in approach; a) NO_2-Ar-COOH was first coupled to the NH_2-CH_2-Ar-GC surface using the HBTU method followed by reaction of GC with $FcCH_2NH_2$ in the presence of HBTU; b) $FcCH_2COOH$ was coupled to the NH_2-CH_2-Ar-GC surface using the HBTU method prior to reaction with $(COCl)_2$-activated FcCOOH.

Table 6.5 summarises data for the mixed films prepared using the routes shown in Scheme 6.4. As shown in Figure 6.11, the mixed film prepared by the route outlined in Scheme 6.4a exhibits well-defined CVs for both redox centres, with estimated surface concentrations of (0.7 ± 0.1) and $(1.4 \pm 0.1) \times 10^{-10}$ mol cm^{-2} for Fc and NP groups, respectively (Table 6.4, Experiment I). Interestingly, the concentration of NP groups is lower than for NP coupled to single-component NH_2-CH_2-Ar films $(2.1 \pm 0.2) \times 10^{-10}$ mol cm^{-2} (Table 6.1), even though the preparation steps are the same. This is not understood as the yield of the coupling reaction

is expected to be same as for the single component films, and for a monolayer all NP groups should be electroactive. A lower Fc concentration compared to that for a single component $FcCH_2NH_2$ film coupled directly to GC ($(1.3 \pm 0.2) \times 10^{-10}$ mol cm^{-2}, Chapter 3) was obtained from this mixed layer as well. This may be because the bare GC surface available for the further coupling reaction is sterically hindered after coupling of NP groups onto NH_2-CH_2-Ar groups.

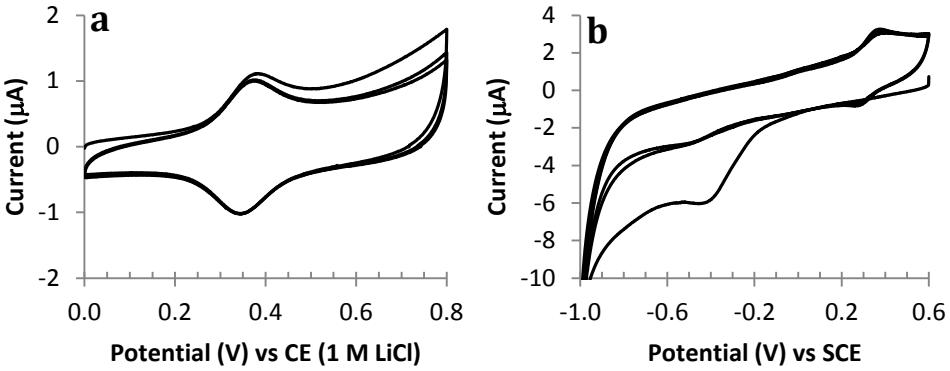

Figure 6.11 Repeat CVs of a GC electrode modified by route 6.4a. Scans were carried out in: a) 0.1 M $LiClO_4$-EtOH at a scan rate of 200 mV s^{-1} and b) 0.1 M H_2SO_4 at a scan rate of 100 mV s^{-1}.

Table 6.5 Conditions for preparation of mixed films by routes shown in Scheme 6.4 and the corresponding surface concentrations of electro-active Fc and NP groups. (The surface concentrations are average values of two repeat experiments and the uncertainties indicate the range of values obtained.)

Expt.	Route	Γ_{Fc} (10^{-10} mol cm^{-2})	Γ_{NP} (10^{-10} mol cm^{-2})
I	6.4a	0.7 ± 0.1	1.4 ± 0.1
II	6.4b	1.0 ± 0.1[a]	N/A
		3.2 ± 0.1[b]	

[a]Reaction with $FcCH_2COOH$

[b]Reaction with $(COCl)_2$-activated FcCOOH

Table 6.5 Experiment II describes experiments similar to those above but in this procedure $FcCH_2COOH$ was first coupled to the NH_2-CH_2-Ar groups using the HBTU method, followed by reaction of GC with $(COCl)_2$-activated FcCOOH (Scheme 6.4b). Figure 6.12

shows the CVs of two sequential Fc/Fc^+ redox couples. The first Fc/Fc^+ couple at $E_{½}$ = 0.36 V arises from the Fc coupled to the NH_2-CH_2-Ar group on the surface, while the second Fc/Fc^+ couple at $E_{½}$ = 0.65 V arises from the Fc coupled directly to the GC surface. The peak area of each Fc/Fc^+ redox couple was integrated by curve fitting the voltammetric peak (of the second scan) using Linkfit software[64] (Chapter 2). The area of each peak was calculated to obtain the corresponding surface concentration of (1.0 ± 0.1) and (3.2 ± 0.1) × 10^{-10} mol cm^{-2} for Fc coupled to NH_2-CH_2-Ar groups and bare GC, respectively. Clearly, the concentration of $(COCl)_2$-activated FcCOOH groups reacted to the modified electrode (Scheme 6.4b) is significantly greater than when the reaction was carried out at bare GC ((1.6 ± 0.2) × 10^{-10} mol cm^{-2}, Table 6.2). Moreover, the concentration of Fc coupled to NH_2-CH_2-Ar groups is lower than coupled to the single-component NH_2-CH_2-Ar films (Table 6.2). A tentative explanation for this difference may be that coupling $FcCH_2COOH$ to NH_2-CH_2-Ar groups with HBTU activation did not result in a quantitative yield, and when in the second step, $(COCl)_2$-activated FcCOOH was reacted with the modified surface, $(COCl)_2$-activated FcCOOH not only reacted with the bare GC surface, but also with the unreacted NH_2-CH_2-Ar groups. However, that explanation is not consistent with the results obtained when NH_2-CH_2-Ar films were reacted with $(COCl)_2$-activated FcCOOH. Only (2.5 ± 0.2) × 10^{-10} mol cm^{-2} of Fc groups was found immobilised to the surface in those experiments (Table 6.2). The total surface concentration of ~4.2 × 10^{-10} mol cm^{-2} obtained from the mixed layer prepared by route of Scheme 6.4b is clearly higher than for the single-component reactions, where reaction on bare GC is also expected. The reason for the high surface concentration of Fc groups obtained by the route shown in Scheme 6.4b is not understood but it may arise from errors determining peak areas from the CVs. This is problematic for the CVs shown in Figure

6.12 due to the small potential separation of the two Fc couples. This makes background correction difficult and introduces uncertainty in curve-fitting the voltammetric peaks.

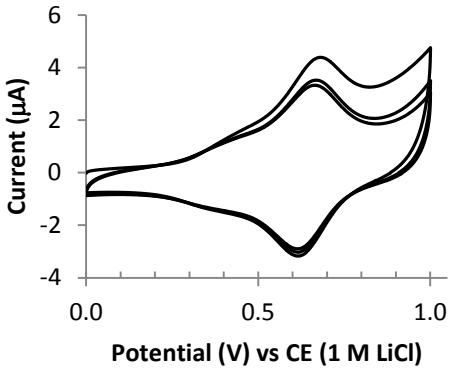

Figure 6.12 Three consecutive cycles obtained in 0.1 M $LiClO_4$-EtOH of GC electrode modified by route 6.4b. Scan rate = 200 mV s^{-1}.

6.3.3 Mixed layers for O_2 reduction

To briefly investigate the use of the mixed layers for electrocatalysis, the O_2 reduction reaction was chosen as an example. Depending on several factors (e.g. electrode material and experimental conditions) the O_2 reduction reaction proceeds by a two-electron pathway to H_2O_2 or by a direct four-electron pathway to H_2O.[65] When reduction of O_2 is catalysed by AQ modified electrodes in aqueous media, the reaction proceeds through the two-electron pathway to form H_2O_2 (Scheme 6.5).[66-68] The aim of the study was to investigate whether the environment of the AQ centres influences the efficiency of the catalytic reaction. Hence, mixed layers were prepared incorporating AQ centres and a variety of other non-electroactive modifiers.

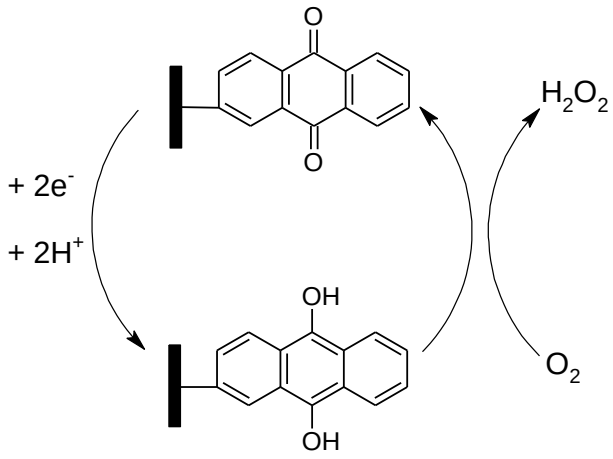

Scheme 6.5 Electrochemical reduction of O_2 to H_2O_2 catalysed by AQ.

To examine O_2 reduction at single-component AQ layers, AQ was immobilised onto a GC surface via a monolayer of H-Eth groups (Scheme 6.6). Figure 6.13 shows CVs of AQ-modified GC obtained in 0.1 M PB, pH 7.1 in the absence of O_2. The broad and ill-defined redox peaks observed for the AQ-modified electrode (rather than the single two-electron process seen in solution) may result from the triazole substituent or from the effect of the film environment on the pH at the surface. Similar voltammetry has previously been reported for surface immobilised AQ groups obtained in pH 7 PB.[69] From the average cathodic and anodic peak areas, the surface concentration of AQ was found to be $(3.2 \pm 0.5) \times 10^{-10}$ mol cm^{-2} (Table 6.6, Experiment I). The theoretical calculated maximum surface concentration for a densely packed monolayer of AQ on a planar surface is 3.5×10^{-10} mol cm^{-2}.[70] Considering the surface roughness of GC and the loosely spaced H-Eth groups, the experimental AQ concentration is within monolayer coverage.

Interestingly, the surface concentration of Fc groups coupled to a monolayer of H-Eth groups was found to be $(2.4 \pm 0.3) \times 10^{-10}$ mol cm^{-2} (Chapter 4). Considering the experimental uncertainty, the concentration of AQ is probably somewhat higher than the concentration of Fc, which may indicate a lower yield for the 'click' reaction between H-Eth groups and $FcCH_2N_3$ than between H-Eth and AQ-N_3. However, as mentioned in Chapter 4, the

measured surface concentration of Fc is dependent on the solvent and electrolyte used. The surface concentration measured in $LiClO_4$-EtOH was assumed to represent the actual Fc concentration, but this may not be the case. This may account for the lower surface concentration measured for Fc than AQ. However, considering the experimental error, the surface concentrations of AQ and Fc groups are similar.

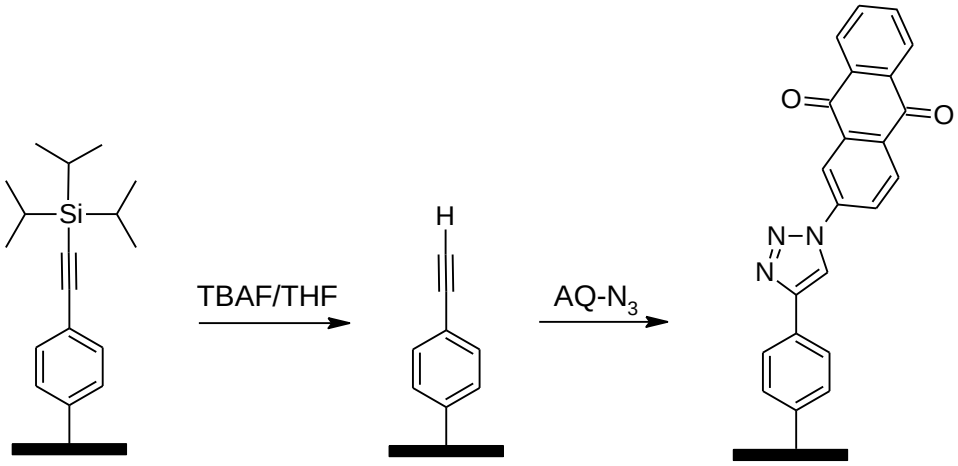

Scheme 6.6 Attachment of AQ-N_3 via click chemistry with H-Eth monolayer.

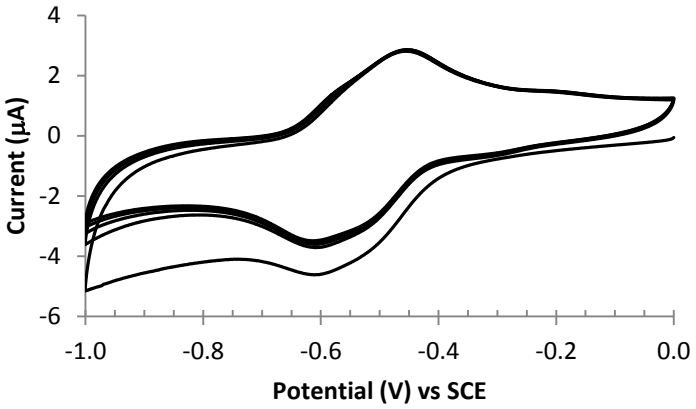

Figure 6.13 Five consecutive cycles obtained in 0.1 M PB, pH 7.1 of GC electrode modified with AQ groups. Scan rate = 100 mV s^{-1}.

To investigate the catalytic activity of AQ towards O_2 reduction, AQ modified GC was scanned in 0.1 M PB, pH 7.1, saturated with O_2 gas. Figure 6.14 shows CVs for the reduction of O_2 at bare GC (black line), and H-Eth (blue line), and AQ (red line) modified GC electrodes. The CVs show an irreversible oxygen reduction peak at -0.63 V, -0.66 V, and

-0.48 V for bare GC, and H-Eth and AQ modified GC, respectively. The less negative reduction potential and the larger peak current obtained at AQ modified GC than at the non-AQ modified electrodes indicates the electrocatalytic ability of AQ towards O_2 reduction.

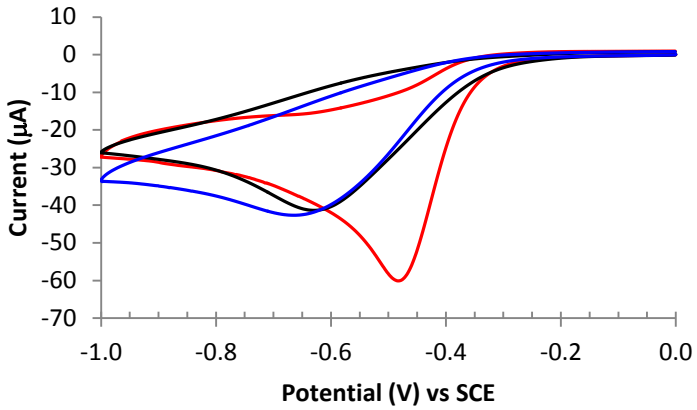

Figure 6.14 CVs of bare GC (black line), H-Eth monolayer (blue line), and AQ modified GC obtained in 0.1 M PB, pH 7.1 saturated with O_2 at scan rate of 100 mV s^{-1}.

To study the effect of mixed layers on the O_2 reduction reaction, three general strategies for preparation of mixed layers were investigated as shown in Scheme 6.7. Figure 6.15 shows CVs of the modified surfaces obtained in 0.1 M PB, pH 7.1 in the absence of O_2. Table 6.6 lists the measured AQ surface concentration for each of the modified surfaces. As shown in Table 6.6 and Figure 6.15, the measured concentrations of AQ groups in the mixed layers prepared by sequential grafting of two aryldiazonium salts (routes 6.7a and 6.7b, Experiments II – VIII) are smaller than for the single component layer (Experiment I). This is not surprising because for the mixed layers, the TIPS-Eth-Ar groups were grafted to a surface with the other component already immobilised and thus a lower amount of H-Eth-Ar tethers is expected to be grafted. Note that this result is different to that found for Fc clicked to single component and mixed films containing H-Eth-Ar groups (Section 5.3.2, Chapter 5). As discussed in Chapter 5, the observation of equal Fc surface concentration in single component and mixed films was unexpected and could not be explained.

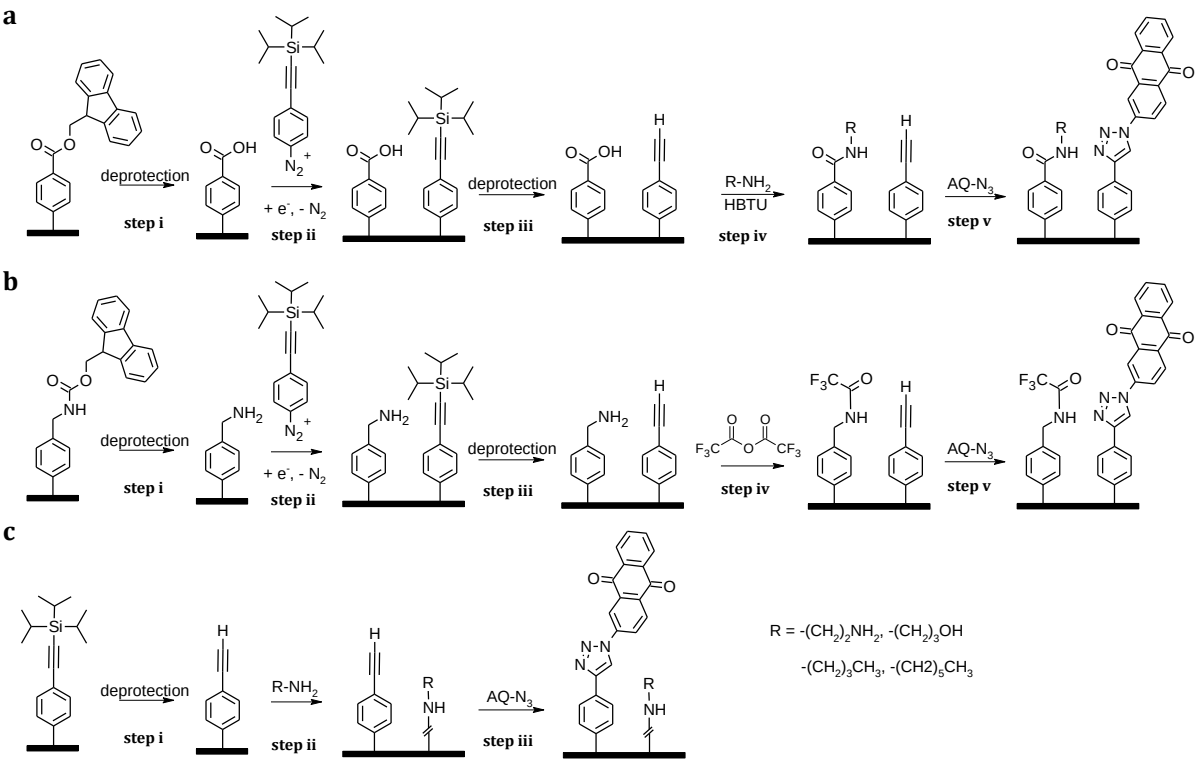

Scheme 6.7 Strategies for the preparation of mixed monolayer films for the O_2 reduction study.

Considering the range of AQ surface concentrations for the mixed layers, it appears that there are additional factors influencing the measured concentrations. Two possible explanations can be considered. First, there may be variable surface concentrations of AQ on the surface due to variable yields for the click reaction. Second, it is possible that the second component affects the electroactivity of the AQ, and therefore the measured surface concentrations of AQ are not the actual surface concentrations.

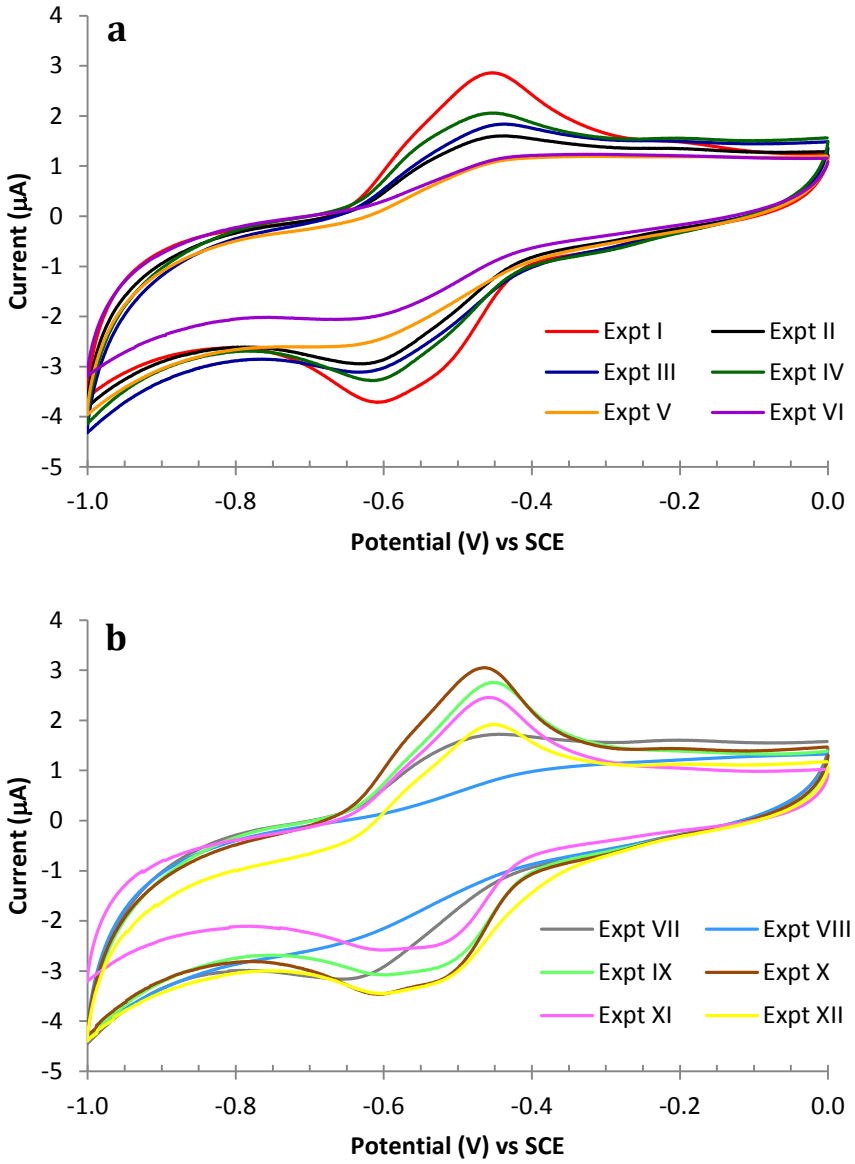

Figure 6.15 CVs obtained at a scan rate of 100 mV s^{-1} in 0.1 M PB, pH 7.1 in the absence of O_2. GCs were modified by the route shown in: a) Schemes 6.6 and 6.7a; b) Schemes 6.7b and 6.7c. Experiment numbers refer to those listed in Table 6.6.

Table 6.6 Conditions for preparation of mixed films by routes shown in Scheme 6.7 and the corresponding surface concentrations of AQ groups and the O_2 reduction peak potential (Scan rate = 100 mV s^{-1}).

Expt.	Route	Modified Surfaces	Γ_{AQ} (10^{-10} mol cm^{-2})	n^a	O_2 $E_{p,c}$ (V) vs SCE
I	6.6	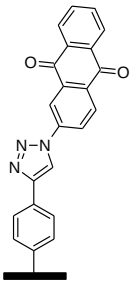	3.2 ± 0.5	4	-0.48 ± 0.02
II	6.7a (without step iv)	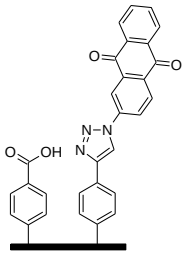	2.3 ± 0.3	2	-0.55 ± 0.02
III	6.7a	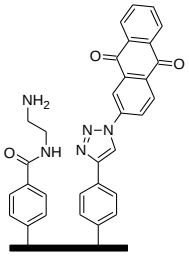	2.3 ± 0.1	2	-0.51 ± 0.01
IV	6.7a	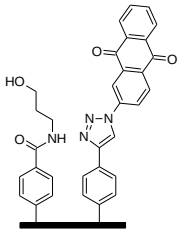	2.4 ± 0.1	2	-0.53 ± 0.01
V	6.7a	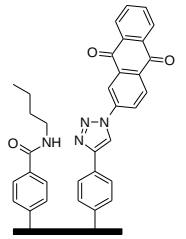	1.1 ± 0.2	2	-0.54 ± 0.01
VI	6.7a	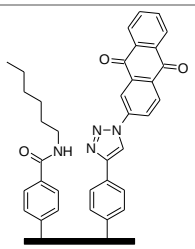	0.9 ± 0.3	4	-0.54 ± 0.02

VII	6.7b (without step iv)	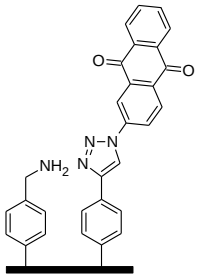	2.1 ± 0.1	2	-0.53 ± 0.01
VIII	6.7b	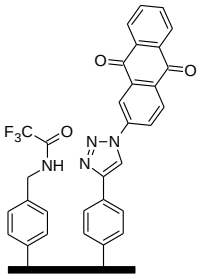	0.7 ± 0.1	2	-0.56 ± 0.01
IX	6.7c	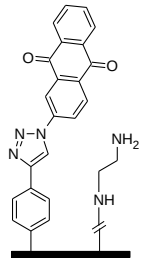	2.8 ± 0.1	2	-0.46 ± 0.01
X	6.7c	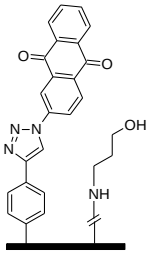	3.1 ± 0.2	2	-0.46 ± 0.01
XI	6.7c	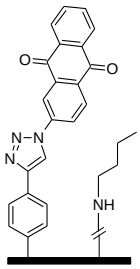	2.6 ± 0.1	2	-0.47 ± 0.01
XII	6.7c	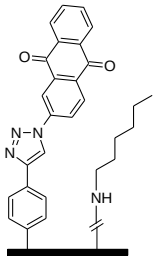	2.5 ± 0.1	2	-0.46 ± 0.01

[a] *n* is the number of samples analysed

To test whether the electroactivity of the AQ groups is influenced by their environment on the surface, the electrochemistry of the single component layer and the mixed layer of

Experiment VI, Table 6.6, were examined in 0.1 M $TBABF_4$-DCM. It was expected that if the film environment was a major factor, the measured AQ surface concentration values would depend on the solvent and electrolyte (as found for immobilised Fc groups, Section 4.3.1, Chapter 4) and that the ratio of measured AQ surface concentrations in the single component film ($\Gamma_{AQ(single)}$) to that in the mixed films ($\Gamma_{AQ(mixed)}$) would be different in PB and in DCM, due to different solvation effects. However, for each layer, the AQ surface concentration was very similar in the two electrolyte solutions and the The $\Gamma_{AQ(single)}$: $\Gamma_{AQ(mixed)}$ ratios were 1.8 and 2.0, in PB and DCM, respectively. These results suggest that the film environment is not influencing the electroactivity of the AQ centres.

Considering the alternative explanation for the variable AQ surface concentrations in the mixed layers, i.e. that there are variable yields for the click reaction in the mixed layers, the data in Table 6.6 show that when a hydrophobic moiety is coupled to the second film component (experiments V, VI and VIII) the measured AQ surface concentration is significantly lower than when the coupled moiety has a hydrophilic terminal group (Experiments III and IV). This suggests that when the H-Eth-Ar groups are in a hydrophobic environment, the yield of the click reaction is decreased compared to that for a hydrophilic environment. This may be due to the better access of hydrophilic azide groups to the H-Eth-Ar groups at the more hydrophilic surface, giving a higher yield for the click reaction. For surface prepared by route 6.7c (Experiments IX – XII), the AQ surface concentrations are all higher than those for mixed layers prepared by routes 6.7a and 6.7b. This is expected because in route 6.7c, the TIPS-Eth-Ar modifier is grafted in the first modification step. However, there is still variability in the AQ surface concentrations, although it is less significant than for surfaces prepared by routes 6.7a and 6.7b. Higher surface concentration of AQ is obtained for the mixed layers with second components with hydrophilic terminal groups (Experiments

IX and X), and for these surfaces the AQ surface concentrations are the same as for the single component layer.

Figure 6.16 shows CVs obtained in O_2 saturated PB at the single component AQ layer and all mixed layers. The peak potentials of O_2 reduction are listed in Table 6.6. As seen from Figure 6.16 and Table 6.6, the O_2 reduction peak potential generally follows the trend in $E_{p,c}$ for the first peak (shoulder) for AQ reduction. This is expected for an electrocatalytic reaction.

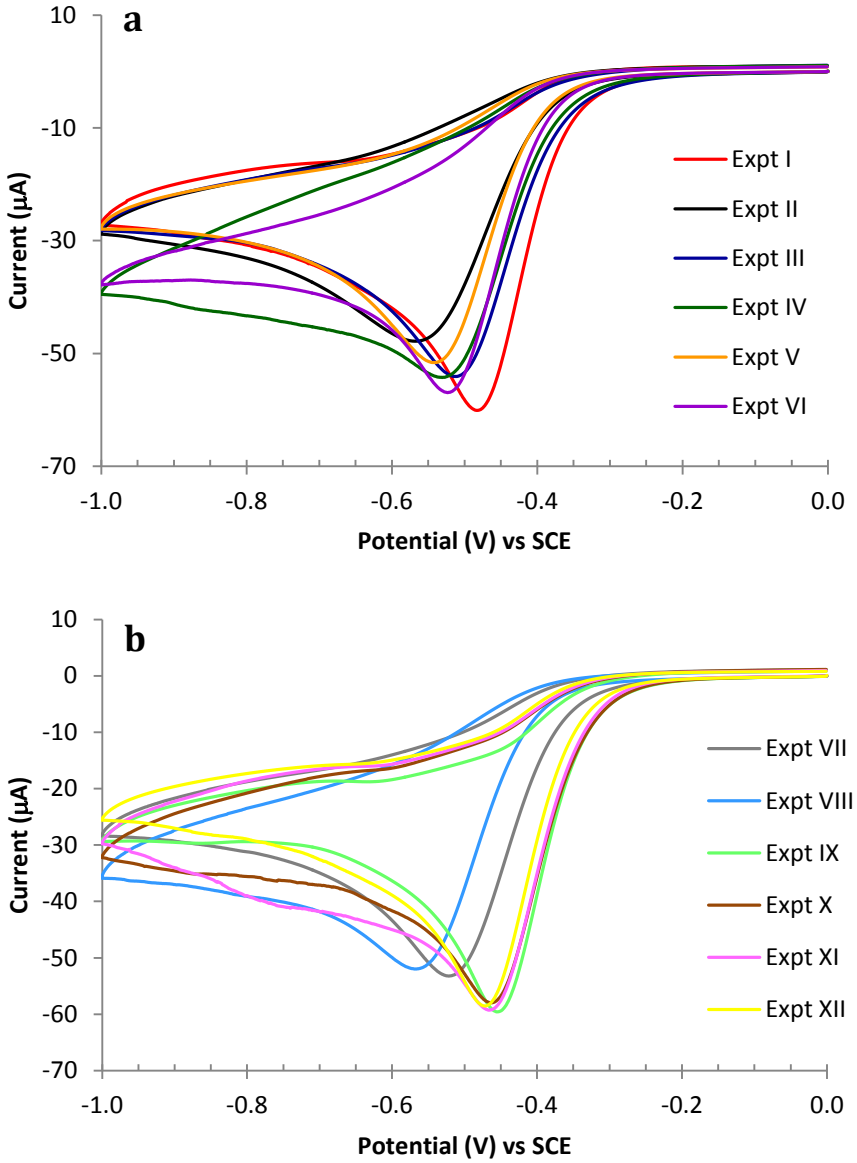

Figure 6.16 CVs obtained at a scan rate of 100 mV s^{-1} in O_2-saturated 0.1 M PB, pH 7.1. GCs were modified with route shown in: a) Schemes 6.6 and 6.7a; b) Schemes 6.7b and 6.7c. Experiment numbers refer to those listed in Table 6.6.

Considering the O_2 reduction peak current in relation to the measured AQ surface concentration (Figure 6.17), it is clear that when $\Gamma_{AQ(mixed)} \approx \Gamma_{AQ(single)}$ (Experiments IX – XII) the peak currents are relatively high and similar. There is no discernible influence of the second film component on the activity of the AQ centres for catalysis of O_2 reduction. On the other hand, when $\Gamma_{AQ(mixed)} < \Gamma_{AQ(single)}$ (Experiments II – VIII), the O_2 reduction peak currents obtained at the mixed layers are significantly lower than those obtained at the single component film. The relationship between the peak current for O_2 reduction and Γ_{AQ}, normalised to that for the single component layer, is shown in Figure 6.18.

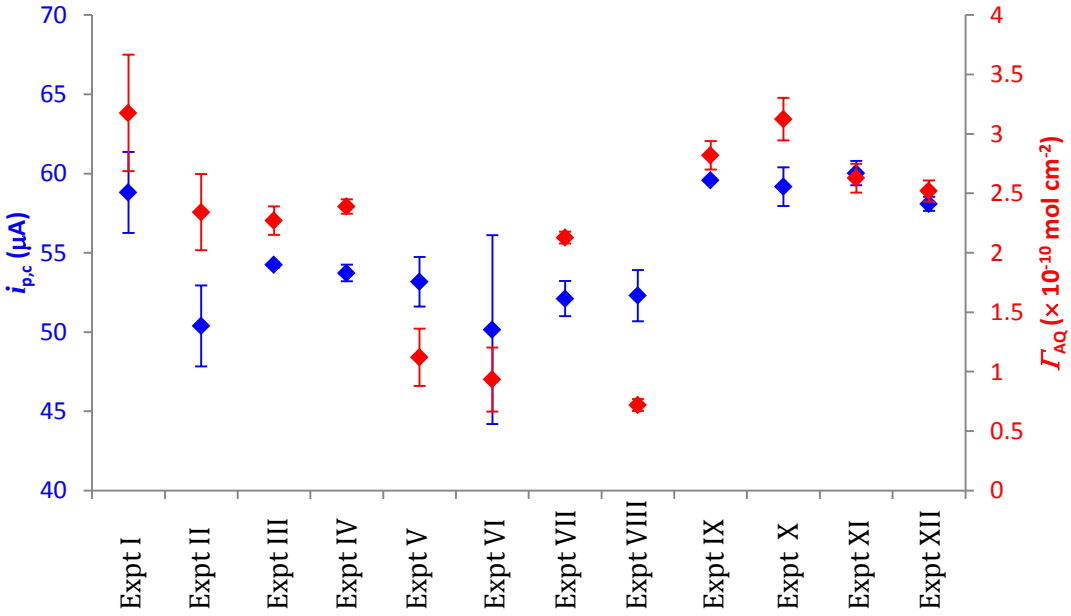

Figure 6.17 Plot of average O_2 reduction current (blue points) and the average surface concentration of AQ (red points) on each of the modified surfaces (Table 6.6).

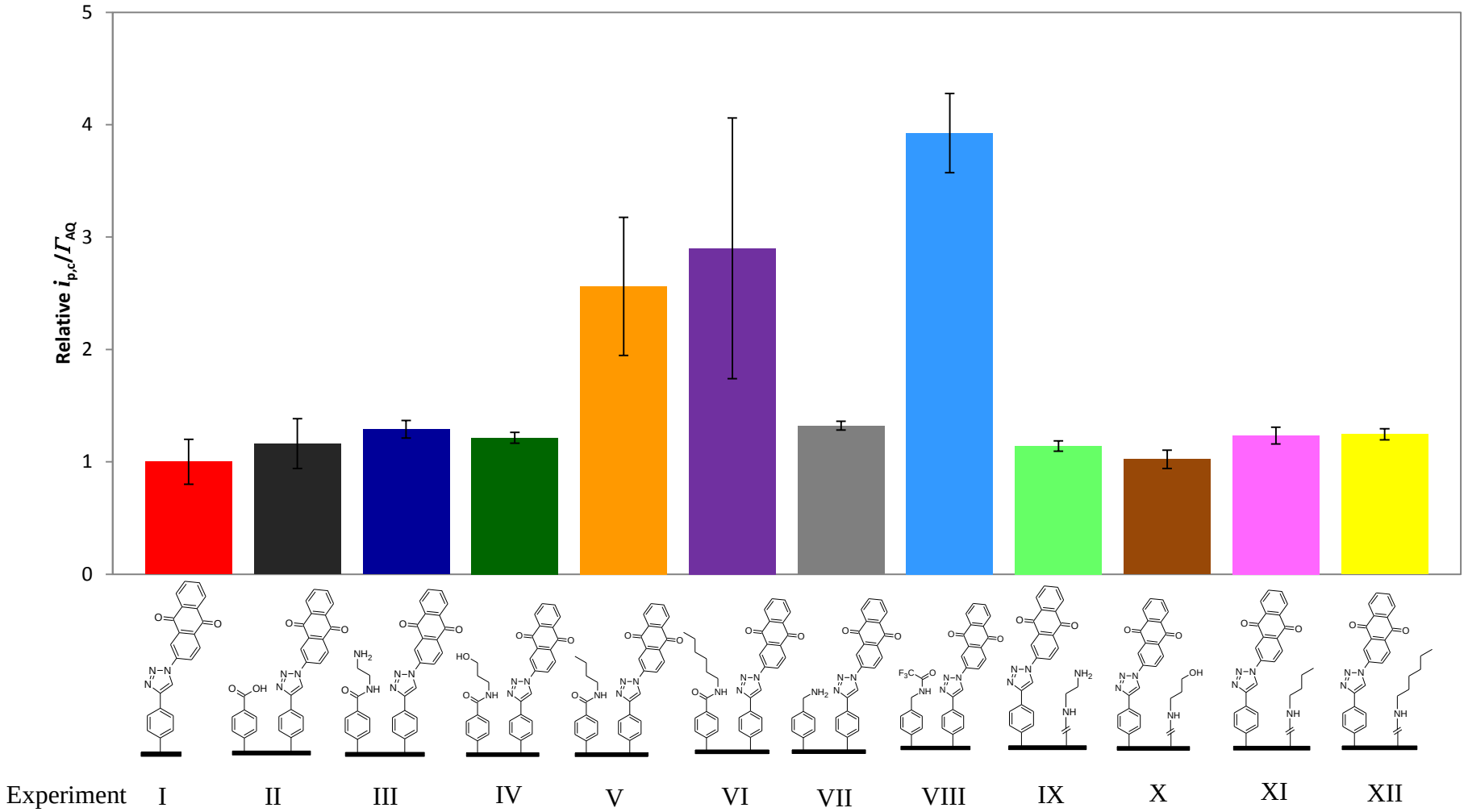

Figure 6.18 Plot of relative O_2 reduction current per amount of AQ on each of the modified surfaces (Table 6.6).

Assuming that the measured surface concentration of AQ groups represents the amount of catalytically active AQ on the surface, these results can be qualitatively analysed by considering the AQ centres as nano-sized active sites in an insulating matrix. Using this model, when the surface concentration of AQ is low, each AQ 'nano-electrode' will have a radial diffusion field resulting in a high flux of O_2 to the surface, and hence a high reduction current. When the surface concentration of AQ is higher, the diffusion fields of the AQ centres overlap, which results in a decreased O_2 flux per AQ centre, but an increased measured current. As expected based on this model, the current for O_2 reduction at the single component AQ layer (highest surface concentration of AQ) is not exceeded (within experimental error) at any of the other modified surfaces. The observed behaviour of mixed layers prepared by direct reaction with GC surface (Experiments IX – XII) is consistent with this model. The surface concentration of AQ groups for these mixed layers is similar to that of single component AQ layers and hence similar O_2 reduction currents are obtained.

The preliminary nature of this investigation prevents more detailed quantitative analysis of the data. However, it is interesting to examine the data for evidence that the environment of the AQ groups affects the efficiency of the O_2 reduction reaction. Figure 6.18 show that the mixed layer with a CF_3 substituent (Experiment VIII), has the highest value of $i_{p,c}/\Gamma_{AQ}$ (not taking into account the large uncertainty for the value for the surface of Experiment VI). Figure 6.17 shows that this surface has the lowest Γ_{AQ}, but the average O_2 reduction current of this surface is higher (not considering the uncertainty) than at surfaces prepared in Experiments II, VI and VII, and is only slightly lower than that at surfaces from Experiments III and IV, all of which have much higher amounts of electroactive AQ. CF_3 groups are known to have an affinity for O_2,[71] and hence it is tentatively suggested that the CF_3 component of the mixed layer improves the efficiency of O_2 reduction.

Figures 6.17 and 6.18 show that a similar argument may be made for the surfaces prepared in Experiment V, although the 'enhanced' O_2 reduction current is less significant. For this experiment, it is tentatively suggested that the hydrophobic component positioned at similar height (1.2 nm, from the structure shown in Figure 6.19a) to that of the AQ group (Figure 6.19c) creates a favourable environment for reduction of O_2. The large experimental uncertainty for currents obtained at the layer prepared by Experiment VI prevents analysis of this surface. Looking at mixed layers prepared by direct reaction with bare GC (Experiments IX – XII), there is no detectable influence of the second modifier on the electrocatalytic activity of AQ towards O_2 reduction, consistent with shorter second modifier, which do not influence the environment of the AQ centres. Figure 6.19b shows that the height of the second modifier in Experiment XII is 0.9 nm, assuming the amine moiety is directly attached to the GC surface.

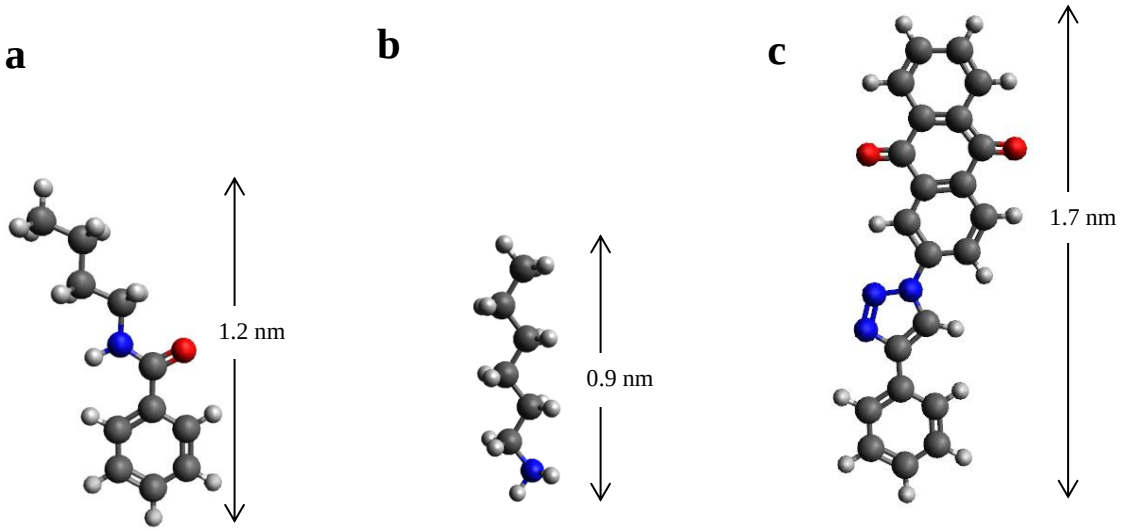

Figure 6.19 Structures of the second component of: a) Experiment V and b) Experiment XII. c) structure of the coupled AQ modifier. Heights of the molecules were estimated using *Avogadro* 1.1.1 freeware.

6.4 Conclusion

Preparation of amine-terminated monolayers by reduction of aryldiazonium salts using the protection-deprotection approach has been achieved. Two different protecting groups, Boc

and Fmoc, and two different amines, aminophenyl and aminomethylphenyl, were investigated. Solution redox probes responses were consistent with the protected and deprotected modified GC surfaces. AFM film thickness measurements confirmed that the films remaining after deprotection of the amine-protected surfaces are monolayers, except for Boc-NH-CH_2-Ar films. Coupling of carboxylic acid derivatives to the amine modified surfaces was also carried out to investigate the reactivity of the tethers and to estimate the amount of amine tethered onto the surface. Different carboxylic acid derivatives were used (FcCOOH and $FcCH_2COOH$) to compare their reactivity towards amide coupling. Coupling via $(COCl)_2$ activation resulted in interference from reactions occurring directly at the bare GC, while coupling in the presence of HBTU is assumed to give a more accurate indication of the amount of amine on the surface. Aminophenyl films are less reactive compared to aminomethylphenyl films and higher surface concentrations of Fc groups were obtained when coupling $FcCH_2COOH$ compared with FcCOOH. To summarise, as a method for coupling Fc to the amine modified film, $FcCH_2COOH$ is the better derivative, in the presence of HBTU, to avoid direct reaction with GC and to give highest possible surface concentration. Coupling to deprotected Fmoc-NH-CH_2-Ar film gives the highest reaction yield in the presence of HBTU. However, to get a maximum monolayer on the surface (through reaction with amine tethers and directly with GC), the deprotected Boc-NH-Ar film in the presence of $(COCl)_2$ as the activating agent is the best choice.

Preparation of binary layers on GC surfaces consisting of H-COO-Ar and NH_2-CH_2-Ar groups, and H-Eth-Ar and NH_2-CH_2-Ar groups was achieved by sequential grafting of the corresponding protected aryl diazonium salts. However, there is strong evidence that grafting of the second modifier can occur on the already grafted groups. An alternative approach was carried out involving immobilising the second component via direct reaction with bare GC

electrode. This method excludes the possibility of grafting on the already grafted layer, and therefore multilayer formation is avoided. However, after coupling of NP groups to the NH_2-CH_2-Ar layer, reaction at bare GC with amine derivatives is limited due to steric hindrance caused by the coupled NP groups. On the other hand, when reaction at bare GC was carried out using $(COCl)_2$-activated FcCOOH, a component ratio of 1 : 3 was obtained for Fc coupled to the NH_2-CH_2-Ar groups and Fc coupled to the bare GC. Therefore, to get a maximum amount of modifier on the surface, the $(COCl)_2$-activation method is preferred over the HBTU method.

Single component and mixed component monolayers incorporating AQ groups were used to study the electrocatalysis of O_2 reduction. The influence of hydrophobic and hydrophilic components, within the AQ monolayers, on the O_2 reduction process was briefly studied. It was found that mixed layers prepared by sequential grafting of two different aryldiazonium salts have lower apparent amounts of AQ than single component layers. The lower amount of AQ is likely due to the H-Eth-Ar groups being grafted to a surface with the other component already immobilised. There was no evidence for electro-inactive AQ groups in the layers. The presence of a second component does not significantly affect the O_2 reduction potential. However, the relative O_2 reduction current per AQ group of a mixed surface having a hydrophobic group, with a similar height to the tethered AQ groups, increased compared to a single component AQ layer. This may be due to the hydrophobic environment provided by the second component increasing the efficiency of the O_2 reduction reaction. This is in agreement with results that showed no influence on the electrocatalytic activity of AQ when the second modifier is shorter than the tethered AQ groups.

6.5 References

1 Leroux, Y.R., Fei, H., Noel, J.M., Roux, C., Hapiot, P., Efficient covalent modification of a carbon surface: Use of a silyl protecting group to form an active monolayer. *J. Am. Chem. Soc.*, **2010**, *132*, 14039.

2 Lee, L., Ma, H.F., Brooksby, P.A., Brown, S.A., Leroux, Y.R., Hapiot, P., Downard, A.J., Covalently anchored carboxyphenyl monolayer via aryldiazonium ion grafting: A well-defined reactive tether layer for on-surface chemistry. *Langmuir*, **2014**, *30*, 7104.

3 Polsky, R., Harper, J.C., Wheeler, D.R., Brozik, S.M., Multifunctional electrode arrays: Towards a universal detection platform. *Electroanal.*, **2008**, *20*, 671.

4 Alonso-Lomillo, M.A., Dominguez-Renedo, O., Hernandez-Martin, A., Arcos-Martinez, M.J., Horseradish peroxidase covalent grafting onto screen-printed carbon electrodes for levetiracetam chronoamperometric determination. *Anal. Biochem.*, **2009**, *395*, 86.

5 Asuncion Alonso-Lomillo, M., Dominguez-Renedo, O., Matos, P., Julia Arcos-Martinez, M., Disposable biosensors for determination of biogenic amines. *Anal. Chim. Acta*, **2010**, *665*, 26.

6 Chretien, J.M., Ghanem, M.A., Bartlett, P.N., Kilburn, J.D., Covalent tethering of organic functionality to the surface of glassy carbon electrodes by using electrochemical and solid-phase synthesis methodologies. *Chem.-Eur. J.*, **2008**, *14*, 2548.

7 Dauphas, S., Corlu, A., Guguen-Guillouzo, C., Ababou-Girard, S., Lavastre, O., Geneste, F., Covalent immobilization of antibodies on electrochemically functionalized carbon surfaces. *New J. Chem.*, **2008**, *32*, 1228.

8 Flavel, B.S., Gross, A.J., Garrett, D.J., Nock, V., Downard, A.J., A simple approach to patterned protein immobilization on silicon via electrografting from diazonium salt solutions. *ACS Appl. Mater. Inter.*, **2010**, *2*, 1184.

9 Ghanem, M.A., Chretien, J.M., Kilburn, J.D., Bartlett, P.N., Electrochemical and solid-phase synthetic modification of glassy carbon electrodes with dihydroxybenzene compounds and the electrocatalytic oxidation of NADH. *Bioelectrochemistry*, **2009**, *76*, 115.

10 Ghanem, M.A., Chretien, J.M., Pinczewska, A., Kilburn, J.D., Bartlett, P.N., Covalent modification of glassy carbon surface with organic redox probes through diamine linkers using electrochemical and solid-phase synthesis methodologies. *J. Mater. Chem.*, **2008**, *18*, 4917.

11 Harper, J.C., Polsky, R., Dirk, S.M., Wheeler, D.R., Brozik, S.M., Electroaddressable selective functionalization of electrode arrays: Catalytic NADH detection using aryl diazonium modified gold electrodes. *Electroanal.*, **2007**, *19*, 1268.

12 Pinczewska, A., Sosna, M., Bloodworth, S., Kilburn, J.D., Bartlett, P.N., High-throughput synthesis and electrochemical screening of a library of modified electrodes for NADH oxidation. *J. Am. Chem. Soc.*, **2012**, *134*, 18022.

13 Sosna, M., Chretien, J.M., Kilburn, J.D., Bartlett, P.N., Monolayer anthracene and anthraquinone modified electrodes as platforms for *Trametes hirsuta* laccase immobilisation. *Phys. Chem. Chem. Phys.*, **2010**, *12*, 10018.

14 Calow, A.D.J., Carbo, J.J., Cid, J., Fernandez, E., Whiting, A., Understanding α,β-unsaturated imine formation from amine additions to α,β-unsaturated aldehydes and ketones: An analytical and theoretical investigation. *J. Org. Chem.*, **2014**, *79*, 5163.

15 Xu, X.Y., Feng, Y., Li, J.J., Li, F., Yu, H.J., A novel protocol for covalent immobilization of thionine on glassy carbon electrode and its application in hydrogen peroxide biosensor. *Biosens. Bioelectron.*, **2010**, *25*, 2324.

16 Hensarling, R.M., Rahane, S.B., LeBlanc, A.P., Sparks, B.J., White, E.M., Locklin, J., Patton, D.L., Thiol-isocyanate "click" reactions: Rapid development of functional polymeric surfaces. *Polym. Chem.*, **2011**, *2*, 88.

17 Martin, C., Alias, M., Christien, F., Crosnier, O., Belanger, D., Brousse, T., Graphite-grafted silicon nanocomposite as a negative electrode for lithium-ion batteries. *Adv. Mater.*, **2009**, *21*, 4735.

18 Li, F., Feng, Y., Yang, L.M., Liu, S.F., Electrochemical sensing platform based on covalent immobilization of thionine onto gold electrode surface via diazotization-coupling reaction. *Talanta*, **2010**, *83*, 205.

19 Revenga-Parra, M., Garcia-Mendiola, T., Gonzalez-Costas, J., Gonzalez-Romero, E., Marin, A.G., Pau, J.L., Pariente, F., Lorenzo, E., Simple diazonium chemistry to develop specific gene sensing platforms. *Anal. Chim. Acta*, **2014**, *813*, 41.

20 Berthelot, T., Garcia, A., Le, X.T., El Morsli, J., Jegou, P., Palacin, S., Viel, P., "Versatile toolset" for DNA or protein immobilization: Toward a single-step chemistry. *Appl. Surf. Sci.*, **2011**, *257*, 3538.

21 de Fuentes, O.A., Ferri, T., Frasconi, M., Paolini, V., Santucci, R., Highly-ordered covalent anchoring of carbon nanotubes on electrode surfaces by diazonium salt reactions. *Angew. Chem. Int. Edit.*, **2011**, *50*, 3457.

22 Flatt, A.K., Chen, B., Tour, J.M., Fabrication of carbon nanotube-molecule-silicon junctions. *J. Am. Chem. Soc.*, **2005**, *127*, 8918.

23 Joyeux, X., Mangiagalli, P., Pinson, J., Localized attachment of carbon nanotubes in microelectronic structures. *Adv. Mater.*, **2009**, *21*, 4404.

24 Radi, A.E., Munoz-Berbel, X., Cortina-Ping, M., Marty, J.L., Novel protocol for covalent immobilization of horseradish peroxidase on gold electrode surface. *Electroanal.*, **2009**, *21*, 696.

25 Viel, P., Le, X.T., Huc, V., Bar, J., Benedetto, A., Le Goff, A., Filoramo, A., Alamarguy, D., Noel, S., Baraton, L., Palacin, S., Covalent grafting onto self-adhesive surfaces based on aryldiazonium salt seed layers. *J. Mater. Chem.*, **2008**, *18*, 5913.

26 Le, X.T., Doan, N.D., Dequivre, T., Viel, P., Palacin, S., Covalent grafting of chitosan onto stainless steel through aryldiazonium self-adhesive layers. *ACS Appl. Mater. Inter.*, **2014**, *6*, 9085.

27 Casas-Solvas, J.M., Ortiz-Salmeron, E., Gimenez-Martinez, J.J., Garcia-Fuentes, L., Capitan-Vallvey, L.F., Santoyo-Gonzalez, F., Vargas-Berenguel, A., Ferrocene-carbohydrate conjugates as electrochemical probes for molecular recognition studies. *Chem.-Eur. J.*, **2009**, *15*, 710.

28 Baramee, A., Coppin, A., Mortuaire, M., Pelinski, L., Tomavo, S., Brocard, J., Synthesis and in vitro activities of ferrocenic aminohydroxynaphthoquinones against *Toxoplasma gondii* and *Plasmodium falciparum. Bioorg. Med. Chem.*, **2006**, *14*, 1294.

29 Isidro-Llobet, A., Alvarez, M., Albericio, F., Amino acid-protecting groups. *Chem. Rev.*, **2009**, *109*, 2455.

30 Yu, S.S.C., Tan, E.S.Q., Jane, R.T., Downard, A.J., An electrochemical and XPS study of reduction of nitrophenyl films covalently grafted to planar carbon surfaces. *Langmuir*, **2007**, *23*, 11074.

31 Lee, J., Kang, M., Shin, M., Kim, J.M., Kang, S.U., Lim, J.O., Choi, H.K., Suh, Y.G., Park, H.G., Oh, U., Kim, H.D., Park, Y.H., Ha, H.J., Kim, Y.H., Toth, A., Wang, Y., Tran, R., Pearce, L.V., Lundberg, D.J., Blumberg, P.M., N-(3-acyloxy-2-benzylpropyl)-n '- 4-(methylsulfonylamino)benzyl thiourea analogues: Novel potent and high affinity antagonists and partial antagonists of the vanilloid receptor. *J. Med. Chem.*, **2003**, *46*, 3116.

32 Ulysse, L., Chmielewski, J., The synthesis of a light-switchable amino-acid for inclusion into conformationally mobile peptides. *Bioorg. Med. Chem. Lett.*, **1994**, *4*, 2145.

33 Bard, A.J., Inner-sphere heterogeneous electrode reactions. Electrocatalysis and photocatalysis: The challenge. *J. Am. Chem. Soc.*, **2010**, *132*, 7559.

34 Chen, P.H., McCreery, R.L., Control of electron transfer kinetics at glassy carbon electrodes by specific surface modification. *Anal. Chem.*, **1996**, *68*, 3958.

35 DuVall, S.H., McCreery, R.L., Control of catechol and hydroquinone electron-transfer kinetics on native and modified glassy carbon electrodes. *Anal. Chem.*, **1999**, *71*, 4594.

36 DuVall, S.H., McCreery, R.L., Self-catalysis by catechols and quinones during heterogeneous electron transfer at carbon electrodes. *J. Am. Chem. Soc.*, **2000**, *122*, 6759.

37 Available from: http://sites.chem.colostate.edu/diverdi/all_courses/CRC%20reference%20data/dissociation%20constants%20of%20organic%20acids%20and%20bases.pdf.

38 Abiman, P., Crossley, A., Wildgoose, G.G., Jones, J.H., Compton, R.G., Investigating the thermodynamic causes behind the anomalously large shifts in pK_a values of benzoic acid-modified graphite and glassy carbon surfaces. *Langmuir*, **2007**, *23*, 7847.

39 Abiman, P., Wildgoose, G.G., Crossley, A., Jones, J.H., Compton, R.G., Contrasting pK_a of protonated bis(3-aminopropyl)-terminated polyethylene glycol "jeffamine" and

the associated thermodynamic parameters in solution and covalently attached to graphite surfaces. *Chem.-Eur. J.*, **2007**, *13*, 9663.

40 Bordwell, F.G., Ji, G.Z., Effects of structural-changes on acidities and homolytic bond-dissociation energies of the H-N bonds in amidines, carboxamides, and thiocarboxamides. *J. Am. Chem. Soc.*, **1991**, *113*, 8398.

41 Belanger, D., Pinson, J., Electrografting: A powerful method for surface modification. *Chem. Soc. Rev.*, **2011**, *40*, 3995.

42 Leroux, Y.R., Hui, F., Hapiot, P., A protecting-deprotecting strategy for structuring robust functional films using aryldiazonium electroreduction. *J. Electroanal. Chem.*, **2013**, *688*, 298.

43 Leroux, Y.R., Hapiot, P., Nanostructured monolayers on carbon substrates prepared by electrografting of protected aryldiazonium salts. *Chem. Mater.*, **2013**, *25*, 489.

44 Han, S.Y., Kim, Y.A., Recent development of peptide coupling reagents in organic synthesis. *Tetrahedron*, **2004**, *60*, 2447.

45 Montalbetti, C., Falque, V., Amide bond formation and peptide coupling. *Tetrahedron*, **2005**, *61*, 10827.

46 Liu, Y.C., McCreery, R.L., Reactions of organic monolayers on carbon surfaces observed with unenhanced Raman-spectroscopy. *J. Am. Chem. Soc.*, **1995**, *117*, 11254.

47 Chidsey, C.E.D., Bertozzi, C.R., Putvinski, T.M., Mujsce, A.M., Coadsorption of ferrocene-terminated and unsubstituted alkanethiols on gold - electroactive self-assembled monolayers. *J. Am. Chem. Soc.*, **1990**, *112*, 4301.

48 McDermott, M.T., McDermott, C.A., McCreery, R.L., Scanning tunneling microscopy of carbon surfaces - relationships between electrode-kinetics, capacitance, and morphology for glassy-carbon electrodes. *Anal. Chem.*, **1993**, *65*, 937.

49 Pontikos, N.M., McCreery, R.L., Microstructural and morphological-changes induced in glassy-carbon electrodes by laser irradiation. *J. Electroanal. Chem.*, **1992**, *324*, 229.

50 Menanteau, T., Levillain, E., Breton, T., Spontaneous grafting of nitrophenyl groups on carbon: Effect of radical scavenger on organic layer formation. *Langmuir*, **2014**, *30*, 7913.

51 Toupin, M., Belanger, D., Thermal stability study of aryl modified carbon black by in situ generated diazonium salt. *J. Phys. Chem. C*, **2007**, *111*, 5394.

52 Mesnage, A., Lefevre, X., Jegou, P., Deniau, G., Palacin, S., Spontaneous grafting of diazonium salts: Chemical mechanism on metallic surfaces. *Langmuir*, **2012**, *28*, 11776.

53 Adenier, A., Cabet-Deliry, E., Chausse, A., Griveau, S., Mercier, F., Pinson, J., Vautrin-Ul, C., Grafting of nitrophenyl groups on carbon and metallic surfaces without electrochemical induction. *Chem. Mater.*, **2005**, *17*, 491.

54 Adenier, A., Chehimi, M.M., Gallardo, I., Pinson, J., Vila, N., Electrochemical oxidation of aliphatic amines and their attachment to carbon and metal surfaces. *Langmuir*, **2004**, *20*, 8243.

55 Baranton, S., Belanger, D., Electrochemical derivatization of carbon surface by reduction of in situ generated diazonium cations. *J. Phys. Chem. B*, **2005**, *109*, 24401.

56 Combellas, C., Delamar, M., Kanoufi, F., Pinson, J., Podvorica, F.I., Spontaneous grafting of iron surfaces by reduction of aryldiazonium salts in acidic or neutral aqueous solution. Application to the protection of iron against corrosion. *Chem. Mater.*, **2005**, *17*, 3968.

57 Doppelt, P., Hallais, G., Pinson, J., Podvorica, F., Verneyre, S., Surface modification of conducting substrates. Existence of azo bonds in the structure of organic layers obtained from diazonium salts. *Chem. Mater.*, **2007**, *19*, 4570.

58 Ortiz, B., Saby, C., Champagne, G.Y., Belanger, D., Electrochemical modification of a carbon electrode using aromatic diazonium salts. 2. Electrochemistry of 4-nitrophenyl modified glassy carbon electrodes in aqueous media. *J. Electroanal. Chem.*, **1998**, *455*, 75.

59 Breton, T., Belanger, D., Modification of carbon electrode with aryl groups having an aliphatic amine by electrochemical reduction of in situ generated diazonium cations. *Langmuir*, **2008**, *24*, 8711.

60 Grivea, S., Mercier, D., Vautrin-Ul, C., Chausse, A., Electrochemical grafting by reduction of 4-aminoethylbenzenediazonium salt: Application to the immobilization of (bio)molecules. *Electrochem. Commun.*, **2007**, *9*, 2768.

61 Jansen, R.J.J., van Bekkum, H., XPS of nitrogen-containing functional groups on activated carbon. *Carbon*, **1995**, *33*, 1021.

62 Lyskawa, J., Belanger, D., Direct modification of a gold electrode with aminophenyl groups by electrochemical reduction of in situ generated aminophenyl monodiazonium cations. *Chem. Mater.*, **2006**, *18*, 4755.

63 Trzebiatowska-Gusowska, M., Gagor, A., Coetsee, E., Erasmus, E., Swart, H.C., Swarts, J.C., Nano islet formation of formyl- and carboxyferrocene, -ruthenocene, -osmocene and cobaltocenium on amine-functionalized silicon wafers highlighted by crystallographic, AFM and XPS studies. *J. Organomet. Chem.*, **2013**, *745*, 393.

64 Loring, J.S., *Linkfit*. **2000**, Ph.D. Dissertation, University of California, Davis: University of California, Davis.

65 Yeager, E., Electrocatalysts for O_2 reduction. *Electrochim. Acta*, **1984**, *29*, 1527.

66 Gong, Z., Zhang, G., Wang, S., Electrochemical reduction of oxygen on anthraquinone/carbon nanotubes nanohybrid modified glassy carbon electrode in neutral medium. *Journal of Chemistry*, **2013**, *2013*, 9.

67 Jurmann, G., Schiffrin, D.J., Tammeveski, K., The pH-dependence of oxygen reduction on quinone-modified glassy carbon electrodes. *Electrochim. Acta*, **2007**, *53*, 390.

68 Sarapuu, A., Vaik, K., Schiffrin, D.J., Tammeveski, K., Electrochemical reduction of oxygen on anthraquinone-modified glassy carbon electrodes in alkaline solution. *J. Electroanal. Chem.*, **2003**, *541*, 23.

69 Weissmann, M., Crosnier, O., Brousse, T., Belanger, D., Electrochemical study of anthraquinone groups, grafted by the diazonium chemistry, in different aqueous media-relevance for the development of aqueous hybrid electrochemical capacitor. *Electrochim. Acta*, **2012**, *82*, 250.

70 Ernst, S., Aldous, L., Compton, R.G., The voltammetry of surface bound 2-anthraquinonyl groups in room temperature ionic liquids: Cation size effects. *Chemical Physics Letters*, **2011**, *511*, 461.

71 Andrieux, C.P., Audebert, P., Hapiot, P., Divisiablohorn, B., Aldebert, P., Electrochemistry in hydrophobic nafion gels .2. Electrochemical-behavior and catalytic properties of electrodes modified by hydrophobic nafion gels loaded with 9-phenylacridinium salts and anthraquinone. *J. Electroanal. Chem.*, **1990**, *296*, 129.

Chapter 7. Electroreduction of Aryldiazonium Salts at Carbon Electrodes: Origin of Two Reduction Peaks

7.1 Introduction

As outlined in Chapter 1, the one-electron reduction of aryldiazonium salts leads to formation of aryl radicals and dinitrogen molecules; the aryl radicals may then react with the electrode surface to form a covalent bond[1-3] (Scheme 1.1, Chapter 1). Interestingly, reported cyclic voltammograms (CVs) obtained at carbon electrodes in diazonium ion solutions often, but not always, show two reduction peaks.[1, 3-32] Figure 7.1 shows CVs of 4-nitrobenzenediazonium salt (NBD) in acetonitrile (ACN) solution, where the CV on the left shows only one reduction peak and the CV on the right shows two reduction peaks, labelled peak 1 and peak 2.

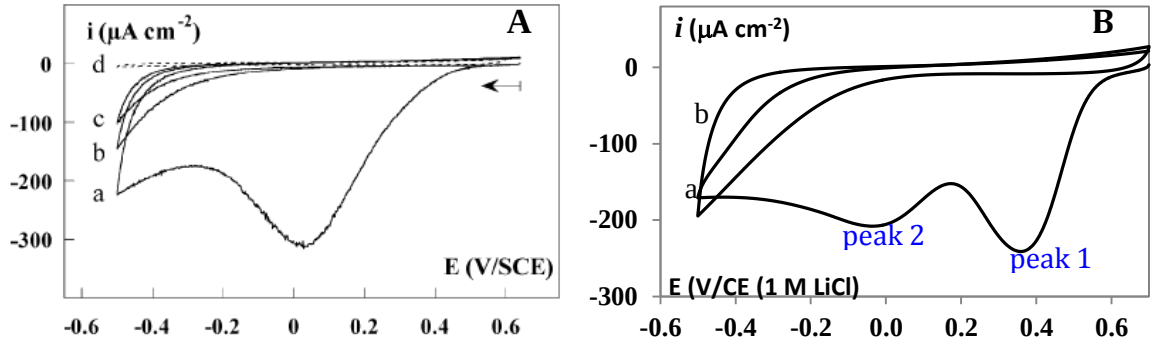

Figure 7.1 Repeat CVs of NBD, 2 mM (A) and 1 mM (B), in 0.1 M $TBABF_4$-ACN on GC. a) 1st scan, b) 2nd scan, and c) 3rd scan. d) CV obtained in 0.1 M $TBABF_4$-ACN without diazonium salt. Scan rate = 200 mV s^{-1}. CVs (A) reproduced from reference 6; CVs (B) this work.

Table 7.1 lists the peak potentials for reduction of some aryldiazonium ions in ACN solution at carbon electrodes. As shown in Table 7.1, the appearance of two reduction peaks is not

limited to a particular aryldiazonium ion. For some derivatives the intensity of peak 1 varies between experiments and is not always present.[7, 11]

Table 7.1 Reported reduction peak potentials for a range of aryldiazonium ions in ACN at carbon electrodes.

Aryldiazonium ions	Peak 1 (V) vs SCE	Peak 2 (V) vs SCE	Concentration (mM)	Scan rate ($V\ s^{-1}$)	Electrode	Ref
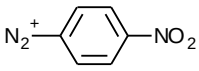	–[a]	0.03	2	0.2	GC	5
	–	0	2	0.2	GC	6
	–[a]	0.20	0.1	0.2	GC	1
	–	0.27	1.8	0.2	HOPG	1
	0.46	0.10	1	0.05	GC	7
	0.41	0.04	1[b]	0.05	GC	8
	–[a]	0.20	3	0.2	GC	9
	0.19	–0.16	0.59	0.2	PPF	11
	0.49	0.09	2	0.2	GC	13
	–	–0.04	0.7	0.2	GC	15
	–	–0.04	1	0.2	Carbon fiber	14
	–	0.04	1	0.1	GC	21
	–	–0.29	1	0.2	GC	22
	–	–0.29[c]	1	0.2	H-terminated GC	22
	–	0.03	0.5	0.1	GC	23
	–[a]	0.08	Not reported		GC	24
	0.37	0.09	1	0.05	GC	27
	–	–0.02	2	Not reported	GC	3
	0.1[d]	–0.2[d]	5	0.2	PPF	28
	0.4	–	2.5	0.1	GC	29
	–	–0.09	1	0.1	GC	30
	–[a]	0.08	1	0.2	GC	16

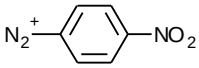	–	0.28	1	0.2	H-terminated diamond	31
	–	0.28	1	0.2	OH-terminated diamond	31
	–	0.02	1	0.2	Reconstructed carbon	31
	–	0.09	1	0.2	O-terminated diamond	31
	0.40	0	1	0.1	GC	*j*
	0.42	–	1	0.1	HOPG	*j*
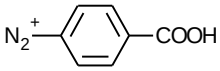	0.25[e]	–0.15[e]	5	0.1	GC	4
	–[a]	0.10	0.1	0.2	GC	1
	0.26	–0.16	1	0.05	GC	7
	–	–0.35[f]	1	0.05	HOPG	10
	0.31	–0.10	1	0.1	GC	*j*
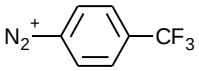	–[a]	–0.34	2	0.2	GC	5
	–[a]	–0.05	3	0.2	GC	9
	–	–0.6[d]	5	0.2	PPF	28
	0.30[g]	0.03	1	0.1	GC	*j*
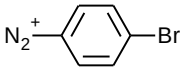	–[a]	–0.35	2	0.2	GC	5
	–[a]	0.02	0.1	0.2	GC	1
	0.16	–0.35	1[b]	0.05	GC	8
	–0.05[g]	–0.39	1	0.1	GC	21
	0.20	0.01[h]	1	0.1	GC	*j*
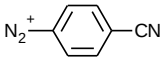	–[a]	0.16	0.1	0.2	GC	1
	0.32	–0.12	1	0.1	GC	*j*
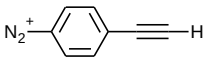	–	0.1	10	0.05	GC	25
	0.19	–0.11	1	0.1	GC	*j*
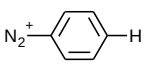	–[a]	–0.06	0.1	0.2	GC	1
	0.14[g]	–0.10	1	0..1	GC	*j*

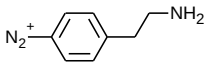	–0.1[g]	–0.51	2	0.1	GC	18
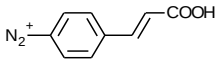	0.2[g]	–0.04	5	0.2	GC	32
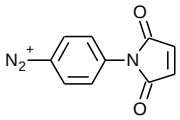	0.5	0.04[h]	1	0.1	GC	19
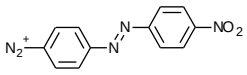	0.24[g]	0.09	1.03	0.2	PPF	11
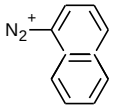	–[a]	0.08	0.1	0.2	GC	1
	0.05[g]	–0.23	1	0.1	GC	21
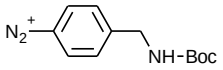	–	–0.44	3	0.05	GC	12
	–	–0.54	5	0.05	GC	20
	–0.14[g]	–0.59	5	0.05	BP[i]	20
	–	–0.49	5	0.05	EP[i]	20
	0.13	–0.58	5	0.05	GC	*j*
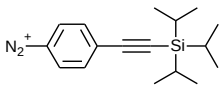	–	–0.05[d]	1	0.05	Carbon paper	17
	–	0	10	0.05	GC	25
	0.2[g]	–0.25	10	0.1	GC	26
	0.27	0.03	5	0.05	GC	*j*
	0.27	–0.17	1	0.1	GC	*j*

[a]CV not shown

[b]*In situ* generated diazonium ion by addition of 3 mM *tert*-butylnitrite

[c]The reduction did not appear on the 1st scan, but on the 2nd scan

[d]V vs Ag/Ag^+ (non-aqueous)

[e]V vs Ag

[f]V vs Pt

[g]Shoulder, rather than a distinct peak, appear at this potential

[h]Total of 3 reduction peaks, values shown are first two reduction potential

[i]EP = edge-plane graphite electrode; BP = basal-plane graphite electrode

[j]From the work carried out in this thesis

The origin of the two reduction peaks for aryldiazonium ions on carbon electrodes has never been explained. From a survey of the literature and from this thesis work (Chapters 4 – 6) the following points can be made. It is clear that when reduction of aryldiazonium ion does not lead to grafting, only one reduction peak is observed, and on the reverse scan, significant reduction current is detected (Figure 7.2).[33] Reduction of aryldiazonium ions with substituents at the *ortho* position (2,6-dimethylbenzene diazonium and 2-ethylbenzenediazonium) does not lead to surface films. It is assumed that the *ortho* substituents sterically prevent the attachment of the radical to the surface, thus the CVs are typical of irreversible diffusion-controlled processes (Figure 7.2). However, it is not possible to establish whether the single peak corresponds to peak 1 or peak 2 (or neither).

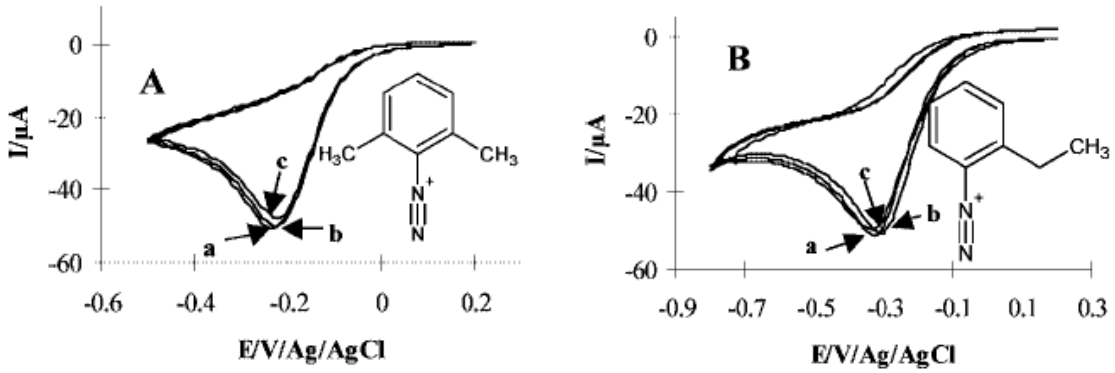

Figure 7.2 CVs in 0.1 M $TBABF_4$-ACN on a GC electrode of: A) 4 mM 2,6-dimethylbenzene diazonium tetrafluoroborate, a) 1st, b) 2nd, and c) 10th scan, and B) 4 mM 2-ethyl benzenediazonium tetrafluoroborate, a) 1st, b) 2nd, and c) 4th scan. Scan rate = 100 mV s^{-1}. Reproduced from reference 33.

Similarly, when a radical scavenger (2,2-diphenyl-1-picrylhydrazyl, DPPH) is added to the grafting solution, the CVs only show one irreversible reduction at the peak 1 position (Figure 7.3A).[27] In Figure 7.3A, the two reversible peaks at $E_{½} \approx$ -0.05 and 0.45 V correspond to the DPPH redox systems (Figure 7.3B). The presence of radical scavengers minimises the formation of thick layers because the aryl radicals produced from the reduction of aryldiazonium ions react with the radical scavengers instead of reacting with the already

grafted layer. It has been shown that electrografting in the presence of an excess amount of radical scavenger results in monolayer coverage.[27] Hence, it can be concluded that the CVs of aryldiazonium ions that do not lead to grafting, or to only a low coverage, only exhibit one reduction peak at the peak 1 position.

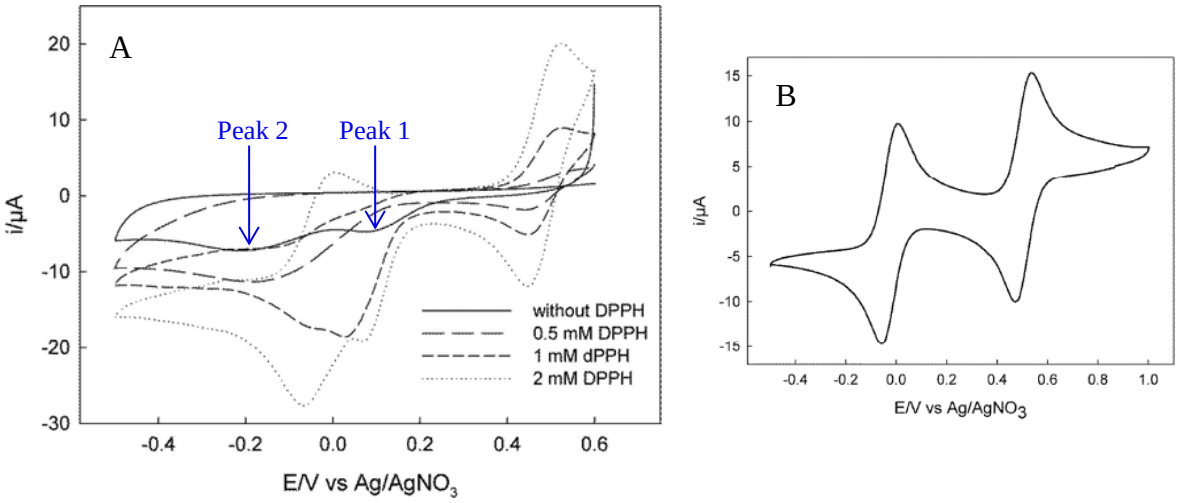

Figure 7.3 A) First CV cycle recorded at a GC electrode in 0.1 M $TBAPF_6$-ACN containing 1 mM NBD without DPPH and with various DPPH concentrations. B) CV recorded in 0.1 M $TBAPF_6$-ACN containing 1 mM DPPH on a GC electrode. Scan rate = 50 mV s^{-1}. Reproduced from reference 27.

In a study of three aryldiazonium ion (benzenediazonium, 4-methylbenzenediazonium and NBD), Andrieux and Pinson[2] showed that under some conditions, the aryl radical that is responsible for the grafting reaction can be reduced to an aryl anion. Figure 7.4 shows that the reduction of aryl radical to aryl anion is observed in CVs as a small peak more negative than the reduction of the diazonium ion itself.[2] The peak of the radical is small because most has reacted by the time the potential is negative enough to reduce it. This aryl radical reduction was only visible if the CVs were scanned fast enough (scan rate ≥ 1 V s^{-1}) to exceed the rate of radical reaction. Hence, reduction of aryl radical is unlikely to correspond to the second peak, often observed for aryldiazonium ion reduction. Moreover, aryl anions are not known to graft to the surface[34, 35] and applying a potential negative of peak 2 usually

results in a thick layer of grafted film. Thus the commonly observed peak 2 is unlikely to correspond to reduction of aryl radicals.

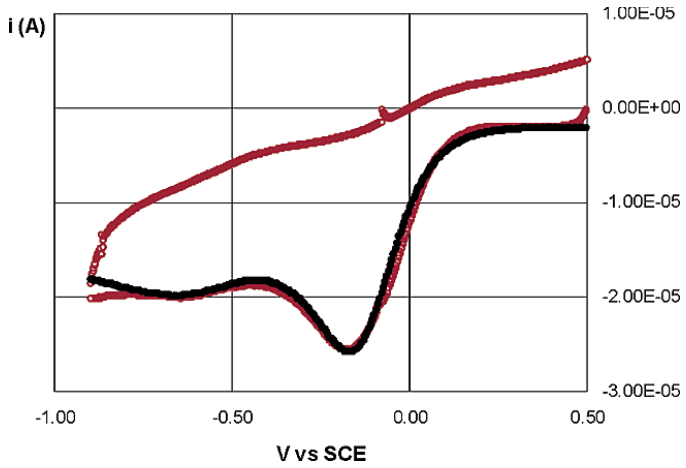

Figure 7.4 CVs obtained at GC electrode in 0.60 mM H-Ar-N_2^+ in 0.1 M $TBABF_4$-ACN at scan rate of 1 V s^{-1}. T = 25 °C. Red points: experimental; black points: simulated curve. Reproduced from reference 2.

Benedetto and co-workers[36] investigated the electroreduction of diazonium salt (C_6F_{13}-S-Ar-N_2^+) on three different crystallographic distributions of Au electrodes: A) polycrystalline Au on glass with an average crystallite size of 20 nm, B) pure Au (111) epitaxied on mica, and C) poorly crystallised Au deposited on bronze coupons. They found three distinct reduction peaks on a polycrystalline Au surface ($E_{p,c}$ = 0.14, 0.03 and -0.45 V), one very sharp peak at 0.13 V and a broad peak at -0.45 V on a monocrystalline Au (111) surface, and only one broad peak on poorly crystallised Au surface (Figure 7.5a). From these results, the authors suggest that each of the reduction peaks corresponds to the one-electron reduction of diazonium ion on different crystalline sites, where the more positive peaks were assigned to Au crystal sites with higher work functions (higher potential of zero charge). Hence the peak at $E_{p,c}$ ~0.14 V corresponds to reduction of diazonium ion on Au (111) facets, the peak at $E_{p,c}$ ~0 V arises from the reduction at Au (100) sites and the broader peak at $E_{p,c}$ ~-0.45 V was attributed to the convolution of the reduction on Au (110), Au (331) and other crystal facets of the Au surface. The other peaks observed in CVs recorded on monocrystalline Au (111)

substrate (Figure 7.5a, solid black line) were presumed to arise from electroreduction on crystallographic defects, grain boundaries and crystallographic steps.[36]

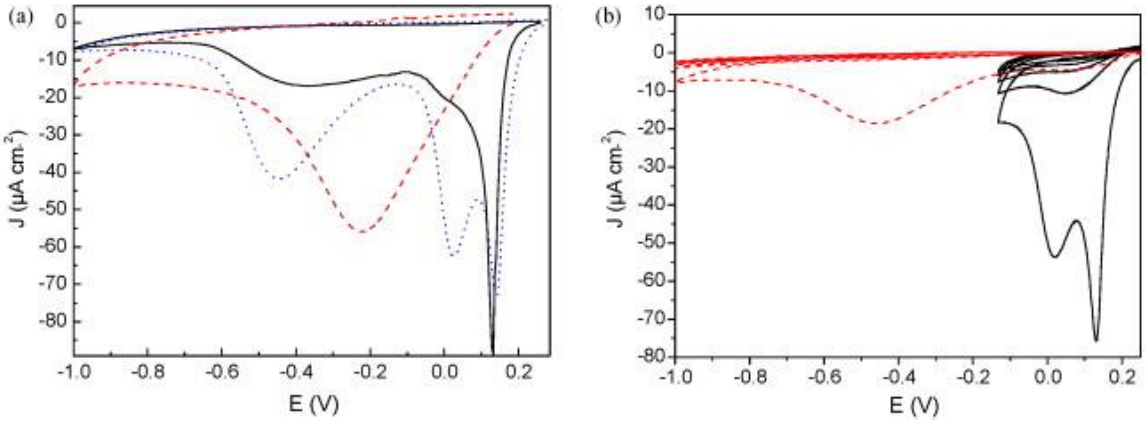

Figure 7.5 a) CVs of 5 mM C_6F_{13}-S-Ar-N_2^+ in ACN (0.05 M tetraethylammonium perchlorate (TEAP) as electrolyte) on different Au substrates: Au (111) epitaxied on mica (solid black line), polycrystalline Au on glass (dotted blue line), poorly crystallised Au on bronze (dashed red line). b) CVs of 5 mM C_6F_{13}-S-Ar-N_2^+ in 0.05 M TEAP-ACN on polycrystalline Au. CVs shown by solid black lines were performed first followed by recording of the dashed red line CV. Reproduced from reference 36.

To further investigate the reduction of diazonium ion at the different crystalline sites, the polycrystalline Au electrode was repetitively cycled from 0.3 to -0.13 V in the presence of C_6F_{13}-S-Ar-N_2^+, and the same surface was then scanned from 0.3 to -1 V (Figure 7.5b).[36] As shown by the solid black line, the two peaks at 0.13 and 0.03 V were observed on the first scan, but almost vanished on the subsequent scans. When scans were extended to -1 V (dashed red line), only a peak at -0.45 V was visible. The authors concluded that the gold facets corresponding to this reduction potential were still electrochemically active for the electroreduction of C_6F_{13}-S-Ar-N_2^+. It was also stated that the cleanliness of the surface is important to observe the multiple peaks; Au surfaces that were left in air for long times only gave one broad reduction peak.[36] The authors also suggested that at GC, the two reduction peaks may be caused by different crystalline structures of GC, however due to the complicated topography of carbon surfaces, it would not be possible to establish a direct

correspondence between work function values and crystallographic sites. The authors did not carry out an experimental investigation on carbon surfaces.

Cline and co-workers[13] made a detailed investigation of the origin of the two reduction peaks for NBD on GC electrodes, however no definitive conclusion was drawn from the investigation. They studied the effect of concentration of aryldiazonium ion on the reduction peaks at GC (Figure 7.6A). As the concentration increases, both peak currents increase and reach a limiting value; at 4 and 8 mM the peak currents are similar within experimental error. Moreover, as the concentration decreases, the current of peak 2 decreases relative to peak 1 and at very low concentration ($\leq$ 0.4 mM) only peak 1 is observed.[13] Under the conditions of low concentration and relatively fast scan rate (200 mV s^{-1}), a negligible amount of grafting is expected and hence the observation of peak 1 only is consistent with the findings discussed above. Cline and co-workers[13] also investigated the influence of electrode pre-treatment on NBD reduction response (Figure 7.6B). Compared with polished GC, electrochemically oxidising GC gives a higher O/C ratio, while sonication in activated charcoal/isopropanol and cyclohexane is expected to yield a lower O/C ratio.[13] After obtaining the CVs shown in Figure 7.6B, the authors conclude that it is not clear whether oxygen functional groups are affecting the appearance of peak 1.[13] In addition, electrodes that were immersed in diazonium ion solution for an hour prior to recording the CV showed a diminished peak 1 relative to peak 2, and it was also noted that the magnitude of peak 1 decreases relative to peak 2 if the GC is placed in water or other aqueous solution without diazonium ion for an hour.[13] From these results and their survey of relevant literature, the authors concluded that the appearance of two distinct reduction peaks in the CVs of NBD is related to: 1) the properties of the material used (different GC samples, pyrolyzed photoresist film (PPF) or highly ordered pyrolytic graphite (HOPG)); 2) different modification conditions (aryldiazonium ion concentration, and scan rate); and 3) surface pre-treatment and history.[13] Futhermore, they

tentatively postulated that two reduction peaks arise from two different sites on the electrode for the adsorption of diazonium ion and /or attachment of aryl radicals: at peak 1, the reduction process is stabilised by the formation of the surface bond, and peak 2 may result from electrografting at a different type of site, either on the native carbon surface or involving an already attached aryl group.[13]

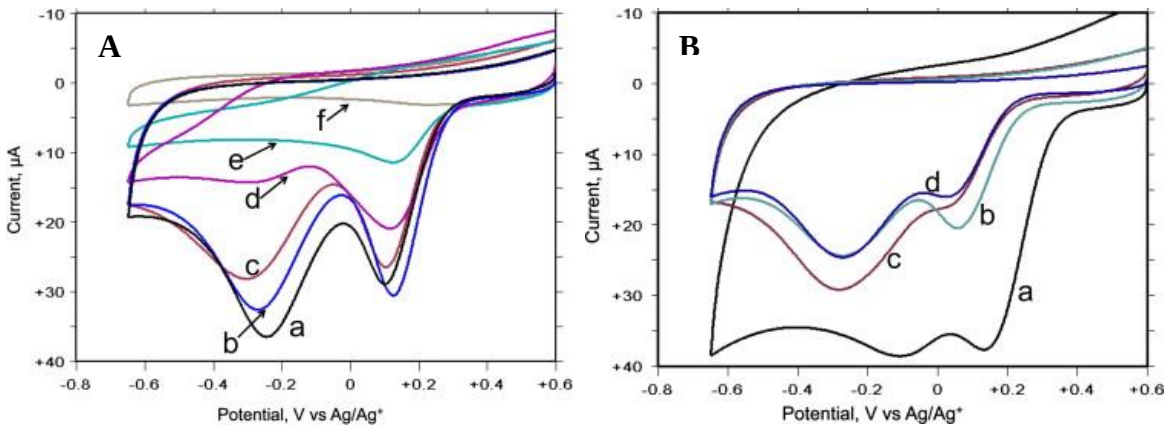

Figure 7.6 A) CVs of NBD in 0.1 M $TBABF_4$-ACN: a) 8 mM, b) 4 mM, c) 2 mM, d) 0.8 mM, e) 0.4 mM, f) 0.02 mM on GC polished with Al_2O_3/H_2O and sonicated in activated charcoal/isopropanol, then H_2O. B) CVs of 2 mM NBD in 0.1 M $TBABF_4$-ACN on GC: a) electrochemically oxidised in 0.1 M H_2SO_4, b) polished with Al_2O_3/H_2O and sonicated in activated charcoal/isopropanol, then H_2O, c) polished and sonicated in cyclohexane, d) polished with Al_2O_3/H_2O and sonicated in H_2O. Scan rate = 200 mV s^{-1}. CVs reproduced from reference 13.

Recently, Richard and co-workers[29] investigated the reduction of NBD at GC surfaces. In their work, CVs of NBD in 0.1 M HCl(aq) solution at a 'fully polished' electrode (GC was polished with 1 μm diamond powder) gave rise to two reduction peaks ($E_{p,c}$ = 0.4 V and 0.05 V vs SCE), while at an 'unpolished' electrode (GC was polished with 9 μm diamond powder) only one reduction peak was observed ($E_{p,c}$ = 0.05 V). However, when CVs were collected in ACN solution only one reduction peak was seen, at $E_{p,c}$ = 0.4 V and 0.05 V for the 'fully polished' and 'unpolished' GC, respectively. Since only one reduction peak was observed in aprotic solution, these authors focussed their attention on the NBD reduction process in protic aqueous solution, and concluded that on a freshly polished GC, peak 1 corresponds to the

reduction of the diazonium moiety of NBD and peak 2 is the reduction of the grafted nitro groups to hydroxylamine groups.[29] However, as the data in Table 7.1 demonstrates, the observation of two distinct reduction peaks is not limited to NBD, and hence this conclusion does not seem feasible, at least as a general explanation.

The observation of multiple peaks is not limited to aryldiazonium ion reduction processes. The electrooxidation of arylhydrazine at GC also sometimes leads to two oxidation peaks.[37, 38] For example, Daasbjerg and co-workers have investigated the electrooxidation of arylhydrazine for grafting of thin films; in their first report[38] the electrooxidation of 4-nitrophenylhydrazine (NPH) shows only one irreversible peak at 0.33 V on the first scan (Figure 7.7A). However, in their second report[37] the CVs show an irreversible peak at ~0.35 V and another small irreversible peak at ~0.65 V (Figure 7.7B). The concentration of NPH used, pH and scan rate are the same for both reports. During the course of this thesis work, two peaks were sometimes observed for the electrooxidation of NPH. In addition, electrooxidation of arylacetate also exhibits multiple peaks, where the first two peaks (peak i and ii, Figure 7.8) lead to grafting.[39, 40] The electropolymerisation of *o*-phenylenediamine (Figure 7.9) sometimes also leads to multiple irreversible peaks.[41, 42] However, none of the authors provide a clear explanation for these phenomena. The similarity between these oxidation processes and aryldiazonium ion reduction may be significant, given that they involve aryl radicals that subsequently bond either to the carbon electrode surface or to neighbouring molecules to form polymeric coatings.

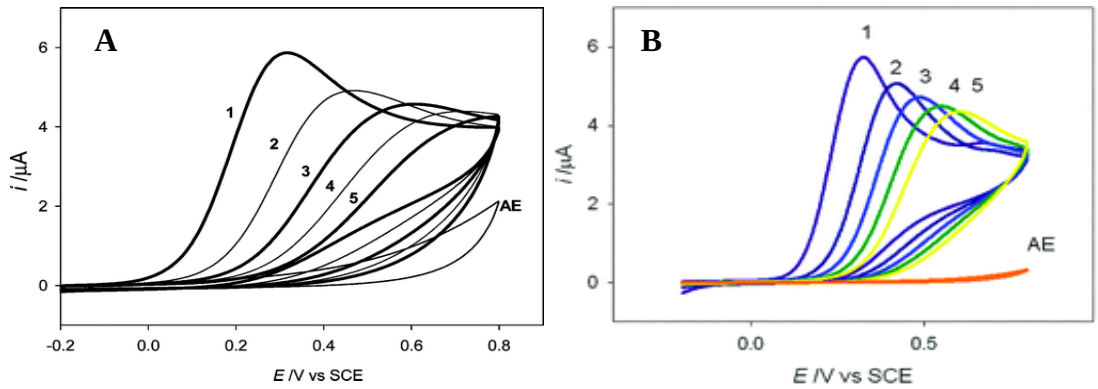

Figure 7.7 CVs of 2 mM NPH in 0.1 M KH_2PO_4 (pH 5) at GC electrode. Numerals refer to scan numbers. "AE" was obtained after potentiostatic electrolysis at 0.8 V vs SCE for 300 s. The solution was stirred in between scans. Scan rate = 200 mV s^{-1}. Figure A reproduced from reference 38 and Figure B reproduced from reference 37.

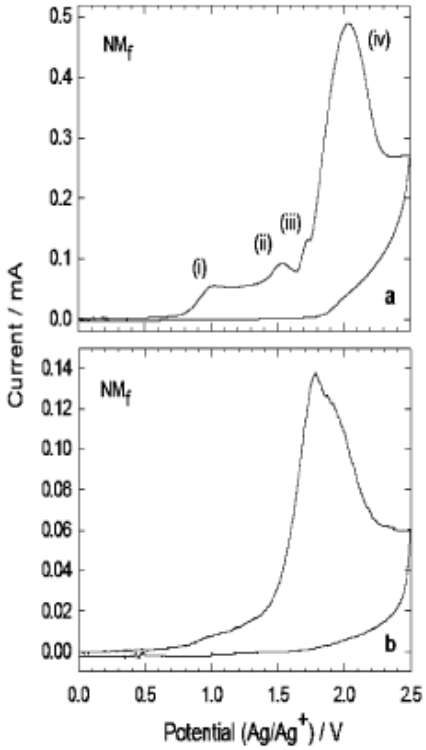

Figure 7.8 CVs of 1-napthylmethylcarboxylate (5.2 mM) in 0.1 M $TBABF_4$-ACN at GC: a) 1st scan, b) 2nd scan. The solution was stirred in between scans. Scan rate = 200 mV s^{-1}. Reproduced from reference 40.

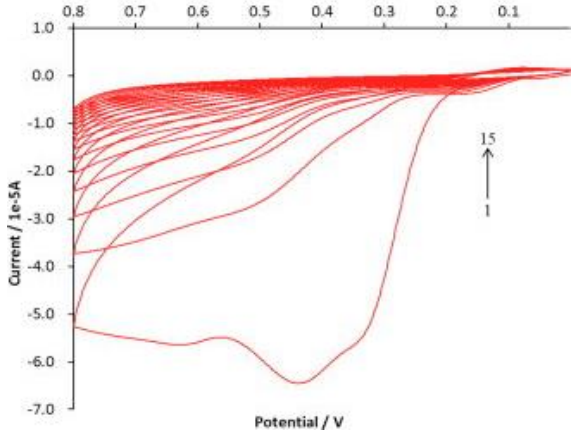

Figure 7.9 CVs for the electropolymerisation of 5 mM *o*-phenylenediamine on GC electrode in phosphate buffer saline (pH 5.2). Numerals refer to scan numbers. Scan rate = 50 mV s^{-1}. Reproduced from reference 41.

From the work of Richard and co-workers[29] and Cline and co-workers,[13] the literature reports of either two reduction peaks or only one reduction peak for a given aryldiazonium ion are likely due to the variation in 'cleanliness' or 'past-history' of the GC electrodes, and the amount of time the GC electrode was left in the diazonium ion solution before the CVs were collected. In this chapter, reduction of aryldiazonium ions in ACN solution was investigated in an attempt to understand the origin of the two reduction peaks. A range of aryldiazonium salts with different substituents at the *para* position were investigated. NBD was further used as a model diazonium ion to study this phenomenon at both GC and highly ordered pyrolytic graphite (HOPG). The effect of GC surface pre-treatment on the CVs of NBD was also studied to give further insight into the appearance of two reduction peaks.

7.2 Experimental

All chemical reagents and materials are described in Chapter 2. The syntheses of aryldiazonium salts are outlined in Chapter 2, Section 2.1.3. All experiments in this chapter were undertaken using Pt mesh as the counter electrode and SCE as the reference electrode in aqueous solution and CE (1 M LiCl) in ACN solution. The ferrocene/ferrocenium couple

appeared at $E_{½}$ = 0.36 V vs CE (1 M LiCl) in 0.1 M $TBABF_4$-ACN solution. The working electrode (GC, PPF or HOPG) used is specified in the text.

Electrochemistry. CVs of aryldiazonium salts were recorded in 0.1 M $TBABF_4$-ACN solution degassed for 5 min by purging with N_2(g). Unless specified otherwise, CVs were obtained immediately after the working electrode was immersed in the solution. Between each experiment, GC electrodes were freshly polished with 1 μm alumina/water slurry, and sonicated in water for 5 min and dried with a stream of N_2(g). A fresh HOPG surface was prepared between each experiment using adhesive tape to remove the top graphite layers. To reduce the nitrophenyl (NP) groups on the modified electrodes, the modified electrodes were first sonicated in ACN for 1 min (for plate electrodes) or 5 min (for GC disks electrode) and dried with a stream of N_2(g) prior to scanning in 0.1 M H_2SO_4 at a scan rate of 100 mV s^{-1}.

Cell setup. Two types of GC working electrodes were used in this chapter: GC disks (area = 0.071 cm^2) and GC plates (area is defined by the O-ring used, 0.290 cm^2 for grafting and 0.106 cm^2 for NP reduction). For GC disks, a standard three-electrode glass cell was used. For GC plates, PPF and HOPG, a glass cell with a hole in the base was used. A working electrode (GC plates, PPF or HOPG) was positioned between the metal base holder and the glass cell. A Kalrez O-ring was placed between the electrode surface and the glass cell to provide a seal to prevent leakage of solution, and a strip of copper was placed onto the electrode to maintain electrical contact (See Chapter 2 for details of the setup).

7.3 Results

One of the interesting characteristics of aryldiazonium ions is the low reduction potential, which is due to the strong electron-withdrawing effect of the N_2^+ group. As the R-group, at the *para* position becomes more electron-withdrawing, the reduction potential shifts to more

positive potential.[1] This ease of reduction allows surface modification to occur spontaneously at graphitic carbon without applied potential.[43] Moreover, Cline and co-workers[13] demonstrated that soaking the GC electrode in the diazonium ion solution diminished the intensity of peak 1. Therefore, unless stated otherwise, to minimise the spontaneous reaction, the CVs were recorded immediately after the working electrode was immersed in the aryldiazonium salt solution.

7.3.1 Investigation at GC electrodes

7.3.1.1 CVs of different para substituent aryldiazonium salts

As can be seen from Table 7.1, aryldiazonium salts are not always reported to show two reduction peaks. Therefore, CVs of range of aryldiazonium salts were obtained at freshly polished GC electrodes under standard conditions. Figure 7.10 shows the CVs of ten different aryldiazonium salts at 1 mM concentration obtained in 0.1 M $TBABF_4$-ACN at a GC electrode using a scan rate of 100 mV s^{-1}. Four types of responses are observed from these CVs. i) Two well-separated peaks on the first scan with very low current on the return scan and a featureless low current on subsequent scans (Figures 7.10a–c). This is consistent with rapid formation of a blocking layer. ii) Two well-separated peaks on the first scan with a small current on the return scan and a broad peak on the second scan followed by a featureless low current on the third scan (Figures 7.10d–f). This suggests a blocking film forms more slowly than for diazonium ions in group (i). iii) Three reduction peaks on the first scan, where the first two peaks at the more positive potential merge together followed by a distinct peak at the most negative position. The first return scan and subsequent scans are similar to (ii) above (Figure 7.10g). iv) On the first scan, the first peak is relatively small and merges with the second peak. On the reverse scan and subsequent forward scan, significant reduction currents are recorded, with the peak potential shifted negative as the scan number

increases (Figures 7.10h–j). These CVs suggest that a blocking film forms most slowly for these derivatives.

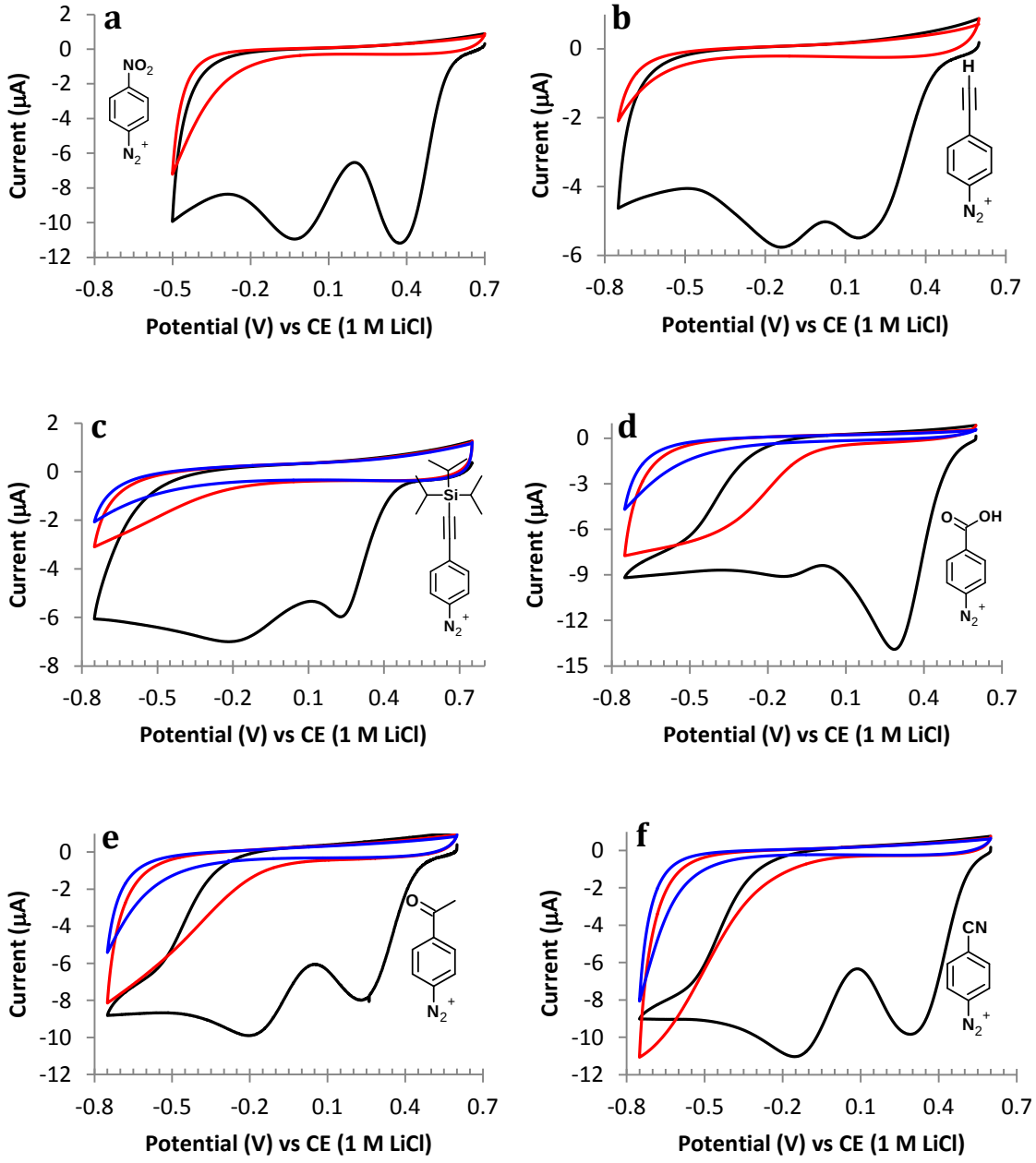

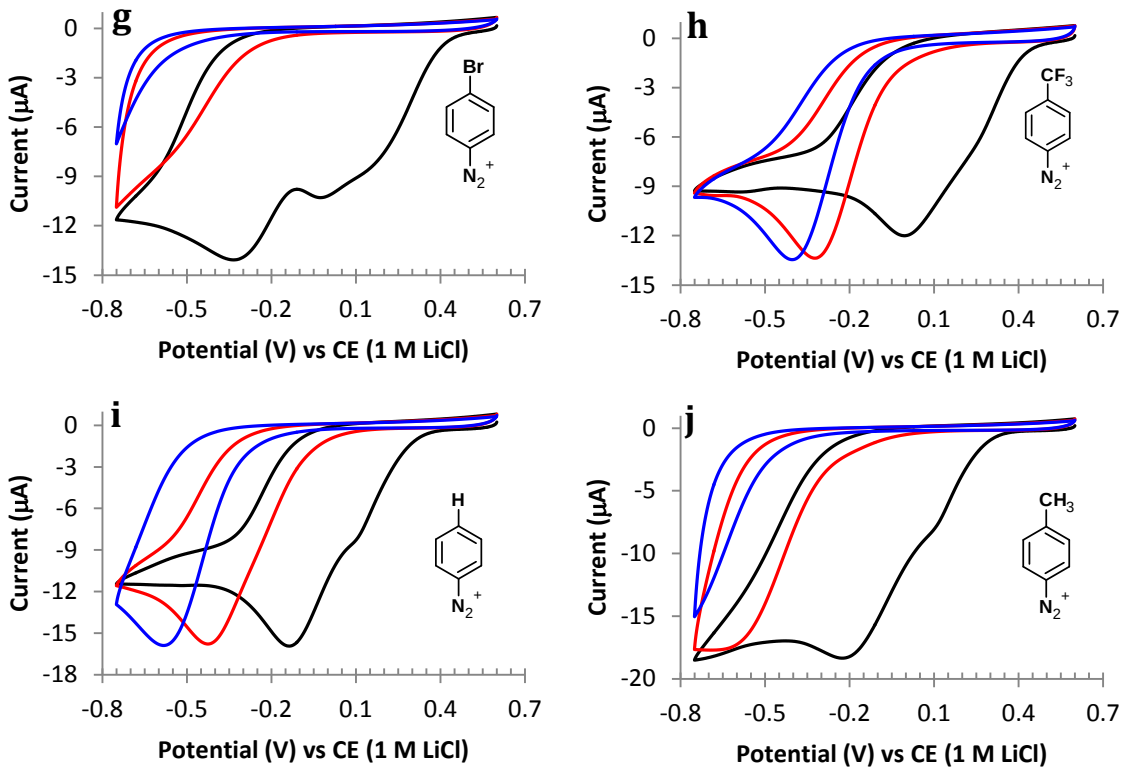

Figure 7.10 CVs at GC electrode obtained in 0.1 M $TBABF_4$-ACN solution containing 1 mM of: a) NBD, b) Eth-Ar-N_2^+, c) TIPS-Eth-Ar-N_2^+, d)HOOC-Ar-N_2^+, e) CH_3OC-Ar-N_2^+, f) NC-Ar-N_2^+, g) Br-Ar-N_2^+, h) F_3C-Ar-N_2^+, i) H-Ar-N_2^+, and j) H_3C-Ar-N_2^+. Black line: 1st scan, red line: 2nd scan, and blue line: 3rd scan. Scan rate = 100 mV s^{-1}.

An alternative explanation may account for the behaviour of H-Ar-N_2^+. Reduction of H-Ar-N_2^+ at metal electrodes has been reported to result in conductive polyphenylene films.[44] Therefore, the CVs of Figure 7.10i may indicate grafting of a conductive polyphenylene film on the GC surface, and thus electron transfer between the electrode surface and diazonium ion in solution is still possible during repeat scans. The shift in potential may be due to the build-up of a moderately conductive layer upon cycling and slowing of electron transfer to diazonium ion in solution.

Reduction of F_3C-Ar-N_2^+ is reported to result in grafted layers.[5, 28, 45] McCreery and co-workers[28, 45] reported CVs recorded at a PPF electrode in a 5 mM solution of F_3C-Ar-N_2^+ in

0.1 M $TBABF_4$-ACN. The first scan showed an irreversible reduction peak, similar to those observed on scans that do not lead to surface modification (Figure 7.2). On subsequent scans a very small decrease in current and a negative shift in potential was observed. It was stated that very low current was observed only after five cycles,[28] and thoroughly degassed ACN was necessary to achieve a high coverage.[45] The CVs shown in Figure 7.10h are consistent with McCreery's observations and it is assumed that little film is grafted under these conditions.

Reduction of H_3C-Ar-N_2^+ also leads to a slow rate of grafting (Figure 7.10j), where a low current is only observed after the third cycle. However, when the concentration of this diazonium salt is increased to 5 mM, a reduction peak at a more negative potential ($E_{p,c}$ = -0.5 V) is recorded on the first scan (Figure 7.11). On the subsequent scans, only featureless low currents are detected, indicating formation of a blocking film. This suggests that the rate of modification is slower in 1 mM concentration than in 5 mM concentration, as expected.

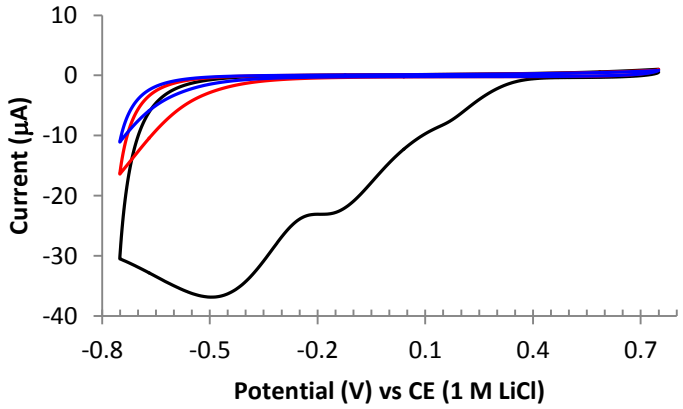

Figure 7.11 CVs at a GC electrode obtained in 5 mM of H_3C-Ar-N_2^+ in 0.1 M $TBABF_4$-ACN at a scan rate of 100 mV s^{-1}. Black line: 1st scan, red line: 2nd scan, and blue line: 3rd scan.

7.3.1.2 Reduction of NBD at varying scan rate

To further investigate the origin of the two reduction peaks, NBD was chosen as the model aryldiazonium salt because it is the most widely studied aryldiazonium ion and gives two

distinct reduction peaks. Figure 7.12 shows the CVs of 1 mM NBD in 0.1 M $TBABF_4$-ACN obtained at different scan rates. As the scan rate increases the potentials of peak 1 and peak 2 shift to slightly more negative values, and the current of peak 1 increases and the magnitude of peak 2 decreases relative to peak 1. At the highest scan rate (500 mV s^{-1}), peak 2 disappears and only peak 1 is observed. From the CVs recorded at fast scan rate (Figure 7.12b), it can be seen that on the reverse scan, the response is similar to that obtained when there is no, or slow, surface modification. Moreover, at fast scan rate, the shape of peak 1 on the first scan is less symmetrical compared to those obtained at slow scan rate and an irreversible peak appears on the second scan (Figures 7.12d). This peak at more negative potentials is assumed to be analogous to peak 2 (present at slower scan rates).

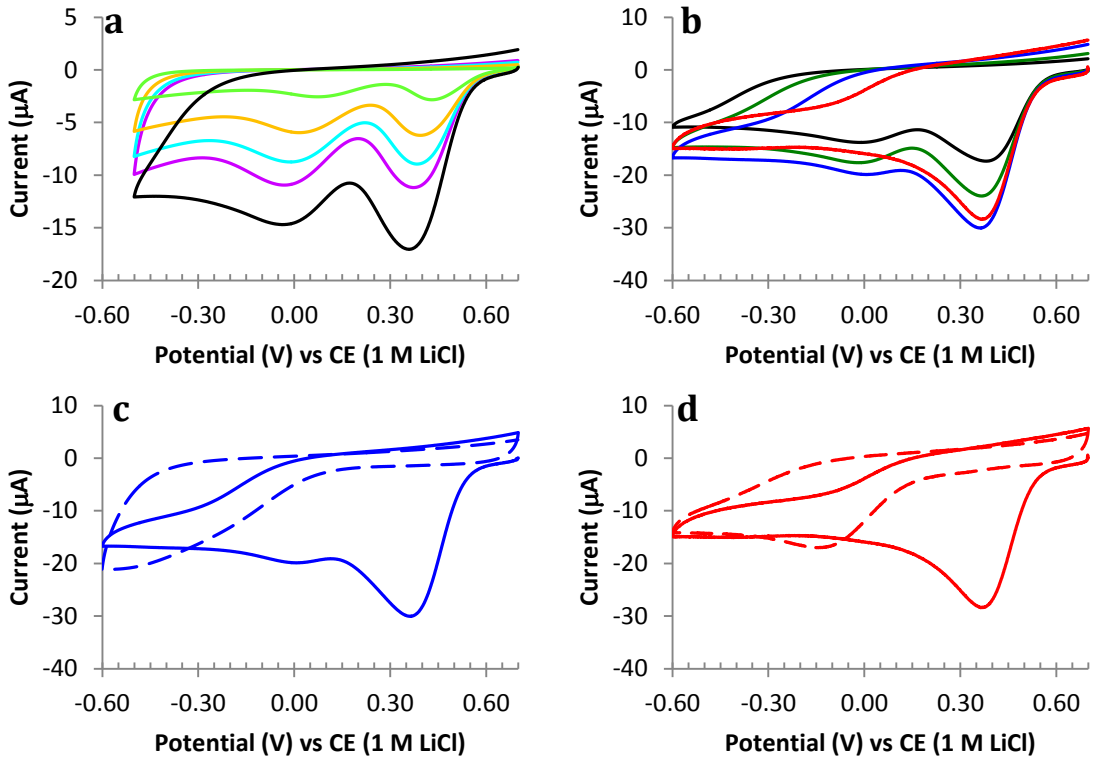

Figure 7.12 CVs obtained at GC in a solution of 1 mM NBD in 0.1 M $TBABF_4$-ACN at: a, b) different scan rate, c) 0.4 V s^{-1}, and d) 0.5 V s^{-1}. Solid line: 1st scan; dashed line: 2nd scan. Light green line: 0.02 V s^{-1}, yellow line: 0.05 V s^{-1}, aqua line: 0.08 V s^{-1}, purple line: 0.1 V s^{-1}, black line: 0.2 V s^{-1}, green line: 0.3 V s^{-1}, blue line: 0.4 V s^{-1}, red line: 0.5 V s^{-1}.

Plots of reduction peak current against the scan rate and square root of scan rate are shown in Figure 7.13. For a surface bound species or a redox species in a thin layer of solution or film, peak currents are proportional to the scan rate, while for a diffusion controlled species, peak currents are proportional to the square root of scan rate.[46] As can be seen from Figure 7.13a, at a slow scan rate the currents of peak 1 and peak 2 are proportional to scan rate, but as the scan rate increases, both peaks show a weaker dependency on scan rate. Tentatively, this suggests less adsorption as the scan rate increases. From Figure 7.13b, the current of peak 1 (blue points) is not proportional to square root of scan rate, while the currents of peak 2 (red points) show reasonable proportionality to the square root of scan rate (R^2 = 0.96). This may indicate that peak 2 is a diffusion controlled process, although the shape of peak 2 is more symmetrical than expected for a diffusion controlled process. Moreover, because reduction of NBD is an irreversible process and the reduction leads to modification of the electrode surface and formation of a blocking film, the peak currents and shapes of the CVs become more difficult to interpret.

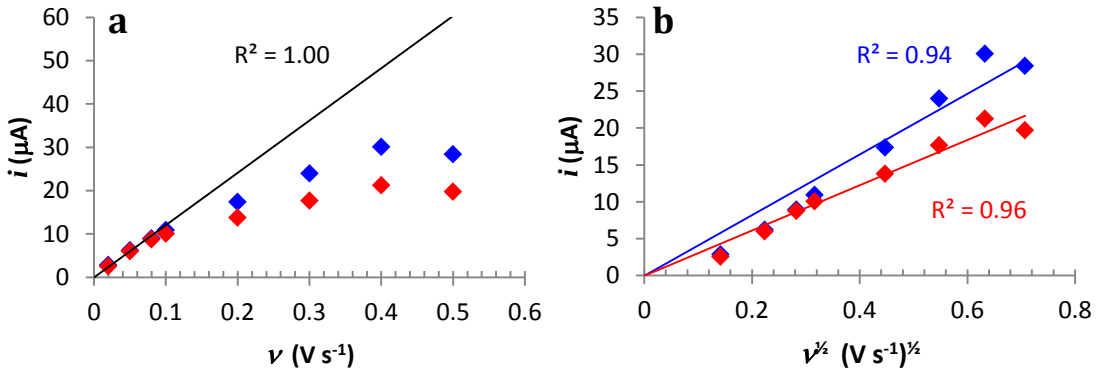

Figure 7.13 a) plot of current against scan rate; b) plot of current against square root of scan rate. Blue: peak 1; red: peak 2. The black line is best fit of the first four points at low scan rate forced through the origin. The red and blue lines are best fit lines of all of the data points forced through the origin.

7.3.1.3 Effect of surface pre-treatment on the NBD reduction

When the GC electrode was immersed in the NBD solution for 30 min prior to collecting the CV (Figure 7.14, red line), peak 1 is diminished compared to the CV that was recorded immediately (black line), while no change was observed for peak 2. Furthermore, the reduction potential of peak 1 is shifted to a more negative value. This observation is similar to that reported by Cline and co-workers,[13] where peak 1 was still present but small compared to peak 2 after immersion in diazonium ion solution for 1 hour. Figure 7.14, blue line, shows that when a 'dirty' GC electrode was used for grafting (GC was left in ferri/ferrocyanide solution for approximately 10 min), peak 1 is almost gone, but peak 2 is somewhat larger than that obtained at freshly polished GC.

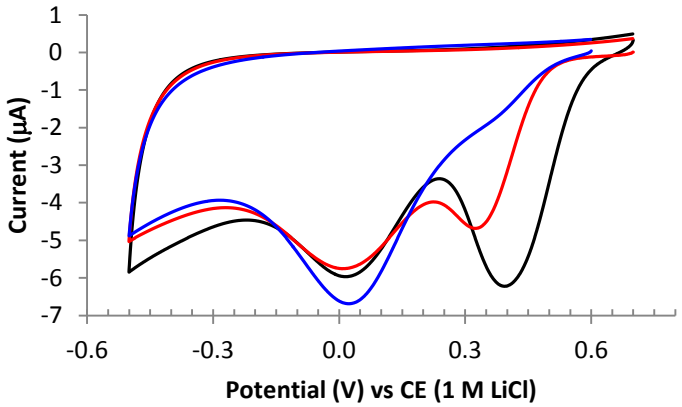

Figure 7.14 First scan of CVs obtained in a solution of 1 mM NBD in 0.1 M $TBABF_4$-ACN at: Black line: freshly polished GC, red line: GC immersed in the NBD solution for 30 min before scan was recorded, blue line: 'dirty' GC. Scan rate = 50 mV s^{-1}.

A similar response was obtained when a CV of TIPS-Eth-Ar-N_2^+ was recorded at a surface already modified with a sparse monolayer of H-COO-Ar groups (Figure 7.15). These results all demonstrate that the relative size and potential of peak 1 depends strongly on the conditions of the surface, while peak 2 does not. From these results, it appears that when peak 2 only is observed on the first scan, this is because peak 1 has shifted to more negative

potential and merged with peak 2. For example, the single reduction peak in Figure 7.1A is assigned to peak 2 with a contribution from merged peak 1.

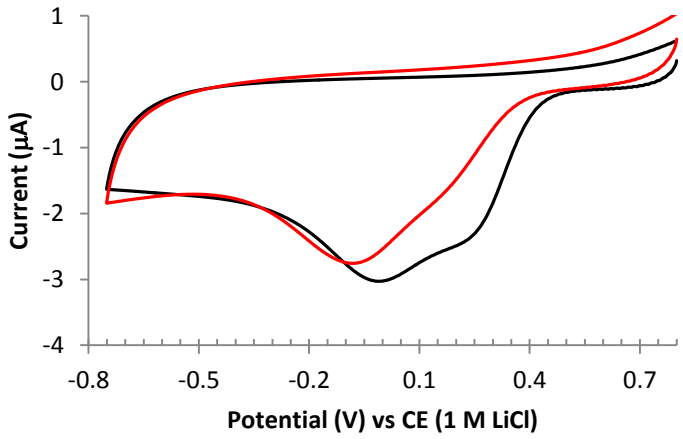

Figure 7.15 First scan of CVs obtained in a solution of 5 mM N_2^+-Ar-Eth-TIPS in 0.1 M $TBABF_4$-ACN at: Black line: freshly polished GC; red line: GC grafted with a monolayer of Ar-COOH (via reduction of N_2^+-Ar-COO-Fm followed by deprotection of Fm group, Chapter 5). Scan rate = 50 mV s^{-1}.

A similar experiment to that of Benedetto and co-workers[36] (Figure 7.5b) was carried out where the GC was first scanned five times from 0.75 to 0.25 V (Figure 7.16, black line) followed by another five cycles from 0.75 to -0.45 V (red line) in 1 mM NBD at 100 mV s^{-1}. As shown by the black line, one reduction peak at 0.37 V (peak 1) is seen on the first scan, and disappears on the subsequent scans. When the same electrode was scanned to -0.45 V (red line), peak 1 is not visible anymore, but peak 2 ($E_{p,c}$ = -0.03 V) appears. The size of peak 2 is similar to that of a CV recorded directly to -0.45 V (dashed line). This indicates that peak 2 is not affected by the first repeat scans up to 0.25 V and that the modified layer formed after these first repeat scans only gives a thin or porous layer so that electron transfer between the GC surface and diazonium ions in solution is still possible.

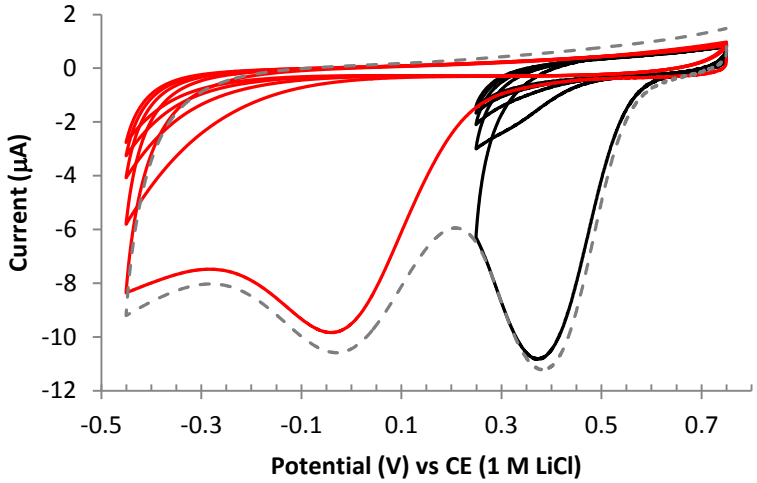

Figure 7.16 CVs obtained in 1 mM NBD in 0.1 M $TBABF_4$-ACN on a GC electrode at a scan rate of 100 mV s^{-1}. Black solid line was collected on freshly polished GC by scanning five cycles from 0.75 to 0.25 V. Red solid line was recorded on the GC surface after the black line CVs by scanning five cycles from 0.75 to -0.45 V. Grey dashed line was recorded on a freshly polished GC by scanning one cycle from 0.75 to -0.45 V.

Figure 7.17 shows the responses of a GC electrode in dopamine (1 mM in 0.1 M H_2SO_4) and ferrocene (1 mM in 0.1 M $TBABF_4$-ACN) after four different modification procedures (Table 7.2). As mentioned in previous chapters, dopamine is an inner sphere redox probe, where the rate of electron transfer is affected by the ability of dopamine to adsorb on the surface,[47] while ferrrocene is an outer sphere redox probe and electron transfer occurs by tunnelling.[48] As seen from Figure 7.17a, the dopamine response is totally blocked after a grafting potential more negative than peak 2 was applied (black and green lines, procedures I and II). When a potential more positive than peak 2 was applied for NBD modification, the dopamine redox response is observed (red and blue lines, procedures III and IV). The response is typical of slow electron transfer or electron transfer through pin holes, indicating that scanning past peak 1 only, creates a porous surface film that has sites available for dopamine adsorption. Scanning past peak 2 creates a dense layer that inhibits the adsorption of dopamine. This is further supported by the ferrocene redox response CVs (Figure 7.17b) which shows no

inhibition of electron transfer to ferrocene after modification by scanning past peak 1 only, but strong inhibition after grafting by scanning more negative than peak 2.

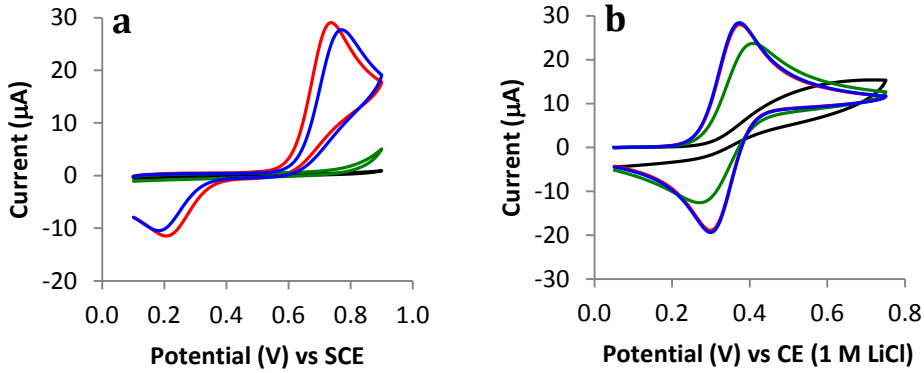

Figure 7.17 CVs obtained in: a) 1 mM dopamine in 0.1 M H_2SO_4; b) 1 mM ferrocene in 0.1 M $TBABF_4$-ACN at a GC electrode modified with 1 mM NBD (in 0.1 M $TBABF_4$-ACN) by: scanning five cycles from 0.75 to 0.25 V followed by five cycles from 0.75 to -0.45 V at a scan rate of 100 mV s^{-1} (black line, procedure I); scanning one cycle from 0.75 to -0.45 V at a scan rate of 100 mV s^{-1} (green line, procedure II); scanning five cycles from 0.75 to 0.25 V at a scan rate of 100 mV s^{-1} (red line, procedure III); applying potential of 0.45 V for 300 s (blue line, procedure IV).

Table 7.2 List of modification conditions at GC electrode in 1 mM NBD (+ 0.1 M $TBABF_4$-ACN) and the corresponding surface concentration of NP groups.

Procedure	Modification conditions	Γ_{NP} [a] (× 10^{-10} mol cm^{-2})
I	Scan 5× from 0.75 to 0.25 V followed by 5× from 0.75 to -0.45 V at 100 mV s^{-1}	18.2 ± 0.6
II	Scan 1× from 0.75 to -0.45 V at 100 mV s^{-1}	18.8 ± 0.9
III	Scan 5× from 0.75 to 0.25 V at 100 mV s^{-1}	14.5 ± 0.2
IV	Applied potential of 0.45 V for 300 s	17.5 ± 0.2

[a]Calculated from CVs recorded in 0.1 M H_2SO_4. Average value of two repeat experiments and the uncertainties indicate the range of values obtained

The NP surface concentrations for grafting carried out by the four procedures are listed in Table 7.2. For GC electrodes modified by procedure I, the surface concentration of NP groups is calculated to be (18.2 ± 0.6) × 10^{-10} mol cm^{-2}, which corresponds to a multilayer film. The calculated surface concentration of a closely packed monolayer of NP groups on a flat surface is 12 × 10^{-10} mol cm^{-2},[49] while the experimentally determined monolayer

equivalent of NP groups is estimated to be $(2.5 \pm 0.5) \times 10^{-10}$ mol cm^{-2}.[11] Surprisingly, when the GC electrode is modified using procedure II, the surface concentration of NP groups is similar to that obtained for procedure I. The grafting conditions for procedure II are expected to generate a thinner film than for procedure I because there are fewer potential scans past peak 2. Additionally, the CVs of Figure 7.17 show a less blocking film after procedure II (green line) than procedure I (black line). Hence, it is likely that not all of the NP groups grafted by procedure I are electroactive. This is a well-established characteristic of thick layers and presumably only the NP groups at the outer layer that are accessible by the electrolyte/solvent are electroactive.[50, 51] When GC electrodes are modified by procedures III and IV, the surface concentrations of NP groups are also greater than that expected for a monolayer. Again this is surprising because Figure 7.17a shows that the dopamine response is well-defined at these surfaces and there is no inhibition of the ferrocene response (Figure 7.17b). Therefore, these results suggest that for modification by electroreduction of NBD, applying a potential more positive than peak 2 results in a porous multilayer, while applying a potential more negative than peak 2, gives a densely packed multilayer.

7.3.2 Investigations at HOPG

To further investigate the influence of electrode surface properties on the electroreduction of diazonium ions in ACN solution, CVs were recorded in NBD solution at GC, PPF and HOPG plate electrodes. To enable easy comparison of data, all aryldiazonium reduction CVs were obtained using the same O-ring to define the electrode area. Figure 7.18a shows the CVs obtained in a solution of 1 mM NBD in 0.1 M $TBABF_4$-ACN solution at GC (black line), PPF (blue line) and HOPG (red line). For these experiments CVs were recorded 2 min after the electrodes were exposed to the diazonium ion solution. Due to the cell set-up used for the plate electrodes, some time is required after the introduction of solution into the cell, to make

sure there is no leakage and no gas bubbles trapped between the O-ring and the glass cell. Therefore, 2 min was adopted as the standard 'wait' time.

As seen from the CVs in Figure 7.18a, the diazonium ion reduction at PPF is similar to that obtained at GC, where two distinct reduction peaks are observed on the first scan. However, the peak 1 current at PPF is smaller than at GC. On the other hand, at HOPG peak 1 is large and at a more negative potential compared to GC and PPF. Peak 2 is very small and broad, and there is significant reduction current over a broad potential range. The negative shift in potential found at HOPG is likely due to a kinetically slower process at HOPG compared to GC and PPF. The CVs recorded at HOPG are not reproducible; sometimes two closely merged peaks are observed as shown in Figure 7.18b. The irreproducibility is presumably because of not forming a reproducible fresh HOPG surface between each repeat experiment. The CVs for reduction of the modified surfaces obtained in 0.1 M H_2SO_4 are shown in Figure 7.18c. It can be seen that similar NP reduction responses are obtained at GC and PPF, while a much smaller current for NP reduction is obtained at HOPG. Table 7.3 lists the charges passed during reduction of NBD and the charges associated with the NP reduction peaks at each surface. The corresponding NP surface concentrations are also listed. Even though the charge passed for the reduction of NBD at HOPG is greater than at GC or PPF, the charge for NP reduction at modified HOPG is only a third that obtained at modified GC and PPF. At GC and PPF, ~60% of diazonium ions reduced gave surface immobilised NP groups. For HOPG, the corresponding value is ~10%. It has previously been noted that the yield of grafting is not 100%, because some of the radicals escape and react in the solution.[1] Savéant and co-workers[1] calculated that for NBD reduction at GC, 84% of electrochemically generated radicals couple to the surface, while at HOPG only 56% couple to the surface. These are higher yields than obtained in this work. This difference may be due to the method used to calculate the yield of reaction; the yield reported by Savéant and co-workers[1] is based on

simulating the current-potential curves for repeat CVs obtained at HOPG and GC in NBD solution. Furthermore, the CVs of NBD at HOPG reported by those authors have a different appearance to those obtained in this work, therefore different yields are not surprising.

Another factor in the lower grafting yields calculated in this work is that during the 2 min wait time, NP groups will graft to GC and PPF through spontaneous reduction of NBD. The presence of these groups will decrease the apparent grafting yield. A slower or negligible spontaneous grafting of NP groups to HOPG may account for the larger peak 1 for NBD reduction seen at this surface. It should be noted that the surface concentration of NP groups at GC and PPF, listed in Table 7.3, are higher than commonly observed. This is tentatively attributed to the difficulty of determining the accessible surface area with using an O-ring on a plate electrode. In other words it is not known which part of the O-ring (inner or outer edge, or halfway across) defines the actual geometric area of the electrode. However, the same O-ring was used for all measurements and hence the trend in NP concentrations is reliable.

The lower yield for NP immobilisation at HOPG than at PPF and GC found in this work is consistent with a different mode of film formation at HOPG, as determined by STM. STM investigation showed that electroreduction of aryldiazonium to aryl radical at the HOPG surface leads to covalent bonding only at the step edges and defect sites, and only physisorbed material on the basal plane.[52] Presumably less material may be deposited by physisorption, and deposited material may be more easily removed during sonication, than for covalently grafted film on GC and PPF.

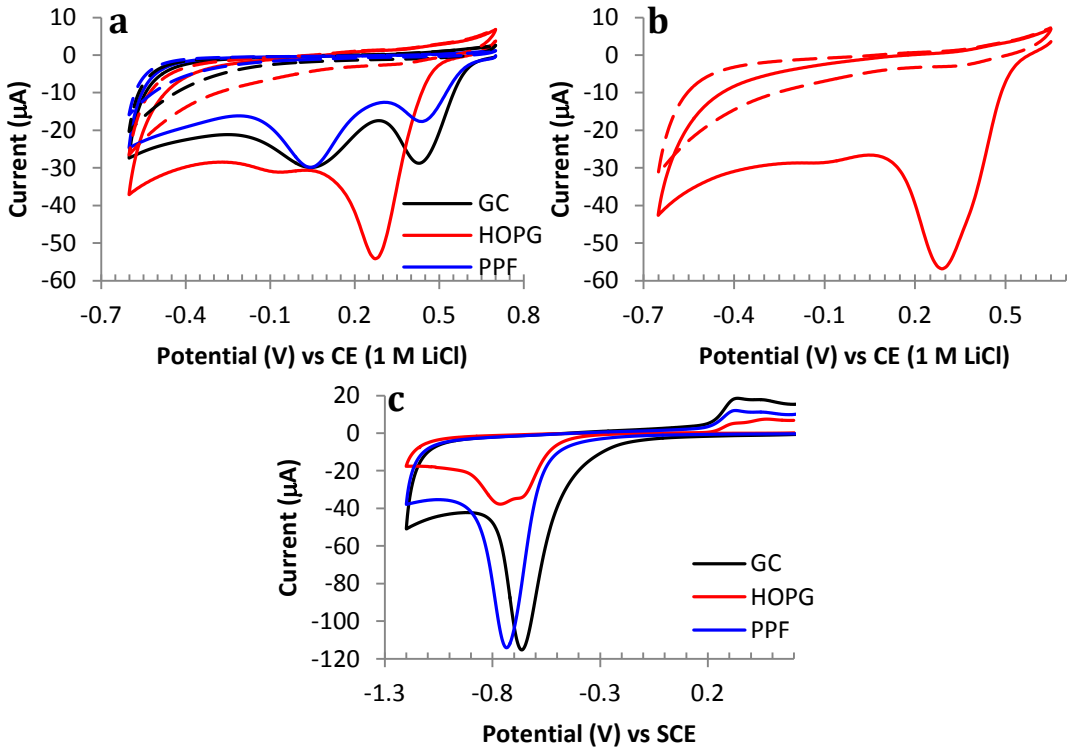

Figure 7.18 CVs obtained in a solution of: a, b) 1 mM NBD in 0.1 M $TBABF_4$-ACN at a scan rate of 50 mV s^{-1}, c) 0.1 M H_2SO_4 at a scan rate of 100 mV s^{-1} of the modified electrodes. Black line: GC plate, red line: HOPG, blue line: PPF. Solid line: 1st scan, dashed line: 2nd scan.

Table 7.3 Charges associated with the electroreduction of NBD at GC, PPF, and HOPG and the corresponding NP surface concentration

Electrode	Charge for NBD reduction (mC cm^{-2})	Charge for NP reduction (mC cm^{-2})	Γ_{NP} (× 10^{-10} mol cm^{-2})	Apparent yield of film formed[a]
GC plate	0.70	2.1	36.4	51%
PPF	0.52	2.0	34.5	64%
HOPG	0.99	0.73	12.6	12%

[a]yield = charge for NP reduction / (6 × charge for NBD reduction)

To examine whether the process at peak 1 of NBD reduction at HOPG is due to the same process as that at GC, experiments were undertaken in which the CVs were collected at HOPG at varying scan rate (Figure 7.19a). As the scan rate increases the reduction peak potential shifts negative, and significant reduction currents are detected on the return scan. This suggests little film is formed as scan rate increases, similar to GC. However, in contrast to GC, at fast scan rate (500 mV s^{-1}) peak 1 is still present on repeat scans although with

lower current (Figure 7.19b). This different behaviour is attributed to the different type of layer formed at HOPG.

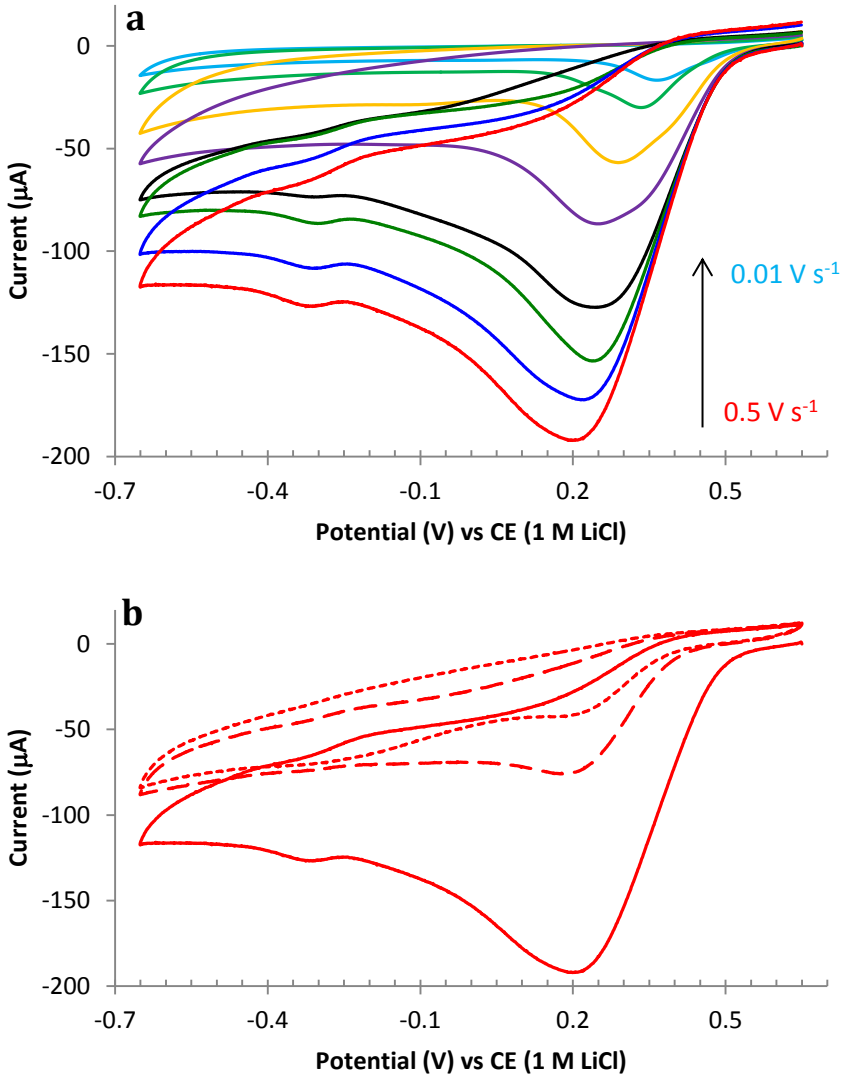

Figure 7.19 CVs obtained at HOPG in a solution of 1 mM NBD in 0.1 M $TBABF_4$-ACN at: a) varying scan rate; b) 0.5 V s^{-1}. Aqua line: 0.01 V s^{-1}, light green line: 0.02 V s^{-1}, yellow line: 0.05 V s^{-1}, purple line: 0.1 V s^{-1}, black line: 0.2 V s^{-1}, green line: 0.3 V s^{-1}, blue line: 0.4 V s^{-1}, red line: 0.5 V s^{-1}. Solid line: 1st scan; dashed line: 2nd scan; dotted line: 3rd scan.

Figure 7.20 shows the plots of reduction peak current against the scan rate at HOPG. The reduction current of NBD is proportional to the square root of scan rate (Figure 7.20a) and not proportional to the scan rate (Figure 7.20b), evidently the aryldiazonium ion reduction is a diffusion controlled process at HOPG. This observation is different to that observed at GC, where the peak 1 is neither proportional to scan rate nor to square root of scan rate.

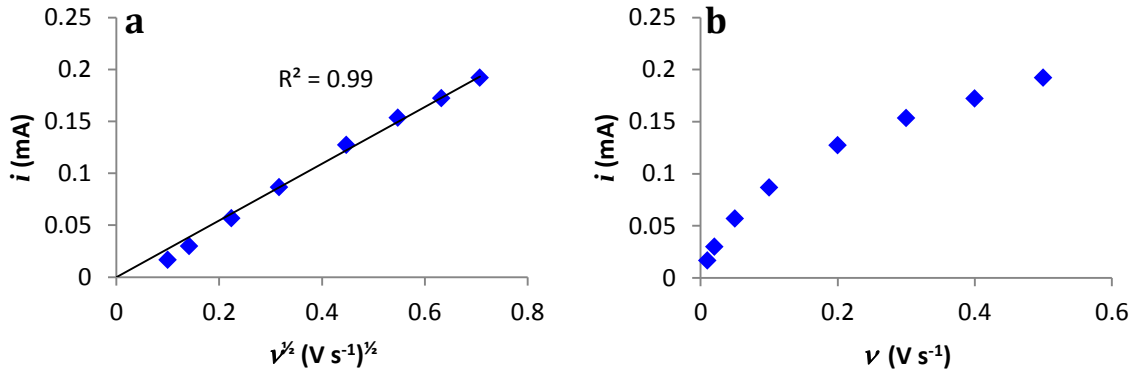

Figure 7.20 Plot of aryldiazonium ion reduction current at HOPG against: a) square root of scan rate; b) scan rate. The best fit line is determined from all of the data points and forced through the origin.

7.4 Discussion

Key findings from this work and the literature which need to be accounted for when considering the origin of the two reduction peaks for aryldiazonium ion reduction are: i) the two peaks commonly observed do not arise from successive reduction of aryldiazonium ion to aryl radical (peak 1) followed by reduction of the aryl radical to aryl anion (peak 2); ii) at scan rates ≤ 500 mV s^{-1}, two peaks are only observed when a film is formed; iii) the CV response depends on the aryldiazonium derivative and on the type of carbon surface and its 'cleanliness' or pre-treatment; iv) both peak 1 and peak 2 correspond to reduction of aryldiazonium ion; v) peak 1 diminishes in size as immersion time in diazonium ion solution increases; vi) covalent attachment of the film to the surface is not essential for observation of two or multiple peaks (at HOPG, physisorbed films are formed on the surface); vii) the potential and magnitude of peak 1, but not peak 2, is strongly dependent on the surface condition; viii) deposition of film occurs at both reduction peaks.

From all of these findings at GC, it is likely that peak 1 corresponds to reduction of aryldiazonium ions to aryl radicals at a 'clean' electrode and peak 2 corresponds to reduction of aryldiazonium ions at the already deposited layers. This suggestion is consistent with the

fact that, when a film is formed, peak 1 is only observed during the first scan, indicating that a very 'clean' surface is required to observe this peak and peak 2 is only observed when a significant amount of film is formed. For example, for modification that does not lead to grafting, only peak 1 is observed (Figure 7.2). Grafting of $H_3C\text{-}Ar\text{-}N_2^+$ at low concentration (1 mM) shows only one main reduction peak (Figure 7.10j), but if the concentration is increased to 5 mM, another peak at more negative potential is observed (Figure 7.11). This indicates that at low concentration, the rate of grafting is slow and at the peak 2 potential there is no observable peak due to not enough build-up of film. However, when the concentration is increased to 5 mM, the grafting is more efficient and therefore peak 2 is observed.

This proposal is also consistent with the variable scan rate experiments at GC. At fast scan rate (Figure 7.12d), only peak 1 is observed on the first scan because grafting is progressing at a relatively slow rate and only peak 2 is observed on the second scan presumably because sufficient film has been deposited by the end of the first cycle. Thus, it is tentatively proposed that two reduction peaks are seen when the surface is modified because reduction of aryldiazonium ion at the 'clean' surface (to give an immobilised layer) is thermodynamically and kinetically more facile (peak 1) than reduction at the already modified surface (peak 2).

The effect of surface pre-treatment experiments is consistent with the explanation outlined above. At a 'dirty' electrode, peak 1 is very small, because a 'clean' electrode is required for the observation of peak 1. Electroreduction at a more positive potential than peak 2 results in a porous film that even after repeat scans cannot block the surface for dopamine electrochemistry (Figure 7.17a). This implies that specific areas of the electrode surface are required for peak 1 reduction. Electroreduction past the peak 2 potential results in a densely packed film that blocks dopamine electron transfer. This suggests that the surface 'sites' that

are available for dopamine adsorption before peak 2 reduction are now unavailable. Hence, the electron transfer for reduction of diazonium ion at peak 2 occurs at the bare sites in the porous film or across the film. It is difficult to distinguish whether the electron transfer occurs across the film or at the bare sites of the porous film because the net result is a denser film.

The larger current for peak 1 at HOPG than at GC and PPF might suggest that the peak 1 reduction process involves basal plane sites. However, GC is considered to consist mainly of edge plane sites,[53] and hence the current for peak 1 at GC is too large to correspond to reduction at basal plane sites only. A more reasonable explanation for the larger peak 1 current at HOPG than at GC and PPF is that for the latter electrodes, peak 1 is 'terminated' by grafting of aryl groups to active sites during reduction at peak 1, whereas at HOPG, active sites are not blocked by the physisorbed film. For NBD reduction at GC, the plot of peak 1 current against square root of scan rate in Figure 7.13b (blue coloured) shows upward curvature consistent with the expected decrease in truncation of the current as the scan rate increases and the amount of grafting decreases. The linear peak current versus square root of scan rate relationship observed for peak 1 at HOPG (Figure 7.20a) supports this explanation. After scanning through peak 1, the physisorbed film formed at HOPG, presumably does not have a well-defined porous structure and hence electron transfer to diazonium ions occurs at a range of rates giving the observed reduction current over a wide potential range.

Analysis of aryldiazonium ion reduction voltammetry is complicated by the irreversibility of the reduction process and because film formation leads to blocking of the electrode surface towards redox species in solution. Therefore, it is difficult to compare these CVs to the classical electrochemical mechanisms. To be able to further understand the origin of the two reduction peaks, computational stimulation of these processes is required.

7.5 Conclusion

In an attempt to understand the origin of two reduction peaks for aryldiazonium salts at carbon electrodes, a series of experiments were conducted at GC and HOPG. The CVs of different *para* substituted aryldiazonium ions were recorded at GC electrodes and the results suggest that the observation of two well-defined reduction peaks is dependent on the type of aryldiazonium salt used. Reduction of NBD was studied in detailed. An important new finding is that modification of GC electrodes by electroreduction at the peak 1 potential results in a porous multilayer that does not affect reduction at peak 2, whereas modification by electroreduction past the peak 2 potential results in a densely-packed multilayer. When reduction of NBD was carried out at HOPG, peak 1 was shifted to a more negative potential compared to at GC and significant reduction current up to the switching potential was detected after peak 1. The different behaviour obtained at HOPG and GC is attributed to the different type of layers formed after peak 1 reduction. Overall, all of these results tentatively suggest peak 1 corresponds to reduction of aryldiazonium ions to aryl radicals at a 'clean' GC electrode, and peak 2 corresponds to reduction of aryldiazonium ions to aryl radical at the already grafted layer.

7.6 References

1 Allongue, P., Delamar, M., Desbat, B., Fagebaume, O., Hitmi, R., Pinson, J., Saveant, J.M., Covalent modification of carbon surfaces by aryl radicals generated from the electrochemical reduction of diazonium salts. *J. Am. Chem. Soc.*, **1997**, *119*, 201.

2 Andrieux, C.P., Pinson, J., The standard redox potential of the phenyl radical/anion couple. *J. Am. Chem. Soc.*, **2003**, *125*, 14801.

3 Pinson, J., Podvorica, F., Attachment of organic layers to conductive or semiconductive surfaces by reduction of diazonium salts. *Chem. Soc. Rev.*, **2005**, *34*, 429.

4 Abiman, P., Crossley, A., Wildgoose, G.G., Jones, J.H., Compton, R.G., Investigating the thermodynamic causes behind the anomalously large shifts in pK_a values of benzoic acid-modified graphite and glassy carbon surfaces. *Langmuir*, **2007**, *23*, 7847.

5 Adenier, A., Barre, N., Cabet-Deliry, E., Chausse, A., Griveau, S., Mercier, F., Pinson, J., Vautrin-Ul, C., Study of the spontaneous formation of organic layers on carbon and metal surfaces from diazonium salts. *Surf. Sci.*, **2006**, *600*, 4801.

6 Adenier, A., Cabet-Deliry, E., Chausse, A., Griveau, S., Mercier, F., Pinson, J., Vautrin-Ul, C., Grafting of nitrophenyl groups on carbon and metallic surfaces without electrochemical induction. *Chem. Mater.*, **2005**, *17*, 491.

7 Baranton, S., Belanger, D., Electrochemical derivatization of carbon surface by reduction of in situ generated diazonium cations. *J. Phys. Chem. B*, **2005**, *109*, 24401.

8 Baranton, S., Belanger, D., In situ generation of diazonium cations in organic electrolyte for electrochemical modification of electrode surface. *Electrochim. Acta*, **2008**, *53*, 6961.

9 Bernard, M.C., Chausse, A., Cabet-Deliry, E., Chehimi, M.M., Pinson, J., Podvorica, F., Vautrin-Ul, C., Organic layers bonded to industrial, coinage, and noble metals through electrochemical reduction of aryldiazonium salts. *Chem. Mater.*, **2003**, *15*, 3450.

10 Bradbury, C.R., Kuster, L., Fermin, D.J., Electrochemical reactivity of HOPG electrodes modified by ultrathin films and two-dimensional arrays of metal nanoparticles. *J. Electroanal. Chem.*, **2010**, *646*, 114.

11 Brooksby, P.A., Downard, A.J., Electrochemical and atomic force microscopy study of carbon surface modification via diazonium reduction in aqueous and acetonitrile solutions. *Langmuir*, **2004**, *20*, 5038.

12 Chretien, J.M., Ghanem, M.A., Bartlett, P.N., Kilburn, J.D., Covalent tethering of organic functionality to the surface of glassy carbon electrodes by using electrochemical and solid-phase synthesis methodologies. *Chem.-Eur. J.*, **2008**, *14*, 2548.

13 Cline, K.K., Baxter, L., Lockwood, D., Saylor, R., Stalzer, A., Nonaqueous synthesis and reduction of diazonium ions (without isolation) to modify glassy carbon electrodes using mild electrografting conditions. *J. Electroanal. Chem.*, **2009**, *633*, 283.

14 Delamar, M., Desarmot, G., Fagebaume, O., Hitmi, R., Pinson, J., Saveant, J.M., Modification of carbon fiber surfaces by electrochemical reduction of aryl diazonium salts: Application to carbon epoxy composites. *Carbon*, **1997**, *35*, 801.

15 Delamar, M., Hitmi, R., Pinson, J., Saveant, J.M., Covalent modification of carbon surfaces by grafting of functionalized aryl radicals produced from electrochemical reduction of diazonium salts. *J. Am. Chem. Soc.*, **1992**, *114*, 5883.

16 Downard, A.J., Potential-dependence of self-limited films formed by reduction of aryldiazonium salts at glassy carbon electrodes. *Langmuir*, **2000**, *16*, 9680.

17 Gietter, A.A.S., Pupillo, R.C., Yap, G.P.A., Beebe, T.P., Rosenthal, J., Watson, D.A., On-surface cross-coupling methods for the construction of modified electrode assemblies with tailored morphologies. *Chem. Sci.*, **2013**, *4*, 437.

18 Grivea, S., Mercier, D., Vautrin-Ul, C., Chausse, A., Electrochemical grafting by reduction of 4-aminoethylbenzenediazonium salt: Application to the immobilization of (bio)molecules. *Electrochem. Commun.*, **2007**, *9*, 2768.

19 Harper, J.C., Polsky, R., Wheeler, D.R., Brozik, S.M., Maleimide-activated aryl diazonium salts for electrode surface functionalization with biological and redox-active molecules. *Langmuir*, **2008**, *24*, 2206.

20 Kocak, I., Ghanem, M.A., Al-Mayouf, A., Alhoshan, M., Bartlett, P.N., A study of the modification of glassy carbon and edge and basal plane highly oriented pyrolytic graphite electrodes modified with anthraquinone using diazonium coupling and solid phase synthesis and their use for oxygen reduction. *J. Electroanal. Chem.*, **2013**, *706*, 25.

21 Kullapere, M., Mirkhalaf, F., Tammeveski, K., Electrochemical behaviour of glassy carbon electrodes modified with aryl groups. *Electrochim. Acta*, **2010**, *56*, 166.

22 Kuo, T.C., McCreery, R.L., Surface chemistry and electron transfer kinetics of hydrogen-modified glassy carbon electrodes. *Anal. Chem.*, **1999**, *71*, 1553.

23 Le Floch, F., Bidan, G., Pilan, L., Ungureanu, E.-M., Simonato, J.-P., Carbon substrate functionalization with diazonium salts toward sensor applications. *Mol. Cryst. Liq. Cryst.*, **2008**, *486*, 1313.

24 Le Floch, F., Simonato, J.-P., Bidan, G., Electrochemical signature of the grafting of diazonium salts: A probing parameter for monitoring the electro-addressed functionalization of devices. *Electrochim. Acta*, **2009**, *54*, 3078.

25 Leroux, Y.R., Fei, H., Noel, J.M., Roux, C., Hapiot, P., Efficient covalent modification of a carbon surface: Use of a silyl protecting group to form an active monolayer. *J. Am. Chem. Soc.*, **2010**, *132*, 14039.

26 Leroux, Y.R., Hapiot, P., Nanostructured monolayers on carbon substrates prepared by electrografting of protected aryldiazonium salts. *Chem. Mater.*, **2013**, *25*, 489.

27 Menanteau, T., Levillain, E., Breton, T., Electrografting via diazonium chemistry: From multilayer to monolayer using radical scavenger. *Chem. Mater.*, **2013**, *25*, 2905.

28 Ranganathan, S., McCreery, R.L., Electroanalytical performance of carbon films with near-atomic flatness. *Anal. Chem.*, **2001**, *73*, 893.

29 Richard, W., Evrard, D., Gros, P., New insight into 4-nitrobenzene diazonium reduction process: Evidence for a grafting step distinct from NO_2 electrochemical reactivity. *J. Electroanal. Chem.*, **2012**, *685*, 109.

30 Saby, C., Ortiz, B., Champagne, G.Y., Belanger, D., Electrochemical modification of glassy carbon electrode using aromatic diazonium salts .1. Blocking effect of 4-nitrophenyl and 4-carboxyphenyl groups. *Langmuir*, **1997**, *13*, 6805.

31 Yang, N., Yu, J., Uetsuka, H., Nebel, C.E., Characterization of diamond surface terminations using electrochemical grafting with diazonium salts. *Electrochem. Commun.*, **2009**, *11*, 2237.

32 Yang, X.H., Hall, S.B., Tan, S.N., Electrochemical reduction of a conjugated cinnamic acid diazonium salt as an immobilization matrix for glucose biosensor. *Electroanal.*, **2003**, *15*, 885.

33 Combellas, C., Jiang, D.E., Kanoufi, F., Pinson, J., Podvorica, F.I., Steric effects in the reaction of aryl radicals on surfaces. *Langmuir*, **2009**, *25*, 286.

34 Barba, F., Batanero, B., Tissaoui, K., Raouafi, N., Boujlel, K., Cathodic reduction of diazonium salts in aprotic medium. *Electrochem. Commun.*, **2010**, *12*, 973.

35 Pinson, J., *Attachment of organic layers to materials surfaces by reduction of diazonium salts*, in *Aryl diazonium salts*, M.M. Chehimi, Editor. 2012, Wiley-VCH. pp. 1.

36 Benedetto, A., Balog, M., Viel, P., Le Derf, F., Salle, M., Palacin, S., Electro-reduction of diazonium salts on gold: Why do we observe multi-peaks? *Electrochim. Acta*, **2008**, *53*, 7117.

37 Malmos, K., Iruthayaraj, J., Ogaki, R., Kingshot, P., Besenbacher, F., Pedersen, S.U., Daasbjerg, K., Grafting of thin organic films by electrooxidation of arylhydrazines. *J. Phys. Chem. C*, **2011**, *115*, 13343.

38 Malmos, K., Iruthayaraj, J., Pedersen, S.U., Daasbjerg, K., General approach for monolayer formation of covalently attached aryl groups through electrografting of arylhydrazines. *J. Am. Chem. Soc.*, **2009**, *131*, 13926.

39 Andrieux, C.P., Gonzalez, F., Saveant, J.M., Derivatization of carbon surfaces by anodic oxidation of arylacetates. Electrochemical manipulation of the grafted films. *J. Am. Chem. Soc.*, **1997**, *119*, 4292.

40 Brooksby, P.A., Downard, A.J., Yu, S.S.C., Effect of applied potential on arylmethyl films oxidatively grafted to carbon surfaces. *Langmuir*, **2005**, *21*, 11304.

41 Duan, Y.Q., Luo, X.P., Qin, Y., Zhang, H.H., Sun, G.B., Sun, X.B., Yan, Y.S., Determination of epigallocatechin-3-gallate with a high-efficiency electrochemical sensor based on a molecularly imprinted poly(*o*-phenylenediamine) film. *J. Appl. Polym. Sci.*, **2013**, *129*, 2882.

42 Liu, X.X., Zhu, H., Yang, X.R., An electrochemical sensor for dopamine based on poly(*o*-phenylenediamine) functionalized with electrochemically reduced graphene oxide. *RSC Advances*, **2014**, *4*, 3706.

43 Barriere, F., Downard, A.J., Covalent modification of graphitic carbon substrates by non-electrochemical methods. *J. Solid State Electr.*, **2008**, *12*, 1231.

44 Adenier, A., Combellas, C., Kanoufi, F., Pinson, J., Podvorica, F.I., Formation of polyphenylene films on metal electrodes by electrochemical reduction of benzenediazonium salts. *Chem. Mater.*, **2006**, *18*, 2021.

45 DuVall, S.H., McCreery, R.L., Control of catechol and hydroquinone electron-transfer kinetics on native and modified glassy carbon electrodes. *Anal. Chem.*, **1999**, *71*, 4594.

46 Bard, A.J., Faulkner, L.R., *Electrochemical methods fundamentals and applications*. Second ed. **2001**: John Wiley & Sons, Inc.

47 DuVall, S.H., McCreery, R.L., Self-catalysis by catechols and quinones during heterogeneous electron transfer at carbon electrodes. *J. Am. Chem. Soc.*, **2000**, *122*, 6759.

48 Bard, A.J., Inner-sphere heterogeneous electrode reactions. Electrocatalysis and photocatalysis: The challenge. *J. Am. Chem. Soc.*, **2010**, *132*, 7559.

49 Liu, Y.C., McCreery, R.L., Reactions of organic monolayers on carbon surfaces observed with unenhanced Raman-spectroscopy. *J. Am. Chem. Soc.*, **1995**, *117*, 11254.

50 Brooksby, P.A., Downard, A.J., Multilayer nitroazobenzene films covalently attached to carbon. An AFM and electrochemical study. *J. Phys. Chem. B*, **2005**, *109*, 8791.

51 Ceccato, M., Nielsen, L.T., Iruthayaraj, J., Hinge, M., Pedersen, S.U., Daasbjerg, K., Nitrophenyl groups in diazonium-generated multilayered films: Which are electrochemically responsive? *Langmuir*, **2010**, *26*, 10812.

52 Ma, H.F., Lee, L., Brooksby, P.A., Brown, S.A., Fraser, S.J., Gordon, K.C., Leroux, Y.R., Hapiot, P., Downard, A.J., Scanning tunneling and atomic force microscopy evidence for covalent and noncovalent interactions between aryl films and highly ordered pyrolytic graphite. *J. Phys. Chem. C*, **2014**, *118*, 5820.

53 McCreery, R.L., Advanced carbon electrode materials for molecular electrochemistry. *Chem. Rev.*, **2008**, *108*, 2646.

Chapter 8. Conclusion

The work in this thesis was aimed at preparing monolayer tethers via reduction of aryldiazonium salts using a protection-deprotection approach. Three new protected diazonium ions were synthesised: protected carboxyphenyl (H-COO-Ar), protected aminophenyl (NH_2-Ar), and protected aminomethylphenyl (NH_2-CH_2-Ar). The H-COO-Ar groups were protected with fluorenylmethyl (Fm) groups, while both the amino groups were protected with *tert*-butyloxycarbonyl (Boc) and fluorenylmethoxycarbonyl (Fmoc) groups. Characterisation of films using electrochemistry and an atomic force spectroscopy (AFM) depth profiling technique suggests that after deprotection, the films are monolayers, except for Boc-NH_2-CH_2-Ar films. Coupling of the electro-active species ferrocenyl (Fc) and/or nitrophenyl (NP) groups was used to estimate the surface concentrations of the monolayer tethers. Amine derivatives were coupled to the H-COO-Ar monolayer to give an estimated surface concentration of ~3.5×10^{-10} mol cm^{-2}, while carboxylic derivatives were coupled to the amine modified films to give an estimated surface concentration of ~1.5×10^{-10} mol cm^{-2} for the Fmoc-NH_2-CH_2-Ar films. The low reactivity of NH_2-Ar films towards coupling reactions prevents the estimation of their surface concentration. Based on the calculated dimensions of the protected diazonium salts, the surface concentrations for a close-packed layer on a flat surface are 1.7×10^{-10} and 1.0×10^{-10} mol cm^{-2} for H-COO-Ar and NH_2-CH_2-Ar monolayers, respectively. Given the roughness of GC surfaces, the measured surface concentrations are consistent with monolayer films.

In addition to grafting from aryldiazonium salts, this thesis has described other methods that can be used to immobilise monolayers on GC surfaces: direct reaction of amine or carboxylic acid derivatives with bare GC, either via activation of acid groups or Michael-type addition.

Table 8.1 lists these methods for coupling a monolayer of Fc groups directly to GC surfaces, and also methods for coupling to monolayer tethers. The corresponding Fc surface concentrations are also listed.

Table 8.1 Conditions for coupling a monolayer of Fc groups on GC surfaces and the corresponding Fc surface concentrations.

Modifier	Fc derivatives	Γ_{Fc} ($\times 10^{-10}$ mol cm^{-2})	Type of linkages or reactions	Chapter
Bare GC	$FcCH_2NH_2$ in ACN	6.2 ± 0.9	Michael-type[a]	3
Bare GC	$FcCH_2NH_2$ in DCM	2.2 ± 0.4	Michael-type	3
Bare GC	$FcCH_2NH_2$ in DMF	2.6 ± 0.2	Michael-type	3
Bare GC + $(COCl)_2$	$FcCH_2NH_2$	2.2 ± 0.6	Amide and/or Michael-type	3
Bare GC + HBTU	$FcCH_2NH_2$	1.3 ± 0.2	Amide and/or Michael-type	3
Bare GC	FcCOOH + $(COCl)_2$	1.6 ± 0.2	Ester	3 and 6
Bare GC	$FcCH_2COOH$ + $(COCl)_2$	2.4 ± 0.4	Ester	3 and 6
H-COO-Ar-GC + $(COCl)_2$	$FcCH_2NH_2$	4.3 ± 0.5	Amide and/or Michael-type	5
H-COO-Ar-GC + $(COCl)_2$	$FcCH_2NH_2$	2.8 ± 0.7	Amide and/or Michael-type	5
NH_2-Ar-GC[b]	FcCOOH + $(COCl)_2$	3.3 ± 0.1	Amide and ester	6
NH_2-Ar-GC[b]	$FcCH_2COOH$ + $(COCl)_2$	2.5 ± 0.2	Amide (and ester)	6
NH_2-CH_2-Ar-GC[c]	FcCOOH + $(COCl)_2$	2.5 ± 0.2	Amide and ester	6
NH_2-CH_2-Ar-GC[c]	$FcCH_2COOH$ + $(COCl)_2$	1.7 ± 0.3	Amide (and ester)	6
NH_2-CH_2-Ar-GC[c]	$FcCH_2COOH$ + HBTU	1.4 ± 0.1	Amide	6

[a]Michael-type addition reaction

[b]Surface obtained from deprotection of Boc-NH-Ar-GC

[c]Surface is obtained from deprotection of Fmoc-NH-CH_2-Ar-GC

Examination of the data in Table 8.1 emphasises that different methods lead to different linkages, and different surface concentrations of Fc groups. To obtain the highest surface concentration of Fc, the Michael-type addition carried out in ACN is the best method. However, due to the short linker between the Fc and GC surface, the Fc has low stability, so attachment via a monolayer of H-COO-Ar-GC may be preferred. To prepare a loosely packed

Fc monolayer, and to avoid ester linkages, which are unstable to hydrolysis, coupling of a monolayer NH_2-CH_2-Ar film with $FcCH_2COOH$ via the HBTU method can be used. On the other hand, to avoid the necessity of synthesis of $FcCH_2NH_2$ or diazonium ions, reaction of bare GC with readily available FcCOOH or $FcCH_2COOH$ can be employed.

The ability to prepare mixed layers (films incorporating more than one modifier) is useful for applications such as biosensors, where the recognition species is diluted in an antifouling film so that interactions with target analytes are not sterically hindered and non-specific adsorption is minimised. In this work, preparation of mixed monolayers using the protected aryldiazonium salts, [Fm-COO-Ar-N_2]BF_4, [Fmoc-NH-CH_2-Ar-N_2]BF_4, and the previously reported [TIPS-Eth-Ar-N_2]BF_4 was investigated using three different methods namely from binary mixtures of diazonium salts and two methods based on sequential grafting. Preparation of mixed layers using mixtures of diazonium salts solution is expected to result in monolayer films. However, this method gives a sparse monolayer after deprotection and it is difficult to control the composition of the binary mixture using this method.

In the first of the sequential grafting methods, the protected diazonium salts were first grafted to the surface followed by cleavage of the protecting group and grafting of the second protected diazonium salt. In this method, the possibility of multilayer formation cannot be discounted, especially when the first modifier is the TIPS-Eth-Ar group.

In the second sequential grafting method, firstly the protected diazonium salts were grafted followed by removal of the protecting group. The second modifier was coupled to the surface via direct reaction of amine or carboxylic acid derivatives with the GC surface. This is the most convenient method for the preparation of mixed monolayers, because direct reaction with bare GC can presumably be carried out with any aliphatic amine or carboxylic acid derivatives, many of which are readily available commercially. Moreover, the attack of the

second modifier on the already grafted groups is not expected in this approach and hence only densely packed monolayer films are formed. In addition, the ratio of the two components can be tailored to fit the desired composition. For example, the bigger Fmoc-NH-CH_2-Ar groups leave a larger space after removal of the Fmoc groups and resulted in a ratio of ~ 1 : 3 for NH-CH_2-Ar groups and directly coupled filler groups. For the smaller TIPS groups a ratio of ~ 1 : 1 is obtained. To apply this strategy to Fm-COO-Ar films, the amine derivatives can only be reacted via the Michael-type addition reaction followed by reaction of amine derivatives with the deprotected H-COO-Ar groups. This is because under activating agent, both coupling reaction, with the bare GC and the H-COO-Ar groups occur.

The use of mixed monolayers for catalysis of O_2 reduction was briefly investigated. Anthraquinone (AQ) was immobilised on the GC surface by coupling of AQ-N_3 with H-Eth-Ar groups. AQ catalyses the reduction of O_2 to H_2O_2 via a two-electron process. The O_2 reduction peak at AQ-modified GC occurs at $E_{p,c}$ = -0.48 V, which is 150 mV more positive than at bare GC surface. This demonstrates the catalytic ability of AQ towards O_2 reduction process. A second modifier was grafted to the AQ-modified surface and the influence of the modifier on O_2 catalysis was examined. From preliminary results, mixed layers consisting of AQ groups diluted with hydrophobic groups increase the O_2 reduction current per AQ group. For these surfaces, the surface concentration of AQ is relatively low and hence, the AQ centres can be considered as nano-electrodes with radial diffusion fields and high fluxes of O_2 to the surface. However, it is tentatively proposed that there is an additional effect arising from the hydrophobic component of the second modifier, which provides a more favourable environment for reduction of the hydrophobic O_2.

Future work on preparation of monolayers via the protection-deprotection approach could be extended to different substrates to investigate the versatility of the method. Other work could

focus on different strategies for preparing monolayers via aryl diazonium ions. For example, aryl diazonium ions with substituted *meta* positions, but with a reactive group at the *para* position should not undergo multilayer formation (Figure 8.1). This approach has the advantage of not requiring a deprotection step. For some substrates, the deprotection step is not possible. For example, TIPS-protected aryldiazonium salt is not suitable for use with a silicon substrate, because upon deprotection of TIPS groups, with TBAF, the TIPS-Eth-Ar group will be cleaved from the silicon surface. Hence, preparation of monolayers without the need of a deprotection step would extend the scope of diazonium-derived monolayers. Preparation of monolayers via the protection-deprotection approach, where the protecting group can be removed either photochemically or thermally may also be of interest.

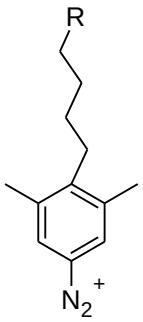

Figure 8.1 Proposed structure of aryldiazonium ions with substituted methyl groups at the *meta* position, to prevent the formation of multilayer and long alkyl chain at the para position consist of R groups (e.g. COOH or NH_2) that can be further used for coupling of functional molecules.

Another interesting area would be to further study the use of mixed layers for catalysis of reactions that require cooperativity between the species. For example, mixed layers could be prepared to have two different species that catalyse two consecutive reactions (Figure 8.2).

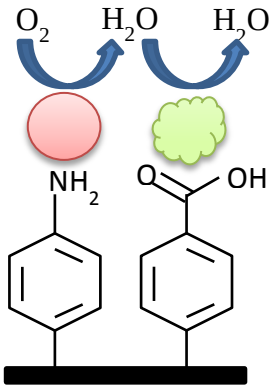

Figure 8.2 Cartoon depiction showing an example of a mixed layer consisting of two different species that catalyse two two-electron reduction of O_2 to H_2O.

Application of mixed monolayers for biosensor preparation is another interesting area. One of the components can be used for tethering the biomolecule and the other component can act as an antifouling layer. This could be applied to low cost screen-printed carbon electrodes for fabrication of stable, sensitive and selective biosensors.